

NIST Special Publication 1086r1
December 2012 Revision

**CFAST – Consolidated Model of Fire
Growth and Smoke Transport
(Version 6)
Software Development and
Model Evaluation Guide**

Richard D. Peacock
Paul A. Renike

<http://dx.doi.org/10.6028/NIST.SP.1086r1>



NIST Special Publication 1086r1
December 2012 Revision

**CFAST – Consolidated Model of Fire
Growth and Smoke Transport
(Version 6)**
**Software Development and
Model Evaluation Guide**

Richard D. Peacock
Paul A. Renike
*Fire Research Division
Engineering Laboratory*

<http://dx.doi.org/10.6028/NIST.SP.1086r1>

April 2013
SVNRepository Revision : 831



U.S. Department of Commerce
Rebecca Blank, Acting Secretary

National Institute of Standards and Technology
Patrick D. Gallagher, Under Secretary of Commerce for Standards and Technology and Director

Disclaimer

The U. S. Department of Commerce makes no warranty, expressed or implied, to users of CFAST and associated computer programs, and accepts no responsibility for its use. Users of CFAST assume sole responsibility under Federal law for determining the appropriateness of its use in any particular application; for any conclusions drawn from the results of its use; and for any actions taken or not taken as a result of analyses performed using these tools. CFAST is intended for use only by those competent in the field of fire safety and is intended only to supplement the informed judgment of a qualified user. The software package is a computer model which may or may not have predictive value when applied to a specific set of factual circumstances. Lack of accurate predictions by the model could lead to erroneous conclusions with regard to fire safety. All results should be evaluated by an informed user.

Intent and Use

The algorithms, procedures, and computer programs described in this report constitute a methodology for predicting some of the consequences resulting from a prescribed fire. They have been compiled from the best knowledge and understanding currently available, but have important limitations that must be understood and considered by the user. The program is intended for use by persons competent in the field of fire safety and with some familiarity with personal computers. It is intended as an aid in the fire safety decision-making process.

Preface

This supplement to the CFAST Technical Reference Guide provides details of the software development process for CFAST and accompanying experimental evaluation of the model. It is based in part on the “Standard Guide for Evaluating the Predictive Capability of Deterministic Fire Models,” ASTM E 1355 [1]. ASTM E 1355 defines *model evaluation* as “the process of quantifying the accuracy of chosen results from a model when applied for a specific use.” The model evaluation process consists of two main components: verification and validation. *Verification* is a process to check the correctness of the solution of the governing equations. Verification does not imply that the governing equations are appropriate; only that the equations are being solved correctly. *Validation* is a process to determine the appropriateness of the governing equations as a mathematical model of the physical phenomena of interest. Typically, validation involves comparing model results with experimental measurement. Differences that cannot be explained in terms of numerical errors in the model or uncertainty in the measurements are attributed to the assumptions and simplifications of the physical model.

Evaluation is critical to establishing both the acceptable uses and limitations of a model. Throughout its development, CFAST has undergone various forms of evaluation, both at the National Institute of Standards and Technology and beyond. This Supplement provides a survey of validation work conducted to date to evaluate CFAST. Documentation of CFAST Verification is contained in the CFAST Technical Reference Guide [2].

Acknowledgments

The following individuals and organizations played a role in the validation process of FDS.

- Continuing support for CFAST is via internal funding at the National Institute of Standards and Technology (NIST).
- In addition, support is provided by other agencies of the U.S. Federal Government, most notably the Nuclear Regulatory Commission (NRC) Office of Research and the U.S. Department of Energy.

The US Nuclear Regulatory Commission Office of Research has funded key validation experiments, the preparation of the CFAST manuals, and the development of various sub-models that are of importance in the area of nuclear power plant safety. Special thanks to Mark Salley, David Stroup, and Jason Dreisbach for their efforts and support.

Support to refine the software development and quality assurance process for CFAST has been provided by the U.S. Department of Energy (DOE). The assistance of Subir Sen and Debra Sparkman in understanding DOE software quality assurance programs and the application of the process to CFAST is gratefully acknowledged. Thanks are also due to Allan Coutts, Washington Safety Management Solutions for his insight into the application of fire models to nuclear safety applications and detailed review of the CFAST document updates for DOE.

- Anthony Hamins, currently Chief of the Fire Research Division at NIST directed the NIST/NRC and WTC experiments, and quantified the experimental uncertainty of these and other experiments used in this study. Alex Maranghides was the Director of the Large Fire Laboratory at NIST at the time these tests were conducted, and he helped to design the experiments. Therese McAllister oversaw the instrumentation of the structural steel during the WTC experiments.
- Anthony Hamins developed the technique of evaluating experimental uncertainty that is used throughout this Guide.
- Kevin McGrattan and Randy McDermott of the Fire Research Devision at NIST developed the automated process for validation and verification testing of the Fire Dynamics Simulator (FDS) model. We use this same process for validation and verification testing of CFAST.
- Kevin McGrattan of the Fire Research Division and Blaza Toman of the Statistical Engineering Division of NIST developed the method of quantifying the model uncertainty at

- For the NIST/NRC tests, Alex Maranghides was in charge of the Large Fire Laboratory at NIST where these tests were conducted, and helped to design the experiments. Thanks also to technicians Laurean Delauter, Jay McElroy, and Jack Lee who constructed and conducted these validation experiments at NIST.
- Steve Nowlen at Sandia National Laboratories provided data, documentation and further information for the NRC-sponsored experiments referred to in this document and the "FM/SNL Test Series" (Factory Mutual and Sandia National Laboratories conducted these experiments).
- Thanks to VTT, Finland, for their contribution of experimental data, referred to in this document as the "VTT Large Hall Experiments."
- Bryan Klein, currently employed at Thunderhead Engineering, Inc., assisted in the development of techniques to automatically generate the plots that are found throughout this Guide.
- David Sheppard, currently of the Bureau of Alcohol, Tobacco and Firearms (ATF), conducted the experiments referred to as the "UL/NFPRF Test Series" on behalf of the Fire Protection Research Foundation (then known as the National Fire Protection Research Foundation) while working at Underwriters Labs in Northbrook, Illinois. Sheppard, along with Bryan Klein, currently employed at Thunderhead Engineering, Inc., conducted the experiments referred to as the "ATF Corridors" series in 2008.
- Steve Nowlen of Sandia National Laboratory provided valuable information about the FM/SNL series.
- Taylor Myers, a student at the University of Maryland and a Summer Undergraduate Research Fellow (SURF) at NIST, analyzed the Vettori Flat sprinkler experiments. Thanks also to Bob Vettori of the U.S. Nuclear Regulatory Commission and formerly of NIST for his help in locating the original test data and laboratory notebooks.
- Taylor Myers also analyzed the NIST Dunes 2000 experiments and the WTC Spray Burner experiments using CFAST.

Contents

Disclaimer	iii
Intent and Use	v
Preface	vii
Acknowledgments	ix
1 Overview	1
1.1 What is Model Validation?	1
1.2 How to Use this Guide	2
1.3 Blind, Specified, and Open Validation Experiments	3
1.4 Software Development and Quality Assurance	4
1.5 Model Validation Scenarios	4
1.6 Input Data Required to Run the Model	5
1.7 Property Data	6
1.8 Model Outputs	6
1.9 Model Accuracy	7
1.10 Uses and Limitations of the Model	7
2 Software Quality Assurance	11
2.1 Relevant Publications	11
2.2 Model Management	12
2.3 SQA Documentation	13
2.4 Standards, Practices, Conventions, and Metrics	14
2.5 Software Reviews	14
2.6 Model Testing	14
2.7 Problem Reporting and Resolution	15
2.8 Tools, Techniques, and Methodologies	15
2.9 Media Control	15
2.10 Supplier Control	15
2.11 Records Collection, Maintenance, and Retention	16
2.12 Training	16
2.13 Risk Management	16

3 Software Structure and Robustness	17
3.1 Structure of the Numerical Routines	17
3.2 Comparison with Analytic Solutions	19
3.3 Code Checking	19
3.4 Numerical Tests	20
4 Survey of Past Validation Work	21
4.1 Comparisons with Full-Scale Tests Conducted Specifically for the Chosen Evaluation	21
4.2 Comparisons with Previously Published Test Data	23
4.2.1 Fire Plumes	23
4.2.2 Multiple Compartments	24
4.2.3 Large Compartments	24
4.2.4 Prediction of Flashover	24
4.3 Comparison with Documented Fire Experience	27
4.4 Comparison with Experiments Which Cover Special Situations	28
4.4.1 Nuclear Facilities	28
4.4.2 Small Scale Testing	29
4.4.3 Unusual Geometry and Specific Algorithms	29
5 Description of Experiments	33
5.1 ATF Corridors Experiments	33
5.2 FM Four Room Including Corridor Test Series	35
5.3 FM / SNL Test Series	36
5.4 iBMB Compartment Tests	37
5.5 LLNL Enclosure Tests	40
5.6 NBS Single Room Tests with Furniture	43
5.7 NBS Multi-Compartment Test Series	47
5.8 NIST Dunes 2000 Experiments	50
5.9 NIST Seven-story Hotel Tests	51
5.10 NIST / NRC Test Series	53
5.11 SP Adiabatic Surface Temperature Experiments	57
5.12 Steckler Compartment Experiments	58
5.13 UL/NFPRF Sprinkler, Vent, and Draft Curtain Study	58
5.14 USN High Bay Hangar Experiments	62
5.15 Vettori Flat Ceiling Experiments	63
5.16 VTT Large Hall Tests	63
5.17 WTC Spray Burner Test Series	69
5.18 Summary of Experiments	69
6 Hot Gas Layer Temperature and Depth	73
6.1 Model / Experiment Comparisons	74
6.2 Summary	79

7 Fire Plumes, Ceiling Jets, and Device Activation	81
7.1 Flame Height	81
7.2 Plume Temperature	81
7.3 Ceiling Jets	83
7.4 Device Activation	85
7.5 Summary	85
8 Gas Species and Smoke	89
8.1 Oxygen and CO ₂	89
8.2 NIST/NRC Test Series, Smoke	92
8.3 Summary	93
9 Pressure	95
10 Heat Flux and Surface Temperature	97
10.1 NIST/NRC Test Series, Cables	97
10.2 NIST/NRC Test Series, Compartment Walls, Floor and Ceiling	99
10.3 Summary	101
11 Summary and Conclusions	103
References	113
Appendices	113
A Calculation of Layer Height and the Average Upper and Lower Layer Temperatures	115
B Model / Experiment Comparison Graphs	117
B.1 FM Four Room Including Corridor Test Series	117
B.2 FM/SNL Test Series	122
B.3 iBMB Compartment Tests	134
B.4 LLNL Enclosure Series	136
B.5 NBS Single Room Tests with Furniture	145
B.6 NBS Multi-Compartment Test Series	148
B.7 NIST Dunes 2000 Experiments	152
B.8 NIST Seven-story Hotel Tests	154
B.9 NIST/NRC Test Series	157
B.10 Steckler Compartment Experiments	203
B.11 UL/NFPRF Series I Experiments	211
B.12 USN High Bay Hangar Experiments	214
B.13 Vettori Flat Ceiling Experiments	218
B.14 VTT Large Hall Tests	225
B.15 WTC Test Series	228

List of Figures

2.1	CFAST SQA Organization Structure.	12
3.1	Subroutine structure for the CFAST model	18
4.1	Comparison of correlations, CFAST predictions, and experimental data for the prediction of flashover in a compartment fire.	26
5.1	Geometry of the ATF Corridors Experiments.	34
5.2	Overview of the Factory Mutual Four Room test series.	35
5.3	Detailed plan, side, and perspective schematic drawings of the FM/SNL experimental arrangement, including the supply and exhaust ducts, and the fuel pan.	38
5.4	Prescribed (dotted line) and measured (solid line) heat release rate as a function of time during Test 21 of the FM/SNL test series	40
5.5	Detailed plan, side, and perspective schematic drawings of the iBMB pool fire experimental arrangement.	41
5.6	Estimated heat release rate for the iBMB fire experiments.	43
5.7	Detailed plan, side, and perspective schematic drawings of the iBMB cable fire experimental arrangement.	44
5.8	Geometry of the LLNL Enclosure Experiments	45
5.9	Plan and elevation view schematic of experimental room for NBS single room tests with furniture.	46
5.10	Burning specimen during NBS single room tests with furniture.	46
5.11	Photo of a 100 kW fire with the burner located against the rear wall of one of the small compartments in the NBS Multi-Compartment test Series.	47
5.12	Overview of the NBS Test Configuration.	48
5.13	Plan, side and perspective schematic drawings of the NBS experimental arrangement, including the burner.	49
5.14	Prescribed and measured heat release rate as a function of time during Tests 100A and 100Z of the NBS multi-room test series.	50
5.15	Geometry of the NIST Dunes 2000 Experiments	51
5.16	Overview of the NIST Seven-story hotel test series including smoke control.	53
5.17	Photograph of a 1 MW heptane fire seen through the open doorway. Photo provided by Anthony Hamins, NIST.	54
5.18	Cross-section View of the NIST NRC Test Configuration.	54
5.19	Plan, side and perspective schematic drawings of the NIST NRC experimental arrangement. The fuel pan and cables B, D, F, and G (dotted lines) are also shown.	55

5.20	Measured and prescribed heat release rate as a function of time during Test 3 of the NIST NRC test series	57
5.21	Plan view of the UL/NFPRF Experiments, Series I.	60
5.22	Plan view of the UL/NFPRF Experiments, Series II	61
5.23	Geometry of the Vettori Flat Ceiling compartment	64
5.24	Cut-Away View of Case 2 of the VTT Large Hall Tests.	65
5.25	Plan, side and perspective schematic drawings of the experimental arrangement of the VTT large hall fire tests, including the fuel pan	66
5.26	Photo of a 2 MW heptane fire during the VTT large hall tests. Photo provided by Simo Hostikka, VTT.	67
5.27	Prescribed Heat Release Rate as a Function of Time for VTT Large Hall Tests.	68
5.28	Geometry of the WTC Experiments	70
6.1	Comparison of Measured and Predicted HGL Temperature and Height.	75
6.2	Measured and Predicted HGL Temperature and Height for a Single Compartment Test.	76
7.1	Comparison of Measured and Predicted Plume Centerline Temperature.	82
7.2	Comparison of Measured and Predicted Ceiling Jet Temperature.	84
7.3	Comparison of Measured and Predicted Ceiling Jet Temperature.	86
8.1	Comparison of Measured and Predicted Oxygen Concentration and Carbon Dioxide Concentration.	90
8.2	Comparison of Measured and Predicted Smoke Concentration.	92
9.1	Comparison of Measured and Predicted Compartment Pressure.	96
10.1	Comparisons of Measured and Predicted Heat Flux to Targets and Target Temperature	98
10.2	Comparisons of Measured and Predicted Heat Flux to Compartment Surfaces and Surface Temperature	100
B.1	Hot Gas Layer Temperature and Height for the FM/NBS Four Compartment Test 19.118	
B.2	Hot Gas Layer Temperature and Height for the FM/NBS Four Compartment Test 21.119	
B.3	Oxygen and Carbon Dioxide Concentration for the FM/NBS Test 19.	120
B.4	Oxygen and Carbon Dioxide Concentration for the FM/NBS Test 21.	121
B.5	Hot Gas Layer Temperature and Height for the FM/SNL Tests.	123
B.6	Hot Gas Layer Temperature and Height for the FM/SNL Tests.	124
B.7	Hot Gas Layer Temperature and Height for the FM/SNL Tests.	125
B.8	Hot Gas Layer Temperature and Height for the FM/SNL Tests.	126
B.9	Hot Gas Layer Temperature and Height for the FM/SNL Tests.	127
B.10	Predicted Plume Centerline Temperature for the FM/SNL Tests.	128
B.11	Predicted Plume Centerline Temperature for the FM/SNL Tests.	129
B.12	Predicted Plume Centerline Temperature for the FM/SNL Tests.	130
B.13	Predicted Plume Centerline Temperature for the FM/SNL Tests.	131
B.14	Predicted Plume Centerline Temperature for the FM/SNL Tests.	132
B.15	Predicted Plume Centerline Temperature for the FM/SNL Tests.	133

B.16 Predicted HGL Temperature and Height for the iBMB Single Compartment Tests. . .	135
B.17 Predicted Oxygen and Carbon Dioxide for the iBMB Cable Test 5.	135
B.18 Predicted HGL Temperature and Height for the NBS Single Compartment Tests. . .	146
B.19 Predicted Oxygen Concentrationfor the NBS Single Compartment Tests.	147
B.20 Predicted Compartment Pressure for the NBS Single Compartment Tests.	147
B.21 Hot Gas Layer Temperature and Height for the NBS Multi-Room Test 100A. . . .	149
B.22 Hot Gas Layer Temperature and Height for the NBS Multi-Room Test 100O. . . .	150
B.23 Hot Gas Layer Temperature and Height for the NBS Multi-Room Test 100Z. . . .	151
B.24 Predicted HGL Temperature and Height for the Seven-Story Hotel Test 7.	155
B.25 Predicted Oxygen and Carbon Dioxide for the Seven-Story Hotel Test 7.	156
B.26 Predicted HGL Temperature and Height for the NIST/NRC Tests 1, 7, 2 and 8. . .	158
B.27 Predicted HGL Temperature and Height for the NIST/NRC Tests 4, 10, 13 and 16. .	159
B.28 Predicted HGL Temperature and Height for the NIST/NRC Tests 17, 3 and 9. . . .	160
B.29 Predicted HGL Temperature and Height for the NIST/NRC Tests 5, 14, 15 and 18. .	161
B.30 Ceiling Jet Temperature for the NIST/NRC Series, Closed Door Tests.	162
B.31 Ceiling Jet Temperature for the NIST/NRC Series, Open Door Tests.	163
B.32 Predicted Oxygen and Carbon Dioxide for the NIST/NRC Tests 1, 7, 2 and 8. . . .	164
B.33 Predicted Oxygen and Carbon Dioxide for the NIST/NRC Tests 4, 10, 13 and 16. .	165
B.34 Predicted Oxygen and Carbon Dioxide for the NIST/NRC Tests 17, 3, and 9. . . .	166
B.35 Predicted Oxygen and Carbon Dioxide for the NIST/NRC Tests 5, 14, 15 and 18. .	167
B.36 Smoke Concentrationfor the NIST/NRC Series, Closed Door Tests.	168
B.37 Smoke Concentrationfor the NIST/NRC Series, Open Door Tests.	169
B.38 Compartment Pressures for the NIST/NRC Series, Closed Door Tests.	170
B.39 Compartment Pressures for the NIST/NRC Series, Open Door Tests.	171
B.40 NIST/NRC Series, Cable B Temperature and Heat Flux, Replicate Tests 1 and 7. .	172
B.41 NIST/NRC Series, Cable B Temperature and Heat Flux, Replicate Tests 2 and 8. .	172
B.42 NIST/NRC Series, Cable B Temperature and Heat Flux, Replicate Tests 4 and 10. .	173
B.43 NIST/NRC Series, Cable B Temperature and Heat Flux, Replicate Tests 13 and 16. .	173
B.44 NIST/NRC Series, Cable B Temperature and Heat Flux, Replicate Tests 3 and 9. .	174
B.45 NIST/NRC Series, Cable B Temperature and Heat Flux, Replicate Tests 5 and 14. .	174
B.46 NIST/NRC Series, Cable B Temperature and Heat Flux, Replicate Tests 15 and 18. .	175
B.47 NIST/NRC Series, Cable D Temperature and Heat Flux, Replicate Tests 1 and 7. .	176
B.48 NIST/NRC Series, Cable D Temperature and Heat Flux, Replicate Tests 2 and 8. .	176
B.49 NIST/NRC Series, Cable D Temperature and Heat Flux, Replicate Tests 4 and 10. .	177
B.50 NIST/NRC Series, Cable D Temperature and Heat Flux, Replicate Tests 13 and 16. .	177
B.51 NIST/NRC Series, Cable D Temperature and Heat Flux, Replicate Tests 3 and 9. .	178
B.52 NIST/NRC Series, Cable D Temperature and Heat Flux, Replicate Tests 5 and 14. .	178
B.53 NIST/NRC Series, Cable D Temperature and Heat Flux, Replicate Tests 15 and 18. .	179
B.54 NIST/NRC Series, Cable F Temperature and Heat Flux, Replicate Tests 1 and 7. .	180
B.55 NIST/NRC Series, Cable F Temperature and Heat Flux, Replicate Tests 2 and 8. .	180
B.56 NIST/NRC Series, Cable F Temperature and Heat Flux, Replicate Tests 4 and 10. .	181
B.57 NIST/NRC Series, Cable F Temperature and Heat Flux, Replicate Tests 13 and 16. .	181
B.58 NIST/NRC Series, Cable F Temperature and Heat Flux, Replicate Tests 3 and 9. .	182
B.59 NIST/NRC Series, Cable F Temperature and Heat Flux, Replicate Tests 5 and 14. .	182
B.60 NIST/NRC Series, Cable F Temperature and Heat Flux, Replicate Tests 15 and 18. .	183

B.61 NIST/NRC Series, Cable G Temperature and Heat Flux, Replicate Tests 1 and 7. . .	184
B.62 NIST/NRC Series, Cable G Temperature and Heat Flux, Replicate Tests 2 and 8. . .	184
B.63 NIST/NRC Series, Cable G Temperature and Heat Flux, Replicate Tests 4 and 10. .	185
B.64 NIST/NRC Series, Cable G Temperature and Heat Flux, Replicate Tests 13 and 16. .	185
B.65 NIST/NRC Series, Cable G Temperature and Heat Flux, Replicate Tests 3 and 9. . .	186
B.66 NIST/NRC Series, Cable G Temperature and Heat Flux, Replicate Tests 5 and 14. .	186
B.67 NIST/NRC Series, Cable G Temperature and Heat Flux, Replicate Tests 15 and 18. .	187
B.68 NIST/NRC Series, Long Wall Temperature and Heat Flux, Replicate Tests 1 and 7. .	188
B.69 NIST/NRC Series, Long Wall Temperature and Heat Flux, Replicate Tests 2 and 8. .	188
B.70 NIST/NRC Series, Long Wall Temperature and Heat Flux, Replicate Tests 4 and 10. .	189
B.71 NIST/NRC Series, Long Wall Temperature and Heat Flux, Replicate Tests 13 and 16.	189
B.72 NIST/NRC Series, Long Wall Temperature and Heat Flux, Replicate Tests 3 and 9. .	190
B.73 NIST/NRC Series, Long Wall Temperature and Heat Flux, Replicate Tests 5 and 14. .	190
B.74 NIST/NRC Series, Long Wall Temperature and Heat Flux, Replicate Tests 15 and 18.	191
B.75 NIST/NRC Series, Short Wall Temperature and Heat Flux, Replicate Tests 1 and 7. .	192
B.76 NIST/NRC Series, Short Wall Temperature and Heat Flux, Replicate Tests 2 and 8. .	192
B.77 NIST/NRC Series, Short Wall Temperature and Heat Flux, Replicate Tests 4 and 10. .	193
B.78 NIST/NRC Series, Short Wall Temperature and Heat Flux, Replicate Tests 13 and 16.	193
B.79 NIST/NRC Series, Short Wall Temperature and Heat Flux, Replicate Tests 3 and 9. .	194
B.80 NIST/NRC Series, Short Wall Temperature and Heat Flux, Replicate Tests 5 and 14. .	194
B.81 NIST/NRC Series, Short Wall Temperature and Heat Flux, Replicate Tests 15 and 18.	195
B.82 NIST/NRC Series, Ceiling Temperature and Heat Flux, Replicate Tests 4 and 10. . .	196
B.83 NIST/NRC Series, Ceiling Temperature and Heat Flux, Replicate Tests 13 and 16. .	196
B.84 NIST/NRC Series, Ceiling Temperature and Heat Flux, Replicate Tests 3 and 9. . .	197
B.85 NIST/NRC Series, Ceiling Temperature and Heat Flux, Replicate Tests 5 and 14. . .	197
B.86 NIST/NRC Series, Ceiling Temperature and Heat Flux, Replicate Tests 15 and 18. .	198
B.87 NIST/NRC Series, Floor Temperature and Heat Flux, Replicate Tests 1 and 7. . . .	199
B.88 NIST/NRC Series, Floor Temperature and Heat Flux, Replicate Tests 2 and 8. . . .	199
B.89 NIST/NRC Series, Floor Temperature and Heat Flux, Replicate Tests 4 and 10. . . .	200
B.90 NIST/NRC Series, Floor Temperature and Heat Flux, Replicate Tests 13 and 16. . .	200
B.91 NIST/NRC Series, Floor Temperature and Heat Flux, Replicate Tests 3 and 9. . . .	201
B.92 NIST/NRC Series, Floor Temperature and Heat Flux, Replicate Tests 5 and 14. . . .	201
B.93 NIST/NRC Series, Floor Temperature and Heat Flux, Replicate Tests 15 and 18. . .	202
B.94 Predicted HGL Temperature and Height for the VTT Large Hall Tests.	226
B.95 Predicted Plume Centerline Temperature for the VTT Large Hall Tests.	227

List of Tables

5.1	Summary of FM/SNL Experiments	39
5.2	Summary of LLNL Enclosure Experiments	42
5.3	Summary of NIST Dunes 2000 experiments selected for model validation.	52
5.4	Test Matrix and Experimental Conditions for NIST NRC Tests	56
5.5	Summary of Steckler compartment experiments.	59
5.6	Thermophysical Properties for VTT Large Hall Tests	65
5.7	Summary of important experimental parameters.	72
6.1	Relative Difference for HGL Temperature and Depth for Two Measurement Locations in Two Single-Room Tests	76
8.1	Relative Difference for Oxygen and Carbon Dioxide in Open and Closed Door Tests in a Single Compartment	91
11.1	Summary of Model Comparisons	104
B.1	Ceiling surface measurement locations for the WTC series	230

Chapter 1

Overview

CFAST is a fire model capable of predicting the fire-induced environmental conditions as a function of time for single- or multi-compartment scenarios. Toward that end, the CFAST software calculates the evolution of temperature, smoke, and fire gases throughout a building during a user-prescribed fire. The model was developed, and is maintained, by the Fire Research Division of the National Institute of Standards and Technology (NIST).

CFAST is a two-zone model, in that it subdivides each compartment into two zones, or control volumes and the two volumes are assumed to be homogeneous within each zone. This two-zone approach has evolved from observations of layering in actual fires and real-scale fire experiments. Differential equations that approximate solution of the mass and energy balances of each zone, equations for heat conduction into the walls, and the ideal gas law simulate the environmental conditions generated by a fire.

This document describes the underlying structure of the CFAST model and the processes used during the development and deployment of the model. It is intended to provide guidelines for

- the planning for modifications to the model,
- any required reviews for both software and associated documentation of the model,
- testing to be conducted prior to the release of an updated model,
- problem reporting and resolution,
- retention of records, source code, and released software over the life of the code.

1.1 What is Model Validation?

Key to ensuring the quality of the software are ongoing validation testing of the model. Validation typically involves comparing model simulations with experimental measurements. To say that CFAST is “validated” means that the model has been shown to be of a given level of accuracy for a given range of parameters for a given type of fire scenario. Although the CFAST developers periodically perform validation studies, it is ultimately the end user of the model who decides if the model is adequate for the job at hand. Thus, this Guide does not and cannot be considered comprehensive for every possible modeling scenario.

Although there are various definitions of model validation, for example those contained in ASTM E 1355 [1], most define it as the process of determining how well the mathematical model predicts the actual physical phenomena of interest. Validation typically involves (1) comparing model predictions with experimental measurements, (2) quantifying the differences in light of uncertainties in both the measurements and the model inputs, and (3) deciding if the model is appropriate for the given application. This Guide only does (1) and (2). Number (3) is the responsibility of the model user.

A common question asked of any mathematical model is whether it is validated. To say that CFAST is “validated” means that the model has been shown to be of a given level of accuracy for a given range of parameters for a given type of fire scenario. Although the CFAST developers continuously perform validation studies, it is ultimately the end user of the model who decides if the model is adequate for the job at hand. Thus, this Guide provides the raw material for a validation study, but it does not and cannot be considered comprehensive.

The following sections discuss key issues that you must consider when deciding whether or not CFAST has been validated. It depends on (a) the scenarios of interest, (b) the predicted quantities, and (c) the desired level of accuracy. Keep in mind that CFAST can be used to model most any compartment fire scenario and predict quantities of interest, but the prediction may not be accurate because of limitations in the description of the fire physics, and also because of limited information about the fuels, geometry, and so on.

1.2 How to Use this Guide

This guide presents a compilation of past and present validation exercises for the CFAST model are presented. As CFAST continues to develop, it will expand to include new experimental measurements of newly modeled physical phenomena. With each change in, the plots and graphs are all be redone to ensure that changes to the model are consistent with any changes in the predictions and the overall accuracy of the model. If you are embarking on a validation study, you might want to consider the following steps:

1. Survey Chapter 4 to learn about past efforts by others to validate the model for applications similar to yours. Keep in mind that most of the referenced validation exercises have been performed with older versions of CFAST, and you may want to obtain the experimental data and the old FDS input files and redo the simulations with the version of CFAST that you plan to use.
2. Identify in Chapter 5 experimental data sets appropriate for your application. In particular, the summary of the experiments found in table 5.7 contains a table listing various non-dimensional quantities that characterize the parameters of the experiments. For example, the equivalence ratio of a compartment fire experiment indicates the degree to which the fire was over or under-ventilated. To say that the results of a given experiment are relevant to your scenario, you need to demonstrate that its parameters “fit” within the parameter space outlined in Table 5.7.
3. Search the Table of Contents to find comparisons of CFAST simulations with the relevant experiments. For a given experiment, there may be numerous measurements of quantities

like the gas temperature, heat flux, and so on. It is a challenge to sort out all the plots and graphs of all the different quantities and come to some general conclusion. For this reason, this Guide is organized by output quantity, not by individual experiment or fire scenario. In this way, it is possible to assess, over a range of different experiments and scenarios, the performance of the model in predicting a given quantity. Overall trends and biases become much more clear when the data is organized this way.

The experimental data sets and CFAST input files described in this Guide are all managed via the on-line project archiving system. You might want to re-run examples of interest to better understand how the calculations were designed, and how changes in the various parameters might affect the results. This is known as a *sensitivity study*, and it is difficult to document all the parameter variations of the calculations described in this report. Thus, it is a good idea to determine which of the input parameters are particularly important.

1.3 Blind, Specified, and Open Validation Experiments

ASTM E 1355 [1] describes three basic types of validation calculations – *Blind*, *Specified*, and *Open*.

Blind Calculation: The model user is provided with a basic description of the scenario to be modeled. For this application, the problem description is not exact; the model user is responsible for developing appropriate model inputs from the problem description, including additional details of the geometry, material properties, and fire description, as appropriate. Additional details necessary to simulate the scenario with a specific model are left to the judgement of the model user. In addition to illustrating the comparability of models in actual end-use conditions, this will test the ability of those who use the model to develop appropriate input data for the models.

Specified Calculation: The model user is provided with a complete detailed description of model inputs, including geometry, material properties, and fire description. As a follow-on to the blind calculation, this test provides a more careful comparison of the underlying physics in the models with a more completely specified scenario.

Open Calculation: The model user is provided with the most complete information about the scenario, including geometry, material properties, fire description, and the results of experimental tests or benchmark model runs which were used in the evaluation of the blind or specified calculations of the scenario. Deficiencies in available input (used for the blind calculation) should become most apparent with comparison of the open and blind calculation.

The calculations presented in this Guide all fall into the *Open* category. There are several reasons for this, the first being the most practical:

- All of the calculations presented in this Guide are routinely rerun. The fact that the experiments have already been performed and the results are known automatically qualify these calculations as *Open*.

- Some of the calculations described in this Guide did originally fall into the *Specified* category because they were first performed before the experiments were conducted. However, in almost every case, the experiment was not conducted exactly as specified, and the calculation results were not particularly useful in determining the accuracy of the model.
- None of the calculations were truly *Blind*, even those performed prior to the experiments. The purpose of a *Blind* calculation is to assess the degree to which the choice of input parameters affects the outcome. However, in such cases it is impossible to discern the uncertainty associated from the choice of input parameters from that associated with the model itself. The primary purpose of this Guide is to quantify the uncertainty of the model itself, in which case *Blind* calculations are of little value.

1.4 Software Development and Quality Assurance

The development and maintenance of CFAST is guided by software quality assurance measures for the planning of modifications to the model that provide required reviews for both software and associated documentation of the model, define testing to be conducted prior to the release of an updated model, describe problem reporting and resolution procedures, and ensure all records, source code, and released software is kept available for the life of the code.

The internal structure of the model also has an impact on the ease of modification and correctness of the model. The method for incorporating new phenomena and ensuring the correctness of the code was adopted as part of the consolidation of CCFM and FAST and has resulted in a more transparent, transportable and verifiable numerical model. This transparency is crucial to a verifiable and robust numerical implementation of the predictive model as discussed in the sections on code checking and numerical analysis. More recently, all of the software development and software tracking has been made available on the web to further enhance the software development process.

1.5 Model Validation Scenarios

Key to ensuring the correctness and accuracy of the model are comparisons of the model with both earlier versions of the model and with documented experimental data applicable to the intended range of application of the model. When doing a validation study, the first question to ask is, “What is the application?” There are countless fire scenarios to consider, but from the point of view of validation, it is useful to divide them into two classes – those for which the fire is *specified* as an input to the model and those for which the fire must be estimated by use of the model. The former is often the case for a design application, the latter for a forensic reconstruction. Consider each in turn.

Design applications typically involve an existing building or a building under design. A so-called “design fire” is prescribed either by a regulatory authority or by the engineers performing the analysis. Because the fire’s heat release rate is specified, the role of the model is to predict the transport of heat and combustion products throughout the room or rooms of interest. Ventilation equipment is often included in the simulation, like fans, blowers, exhaust hoods, ductwork, smoke management systems, *etc.* Sprinkler and heat and smoke detector activation are also of interest.

The effect of the sprinkler spray on the fire is usually less of interest since the fire is prescribed rather than predicted. Detailed descriptions of the contents of the building are usually not necessary because these items are not assumed to be burning, and even if they are, the burning rate will be fixed, not predicted. Sometimes, it is necessary to predict the heat flux from the fire to a nearby “target,” and even though the target may heat up to some prescribed ignition temperature, the subsequent spread of the fire usually goes beyond the scope of the analysis because of the uncertainty inherent in object to object fire spread.

Forensic reconstructions require the model to simulate an actual fire based on information that is collected after the event, such as eye witness accounts, unburned materials, burn signatures, *etc.* The purpose of the simulation is to connect a sequence of discrete observations with a continuous description of the fire dynamics. Usually, reconstructions involve more gas/solid phase interaction because virtually all objects in a given room are potentially ignitable, especially when flashover occurs. Thus, there is much more emphasis on such phenomena as heat transfer to surfaces, pyrolysis, flame spread, and suppression. In general, forensic reconstructions are more challenging simulations to perform because they require more detailed information about the room geometry and contents, and there is much greater uncertainty in the total heat release rate as the fire spreads from object to object.

CFAST has been applied for both design and reconstruction scenarios. For the former, specified design fires are typically used (e.g., reference [3]). For the latter, iterative simulation with multiple model runs allow the user to develop fire growth inputs consistent with observed post fire conditions.

1.6 Input Data Required to Run the Model

All of the data required to run the CFAST model reside in a primary data file, which the user creates. Some instances may require databases of information on objects, thermophysical properties of boundaries, and sample prescribed fire descriptions. In general, the data files contain the following information:

- compartment dimensions (height, width, length)
- construction materials of the compartment (e.g., concrete, gypsum)
- material properties (e.g., thermal conductivity, specific heat, density, thickness, heat of combustion)
- dimensions and positions of horizontal and vertical flow openings such as doors, windows, and vents
- mechanical ventilation specifications
- fire properties (e.g., heat release rate, lower oxygen limit, and species production rates as a function of time)
- sprinkler and detector specifications
- positions, sizes, and characteristics of targets

The CFAST User's Guide [4] provides a complete description of the required input parameters. Some of these parameters have default values included in the model, which are intended to be representative for a range of fire scenarios. Unless explicitly noted, default values were used for parameters not specifically included in this validation study.

1.7 Property Data

Required inputs for CFAST must be provided with a number of material properties related to compartment bounding surfaces, objects (called targets) placed in compartments for calculation of object surface temperature and heat flux to the objects, or fire sources. For compartment surfaces and targets, CFAST needs the density, thermal conductivity, specific heat, and emissivity.

For fire sources, CFAST needs to know the pyrolysis rate of fuel, the heat of combustion, stoichiometric fuel-oxygen ratio, yields of important combustion products in a simplified combustion reaction (carbon monoxide, carbon dioxide, soot, and others), and the fraction of energy released in the form of thermal radiation.

These properties are commonly available in fire protection engineering and materials handbooks. Experimentally determined property data may also be available for certain scenarios. However, depending on the application, properties for specific materials may not be readily available. A small file distributed with the CFAST software contains a database with thermal properties of common materials. These data are given as examples, and users should verify the accuracy and appropriateness of the data.

1.8 Model Outputs

Once the simulation is complete, CFAST produces an output file containing all of the solution variables. Typical outputs include (but are not limited to) the following:

- environmental conditions in the room (such as hot gas layer temperature; oxygen and smoke concentration; and ceiling, wall, and floor temperatures)
- heat transfer-related outputs to walls and targets (such as incident convective, radiated, and total heat fluxes)
- fire intensity and flame height
- flow velocities through vents and openings
- detector and sprinkler activation times

Thus, for a given fire scenario, there are a number of different quantities that the model predicts. A typical fire experiment can produce hundreds of time histories of point measurements, each of which can be reproduced by the model to some level of accuracy. It is a challenge to sort out all the plots and graphs of all the different quantities and come to some general conclusion. For this reason, this Guide is organized by output quantity, not by individual experiment or fire scenario. In this way, it is possible to assess, over a range of different experiments and scenarios,

the performance of the model in predicting a given quantity. Overall trends and biases become much more clear when the data is organized this way.

1.9 Model Accuracy

The degree of accuracy for each output variable required by the user is highly dependent on the technical issues associated with the analysis. The user must ask: How accurate does the analysis have to be to answer the technical question posed? Thus, a generalized definition of the accuracy required for each quantity with no regard as to the specifics of a particular analysis is not practical and would be limited in its usefulness.

Returning to the earlier definitions of “design” and “reconstruction,” fire scenarios, design applications typically are more accurate because the heat release rate is prescribed rather than predicted, and the initial and boundary conditions are far better characterized. Mathematically, a design calculation is an example of a “well-posed” problem in which the solution of the governing equations is advanced in time starting from a known set of initial conditions and constrained by a known set of boundary conditions. The accuracy of the results is a function of the fidelity of the numerical solution, which is largely dependent on the quality of the model inputs. This CFAST validation guide includes efforts to date involving well-characterized geometries and prescribed fires. These studies show that CFAST predictions vary from being within experimental uncertainty to being about 30 % different than measurements of temperature, heat flux, gas concentration, *etc* (see, for example, reference [5]).

A reconstruction is an example of an “ill-posed” problem because the outcome is known whereas the initial and boundary conditions are not. There is no single, unique solution to the problem. Rather, it is possible to simulate numerous fires that produce the given outcome. There is no right or wrong answer, but rather a small set of plausible fire scenarios that are consistent with the collected evidence and physical laws incorporated into the model. These simulations are then used to demonstrate why the fire behaved as it did based on the current understanding of fire physics incorporated in the model. Most often, the result of the analysis is only qualitative. If there is any quantification at all, it could be in the time to reach critical events, like a roof collapse or room flashover.

1.10 Uses and Limitations of the Model

CFAST has been developed for use in solving practical fire problems in fire protection engineering. It is intended for use in system modeling of building and building components. A priori prediction of flame spread or fire growth on objects is not modeled. Rather, the consequences of a specified fire is estimated. It is not intended for detailed study of flow within a compartment, such as is needed for smoke detector siting. It includes the activation of sprinklers and fire suppression by water droplets.

The most extensive use of the model is in fire and smoke spread in complex buildings. The efficiency and computational speed are inherent in the few computation cells needed for a zone model implementation. The use is for design and reconstruction of time-lines for fire and smoke spread in residential, commercial, and industrial fire applications. Some applications of the model

have been for design of smoke control systems.

- Compartments: CFAST is generally limited to situations where the compartment volumes are strongly stratified. However, in order to facilitate the use of the model for preliminary estimates when a more sophisticated calculation is ultimately needed, there are algorithms for corridor flow, smoke detector activation, and detailed heat conduction through solid boundaries. This model does provide for non-rectangular compartments, although the application is intended to be limited to relatively simple spaces. There is no intent to include complex geometries where a complex flow field is a driving force. For these applications, computational fluid dynamics (CFD) models are appropriate.
- Gas Layers: There are also limitations inherent in the assumption of stratification of the gas layers. The zone model concept, by definition, implies a sharp boundary between the upper and lower layers, whereas in reality, the transition is typically over about 10 % of the height of the compartment and can be larger in weakly stratified flow. For example, a burning cigarette in a normal room is not within the purview of a zone model. While it is possible to make predictions within 5 % of the actual temperatures of the gas layers, this is not the optimum use of the model. It is more properly used to make estimates of fire spread (not flame spread), smoke detection and contamination, and life safety calculations.
- Heat Release Rate: CFAST does not predict fire growth on burning objects. Heat release rate is specified by the user for one or more fire objects. The model does include the ability to limit the specified burning based on available oxygen. There are also limitations inherent in the assumptions used in application of the empirical models. As a general guideline, the heat release should not exceed about 1 MW/m^3 . This is a limitation on the numerical routines attributable to the coupling between gas flow and heat transfer through boundaries (conduction, convection, and radiation). The inherent two-layer assumption is likely to break down well before this limit is reached.
- Radiation: Because the model includes a sophisticated radiation model and ventilation algorithms, it has further use for studying building contamination through the ventilation system, as well as the stack effect and the effect of wind on air circulation in buildings. Radiation from fires is modeled with a simple point source approximation. This limits the accuracy of the model near fire sources. Calculation of radiative exchange between compartments is not modeled.
- Ventilation and Leakage: In a single compartment, the ratio of the area of vents connecting one compartment to another to the volume of the compartment should not exceed roughly $1/2 \text{ m}$. This is a limitation on the plug flow assumption for vents. An important limitation arises from the uncertainty in the scenario specification. For example, leakage in buildings is significant, and this affects flow calculations especially when wind is present and for tall buildings. These effects can overwhelm limitations on accuracy of the implementation of the model. The overall accuracy of the model is closely tied to the specificity, care, and completeness with which the data are provided.
- Thermal Properties: The accuracy of the model predictions is limited by how well the user can specify the thermophysical properties. For example, the fraction of fuel which ends up

as soot has an important effect on the radiation absorption of the gas layer and, therefore, the relative convective versus radiative heating of the layers and walls, which in turn affects the buoyancy and flow. There is a higher level of uncertainty of the predictions if the properties of real materials and real fuels are unknown or difficult to obtain, or the physical processes of combustion, radiation, and heat transfer are more complicated than their mathematical representations in CFAST.

In addition, there are specific limitations and assumptions made in the development of the algorithms. These are detailed in the discussion of each of these sub-models in the NIST Technical Reference Guide [2].

Chapter 2

Software Quality Assurance

This chapter describes the processes used during the development and deployment of the Consolidated Fire and Smoke Transport model (CFAST). This software quality assurance (SQA) plan is intended to guide the planning for modifications to the model, provide required reviews for both software and associated documentation of the model, define testing to be conducted prior to the release of an updated model, describe problem reporting and resolution procedures, and ensure all records, source code, and released software is kept available for the life of the code. While this memorandum and many of our practices follow the Institute of Electrical and Electronics Engineers (IEEE) standard for software quality assurance, IEEE 730-2002 [6], other standards have been followed as well. Most notably, ASTM 1355-05, Standard Guide for Evaluating the Predictive Capability of Deterministic Fire Models [1] has been used extensively to guide the documentation, verification, and validation of the model.

CFAST is intended for use only by those competent in the field of fire safety and is intended only to supplement the informed judgment of the qualified user. The software package is a computer model which has limitations based on the way it is used, and the data used for calculations. All results should be evaluated by a qualified user.

The SQA process and requirements outlined in this chapter apply specifically to the CFAST and is focused on ensuring the quality of the numerical predictions of the model. The user interface that may be used to develop input for the model is included in this process to insure that changes to the model are reflected in the user interface and in the data files created by the user interface for use by the model. Of course, users must ensure that the input files developed for the simulations accurately reflect the desired model inputs, whether developed using the supplied user interface, another third-party interface, or manually input with a spreadsheet or text editor program. Documentation of these inputs is included as part of the model documentation outlined below.

2.1 Relevant Publications

To accompany the model and simplify its use, NIST has developed a Technical Reference Guide [2] and a User's Guide [4] and this Software and Validation Guide. The Technical Reference Guide describes the underlying physical principles and summarizes sensitivity analysis, model validation, and model limitations consistent with ASTM E 1355 [1]. The Users Guide describes how to use the model.

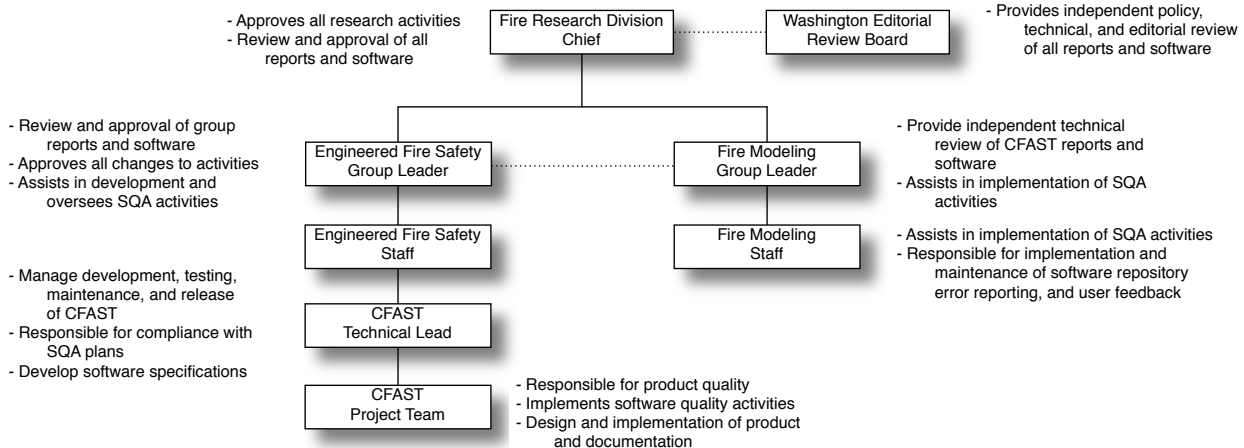


Figure 2.1: CFAST SQA Organization Structure.

The U.S. Nuclear Regulatory Commission has published a verification and validation study of five selected fire models commonly used in support of risk-informed and performance-based fire protection at nuclear power plants [5]. In addition to an extensive study of the CFAST model, the report compares the output of several other models ranging from simple hand calculations to more complex CFD codes such as the Fire Dynamics Simulator (FDS) developed by NIST.

While this document and many of our practices make extensive use of ASTM 1355, Standard Guide for Evaluating the Predictive Capability of Deterministic Fire Models [1] to guide the documentation, verification, and validation of the model, other standards have been followed as well. Most notably, our software quality assurance processes were guided by the IEEE standard for software quality assurance, IEEE 730-2002 [6].

In addition, numerous related documents available at <http://cfast.nist.gov> provide a wealth of information concerning including earlier versions of the model and its user interface. Software quality assurance (SQA) plan is intended to guide the planning for modifications to the model, provide required reviews for both software and associated documentation of the model, define testing to be conducted prior to the release of an updated model, describe problem reporting and resolution procedures, and ensure all records, source code, and ensure released software is kept available for the life of the code.

2.2 Model Management

CFAST is developed and maintained by the Building and Fire Research Laboratory (BFRL) at the National Institute of Standards and Technology (NIST). Like all projects at BFRL, a designated project leader is responsible for directing and prioritizing model development, error correction, and preparation of documentation for the model development. The organization chart in Figure 2.1 provides a graphical representation of the software quality organization structure for CFAST.

Review and approval of software and documentation is part of the standard review process for any report or other product developed by NIST. A minimum of five reviews are required prior to

release of reports or software, including two independent technical peer reviews, two technical and management reviews at the technical workgroup and division level, and a policy review at the NIST-wide level. This review is documented and recorded on the NIST standard form NIST 114 along with official approval notification provided to the primary author of the product.

CFAST is distributed exclusively through a NIST website dedicated to the CFAST model (<http://cfast.nist.gov>). Content of the website is the responsibility of the CFAST project leader and the BFRL webmaster. Additions and changes to the website are made only with the approval of the CFAST project leader after any required NIST reviews.

2.3 SQA Documentation

The released version of CFAST is documented by three primary publications, the Technical Reference Guide[2], the Users Guide [4], and this Software and Model Evaluation Guide. The documents apply to the newest version of the model available on the NIST website. The Technical Reference Guide describes the underlying physical principles, provides a review of model verification and validation efforts by NIST and others, and describes the limitations of the model. The User's Guide describes how to use the model, includes a detailed description of the model inputs and outputs, and provides a process to ensure the correct installation of the model. There are also documents archived on the website that are applicable to older versions of both the model and user interface.

During development of new or corrected features for the model, the following documents are developed:

- *Software Requirements and Design Specifications:* This is an internal memorandum that documents the intended function of a new or enhanced feature, describes its implementation in sufficient detail to allow an independent review of the feature, and identifies any new or existing testing and validation required prior to acceptance of the feature in a release version of the model. This document forms the basis for necessary changes to the technical reference guide and users guide for the model once the new feature is ready for general release. As defined in IEEE 730-2002 [6], this document includes the software requirements specification, software design description, and software verification and validation plan. The level of detail in this document depends on the complexity of the change to the model.
- *Software Validation and Testing Results:* This is an internal memorandum that demonstrates the use of the new feature through appropriate test cases and describes validation and verification tests performed to ensure the new feature is implemented properly without unexpected changes in other features. This document forms the basis for the model verification and validation documentation included as part of this Software and Experimental Validation guide. As defined in IEEE 730-2002 [6], this document includes the software verification and validation report. The level of detail in this document depends on the complexity of the change to the model.

Both of these documents are reviewed internally to NIST by group staff not directly involved with model development. In addition, the NIST review process documents the review and approval of released versions of the model as described above.

Source code for released versions of the model is maintained with version control software that allows tracking of specific changes to the model from version to version. Each version of the model released includes a unique version number that identifies the major and minor version numbers of the release as well as the date of release. Differences with prior versions are documented and provided as part of the release and on the CFAST website so that users can ascertain what effect these changes will have on prior calculations.

2.4 Standards, Practices, Conventions, and Metrics

Prior to final implementation of a new feature or change, a review of the proposed modification is conducted by a developer who is not involved in the modification. This review includes review and concurrence of the software requirements and design specification as well as more detailed review of code changes as the complexity of the modification requires. Review and acceptance of the software requirements and design specification by interested project sponsors or users may be included as appropriate. Name and date of approval and/or review is noted electronically in the document.

Review of the testing and validation report is also conducted by a developer who is not involved in the modification prior to proposed model release. Any significant changes in model output (typically a change greater than 1 % of a given output) should be explained based on changes to the code as a result of a new feature. Name and date of approval and/or review is noted electronically in the document.

2.5 Software Reviews

Software reviews are outlined as part of the standard practices described above. The standard NIST review process includes review of software and documentation prior to any report or product release by NIST.

2.6 Model Testing

Individual testing of model algorithms are made by the developers during any revision of the model. Often, this testing forms the basis for any new standard test cases included with future model releases. System release testing of the model prior to release includes the following:

- Examination of results of test cases specific to any model modifications made as appropriate. Comparison with analytic solutions to simplified problems is desirable when available.
- Examination of results of standard test cases included with the release version of the model. Any changes in the output from prior versions is explained (and documented in the software testing and validation results report) by modifications made to the model.
- For major new releases of the model, a complete suite of test cases should be compared to those from previous versions of the model. At a minimum this includes the set of valida-

tion exercises described in NUREG 1824 [7], but may include additional example cases or validation exercises as appropriate.

2.7 Problem Reporting and Resolution

NIST maintains an e-mail address specifically for inquiries and problem reporting for the CFAST model (cfast@nist.gov). These e-mails are directed to the CFAST project leader for response and resolution as appropriate. Inquiries and responses are catalogued and retained by the project leader.

NIST has developed an automated reporting and resolution tracking website for use with the CFAST model to facilitate tracking and cataloging of inquiries, problems, and model enhancements / revisions. This is included as part of the CFAST website at <http://cfast.nist.gov>

2.8 Tools, Techniques, and Methodologies

NIST will use an automated comparison tool (under development) to compare CFAST predictions between different versions of the model and with experimental data to simplify testing and validation for the CFAST model.

2.9 Media Control

Release versions of the CFAST model are available exclusively on the CFAST specific website maintained by the Building and Fire Research Laboratory (BFRL) at NIST. This website is included in NISTs automated backup and recovery system for computer systems organization wide.

Development versions of the model are maintained by the CFAST project leader. All software and documents are included in NISTs automated backup and recovery system for computer systems organization wide. As part of its model development, NIST maintains a web-based system for version control and history of both the CFAST source code and of pre-release and release executables for the software.

These computer systems are available only to specified personnel, including the CFAST project leader and project team members.

2.10 Supplier Control

CFAST is entirely a product of BFRL / NIST and as such does not include any commercial software libraries. The differential equation solver used by CFAST, DASSL, is a publicly available software package. Full source code for the solver as used by CFAST is maintained under version control with the rest of the model code.

BFRL currently uses Microsoft Visual Studio 2010 and Intel Fortran XE 2011 for development¹. Prior to any change to a different development system, a full test suite of test cases are

¹Certain commercial entities, equipment, or materials may be identified in this document in order to describe an experimental procedure or concept adequately. Such identification is not intended to imply recommendation or endorsement by the National Institute of Standards and Technology, nor is it intended to imply that the entities,

compared to verify consistent operation of the model and model results.

2.11 Records Collection, Maintenance, and Retention

All software, documentation, and SQA documents are retained by the CFAST project leader, typically in electronic form. Software and documentation is also maintained and archived on the NIST CFAST website as part of the version control software for the model.

BFRL management approval is required prior to destruction of old or out-of-date records. Records are typically maintained for a minimum of 25 years.

2.12 Training

No specific training is identified for use of this SQAP. Details of training requirements for use of the model included in the CFAST users guide is applicable to developers of the model as well.

2.13 Risk Management

The primary risk management tool for software developed and released by NIST is the official NIST review process for software, documents, and other products of NIST. Official approval is required prior to release of the model for general use.

materials, or equipment are necessarily the best available for the purpose.

Chapter 3

Software Structure and Robustness

The mathematical and numerical robustness of a deterministic computer model depends upon three issues: the code must be transparent so that it can be understood and modified by visual inspection; it must be possible to check and verify with automated tools; and there must be a method for checking the correctness of the solution, at least for asymptotic (steady state) solutions (numerical stability and agreement with known solutions). In order to understand the meaning of accuracy and robustness, it is necessary to understand the means by which the numerical routines are structured. In this chapter, details of the implementation of the model are presented, including the tests used to assess the numerical aspects of the model. These include:

- the structure of the model, including the major routines implementing the various physical phenomena included in the model,
- the organization of data initialization and data input used by the model,
- the structure of data used to formulate the differential equations solved by the model,
- a summary of the main control routines in the model that are used to control all input and output, initialize the model and solve the appropriate differential equation set for the problem to be solved,
- the means by which the computer code is checked for consistency and correctness,
- analysis of the numerical implementation for stability and error propagation, and
- comparison of the results of the system model with simple analytical or numerical solutions.

3.1 Structure of the Numerical Routines

A methodology which is critical to verification of the model is the schema used to incorporate physical phenomena. This is the subroutine structure discussed below. The method for incorporating new phenomena and ensuring the correctness of the code was adopted as part of the consolidation of CCFM and FAST. This consolidation occurred in 1990 and has resulted in a more transparent, transportable and verifiable numerical model. This transparency is crucial to a verifiable and robust

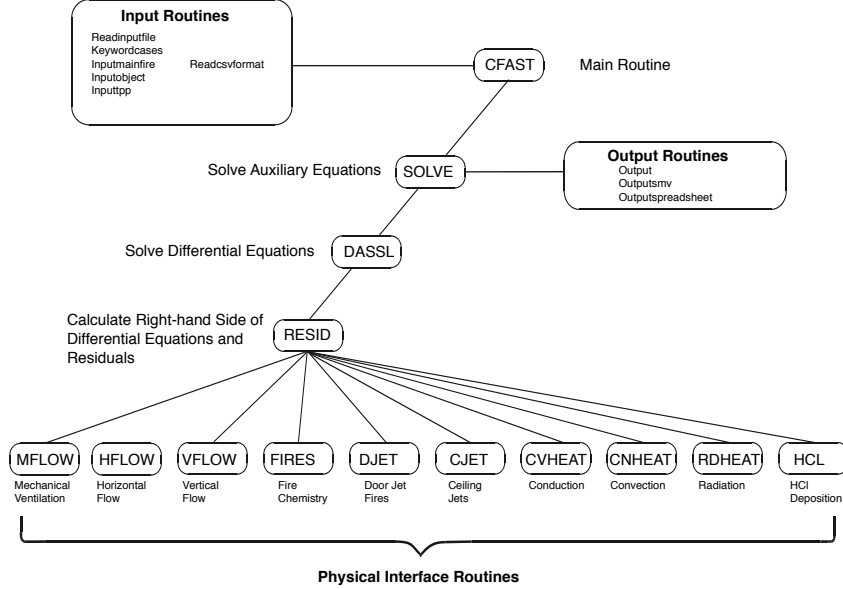


Figure 3.1: Subroutine structure for the CFAST model showing major routines and calling structure.

numerical implementation of the predictive model as discussed in the sections on code checking and numerical analysis.

The model can be split into distinct parts. There are routines for reading data, calculating results and reporting the results to a file or printer. The major routines for performing these functions are identified in figure 3.1. These physical interface routines link the CFAST model to the actual routines which calculate quantities such as mass or energy flow at one particular point in time for a given environment.

The routines SOLVE, RESID and DASSL are the key to understanding how the physical equations are solved. SOLVE is the control program that oversees the general solution of the problem. It invokes the differential equation solver DASSL [8] which in turn calls RESID to solve the transport equations. Given a solution at time t , what is the solution at time t plus a small increment of time, Δt ? The differential equations are of the form

$$\begin{aligned} \frac{dy}{dx} &= f(y, t) \\ y(t_0) &= y_0 \end{aligned} \tag{3.1}$$

where y is a vector representing pressure, layer height, mass and such, and f is a vector function that represents changes in these values with respect to time. The term y_0 is an initial condition at the initial time t_0 . The time increment is determined dynamically by the program to ensure convergence of the solution at $t + \Delta t$. The subroutine RESID computes the right hand side of eq 3.1 and returns a set of residuals of that calculation to be compared to the values expected by DASSL. DASSL then checks for convergence. Once DASSL reaches an error limit (defined as convergence of the equations) for the solution at $t + \Delta t$, SOLVE then advances the solution

of species concentration, wall temperature profiles, and mechanical ventilation for the same time interval. Note that there are several distinct time scales that are involved in the solution of this type of problem. The fastest will be chemical kinetics. In CFAST, chemical reactions are assumed to be instantaneous so we ignore the impact of chemical kinetics. The next larger time scale is that associated with the flow field. These are the equations which are cast into the form of ordinary differential equations. Then there is the time scale for mechanical ventilation, and finally, heat conduction through objects.

Chemical kinetic times are typically on the order of milliseconds. The transport time scale are on the order of 0.1 s. The mechanical ventilation and conduction time scales are typically several seconds, or even longer. The time step is dynamically adjusted to a value appropriate for the solution of the currently defined equation set. In addition to allowing a more correct solution to the pressure equation, very large time steps are possible if the problem being solved approaches steady-state.

3.2 Comparison with Analytic Solutions

Certain CFAST sub-models address phenomena that have analytical solutions, for example, one dimensional heat conduction through a solid or pressure increase in a sealed or slightly leaky compartment as a result of a fire or fan. The developers of CFAST use analytical solutions to test sub-models to verify the correctness of the coding of the model as part of the development. Such verification efforts are relatively simple and the results may not always be published or included in the documentation. Two additional types of verification are possible. The first type, discussed in Section 3, Theoretical Basis, involves validating individual algorithms against experimental work. The second involves simple experiments, especially for conduction and radiation, for which the results are asymptotic (e.g., a simple single-compartment test case with no fire, all temperatures should equilibrate asymptotically to a single value). Such comparisons are common and not usually published.

3.3 Code Checking

Two standard programs have been used to check the CFAST model structure and language. Specifically, FLINT and LINT have been applied to the entire model to verify the correctness of the interface, undefined or incorrectly defined (or used) variables and constants, and completeness of loops and threads.

The CFAST code has also been checked by compiling and running the model on a variety of computer platforms. Because FORTRAN and C are implemented differently for various computers, this represents both a numerical check as well as a syntactic check. CFAST has been compiled for Sun (Solaris), SGI (Irix), Microsoft Windows-based PCs (Lahey, Digital, and Intel FORTRAN), and Concurrent computer platforms. Within the precision afforded by the various hardware implementations, the model outputs are identical on the different platforms.¹

¹Typically an error limit of one part in 10^6 which is the limit set for the differential equation solver in the solution of the CFAST equations

The CFAST Technical Reference Guide [2] contains a detailed description of the CFAST subroutine structure and interactions between the subroutines.

3.4 Numerical Tests

CFAST is designed to use 64-bit precision for real number calculations to minimize the effects of numerical error.

The differential and algebraic equation solver (called DASSL) has been tested for a variety of differential equations and is widely used and accepted [8]. The radiation and conduction routines have also been tested against known solutions for asymptotic results [9].

Coupling between the physical algorithms of the model and the differential equation solver also works to ensure numerical accuracy by dynamically adjusting the time step used by the model to advance the solutions of the equation set. Solution tolerances are set to require solution of the model equations within one part in 10^6 . This ensures that the error attributable to numerical solution is far less than that associated with the model assumptions.

Chapter 4

Survey of Past Validation Work

CFAST has been subjected to extensive validation studies by NIST and others. There are two ways of comparing predictive capability with actual events. The first is simply graphing the time series curves of model results with measured values of variables such as temperature. Another approach is to consider the time to critical conditions such as flashover. Making such direct comparisons between theory and experiment provides a sense of whether predictions are reasonable. This chapter provides a review of CFAST validation efforts by NIST and others to better understand the quality of the predictions by the model.

Some of the work has been performed at NIST, some by its grantees and some by engineering firms using the model. Because each organization has its own reasons for validating the model, the referenced papers and reports do not follow any particular guidelines. Some of the works only provide a qualitative assessment of the model, concluding that the model agreement with a particular experiment is “good” or “reasonable.” Sometimes, the conclusion is that the model works well in certain cases, not as well in others. These studies are included in the survey because the references are useful to other model users who may have a similar application and are interested in qualitative assessment. It is important to note that some of the papers point out flaws in early releases of CFAST that have been corrected or improved in more recent releases. Some of the issues raised, however, are still subjects of active research. Continued updates for CFAST are greatly influenced by the feedback provided by users, often through publication of validation efforts.

4.1 Comparisons with Full-Scale Tests Conducted Specifically for the Chosen Evaluation

Several studies have been conducted specifically to validate the use of CFAST in building performance design. Dembsey [10] used CFAST version 3.1 to predict the ceiling jet temperatures, surface heat fluxes and heat transfer coefficients for twenty compartment fire experiments in a compartment that is similar in size, geometry, and construction to the standard fire test compartment specified in the Uniform Building Code [11]¹. Results from 330 kW, 630 kW, and 980 kW fires were used. In general, CFAST made predictions which were higher than the experimental

¹The 1997 Uniform Building Code has been superceded by the International Building Code, 2003 Edition, International Code Council, Country Club Hills, Illinois.

results. In these cases, the temperature prediction is typically 20 % to 30 % higher than measured values. Much of this can be attributed to not knowing the species production (soot) and relative absorption of radiation by the gas layers which highlights the importance of scenario specification. This is the most common cause of over prediction of temperature by CFAST. A secondary source of discrepancy is correcting for radiation from thermocouple beads. The authors provide for this correction, but the corrections cited are not as large as has been reported in other fire experiments [12].

He et al. [13] describe a series of full-scale fire experiments that were designed to investigate the validity of two zone models including CFAST version 3.1. The experiments, involving steady state burning rates and a number of ventilation conditions, were conducted in a four-story building. Temperature, pressure, flow velocity, smoke density and species concentrations were measured in various parts of the building. The stack effect and its influence on temperature distribution in a stair shaft were observed. Comparisons were then made between the experimental results and the model predictions. Early in the fire there is a few percent difference² between the predictions and measurements; beyond 10 min, there are significant variations. Both the experiment and the model are internally consistent; that is, higher flow leads to a higher interface height (figure 13 in the paper). Once again, the difference is about 25 %. The authors discuss the effect of fuel composition and correction for radiation from thermocouple beads but did not draw firm conclusions based on their measurements of fuel products.

A series of experimental results for flaming fires, obtained using realistic fires in a prototype apartment building were performed by Luo et al. [14]. Fuel configurations in the fire test included a horizontal plain polyurethane slab, mock-up chair (polyurethane slabs plus a cotton linen cover), and a commercial chair. CFAST version 3.1 typically over-predicted upper layer temperatures by 10 % to 50 % depending on the test conditions and measurement location in that test. The predicted and experimental time dependent upper layer temperatures were similar in shape. The time to obtain peak upper layer temperatures was typically predicted to within 15 % of the experimental measurements. The authors concluded that CFAST was conservative in terms of life safety calculations.

In order to optimize fire service training facilities, the best use of resources is imperative. The work reported by Poole et al. [15] represents one aspect of a cooperative project between the city of Kitchener Fire Department (Canada) and the University of Waterloo aimed at developing design criteria for the construction of a fire fighter training facility. One particular criterion is that realistic training with respect to temperature, heat release and stratification be provided in such a facility. The purpose of this paper was to compare existing analytical heat release and upper and lower gas temperature rise correlations and models with data from actual structures which were instrumented and burned in collaboration with the Kitchener Fire Department. According to the authors, the CFAST model was used ‘successfully’ to predict these conditions and will be used in future design of such facilities.

A report by Bailey et al. [16] compares predictions by CFAST version 3.1 to data from real scale fire tests conducted onboard ex-USS SHADWELL, the Navy’s R&D damage control platform. The phenomenon of particular interest in this validation series was the conduction of heat in the vertical direction through compartment ceilings and floors. As part of this work, Bailey et al. [17] compared CFAST temperature predictions on the unexposed walls of large metal

²Unless otherwise noted, percent differences are defined as (model-experiment)/experiment x100.

boxes, driven by steady state fires. This tested the model's prediction of radiation and conduction in both the vertical and horizontal directions. Indirectly it quantifies the quality of the conduction/convection/radiation models. The model and experiment compared well within measurement error bounds of each. The comparison was particularly good for measurements in the fire compartment as well as for the compartment and deck directly above it, with predictions typically agreeing with experiments within measurement uncertainty. The model under-predicted the temperatures of the compartments and decks not directly adjacent to the fire compartment early in the tests. Most of the error arose due to uncertainty in modeling the details of the experiment. The size of the vent openings between decks and to the outside must be included, but these were not always known. Cracks formed in the deck between the fire compartment and the compartment above due to the intense fire in the room of origin, but a time dependent record was not kept. The total size of the openings to the outside of warped doors in both compartments was not recorded. As can be seen in figures 7 and 8 of reference [16], the steady state predictions are identical (within error bounds of the experiment and prediction). The largest error is after ignition (uncertainty in the initial fire) and during development of the cracks between the compartments. While this does not affect the agreement in the room of origin, it does lead to an uncertainty of about 30 % in the adjacent compartment.

4.2 Comparisons with Previously Published Test Data

A number of researchers have studied the level of agreement between computer fire models and real-scale fires. These comparisons fall into two broad categories: fire reconstruction and comparison with laboratory experiments. Both categories provide a level of verification for the models used. Fire reconstruction, although often more qualitative, provides a higher degree of confidence for the user when the models successfully simulate real-life conditions. Comparisons with laboratory experiments, however, can yield detailed comparisons that can point out weaknesses in the individual phenomena included in the models.

Deal [18] reviewed four computer fire models (CCFM [19], FIRST [20], FPETOOL [21] and FAST [22] version 18.5 (the immediate predecessor to CFAST)) to ascertain the relative performance of the models in simulating fire experiments in a small room (about 12 m³ in volume) in which the vent and fuel effects were varied. Peak fire size in the experiments ranged up to 800 kW. According to the author, all the models simulated the experimental conditions including temperature, species generation, and vent flows 'quite satisfactorily.' With a variety of conditions, including narrow and normal vent widths, plastic and wood fuels, and flashover and sub-flashover fire temperatures, competence of the models at these room geometries was 'demonstrated.'

4.2.1 Fire Plumes

Davis compared predictions by CFAST version 5 (and other models) for high ceiling spaces [23]. In this paper, the predictive capability of two algorithms designed to calculate plume centerline temperature and maximum ceiling jet temperature in the presence of a hot upper layer were compared to measurements from experiments and to predictions using CFASTs ceiling jet algorithm. The experiments included ceiling heights of 0.58 m to 22 m and heat release rates of 0.62 kW to 33 MW. When compared to the experimental results CFASTs ceiling jet algorithm tended to

over-predict the upper layer temperature by 20 %. With proper adjustment for radiation effects in the thermocouple measurements, some of this difference disappears. The effect of entrainment of the upper layer gases was identified for improvement.

4.2.2 Multiple Compartments

Jones and Peacock [24] presented a limited set of comparisons between the FAST model (version 18.5) and a multi-room fire test. The experiment involved a constant fire of about 100 kW in a three-compartment configuration of about 100 m³. They observed that the model predicted an upper layer temperature that was too high by about 20 % with satisfactory prediction of the layer interface position. These observations were made before the work of Pitts et al. [12] showed that the thermocouple measurements need to be corrected for radiation effects. Convective heating and plume entrainment were seen to limit the accuracy of the predictions. A comparison of predicted and measured pressures in the rooms showed within 20 %. Since pressure is the driving force for flow between compartments, this agreement was seen as important.

Levine and Nelson [25] used a combination of full-scale fire testing and modeling to simulate a fire in a residence. The 1987 fire in a first-floor kitchen resulted in the deaths of three persons in an upstairs bedroom, one with a reported blood carboxyhemoglobin content of 91 %. Considerable physical evidence remained. The fire was successfully simulated at full scale in a fully-instrumented seven-room two-story test structure. The data collected during the test have been used to test the predictive abilities of two multiroom computer fire models: FAST and HARVARD VI. A coherent ceiling layer flow occurred during the full-scale test and quickly carried high concentrations of carbon monoxide to remote compartments. Such flow is not directly accounted for in either computer code. However, both codes predicted the carbon monoxide buildup in the room most remote from the fire. Prediction of the pre-flashover temperature rise was also ‘good’ according to the authors. Prediction of temperatures after flashover that occurred in the room of fire origin was seen as ‘less good.’ Other predictions of conditions throughout the seven test rooms varied from ‘good approximations’ to ‘significant deviations’ from test data. Some of these deviations are believed to be due to combustion chemistry in the not upper layer not considered in detail in either of the two models.

4.2.3 Large Compartments

Duong [26] studied the predictions of several computer fire models (CCFM, FAST, FIRST, and BRI [27]), comparing the models with one another and with large fires (4 MW to 36 MW) in an aircraft hanger (60 000 m³). For the 4 MW fire size, he concluded that all the models are ‘reasonably accurate.’ At 36 MW, however, ‘none of the models did well.’ Limitations of the heat conduction and plume entrainment algorithms were thought to account for some of the inaccuracies.

4.2.4 Prediction of Flashover

A chaotic event that can be predicted by mathematical modeling is that of flashover. Flashover is the common term used for the transition a fire makes from a few objects pyrolyzing to full room involvement. It is of interest to the fire service because of the danger to fire fighters and to building

designers because of life safety and the attendant impact on occupants. Several papers have looked at the capability of CFAST to predict the conditions under which flashover can occur.

Chow [28] concluded that FAST correctly predicted the onset of flashover if the appropriate criteria were used. The criteria were gas temperature near the ceiling, heat flux at the floor level and flames coming out of the openings. This analysis was based on a series of compartment fires.

A paper by Luo et al. [29] presents a comparison of the results from CFAST version 3 against a comprehensive set of data obtained from one flashover fire experiment. The experimental results were obtained from a full-scale prototype apartment building under flashover conditions. Three polyurethane mattresses were used as fuel. It was found that the predicted temperatures from the CFAST fire model agreed well with the experimental results in most areas, once radiation corrections are applied to the thermocouple data.

Collier [30] makes an attempt to quantify the fire hazards associated with a typical New Zealand dwelling with a series of experiments. These tests, done in a three-bedroom dwelling, included both non-flashover and flashover fires. The predictions by CFAST version 2 were seen by the author as consistent with the experiments within the uncertainty of each.

Post-flashover fires in shipboard spaces have a pronounced effects on adjacent spaces due to highly conductive boundaries. CFAST (version 3.1) predictions for the gas temperature and the cold wall temperature were compared with shipboard fires [31]. The comparisons between the model and experimental data show ‘conservative predictions’ according to the authors. The authors attribute this to an overestimation of the average hot wall temperature and an underestimation of external convective losses due to wind effects.

Finally, a comparison of CFAST with a number of simple correlations was used by Peacock and Babrauskas [32, 33] to simulate a range of geometries and fire conditions to predict the development of the fire up to the point of flashover. The simulations represent a range of compartment sizes and ceiling heights. Both the correlations and CFAST predictions were seen to provide a lower bound to observed occurrence of flashover. For very small or very large compartment openings, the differences between the correlations, experimental data, and CFAST predictions was more pronounced.

The important test of all these prediction methods is in the comparison of the predictions with actual fire observations. Figure 4.1 (reference [33]) presents estimates of the energy required to achieve flashover for a range of room and vent sizes. This figure is an extension of the earlier work of Babrauskas [34] and includes additional experimental measurements from a variety of sources, most notably the work of Deal and Beyler [35]. For a number of the experimental observations, values are included that were not explicitly identified as being a minimum value at flashover. In addition, figure 4.1 includes predictions from the CFAST model (version 5).

As with some of the experimental data defining flashover as an upper layer temperature reaching 600 °C, many experimental measures were reported as peak values rather than minimum values necessary to achieve flashover. Thus, ideally all the predictions should provide a lower bound for the experimental data. Indeed, this is consistent with the graph the vast majority of the experimental observations lie above the correlations and model predictions. For a considerable range in the ratio $A_T/A\sqrt{h}$, the correlations of Babrauskas [34] Thomas [36], and the MQH correlation of McCaffrey et al. [37] provide similar estimates of the minimum energy required to produce flashover. The estimates of Hägglund [38] yields somewhat higher estimates for values of $A_T/A\sqrt{h}$ greater than $20 \text{ m}^{-1/2}$.

The results from the CFAST model for this single compartment scenario provide similar results

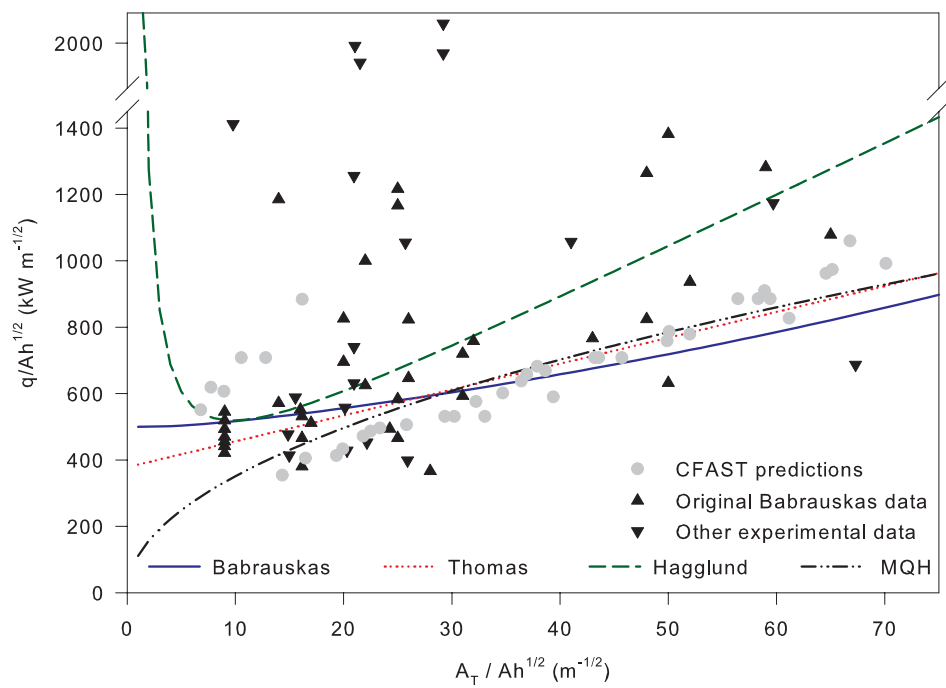


Figure 4.1: Comparison of correlations, CFAST predictions, and experimental data for the prediction of flashover in a compartment fire.

to the experiments and the correlations for most of the range of $A_T/A\sqrt{h}$. For small values of $A_T/A\sqrt{h}$, the CFAST values rise somewhat above the values from the correlations. These small values of $A_T/A\sqrt{h}$ result from either very small compartments (small A_T) or very large openings (large $A_T/A\sqrt{h}$), both of which stretch the limits of the assumptions inherent in the model. For very small compartments, radiation from the fire to the compartment surfaces becomes more important, enhancing the conductive heat losses through the walls. However, the basic two-zone assumption may break down as the room becomes very small. For very large openings, the calculation of vent flow via an orifice flow coefficient approach is likely inaccurate. Indeed, for such openings, this limitation has been observed experimentally [34]. The estimates are close to the range of uncertainty shown by the correlations which also diverge at very small values of $A_T/A\sqrt{h}$.

Perhaps most significant in these comparisons is that all the simple correlations provide estimates similar to the CFAST model and all the models are consistent with a wide range of experimental data. For this simple scenario, little is gained with the use of the more complex models. For more complicated scenarios, the comparison may not be as simple.

4.3 Comparison with Documented Fire Experience

There are numerous cases of CFAST being used to adjudicate legal disputes. Since these are discussed in courts of law, there is a great deal of scrutiny of the modeling, assumptions, and results. Most of these simulations and comparisons are not available in the public literature. A few of the cases which are available are discussed below. The metric for how well the model performed is its ability to reproduce the time-line as observed by witnesses and the death of occupants or the destruction of property as was used in evidence in legal proceedings.

As mentioned in section 4.2.2, Levine and Nelson describe the use of FAST for understanding the deaths of two adults in a residence in Sharon, Pennsylvania in 1987 [25]. The paper compared the evidence of the actual fire, a full scale mockup done at NIST and the results from FAST (version 18) [39] and Harvard VI [40]. The most notable shortcoming of the models was the lower than actual temperatures in the bedrooms, caused by loss of heat through the fire barriers. This led to the improvement in CFAST in the mid-90s to couple compartments together so that both horizontal and vertical heat transfer can occur to adjacent compartments.

Bukowski used CFAST version 3.1 to analyze a fire in New York City [41] in 1994 which resulted in the death of three fire fighters. The CFAST model was able to reproduce the observed conditions and supported the theory as to how the fire began and the cause of death of the three fire fighters.

Chow describes the use and comparison of CFAST simulations with a 1996 high rise building fire in Hong Kong [42]. CFAST simulations were performed to help understand the probable fire environment under different conditions. Three simulations were performed to study the consequences of a fire starting in the lift shaft. Smoke flow in the simulations qualitatively matched those observed during the incident.

In the early morning hours of March 25, 1990 a tragic fire took the lives of 87 persons at a neighborhood club in the Bronx, New York [43]. The New York City Fire Department requested the assistance of the NIST Center for Fire Research (CFR) in understanding the factors which contributed to this high death toll and to develop a strategy that might reduce the risk of a similar occurrence in the many similar clubs operating in the city. The simulation showed the potential for

development of untenable conditions within the club and particularly in the single exit stairway.

4.4 Comparison with Experiments Which Cover Special Situations

There are several sets of comparisons used in the development of the model or specific applications beyond those discussed more generally above.

4.4.1 Nuclear Facilities

Floyd validated CFAST version 3.1 by comparing the modeling results with measurements from fire tests at the Heiss-Dampf Reaktor (HDR) facility [44]. The structure was originally the containment building for a nuclear power reactor in Germany. The cylindrical structure was 20 m in diameter and 50 m in height topped by a hemispherical dome 10 m in radius. The building was divided into eight levels. The total volume of the building was approximately 11 000 m³. From 1984 to 1991, four fire test series were performed within the HDR facility. The T51 test series consisted of 11 propane gas tests and three wood crib tests. To avoid permanent damage to the test facility, a special set of test rooms were constructed, consisting of a fire room with a narrow door, a long corridor wrapping around the reactor vessel shield wall, and a curtained area centered beneath a maintenance hatch. The fire room walls were lined with fire brick. The doorway and corridor walls had the same construction as the test chamber. Six gas burners were mounted in the fire room. The fuel source was propane gas mixed with 10 % air fed at a constant rate to one of the six burners.

In general, the comparison between CFAST and the HDR results was seen as ‘good’ by the author, with two exceptions. The first is the over estimate of the temperature of the upper layer, typically within about 15 % of the experimental measurements. This is common and generally results from using too low a value for the production of soot, water (hydrogen) and carbon monoxide. The other exception consists of predictions in spaces where the zone model concept breaks down, for example in the stairways between levels. In this case, CFAST has to treat the space either in the filling mode (two layer approximation) or as a fully mixed zone (using the SHAFT option). Neither is quite correct, and in order to understand the condition in such spaces in detail (beyond the transfer of mass and energy), a more detailed CFD model must be used, for example, FDS [45].

The U.S. Nuclear Regulatory Commission performed an extensive verification and validation of several fire models commonly used in nuclear power plant applications [7]. These models included simple spreadsheet calculations, zone models (including CFAST [5]), and CFD models. The results of this study are presented in the form of relative differences between fire model predictions and experimental data for fire modeling attributes such as temperature or heat flux that are important to NPP fire modeling applications. These relative differences are affected by the capabilities of the models, the availability of accurate applicable experimental data, and the experimental uncertainty of these data. Evaluation of the two-zone models showed that the models simulated the experimental results within experimental uncertainty for many of the parameters of interest. The reason for this may be that the relatively simple experimental configurations selected for this study

conform well to the simple two-layer assumption that is the basis of these models.

While the relative differences sometimes show agreement for many parameters, they also show both under-prediction and over-prediction in some circumstances, most notably when conditions vary within a compartment or detailed local conditions are important to accurate prediction (for example, plume temperature or heat flux near to the fire source). The results and comparisons included the the NRC study are included in this report for the current version of CFAST.

4.4.2 Small Scale Testing

As an implementation of the zone model concept, CFAST is applicable to a wide range of scenarios. One end of this spectrum are small compartments, one to two meters on a side. Several research efforts have looked at small scale validation. There are three papers by Chow [46, 47, 48] which examine this issue. The first is the use of an electric heater with adjustable thermal power output was to verify temperature predictions by CFAST version 3.1. The second was closed chamber fires studied by burning four types of organic liquids, namely ethanol, N-heptane, and kerosene. The burning behavior of the liquids was observed, and the hot gas temperature measured. These behaviors along with the transient variations of the temperature were then compared with those predicted by the CFAST model. Finally, in another series of experiments, three zone models, one of which was CFAST, were evaluated experimentally using a small fire chamber. Once again, liquid fires were chosen for having better control on the mass loss rate. The results on the development of smoke layer and the hot gas temperature predicted by the three models were compared with those measured experimentally. According to Chow, ‘fairly good agreement’ was found if the input parameters were carefully chosen.

4.4.3 Unusual Geometry and Specific Algorithms

A zone model is inherently a volume calculation. There is an assumption in the derivation of the equations that gas layers are strongly stratified. This allows for the usual interpretation that a volume can then be thought of as a rectangular parallelepiped, which allows the developers to express the volume in terms of a floor area and height of a compartment, saying simply that the height times the floor area is the volume. However, there are other geometries which can be adequately described by zone models. Tunnels, ships, and attics are the most common areas of application which fall outside of the usual scope.

Railway and Vehicle Tunnels

Altinakar et al. [49] used a *modified version* of CFAST for predicting fire development and smoke propagation in vehicle or railroad tunnels. The two major modifications made to the model dealt with mixing between the upper and lower layers and friction losses along the tunnel. The model was tested by simulating several full-scale tests carried out at memorial Tunnel Ventilation Test Program in West Virginia, and the Offeneg Tunnel in Switzerland. His article compares simulated values of temperature, opacity and similar sensible quantities with measured values and discusses the limits of the applicability of zone models for simulating fire and smoke propagation in vehicle and railroad tunnels.

Peacock et al. [50] compared times to untenable conditions determined from tests in a passenger rail car with those predicted by CFAST for the same car geometry and fire scenarios. For a range of fire sizes and growth rates, they found agreement that averaged approximately 13 %.

Non-Uniform Compartments

In January 1996, the U.S. Navy began testing how the CFAST model would perform when tasked with predicting shipboard fires. These conditions include mass transport through vertical vents (representing hatches and scuttles), energy transport via conduction through decks, improvement to the radiation transport sub-model, and geometry peculiar to combat ships. The purpose of this study was to identify CFAST limitations and develop methods for circumnavigating these problems [51]. A retired ship representing the forward half of a USS Los Angeles class submarine was used during this test. Compartments in combat ships are not square in floor area, nor do they have parallel sides.

Application of CFAST to these scenarios required a direct integration of compartment cross-sectional area as a function of height to correctly interpret the layer interface position and provide correct predictions for flow through doors and windows (vertical vents). This required user specification of the area as a function of height (ROOMA and ROOMH inputs) to provide a description for the model to use. For most applications of CFAST, the effort required for the input outweighs any additional precision in the calculated results gained by use of the ROOMA and ROOMH inputs in the model.

Long Corridors

Prior to development of the corridor flow model, the implementation of flow in compartments assumed that smoke traveled instantly from one side of a compartment to another. The work of Bailey et al. [52] provided the basis for the corridor flow model in CFAST. According to the author, it shows ‘good agreement’ for the delay time calculated using CFAST version 5 and measured flow along high aspect ratio passageways.

Mechanical Ventilation

There have been two papers which have looked at the effectiveness of the mechanical ventilation system. The first considered a fire chamber of length 4.0 m, width 3.0 m and height 2.8 m with adjustable ventilation rates [53]. Burning tests were carried out with wood cribs and methanol to study the preflashover stage of a compartmental fire and the effect of ventilation. The mass loss rate of fuel, temperature distribution of the compartment and the air intake rate were measured. The heat release rates of the fuel were calculated and the smoke temperature was used as a validation parameter. A scoring system was proposed to compare the results predicted by the three models. According to the author, CFAST does ‘particularly well,’ though there are some differences which can be attributed to the zone model approach.

A second series of experiments by Luo [54] indicate that the CFAST model (version 3.1) generally over predicts the upper layer temperature in the burn room because the two-zone assumption is likely to break down in the burn room. It was found that the room averaged temperatures obtained from CFAST were in ‘good overall agreement’ with the experimental results. The discrepancies

can be attributed to the correction needed for thermocouple measurements. The CO concentration, however, was inconsistent. CFAST tended to overestimate CO concentration when the air handling system was in operation. This was seen due to inconsistencies in what is measured (point measurements) and predicted (global measurements).

Sprinkler Activation

A suppression algorithm [55] was incorporated into CFAST. Chow [56] evaluates the predictive capability for a sprinkler installed in an atrium roof. There were three main points being considered: the possibility of activating the sprinkler, thermal response, and water requirement. The zone model CFAST was used to analyze the possibility of activation of a sprinkler head. Results derived from CFAST were seen to be ‘accurate, that is, providing good agreement with experimental measurements.’

t^2 Fires

Matsuyama conducted a series of full-scale experiments [57] using t^2 fires. Fire room and corridor smoke filling processes were measured. The size of the corridors and arrangements of smoke curtains were varied in several patterns. Comparisons were then made between the experimental results and those predicted by CFAST. The author concludes that while the model does a ‘good job’ of predicting experimental results, there are systematic differences which could be reduced with some revision to zone model formulation to include the impact of smoke curtains.

Chapter 5

Description of Experiments

This chapter summarizes the range of experiments used in the current evaluation for the CFAST model. This study focused on the predicted results of the CFAST fire model and did not include an assessment of the user interface for the model. However, all input files used for the simulations were prepared using the CFAST graphical user interface (GUI) and reviewed for correctness prior to the simulations. The comparisons between the experiments and model predictions were characterized as semi-blind calculations, i.e., the modelers were given detailed descriptions of the test conditions, test geometry, and fire source, but did not modify model inputs from these given conditions to improve model predictions. As such, the comparisons in this report provide an assessment of the predictive capability of the model, but not an assessment of the ability of different modelers to develop appropriate model inputs.

5.1 ATF Corridors Experiments

A series of eighteen experiments were conducted in a two-story structure with long hallways and a connecting stairway in the large burn room of the ATF Fire Research Laboratory in Ammendale, Maryland, in 2008 [58]. The test enclosure consisted of two 17.0 m long hallways connected by a stairway consisting of two staircases and an intermediary landing. There was a door at the opposite end of the first floor hallway, which was closed during all tests. The end of the second floor hallway was open with a soffit near the ceiling.

The walls and ceilings of the test structure were constructed of 1.2 cm gypsum wallboard. The flooring throughout the structure, including the stairwell landing floor, consisted of one layer of 1.3 cm thick cement board on one layer of 1.9 cm thick plywood supported by wood joists. The first set of stairs, which had eight risers, led from the first floor up to the landing area. The second set of stairs, which had nine risers, led from the landing area up to the second floor. The stairs were constructed of 2.5 cm thick clear pine lumber. The two set of stairs were separated by an approximately 0.42 m wide gap in the middle of the stairwell. This gap was separated from the stairs by a 0.91 m tall barrier constructed of a single piece of gypsum board. The flue space was open to the first floor. The flue space was separated from the second floor by a 0.9 m tall barrier constructed of gypsum board. There was a metal exterior type door at the end of the first floor near the burner. The door was closed during all experiments.

The fire source was a natural gas diffusion burner. The burner surface was horizontal, square

and 0.45 m on each side, its surface was 0.37 m above the floor, and it was filled with gravel. The burner was located near the end of the first floor away from the stairs. A diagram of the test structure is displayed in Figure 5.1.

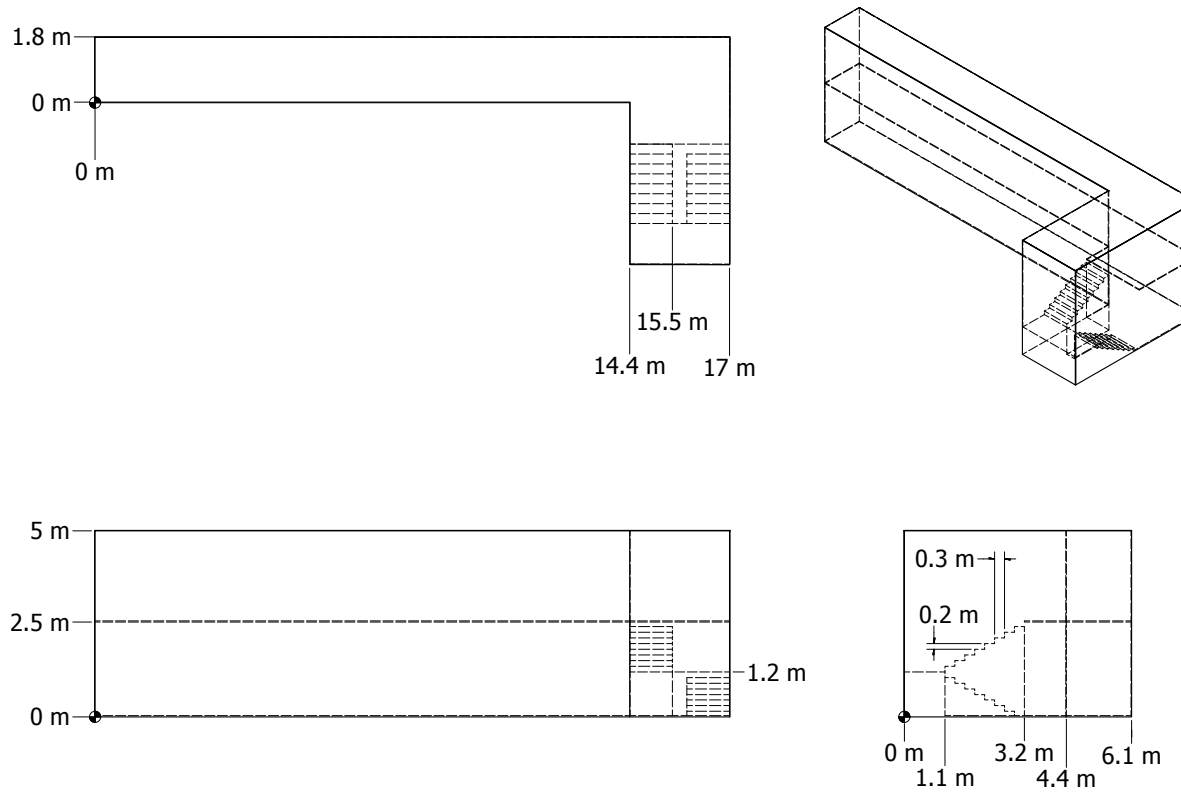


Figure 5.1: Geometry of the ATF Corridors Experiments.

5.2 FM Four Room Including Corridor Test Series

This data set describes a series of tests conducted in a multiple room configuration with more complex gas burner fires than the previous data set. This study [59] was included because, in many ways, it is similar to the smoke movement study performed at NBS [60], and permits comparisons between two different laboratories. In addition, it expands upon that data set by providing larger a time-varying gas burner fires in a room-corridor configuration. Fire size was about up to 1 MW with a total volume of 200 m³.

This study was performed to collect data allowing for variations in fire source, ventilation, and geometry in a multi-compartment structure, especially for situations with closed doors. This test program was carried out at Factory Mutual Research Corporation (FMRC) in West Gloucester, RI, in which 60 fire experiments were conducted in a multiple-room enclosure to furnish validation data for theoretical fire models.

Figure 5.2 shows a diagram of the basic facility with indications of instrumentation location. The facility was built on the floor of FMRC's fire test building, using part of the 67 m by 76 m test building where the ceiling height is 18.3 m. The layout in figure 25 shows a burn room and two target rooms connected to a corridor. The corridor was 2.43 m wide x 18.89 m long x 2.43 m high. The burn room measured 3.63 m deep x 3.64 m wide x 2.45 m high; a sealable window opening, measuring 0.85 m square, was centered on the rear wall, 0.34 m down from the top, and a door, measuring 0.92 m by 2.05 m high, was centered on the front wall (opening to the corridor). For closed window experiments, the wood-framed calcium silicate board window cover was pressed against a bead of caulking around the steel window frame and held by drop bars positioned into slots on the outside wall.

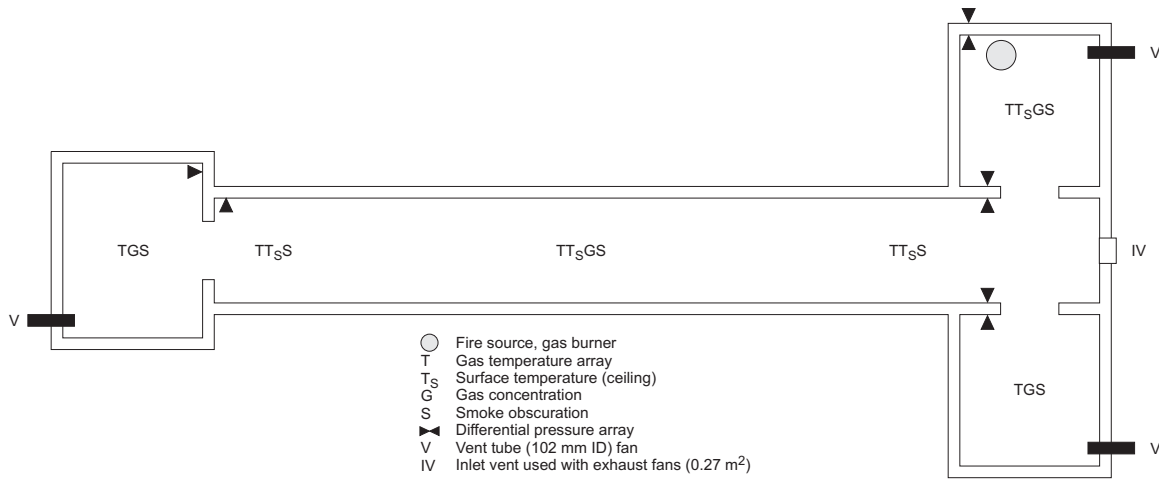


Figure 5.2: Overview of the Factory Mutual Four Room test series.

Room 3, located opposite the burn room, measured 3.65 m deep x 3.64 m wide x 2.45 m high; a door, measuring 0.88 m by 2.02 m high, was centered on the front wall (opening to the corridor). Room 4, located at the opposite end of the corridor, measured 3.65 m deep x 3.65 m wide x 2.43 m high and had a 0.88 m by 2.02 m high door centered on the front wall (opening to the corridor); an observation alcove, measuring 1.28 m by 0.86 m by 1.99 m high, was located in the front corner of

room 4. Each room was equipped with a 102 mm inside diameter vent tube with a 61 mm inside diameter orifice meter and thermocouple, with option of exhaust fan (tube centered 0.27 m from the floor and 0.17 m from the closest parallel wall). An inlet vent (0.29 m^2) used with exhaust fans was centered 0.43 m above the floor at the end of the corridor between the burn room and room 3. When not in use, the inlet vent was sealed with a gypsum board cover taped in place.

The target room doors were commercial fire doors (wood-faced composite doors with calcium silicate cores, 14 h rated) mounted on 16 gage steel frames. The burn room door was fabricated from 12.7 mm calcium silicate, mounted in a steel frame lined with calcium silicate. Details of the doors and the spacings (cracks) are given in the original reference [59].

Gypsum wallboard, 12.7 mm thick, on wood studs was used throughout the experimental facility. In addition, the walls and ceiling of the burn room were overlaid with calcium silicate, also 12.7 mm thick, to harden against repeated fire exposure. The existing concrete floor of the test building was used.

Two types of fire sources were used: 1) steady propylene fires at 56 kW on a 0.30 m diameter sand burner and 522 kW on a 0.91 m diameter burner and 2) propylene fires on the 0.91 m diameter burner programmed under computer control to grow with the square of time, exceeding 1 MW in 1, 2, 4, or 8 min.

The 0.91 m diameter, 0.58 in high propylene burner was used for most of the tests. Its design consisted of a 12 gage steel container with a gas distributor near the bottom, filled with gravel to a 67 percent height, where there was wire mesh screen, and coarse sand to the full height of the burner. The 0.30 m diameter burner was a scaled-down version of similar design.

5.3 FM / SNL Test Series

The Factory Mutual and Sandia National Laboratories (FM/SNL) Test Series was a series of 25 fire tests conducted in 1985 for the NRC by Factory Mutual Research Corporation (FMRC), under the direction of Sandia National Laboratories (SNL). The primary purpose of these tests was to provide data with which to validate computer models for various types of NPP compartments. The experiments were conducted in an enclosure measuring 18 m x 12 m x 6 m, constructed at the FMRC fire test facility in Rhode Island. Figure 5.3 shows detailed schematic drawings of the compartment from various perspectives. The FM/SNL test series is described in detail, including the types and locations of measurement devices, as well as some results in References [61, 62]. Six of the experiments were conducted with a full-scale control room mock-up in place. Parameters varied during the experiments included fire intensity, enclosure ventilation rate, and fire location. The current guide uses data from nineteen experiments (Tests 1-17, 21, and 22). In these tests, propylene gas burners, heptane pools, and methanol pools were used as fire sources. Table 5.1 lists the test parameters.

The following information was provided by the test director, Steve Nowlen of Sandia National Laboratory. In particular, Tests 4, 5, and 21 were given extra attention.

Heat Release Rate: The HRR was determined using oxygen consumption calorimetry in the exhaust stack with a correction applied for the carbon dioxide in the upper layer of the compartment. The uncertainty of the fuel mass flow was not documented. Several tests selected for this study had the same target peak heat release rate of 516 kW following a 4 min “t-squared” growth profile. The test report contains time histories of the measured HRR, for

which the average, sustained HRR following the ramp up for Tests 4, 5, and 21 have been estimated as 510 kW, 480 kW, and 470 kW, respectively. Once reached, the peak HRR was maintained essentially constant during a steady-burn period of 6 min in Tests 4 and 5, and 16 min in Test 21. Note that in Test 21, Nowlen reports a “significant” loss of effluent from the exhaust hood that could lead to an under-estimate of the HRR towards the end of the experiment.

Radiative Fraction: The radiative fraction was not measured during the experiment, but in this study it is assumed to equal 0.35, which is typical for a smoky hydrocarbons. It was further assumed that the radiative fraction was about the same in Test 21 as the other tests, as fuel burning must have occurred outside of the electrical cabinet in which the burner was placed.

Measurements: Four types of measurements were conducted during the FM/SNL test series that are used in the current model evaluation study, including the HGL temperature and depth, and the ceiling jet and plume temperatures. Aspirated thermocouples (TCs) were used to make all of the temperature measurements. Generally, aspirated TC measurements are preferable to bare-bead TC measurements, as systematic radiative exchange measurement error is reduced.

HGL Depth and Temperature: Data from all of the vertical TC trees were used when reducing the HGL height and temperature. For the majority of the tests, Sectors 1, 2, and 3 were used, all weighted evenly. For Tests 21 and 22, Sectors 1 and 3 were used, evenly weighted. Sector 2 was partially within the fire plume.

All of the tests involved forced ventilation to simulate typical nuclear power plant installation practices.

5.4 iBMB Compartment Tests

A series of small compartment kerosene pool fire experiments, conducted at the Institut für Baustoffe, Massivbau und Brandschutz (iBMB) of Braunschweig University of Technology in Germany in 2004 [63]. The results from Test 1 were considered here. These experiments involved relatively large fires in a relatively small (3.6 m x 3.6 m x 5.7 m) concrete enclosure. Figure 5.5 shows plan, side and perspective schematic drawings of the experimental arrangement, including the location of the fuel pan, which was located at the center of the compartment.

Only a portion of Test 1 was selected for consideration in the present study, because a significant amount of data was lost in Test 2, and the measured \dot{Q} during Test 3 exhibited significant amounts of fluctuation. Five types of measurements that were conducted during the test series were used in the model evaluation reported here. These included the HGL temperature and depth, the temperature of targets and compartment surfaces, and heat flux. In addition, figure 5.6 shows the heat release rate for Test 1, which was estimated from a mass loss rate measurement. In this calculation, the heat of combustion and the combustion efficiency were taken as 42.8 MJ/kg and 1, respectively, as suggested by Refs. [64, 65]. There were several reported difficulties in measuring the mass loss rate, including data loss due to an instrument malfunction and significant fluctuations

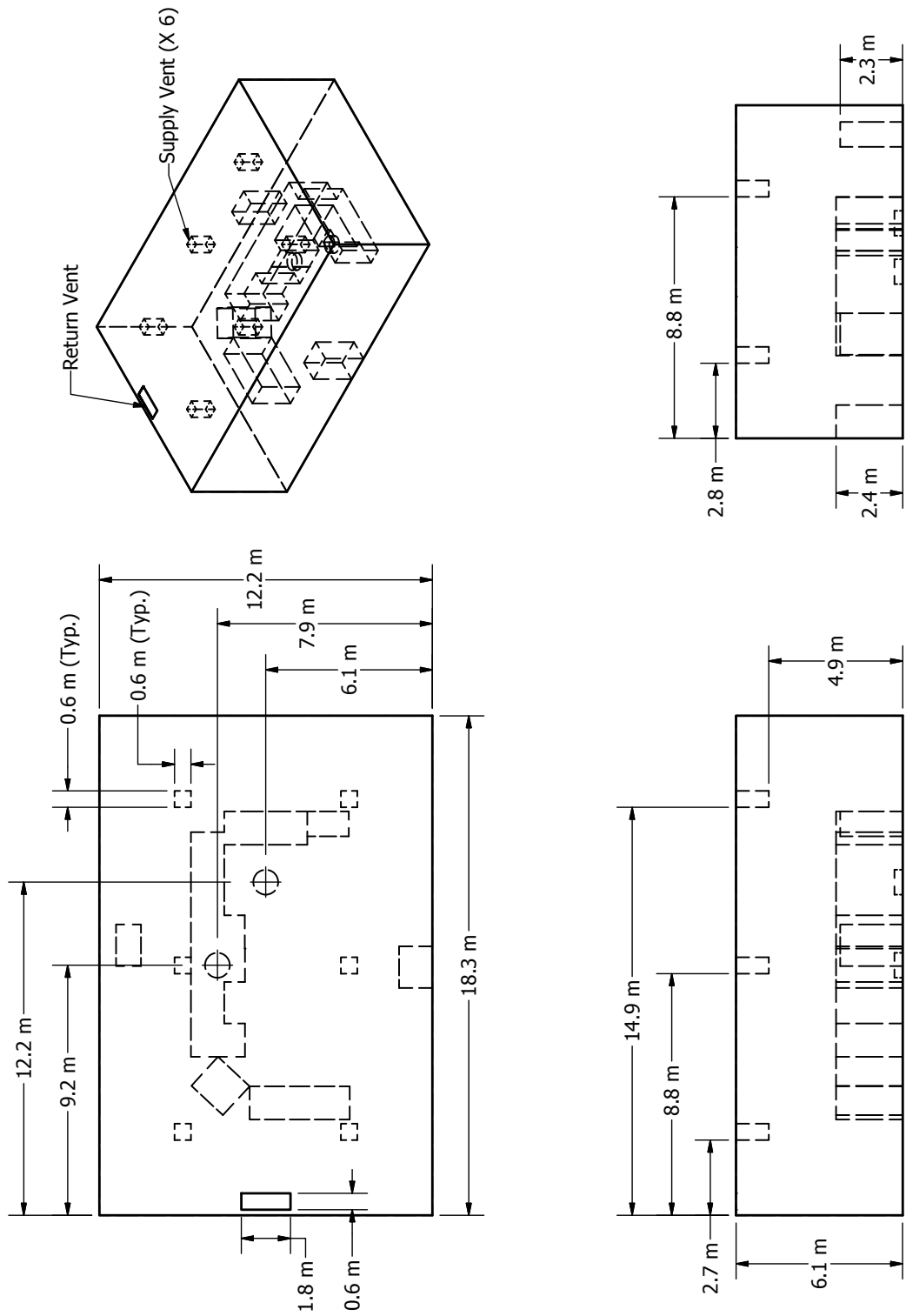


Figure 5.3: Detailed plan, side, and perspective schematic drawings of the FM/SNL experimental arrangement, including the supply and exhaust ducts, and the fuel pan.

Table 5.1: Summary of FM/SNL Experiments.

Test No.	Fuel Type	Nominal Peak HRR (kW)	Fire Position	Ventilation Rate (ach)	Room Configuration	Used in Guide?
1	Propylene Burner	516	Center	10	Empty	Yes
2	Propylene Burner	516	Center	10	Empty	Yes
3	Propylene Burner	2000	Center	10	Empty	Yes
4	Propylene Burner	516	Center	1	Empty	Yes
5	Propylene Burner	516	Center	10	Empty	Yes
6	Heptane Pool	500	Wall	1	Empty	Yes
7	Propylene Burner	516	Center	1	Empty	Yes
8	Propylene Burner	1000	Center	1	Empty	Yes
9	Propylene Burner	1000	Center	8	Empty	Yes
10	Heptane Pool	1000	Wall	4.4	Empty	Yes
11	Methanol Pool	500	Wall	4.4	Empty	Yes
12	Heptane Pool	2000	Wall	4.4	Empty	Yes
13	Heptane Pool	2000	Wall	8	Empty	Yes
14	Methanol Pool	500	Wall	1	Empty	Yes
15	Heptane Pool	1000	Wall	1	Empty	Yes
16	Heptane Pool	500	Corner	1	Empty	Yes
17	Heptane Pool	500	Corner	10	Empty	No
18	PMMA Slab	1000	Wall	1	Empty	No
19	Heptane Pool	1000	Center	1	Furnished	No
20	Heptane Pool	1000	Corner	8	Furnished	Yes
21	Propylene Burner	500	Cabinet	1	Furnished	Yes
22	Propylene Burner	1000	Cabinet	1	Furnished	No
23	Qualified Cable	N/A	Cabinet	1	Furnished	No
24	Unqualified Cable	N/A	Cabinet	1	Furnished	No
25	Unqualified Cable	N/A	Cabinet	8	Furnished	No

in the measured mass loss rate. Due to these measurement issues and because the combustion efficiency was not well-characterized, the \dot{Q} uncertainty was assigned a relatively large expanded uncertainty of $\pm 25\%$ [64].

A second series of fire experiments in 2004, conducted under the International Collaborative Fire Model Project (ICFMP) involved realistically routed cable trays inside the same concrete enclosure at iBMB [65]. The compartment was configured slightly differently with a ceiling height of 5.6 m. A schematic diagram from plan, side, and perspective views of the experimental arrangement is shown in figure 5.7. Six types of measurements conducted during the test series were used in the evaluation conducted here, including the HGL temperature and depth, oxygen gas concentration, the temperature of targets and compartment surfaces, and heat flux.

The results of four tests were available, of which one has been used in the current study. These tests were conducted primarily for the evaluation of cable ignition and flame spread. The results

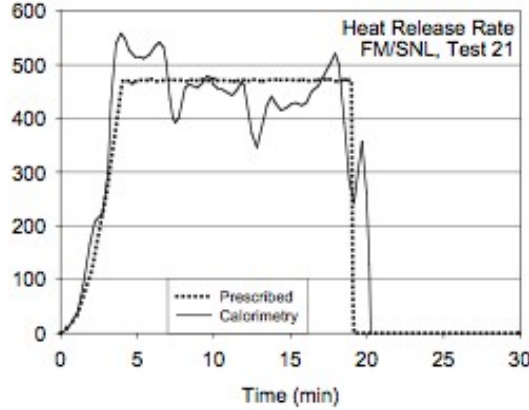


Figure 5.4: Prescribed (dotted line) and measured (solid line) heat release rate as a function of time during Test 21 of the FM/SNL test series

were erratic, and no replicate experiments were performed. Given the primitive nature of the ignition and spread algorithms within the models, it was decided that only a qualitative analysis would be possible with the data from three of the four experiments. However, in one experiment, the first 20 minutes involved a fairly well-characterized ethanol pool fire burning on the opposite side of the compartment from the cable tray. This part of the experiment has been used as part of the model evaluation.

The first part of the test consisted of preheating the cable trays in the room with a 1 m² round pan on the floor filled with ethanol (ethyl alcohol) used as the preheating source. At 30 min, a propane gas burner was used as the fire source – this was not considered because only the first 20 min of the test was used in this validation study. Exhaust products were collected in an exhaust duct and the \dot{Q} was measured using the oxygen calorimetry. For the purpose of this study, the measured \dot{Q} was used as direct input to the various fire models. The first 20 min of data were used for the model evaluation. After 20 min, the \dot{Q} became relatively noisy. Figure 5.6 shows the HRR. The relative combined expanded uncertainty was assigned a value of $\pm 15\%$, consistent with typical values of this parameter [64].

5.5 LLNL Enclosure Tests

Sixty-four enclosure fire tests were conducted by Lawrence Livermore National Laboratory (LLNL) in 1986 to study the effects of ventilation on enclosure fires [66]. The test enclosure was 6 m long, 4 m wide, and 4.5 m high. It contained a methane rock burner which was placed in the center of the space. For most of the tests the burner was placed on the floor. The fires varied in size from 50 kW to 400 kW. The burner was 0.57 m in diameter and 0.23 m height.

The door (2.06 m high by 0.76 m wide) was closed and sealed for most tests, and air was pulled through the space at rates varying from 100 to 500 g/s. In some tests the enclosure included a plenum space, where make-up air could be injected from above or below. The test matrix is listed in Table 5.2.

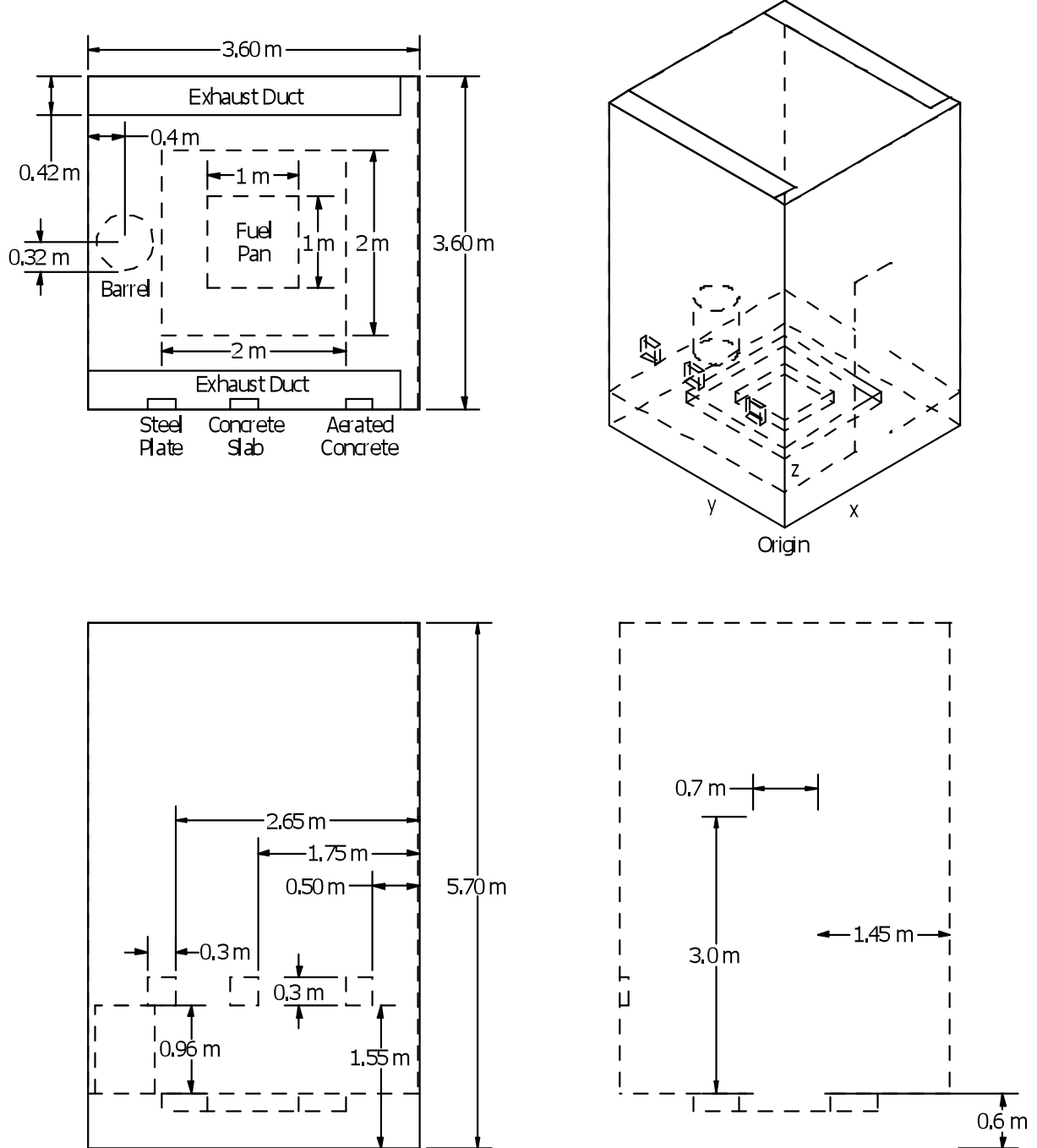


Figure 5.5: Detailed plan, side, and perspective schematic drawings of the iBMB pool fire experimental arrangement.

Table 5.2: Summary of LLNL Enclosure Experiments.

Test No.	Room Config.	h_0 m	\dot{Q} kW	\dot{m} g/s	T_∞ °C	Test No.	Room Config.	h_0 m	\dot{Q} kW	\dot{m} g/s	T_∞ °C
1	TL	0	200	0	23	33	PH	0	100	200	23
2	TL	0	200	0	27	34	PH	0	100	300	34
3	TL	0	400	0	27	35	PH	0	100	400	22
4	TL	0	300	0	24	36	PH	0	100	500	29
5	TL	0	50	0	28	37	PH	0	200	100	20
6	TL	0	100	0	29	38	PH	0	200	300	29
7	TL	0	100	0	35	39	PH	0	250	100	18
8	TL	0	200	0	35	40	PH	0	200	400	28
9	TL	0	200	500	33	41	PH	0	150	100	20
10	TL	0	200	100	28	42	PHE	2	200	180	30
11	TL	0	200	200	18	43	PHE	2	200	0	32
12	TL	0	200	300	21	44	PHE	1	200	180	19
13	TL	0	200	400	28	45	PHE	1	200	0	30
14	TL	0	200	400	28	46	PHE	0.6	200	180	19
15	TL	0	100	300	24	47	PHE	0.6	200	0	19
16	TL	0	200	300	21	48	PHE	0.3	200	0	21
17	PL	0	200	500	26	49	PHE	0.3	200	180	26
18	PL	0	200	400	21	50	PHE	1	200	180	21
19	PL	0	200	300	18	51	PNE	1	200	NAT	33
20	PL	0	200	200	16	52	PN	0	200	NAT	23
21	PL	0	200	100	23	53	PHGS	0	200	185	33
22	PH	0	200	190	30	54	PHGS	0	200	215	21
23	PH	0	200	215	28	55	PN	0	100	NAT	31
24	PH	0	200	205	26	56	PHGW	0	200	190	20
25	PH	0	200	205	25	57	PHGW	0	200	215	29
26	PH	0	200	500	24	58	PHX	0	200	190	18
27	PH	0	200	100	23	59	PHXE	1	200	190	24
28	PH	0	150	150	31	60	PN	0	400	NAT	22
29	PH	0	250	250	28	61	TN	0	200	NAT	31
30	PH	0	250	300	34	62	TN	0	400	NAT	22
31	PH	0	250	500	36	63	TN	0	50	NAT	28
32	PH	0	100	100	33	64	TN	0	100	NAT	17

T	full compartment	N	natural ventilation (door open)
P	plenum configuration	X	3 ft extension on inlet opening
L	low inlet duct	GS	grate on inlet, north/south configuration
H	high inlet duct	GW	grate on inlet, east/west configuration
E	elevated fire, h_0		

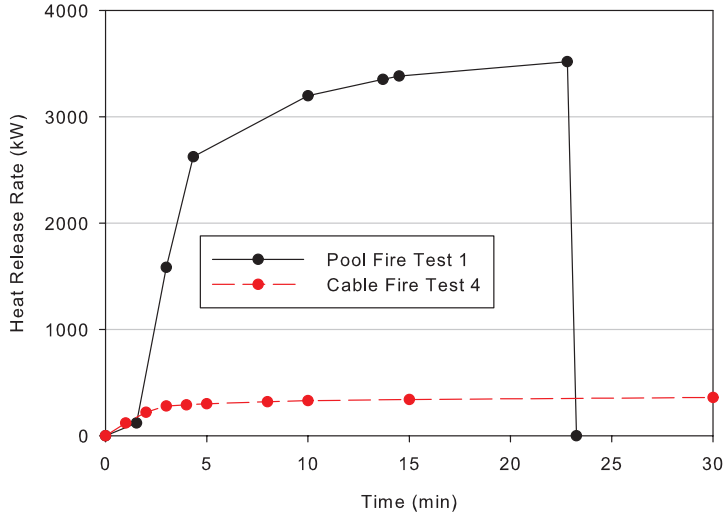


Figure 5.6: Estimated heat release rate for the iBMB fire experiments.

5.6 NBS Single Room Tests with Furniture

These data describe a series of room fire tests using upholstered furniture items in a room of fixed size but with varying opening sizes and shapes [34] conducted by the National Bureau of Standards (NBS, former name of NIST). It was selected for its well characterized and realistic fuel sources in a simple single-room geometry. In addition, the wide variation in opening size should provide challenges for current zone fire models. Peak fire size was about 2.9 MW with a total room volume of 21 m^3 . A series of four single-room fire tests were conducted using upholstered furniture items for comparison with their free burning behavior, previously determined in a furniture calorimeter. The experiments were conducted in a single room enclosure; ventilation to the room was provided by window openings of varying sizes. The room was equipped with an instrumented exhaust collection system outside the window opening.

A second similar test series also utilized a single-room fire test with furniture as the fire source [67]. It expanded upon the first data set by adding the phenomenon of wall burning. Peak fire size was about 7 MW. The room size was similar to the first test series. Figure 5.9 illustrates the configuration for the two test series.

The test furniture included a 28.3 kg armchair or a similar 40.0 kg love seat for the first test series. Both were of conventional wood frame construction and used polyurethane foam padding, made to minimum California State flammability requirements, and polyolefin fabric. A single piece of test furniture and igniting wastebasket were the only combustibles in the test room.

For the second test series, room furnishings consisted of a 1.37 m wide x 1.91 m long x 0.53 m high double bed, a 2.39 m X 0.89 m high headboard, and 0.51 m wide x 0.41 m deep x 0.63 m high night table. Both headboard and night table were fabricated from 12.7 mm thick plywood. The bedding was comprised of two pillows, two pillow cases, two sheets, and one blanket. The pillows had a polypropylene fabric with a polyester filling. The pillow cases and sheets were polyester-cotton. The blanket was acrylic material. The bedding was left in a "slept in" condition which was

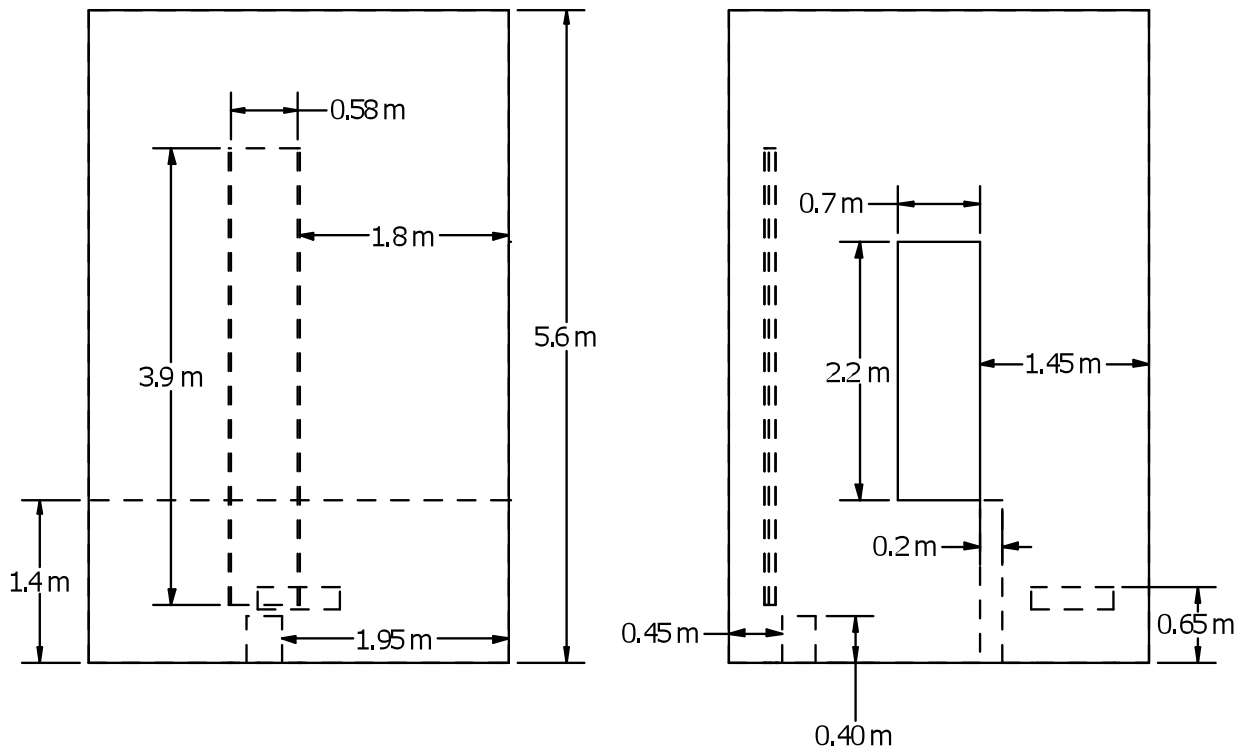
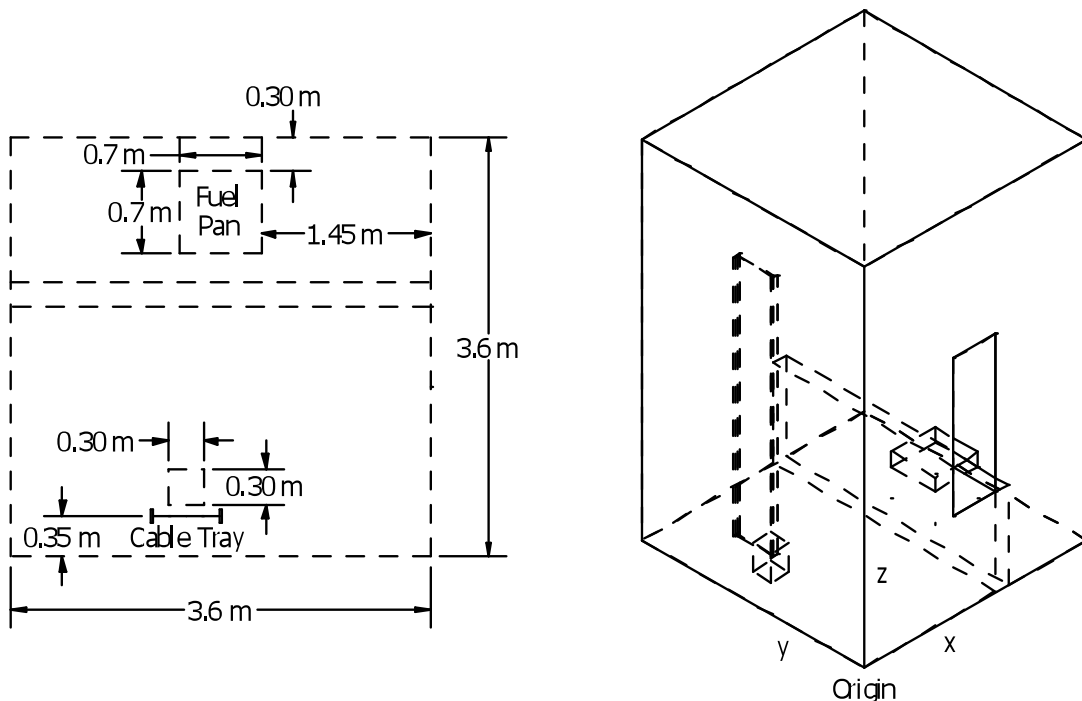


Figure 5.7: Detailed plan, side, and perspective schematic drawings of the iBMB cable fire experimental arrangement.

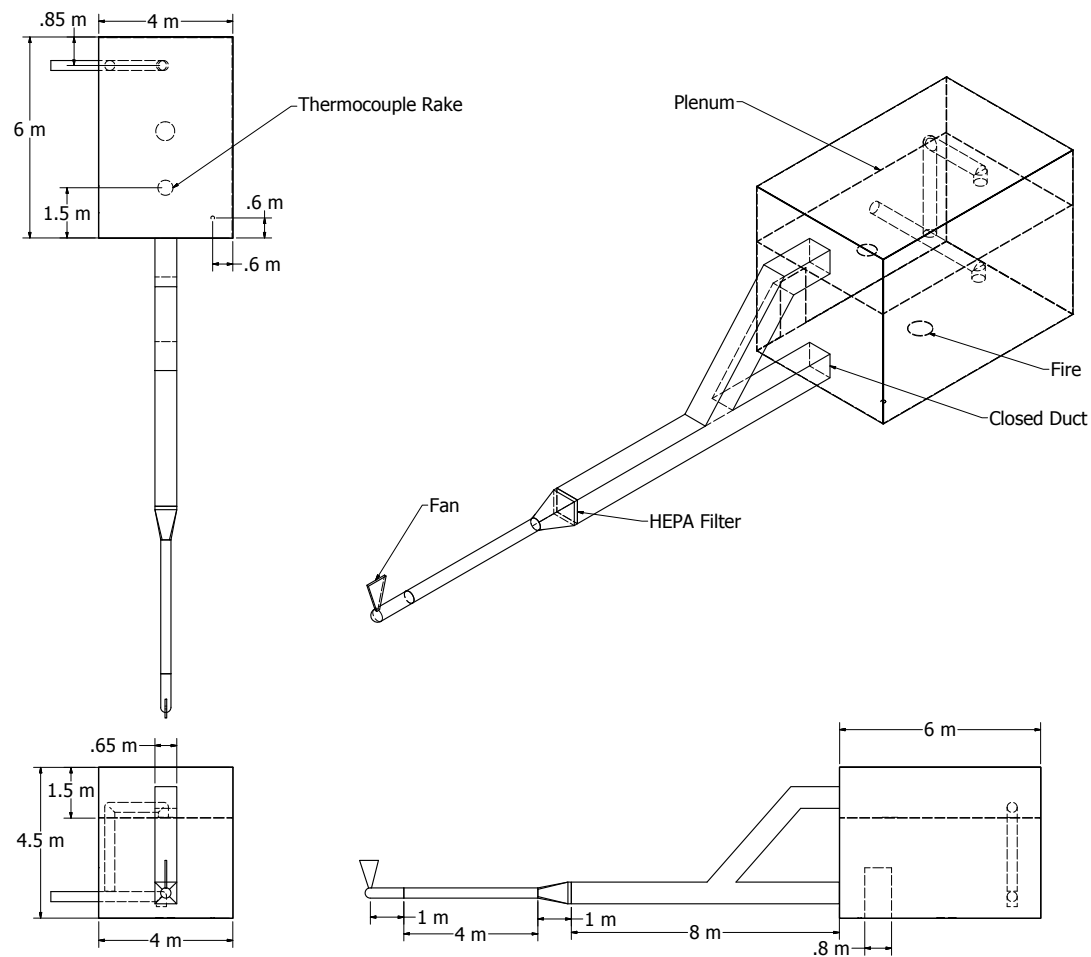


Figure 5.8: Geometry of the LLNL Enclosure Experiments.

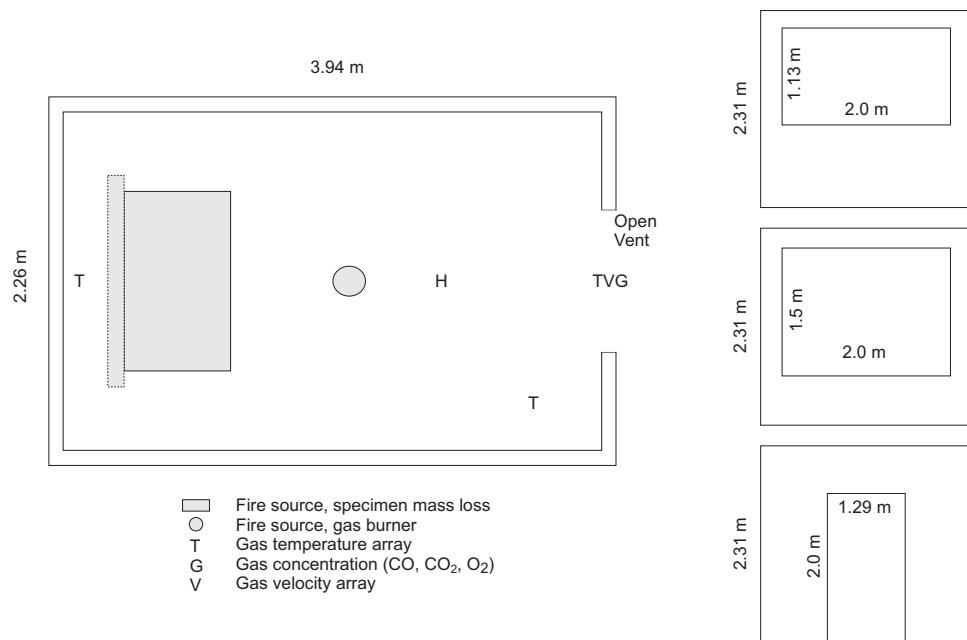


Figure 5.9: Plan and elevation view schematic of experimental room for NBS single room tests with furniture. Note dotted lines on burning specimen indicates vertical surface for wall burning experiments. Specimen and instrumentation placement are approximate.



Figure 5.10: Burning specimen during NBS single room tests with furniture.



Figure 5.11: Photo of a 100 kW fire with the burner located against the rear wall of one of the small compartments in the NBS Multi-Compartment test Series.

duplicated to the degree possible in each test. In all of the tests, the fire was started with match flame ignition of a 0.34 kg (240 mm x 140 mm x 240 mm high) wastebasket, filled with 0.41 kg of trash, positioned adjacent to the bed.

5.7 NBS Multi-Compartment Test Series

The National Bureau of Standards (NBS, former name of NIST) Multi-Compartment Test Series consisted of 45 fire tests representing 9 different sets of conditions were conducted in a three-room suite. The experiments were conducted in 1985 and are described in detail in reference [60]. The suite consisted of two relatively small rooms, connected via a relatively long corridor. Total volume of the structure was approximately 100 m². The fire source, a gas burner, was located against the rear wall of one of the small compartments as seen in Figure 5.11 for a 100 kW fire. Figures 5.12 and 5.13 presents the experimental arrangement in the form of plan, side and perspective schematic drawings of the compartments. Fire tests of 100 kW, 300 kW and 500 kW were conducted. For the current study, three 100 kW fire experiments have been used, including Test 100A from Set 1, Test 100O from Set 2, and Test 100Z from Set 4. For the NBS Multi-room series, Tests 100A, 100O and 100Z were selected for study, because they were constructively used in a previous validation study [[68]], and because these tests had the steadiest values of measured heat release rate during the steady burning period. The selected data are also available in Reference [68]. Reference [64] provides information used as model input for simulation of the NBS tests, including information on the compartment, the fire, the ventilation, and ambient conditions. The data in the NBS data set was acquired every 10 s with a 6 s time-average. This time-averaging interval was somewhat smaller than all of the other experimental series, which were time-averaged over a 10 s interval.

Figures 5.14 show the experimentally measured \dot{Q} as a function of time during Tests 100A

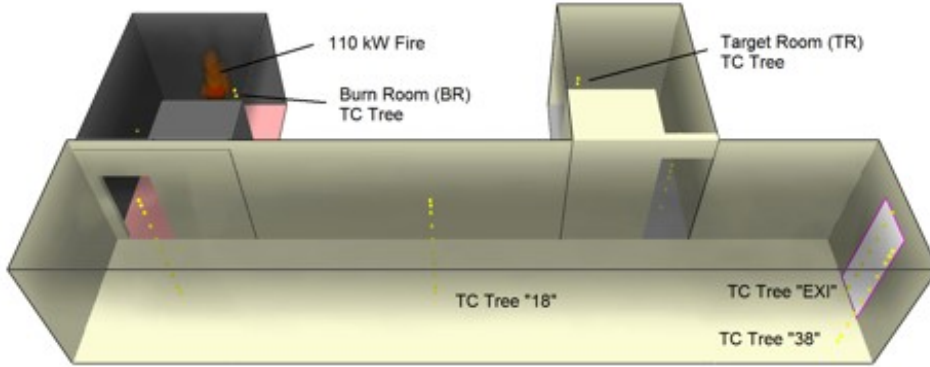


Figure 5.12: Overview of the NBS Test Configuration.

and 100Z, respectively, of the NBS multi-room test series, typically averaging about 100 kW. In these two tests, for which the door was open, the \dot{Q} during the steady burning period measured via oxygen consumption calorimetry was about $110 \text{ kW} \pm 17 \text{ kW} (\pm 15\%)$ [64]. The combined relative expanded (2σ) uncertainty in the calorimetric \dot{Q} is assigned a value of $\pm 15\%$, consistent with the replicate measurements made during the experimental series and the uncertainty typical of oxygen consumption calorimetry [64]. This value is also consistent with the measurement variation evident in the figures. It was assumed that the closed door test (Test 100O) had the same \dot{Q} as the open door tests [64].

The specified or prescribed \dot{Q} is also shown in the figures. The mass flow of the fuel (natural gas in Test 100A, or natural gas mixed with acetylene in Tests 100O and 100Z) was not metered; rather, the effluent was captured in a hood mounted above the open door in the corridor and the was measured using oxygen consumption calorimetry. The manner by which the fuel flow was controlled is not documented. In Test 100A, candles were used to increase smoke in the upper layer to promote visualization. In Tests 100O and 100Z, acetylene was used (about 20 % by volume) to produce smoke. In those tests, the flow of natural gas and acetylene were adjusted to obtain approximately the same \dot{Q} as in Test 100A. The addition of acetylene increased the radiative fraction of the fire.

For practical reasons, piped natural gas supplied by large utility companies is often used in fire experiments. While its composition may vary from day to day, there is little change expected in the value of the radiative fraction [64]. As mentioned above, natural gas was used as the fuel in Test 100A. In Tests 100O and 100Z, acetylene was added to the natural gas to increase the smoke yield, and as a consequence, the radiative fraction increased. The radiative fraction of natural gas has been studied previously, whereas the radiative fraction of the acetylene/natural gas mixture has not been studied. The radiative fraction for the natural gas fire was assigned a value of 0.20, whereas a value of 0.30 was assigned for the natural gas/acetylene fires [64, 69].

The relative combined expanded (2σ) uncertainty in this parameter was assigned a value of $\pm 20\%$ in Test 100A and $\pm 30\%$ in 100O and 100Z. The 20 % expanded deviation value is consistent with typical values of the deviation reported in the literature for the measured radiative fraction. The 100O and 100Z tests had a 50 % larger value assigned, because the effect on the

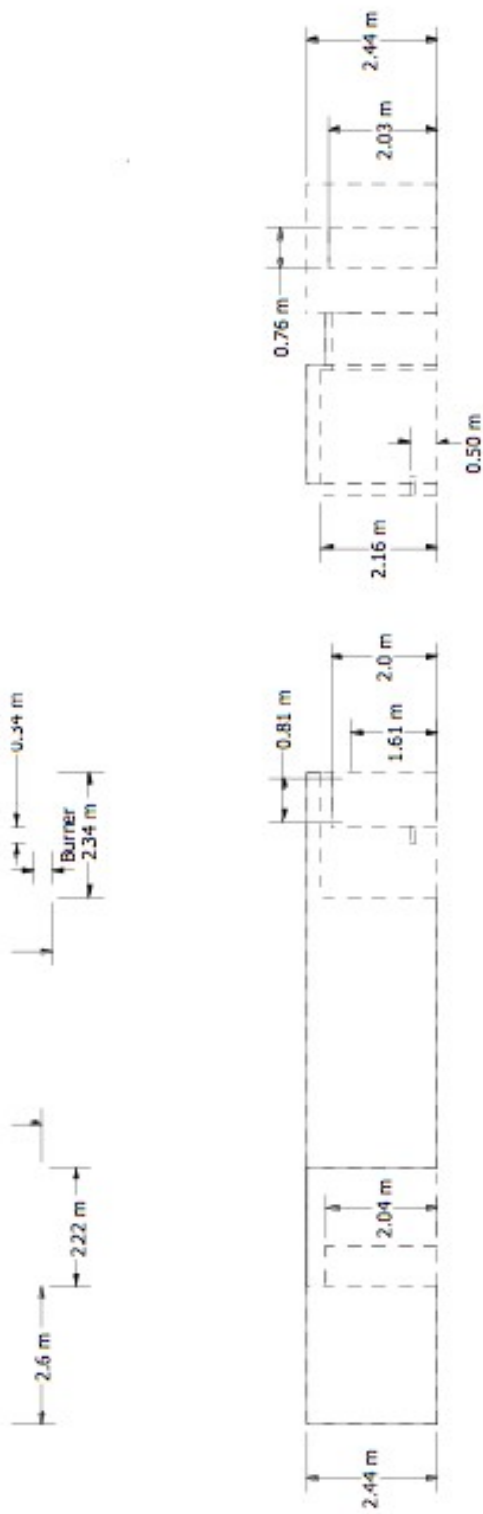


Figure 5.13: Plan, side and perspective schematic drawings of the NBS experimental arrangement, including the burner.

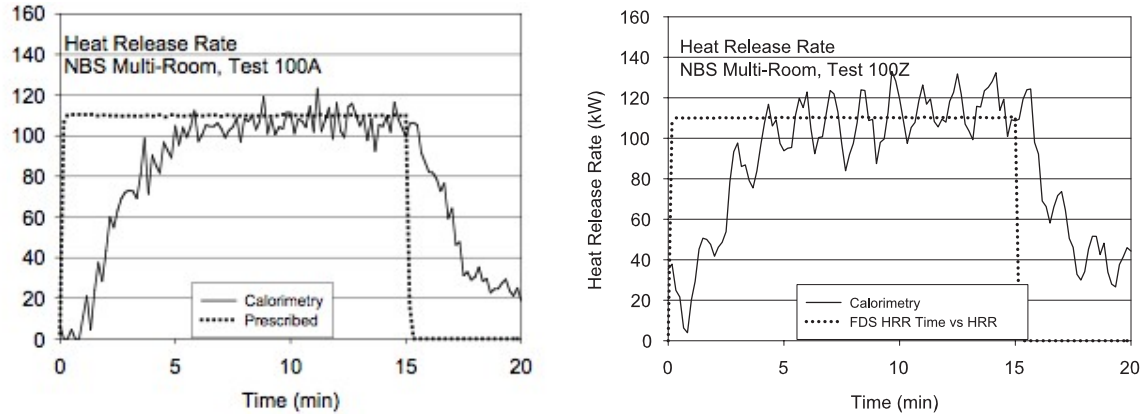


Figure 5.14: Prescribed and measured heat release rate as a function of time during Tests 100A and 100Z of the NBS multi-room test series.

radiative fraction of adding acetylene to the natural gas was not measured [64].

Measurements made during the NBS test series included gas and surface temperature, pressure, smoke and major gas species concentration, and doorway gas velocity. Only two types of measurements conducted during the NBS test series were used in the evaluation considered here, because there was less confidence in the other measurements. The measurements considered here were the HGL temperature and depth, in which bare bead thermocouples were used to make these measurements. Single point measurements of temperature within the burn room were not used in the evaluation of plume or ceiling jet algorithms. This is because, in neither instance, was the geometry consistent with the assumptions used in the model algorithms of plumes or jets. Specifically, the burner was mounted against a wall, and the room width to height ratio was less than that assumed by the various ceiling jet correlations.

5.8 NIST Dunes 2000 Experiments

A series of experiments was conducted by NIST to measure the activation time of ionization and photoelectric smoke alarms in a residential setting [70]. Tests were conducted in actual homes with representative sizes and floor plans, utilized actual furnishings and household items for fire sources, and tested actual smoke alarms sold in retail stores at that time. Thirty-six tests were conducted in two homes; 27 in a single-story manufactured home, and 8 in a two-story home.

Figure 5.15 shows a diagram of the layout and instrumentation in the manufactured home. The primary partitioning of the 84.7 m^2 floor plan consisted of three bedrooms: one full bathroom, one kitchen/dining area, one living room, and two hallways. For testing, the doors to bedroom 3 and the bathroom were always closed. The ceiling was peaked on the long axis, reaching a height of 2.4 m. The outside walls were approximately 2.1 m in height. The slope of the ceiling was approximately 8.4° .

An upholstered chair, mattress, or pan of cooking oil was used as the fire source in each test. There were three primary ignition sources: flaming, smoldering, and cooking. The flaming ignition source used a moderate flame source to quickly ignite the fuel package. Groups of smoke alarms

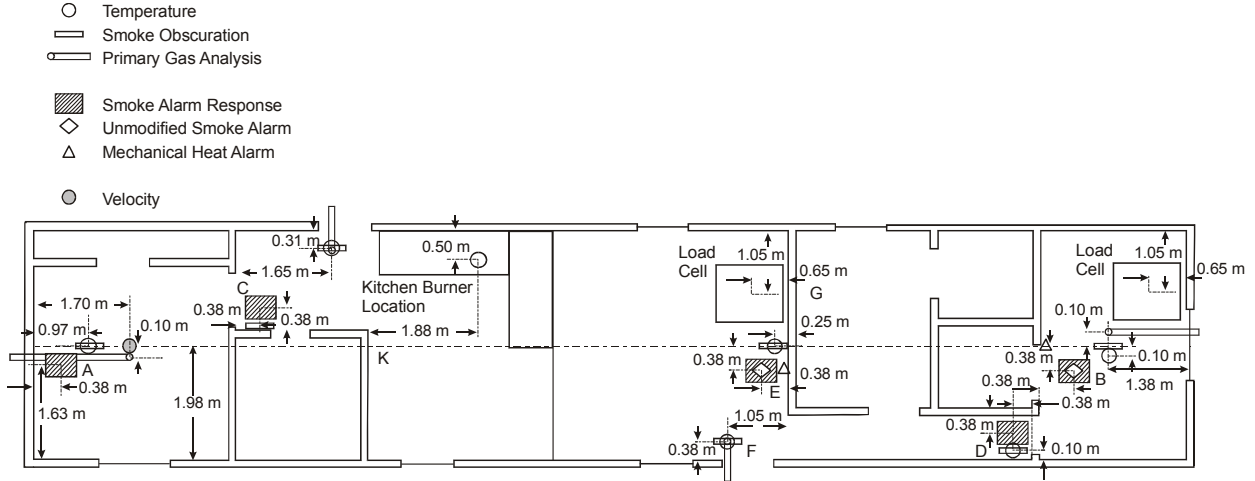


Figure 5.15: Geometry of the NIST Dunes 2000 Experiments.

were located in the room of fire origin, at least one bedroom, and in a central location. Five stations (A-E) containing smoke alarm arrays were mounted parallel to the ceiling.

Nine experiments that were conducted in the single-story manufactured home were selected for model validation. Only tests that used a flaming ignition source with a couch or mattress fuel package were considered; the cooking oil fires and tests that used a smoldering ignition source were not considered.

Although a load cell was used in the experiments to measure the mass loss rate of the fuel package, the mass loss data were not reliable enough to reconstruct the HRR curves for each test. Instead, the HRR curves were determined by approximating the fire growth using a t^2 ramp, as in Eq. (5.1). The parameters for the t^2 ramp were calibrated in FDS by using the temperature measured at the highest thermocouple in the tree (2 cm below the ceiling) in the fire room.

$$\dot{Q} = \dot{Q}_0 \left(\frac{t}{\tau} \right)^2 \quad (5.1)$$

A time offset was used to align the predicted ceiling thermocouple temperatures with the measured temperatures. This offset is reported as the time at which the t^2 ramp begins. The t-squared calibration parameters and time offsets for the HRR ramps are shown in Table 5.3. Additionally, the ignition source had a small effect on the measured ceiling thermocouple temperatures. Therefore, the size of the ignition source was approximated as either 3 kW or 7 kW, and the time offset of the ignition source was also calibrated by using the measured ceiling thermocouple temperatures. The resulting HRR curve was input into FDS as a fire ramp.

A summary of the nine tests selected for model validation is shown in Table 5.3.

5.9 NIST Seven-story Hotel Tests

By far the most complex test, this data set is part of a series of full-scale experiments conducted to evaluate zoned smoke control systems, with and without stairwell pressurization [71]. It was

Table 5.3: Summary of NIST Dunes 2000 experiments selected for model validation.

Test No.	Fire Source	Fire Location	\dot{Q}_0 (kW)	τ (s)	Time Offset (s)
SDC02	Chair	Living Room	150	180	20
SDC05	Mattress	Bedroom	200	180	20
SDC07	Mattress	Bedroom	350	180	50
SDC10	Chair	Living Room	150	180	40
SDC15	Chair	Living Room	225	400	180
SDC33	Chair	Living Room	100	180	10
SDC35	Chair	Living Room	100	180	10
SDC38	Mattress	Bedroom	120	180	25
SDC39	Mattress	Bedroom	200	180	25

conducted in a seven story hotel with multiple rooms on each floor and a stairwell connecting all floors. This data set was chosen because it would challenge the scope of most current fire models. Measured temperatures and pressure differences between the rooms and floors of the building are extensive and consistent. Peak fire size was 3 MW with a total building volume of 140 000 m³.

Smoke movement and the performance of smoke control systems were studied in a seven story hotel building with smoke generated from wood fires and theatrical smoke. A total of 12 single experiments were conducted under a variety of conditions: two different fire sizes; sprinklered vs non-sprinklered wood fires; zoned smoke control on or off; stairwell pressurization on or off; with and without ventilation to the outside; and open and closed doors.

The Plaza Hotel building was a masonry structure consisting of two wings, one three stories and the other seven stories tall. The two wings were built at different times. The wings were connected to each other at only one location on each floor. The connections between the wings at each floor were sealed off, and the fires were set on the second floor of the seven-story wing, using the shorter wing as an instrumentation area. Areas of the second floor were fire hardened to minimize structural damage to the building.

The smoke control systems were designed using the methods presented in the smoke control manual of the American Society of Heating, Refrigerating, and Air-Conditioning Engineers [72], and the design analysis is discussed in detail by Klote [73]. The minimum design pressure difference was 25 Pa, meaning that the system should be able to maintain at least this value without a fire. The Plaza Hotel building had no central forced air heating, ventilating, and air-conditioning (HVAC) system, so a dedicated system of fans and ducts was installed for zoned smoke control and stairwell pressurization. The smoke control system consisted of the three 0.944 m³/s centrifugal fans shown in 5.16, plus another centrifugal fan (not shown) located outside and supplying 4.25 m³/s of pressurization air to the stairwell at the first floor. The smoke control system is illustrated in figure 5.16. All the test fires were located in the second floor smoke zone. This smoke was exhausted at about six air changes per hour. The first and second floors were pressurized at about six air changes per hour. When the stairwell pressurization system was activated, the exterior stairwell door was open. This approach is intended to minimize fluctuations due to opening and closing doors.

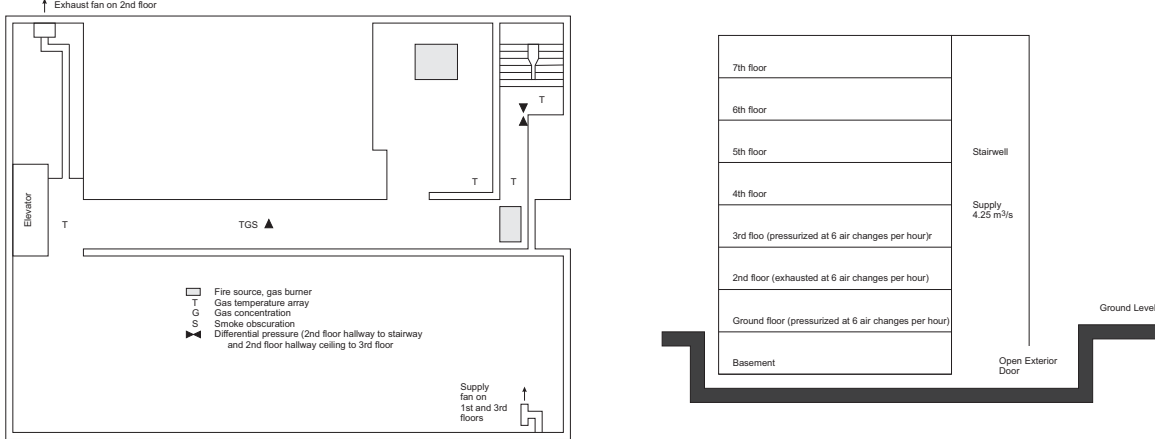


Figure 5.16: Overview of the NIST Seven-story hotel test series including smoke control.

5.10 NIST / NRC Test Series

These experiments, sponsored by the US NRC and conducted at NIST, consisted of 15 large-scale experiments performed in June 2003. All 15 tests were included in the validation study. The experiments are documented in Ref. [74]. The fire sizes ranged from 350 kW to 2.2 MW in a compartment with dimensions 21.7 m by 7.1 m by 3.8 m high, designed to represent a compartment in a nuclear power plant containing power and control cables. A photo of the fire seen through the compartment doorway is shown in figure 5.17. Figure 5.18 shows the important features of the test hall. Figure 5.19 shows detailed plan, side and perspective schematic diagrams of the experimental arrangement. The walls and ceiling were covered with two layers of marinate boards, each layer 0.0125 m thick. The floor was covered with one layer of gypsum board on top of a layer of plywood. Thermo-physical and optical properties of the marinate and other materials used in the compartment are given in reference [74]. The room had one door and a mechanical air injection and extraction system. Ventilation conditions, the fire size, and fire location were varied. Numerous measurements (approximately 350 per test) were made including gas and surface temperatures, heat fluxes and gas velocities. Detailed schematic diagrams of the experimental arrangement are shown in figure 5.19. Table 5.4 shows the experimental conditions for all 15 tests.

The compartment had a 2 m by 2 m door in the middle of the west wall. Some of the tests had a closed door and no mechanical ventilation, and in those tests the measured compartment leakage was an important consideration. Reference [74] reports leakage area based on measurements performed periodically during the test series. For the closed door tests, the leakage area used in the simulations was based on the last available measurement. It should be noted that the chronological order of the tests differed from the numerical order [74].

The mechanical ventilation and exhaust was used during some test, providing about 5 air changes per hour. The supply duct was positioned on the long wall, about 2 m off the floor. An exhaust duct of equal area to the supply duct was positioned on the opposite wall at a comparable location. The flow rates through the supply and exhaust ducts were measured in detail during breaks in the testing, in the absence of a fire. During the tests, the flows were monitored with single bi-directional probes during the tests themselves.



Figure 5.17: Photograph of a 1 MW heptane fire seen through the open doorway. Photo provided by Anthony Hamins, NIST.

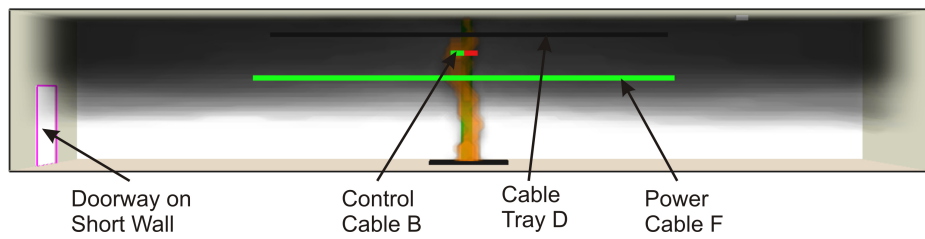


Figure 5.18: Cross-section View of the NIST NRC Test Configuration.

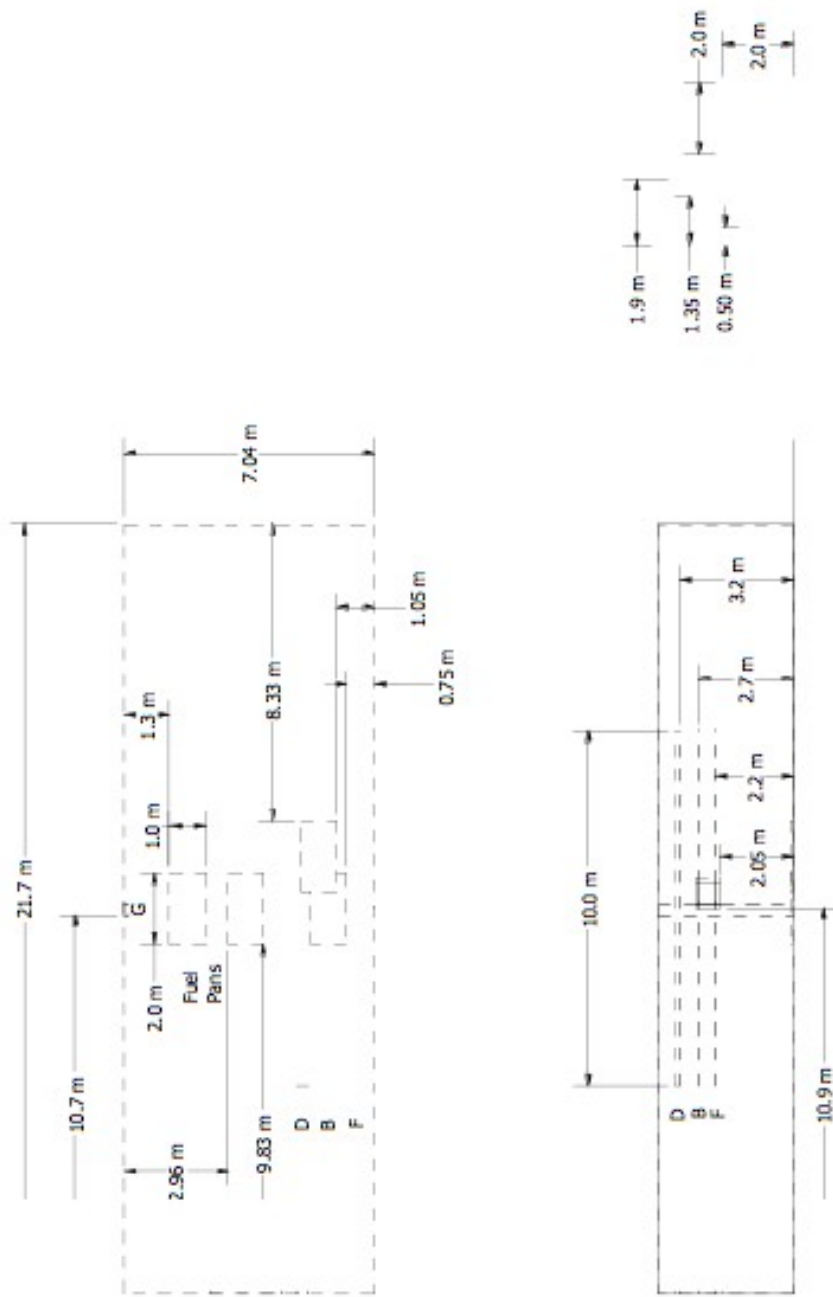


Figure 5.19: Plan, side and perspective schematic drawings of the NIST NRC experimental arrangement. The fuel pan and cables B, D, F, and G (dotted lines) are also shown.

Table 5.4: Test Matrix and Experimental Conditions for NIST NRC Tests

Test	Nominal Peak \dot{Q} (MW)	Cable Type	Fuel; Burner Location	Door	Mechanical Ventilation
1	0.35	XPE ^a	Heptane; Center	Closed	Off
2	1	XPE	Heptane; Center	Closed	Off
3	1	XPE	Heptane; Center	Open	Off
4	1	XPE	Heptane; Center	Closed	On
5	1	XPE	Heptane; Center	Open	On
6			Not Conducted		
7	0.35	PVC ^b	Heptane; Center	Closed	Off
8	1	XPE	Heptane; Center	Closed	Off
9	1	XPE	Heptane; Center	Open	Off
10	1	PVC	Heptane; Center	Closed	On
11			Not Conducted		
12			Not Conducted		
13	2	XPE	Heptane; Center	Closed	Off
14	1	XPE	Heptane; 1.8 m from N wall on E-W centerline	Open	Off
15	1	PVC	Heptane; 1.25 m from S wall on E-W centerline	Open	Off
16	2	PVC	Heptane; Center	Closed	On
17	1	PVC	Toluene; Center	Closed	Off
18	1	XPE	Heptane; 1.55 m from S wall 1.50 m E of centerline	Open	Off

a - XPE cable has crosslinked polyethylene jacket insulation

b - PVC cable has a polyvinylchloride jacket insulation

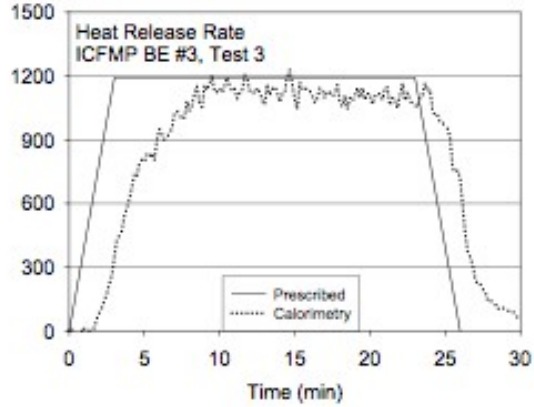


Figure 5.20: Measured and prescribed heat release rate as a function of time during Test 3 of the NIST NRC test series

A single nozzle was used to spray liquid hydrocarbon fuels onto a 1 m by 2 m fire pan that was about 0.02 m deep. The test plan originally called for the use of two nozzles to provide the fuel spray. Experimental observation suggested that the fire was more steady with the use of a single nozzle. In addition, it was observed that the actual extent of the liquid pool was well-approximated by a 1 m circle in the center of the pan. For safety reasons, the fuel flow was terminated when the lower-layer oxygen concentration dropped to approximately 15 % by volume. The fuel used in 14 of the tests was heptane, while toluene was used for one test. The HRR was determined using oxygen consumption calorimetry (figure 5.20 shows a sample heat release rate for one of the tests in the series). The recommended uncertainty values for HRR were 17 % for all of the tests. The radiative fraction was measured in an independent study for the same fuels using the same spray burner as used in the test series [75]. The value of the radiative fraction and its uncertainty were reported as $0.44 \pm 16\%$ and $0.40 \pm 23\%$ for heptane and toluene, respectively. Further details of the model inputs used for these simulations are included in reference [64].

5.11 SP Adiabatic Surface Temperature Experiments

In 2008, three compartment experiments were performed at SP Technical Research Institute of Sweden under the sponsorship of Brandforsk, the Swedish Fire Research Board [76]. The objective of the experiments was to demonstrate how plate thermometer measurements in the vicinity of a simple steel beam can be used to supply the boundary conditions for a multi-dimensional heat conduction calculation for the beam. The adiabatic surface temperature was derived from the plate temperatures and used by TASEF, a finite-element thermal-structural program.

The experiments were performed inside a standard compartment designed for corner fire testing (ISO 9705). The compartment is 3.6 m deep, 2.4 m wide and 2.4 m high and includes a door opening 0.8 m by 2.0 m. The room was constructed of 20 cm thick light weight concrete blocks with a density of $600 \text{ kg/m}^3 \pm 100 \text{ kg/m}^3$. The heat source was a gas burner run at a constant power of 450 kW. The top of the burner, with a square opening 30 cm by 30 cm, was placed 65 cm above the floor, 2.5 cm from the walls. A single steel beam was suspended 20 cm below the ceiling

along the centerline of the compartment. There were three measurement stations along the beam at lengths of 0.9 m (Position A), 1.8 m (Position B), and 2.7 m (Position C) from the far wall where the fire was either positioned in the corner (Tests 1 and 2), or the center (Test 3). The beam in Test 1 was a rectangular steel tube filled with an insulation material. The beam in Tests 2 and 3 was an I-beam..

5.12 Steckler Compartment Experiments

Steckler, Quintiere and Rinkinen performed a set of 55 compartment fire tests at NBS in 1979 [77]. The compartment was 2.8 m by 2.8 m by 2.13 m high¹, with a single door of various widths, or alternatively a single window with various heights. A 30 cm diameter methane burner was used to generate fires with heat release rates of 31.6 kW, 62.9 kW, 105.3 kW and 158 kW. Vertical profiles of velocity and temperature were measured in the doorway, along with a single vertical profile of temperature within the compartment. A full description and results are reported in Reference [77]. The basic test matrix is listed in Table 5.5. Note that the test report does not include a detailed description of the compartment. However, an internal report² by the test sponsor, Armstrong Cork Company, reports that the compartment floor was composed of 19 mm calcium silicate board on top of 12.7 mm plywood on wood joists. The walls and ceiling consisted of 12.7 mm ceramic fiber insulation board over 0.66 mm aluminum sheet attached to wood studs.

5.13 UL/NFPRF Sprinkler, Vent, and Draft Curtain Study

In 1997, a series of 34 heptane spray burner experiments was conducted at the Large Scale Fire Test Facility at Underwriters Laboratories (UL) in Northbrook, Illinois [78]. The experiments were divided into two test series. Series I consisted of 22 4.4 MW experiments. Series II consisted of 12 10 MW experiments. The objective of the experiments was to characterize the temperature and flow field for fire scenarios with a controlled heat release rate in the presence of sprinklers, draft curtains, and smoke & heat vents. The Large Scale Fire Test Facility at UL contains a 37 m by 37 m (120 ft by 120 ft) main fire test cell, equipped with a 30.5 m by 30.5 m (100 ft by 100 ft) adjustable height ceiling. The layout of the experiments is shown in Figs. 5.21 and 5.22.

Ceiling: The ceiling was raised to a height of 7.6 m and instrumented with thermocouples and other measurement devices. The ceiling was constructed of 0.6 m by 1.2 m by 1.6 cm UL fire-rated Armstrong Ceramaguard (Item 602B) ceiling tiles. The manufacturer reported the thermal properties of the material to be: specific heat 753 J/(kg·K), thermal conductivity 0.0611 W/(m·K), and density 313 kg/m³.

Draft Curtains: Sheet metal, 1.2 mm thick and 1.8 m deep, was suspended from the ceiling for 16 of the 22 Series I tests, enclosing an area of about 450 m² and 49 sprinklers. The curtains were in place for all of the Series II tests.

¹The test report gives the height of the compartment as 2.18 m. This is a misprint. The compartment was 2.13 m high.

² *Technical Research Report, Fire Induced Flows Through Room Openings - Flow Coefficients*, Project 203005-003, Armstrong Cork Company, Lancaster, Pennsylvania, May, 1981.

Table 5.5: Summary of Steckler compartment experiments.

Test	Opening Width (m)	Opening Height (m)	HRR \dot{Q} (kW)	Burner Location	Test	Opening Width (m)	Opening Height (m)	HRR \dot{Q} (kW)	Burner Location
10	0.24	1.83	62.9	Center	224	0.74	0.92	62.9	Back Corner
11	0.36	1.83	62.9	Center	324	0.74	0.92	62.9	Back Corner
12	0.49	1.83	62.9	Center	220	0.74	1.83	31.6	Back Corner
612	0.49	1.83	62.9	Center	221	0.74	1.83	105.3	Back Corner
13	0.62	1.83	62.9	Center	514	0.24	1.83	62.9	Back Wall
14	0.74	1.83	62.9	Center	544	0.36	1.83	62.9	Back Wall
18	0.74	1.83	62.9	Center	512	0.49	1.83	62.9	Back Wall
710	0.74	1.83	62.9	Center	542	0.62	1.83	62.9	Back Wall
810	0.74	1.83	62.9	Center	610	0.74	1.83	62.9	Back Wall
16	0.86	1.83	62.9	Center	510	0.74	1.83	62.9	Back Wall
17	0.99	1.83	62.9	Center	540	0.86	1.83	62.9	Back Wall
22	0.74	1.38	62.9	Center	517	0.99	1.83	62.9	Back Wall
23	0.74	0.92	62.9	Center	622	0.74	1.38	62.9	Back Wall
30	0.74	0.92	62.9	Center	522	0.74	1.38	62.9	Back Wall
41	0.74	0.46	62.9	Center	524	0.74	0.92	62.9	Back Wall
19	0.74	1.83	31.6	Center	541	0.74	0.46	62.9	Back Wall
20	0.74	1.83	105.3	Center	520	0.74	1.83	31.6	Back Wall
21	0.74	1.83	158.0	Center	521	0.74	1.83	105.3	Back Wall
114	0.24	1.83	62.9	Back Corner	513	0.74	1.83	158.0	Back Wall
144	0.36	1.83	62.9	Back Corner	160	0.74	1.83	62.9	Center*
212	0.49	1.83	62.9	Back Corner	163	0.74	1.83	62.9	Back Corner*
242	0.62	1.83	62.9	Back Corner	164	0.74	1.83	62.9	Back Wall*
410	0.74	1.83	62.9	Back Corner	165	0.74	1.83	62.9	Left Wall*
210	0.74	1.83	62.9	Back Corner	162	0.74	1.83	62.9	Right Wall*
310	0.74	1.83	62.9	Back Corner	167	0.74	1.83	62.9	Front Center*
240	0.86	1.83	62.9	Back Corner	161	0.74	1.83	62.9	Doorway*
116	0.99	1.83	62.9	Back Corner	166	0.74	1.83	62.9	Front Corner*
122	0.74	1.38	62.9	Back Corner					* Raised burner

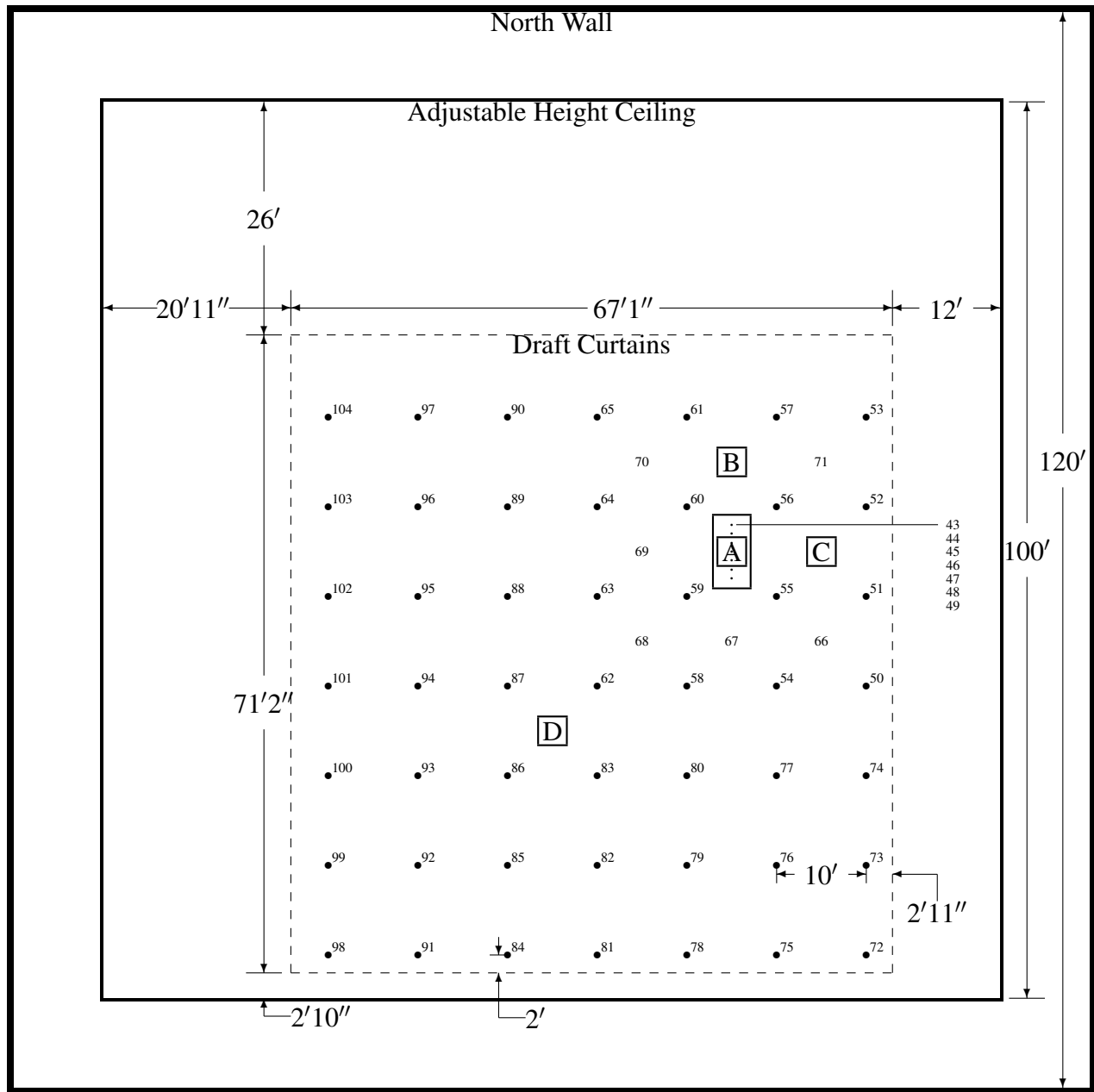


Figure 5.21: Plan view of the UL/NFPRF Experiments, Series I. The sprinklers are indicated by the solid circles and are spaced 3 m apart. The number beside each sprinkler location indicates the channel number of the nearest thermocouple. The vent dimensions are 4 ft by 8 ft. The boxed letters A, B, C and D indicate burner positions. Corresponding to each burner position is a vertical array of thermocouples. Thermocouples 1–9 hang 7, 22, 36, 50, 64, 78, 92, 106 and 120 in from the ceiling, respectively, above Position A. Thermocouples 10 and 11 are positioned above and below the ceiling tile directly above Position B, followed by 12–20 that hang at the same levels below the ceiling as 1–9. The same pattern is followed at Positions C and D, with thermocouples 21–31 at C and 32–42 at D.

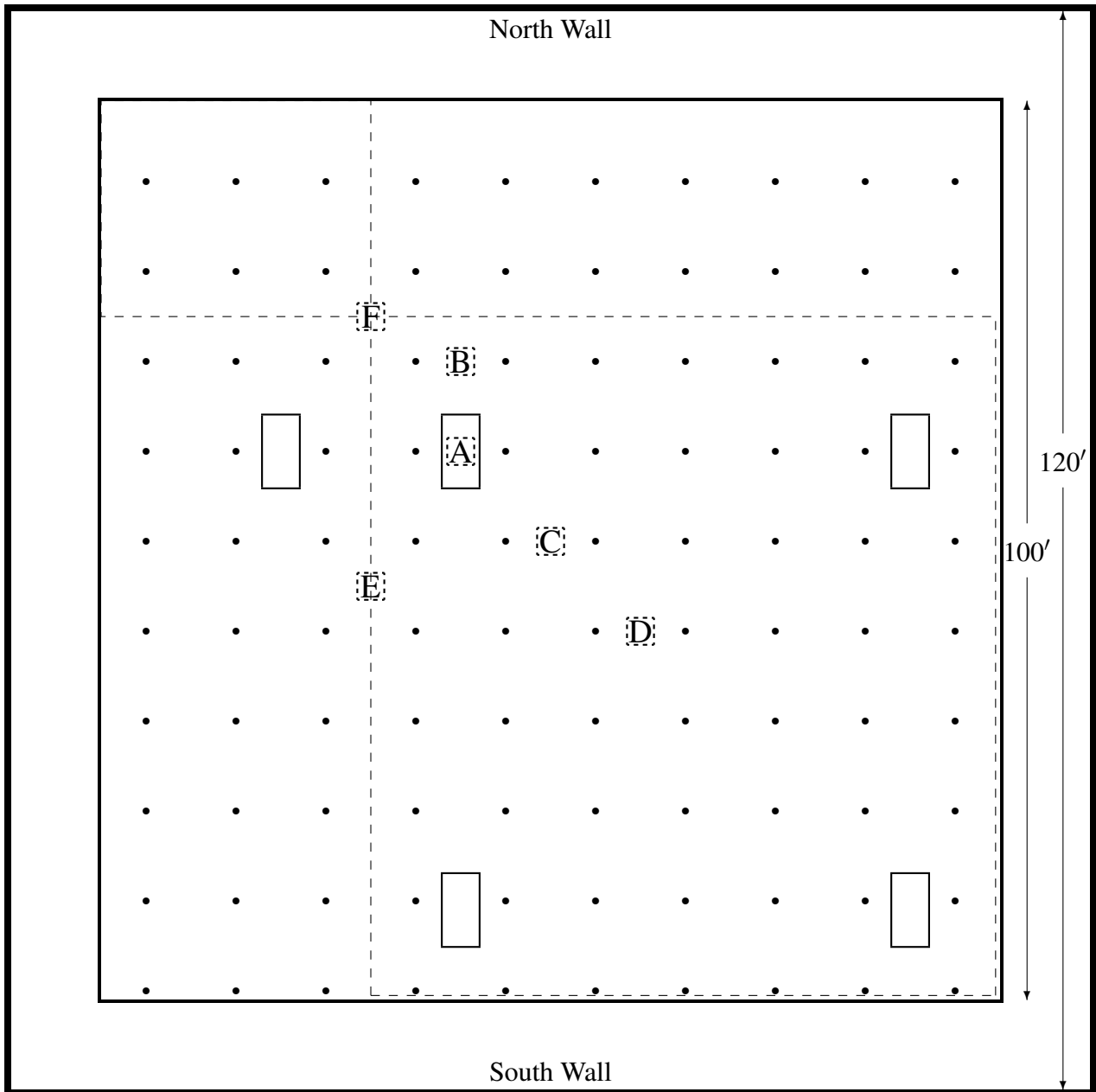


Figure 5.22: Plan view of the UL/NFPRF Experiments, Series II. The boxed letters A, B, C, D, E and F indicate burner positions. The sprinklers are indicated by the solid circles and are spaced 10 ft apart. The branch lines run north to south. The vents are 4 ft by 8 ft.

Sprinklers: Central ELO-231 (Extra Large Orifice) uprights were used for all the tests. The orifice diameter of this sprinkler is reported by the manufacturer to be nominally 1.6 cm (0.64 in), the reference actuation temperature is reported by the manufacturer to be 74°C (165°F). The RTI (Response Time Index) and C-factor (Conductivity factor) were reported by UL to be $148 \text{ (m}\cdot\text{s)}^{\frac{1}{2}}$ and $0.7 \text{ (m/s)}^{\frac{1}{2}}$, respectively [78]. When installed, the sprinkler deflector was located 8 cm below the ceiling. The thermal element of the sprinkler was located 11 cm below the ceiling. The sprinklers were installed with nominal 3 m by 3 m (exact 10 ft by 10 ft) spacing in a system designed to deliver a constant $0.34 \text{ L/(s}\cdot\text{m}^2)$ (0.50 gpm/ft^2) discharge density when supplied by a 131 kPa (19 psi) discharge pressure.

Vent: UL-listed double leaf fire vents with steel covers and steel curb were installed in the adjustable height ceiling in the position shown in Figs. 5.21 and 5.22. The vent is designed to open manually or automatically. The vent doors were recessed into the ceiling about 0.3 m (1 ft).

Heat Release Rate: The heptane spray burner consisted of a 1 m by 1 m square of 1.3 cm pipe supported by four cement blocks 0.6 m off the floor. Four atomizing spray nozzles were used to provide a free spray of heptane that was then ignited. For all but one of the Series I tests, the total heat release rate from the fire was manually ramped up following a “t-squared” curve to a steady-state in 75 s (150 s was used in Test I-16). The fire was ramped to 10 MW in 75 s for the Series II tests. The fire growth curve was followed until a specified fire size was reached or the first sprinkler activated. After either of these events, the fire size was maintained at that level until conditions reached roughly a steady state, i.e., the temperatures recorded near the ceilings remained steady and no more sprinkler activations occurred. The heat release rate from the burner was confirmed by placing it under the large product calorimeter at UL, ramping up the flow of heptane in the same manner as in the tests, and measuring the total and convective heat release rates. It was found that the convective heat release rate was 0.65 ± 0.02 of the total.

Instrumentation: The instrumentation for the tests consisted of thermocouples, gas analysis equipment, and pressure transducers. The locations of the instrumentation are referenced in the plan view of the facility (Fig. 5.21). Temperature measurements were recorded at 104 locations. Type K 0.0625 in diameter Inconel sheathed thermocouples were positioned to measure (i) temperatures near the ceiling, (ii) temperatures of the ceiling jet, and (iii) temperatures near the vent.

5.14 USN High Bay Hangar Experiments

The U.S. Navy sponsored a series of 33 tests within two hangars examining fire detection and sprinkler activation in response to spill fires in large enclosures [79, 80]. Experiments were conducted using JP-5 and JP-8 fuels in two Navy high bay aircraft hangars located in Naval Air Stations in Barber's Point, Hawaii and Keflavik, Iceland.

The Hawaii tests were conducted in a 15 m high hangar measuring 97.8 m in length and 73.8 m in width. Of the 13 tests conducted in the facility 11 were conducted in pans ranging from $.09 \text{ m}^2$ to 4.9 m^2 in area with heat release rates varying from 100 kW to 7.7 MW. The burner was placed

in the center of the room on a scale that continuously recorded the pans weight. The facility was equipped with a number of detection devices including thermocouples, electronic smoke and spot heat detectors, projected beam smoke detectors, combination UV/IR optical flame detectors, line-type heat detectors, as well as sprinklers. Measurements were recorded at a large number of locations allowing for a through profile of compartment behavior.

It was suspected that fire plume behavior and response of detection devices in a cold building may not have been well replicated by the experiments held in the warm hangar in Hawaii. The Iceland tests were conducted under a 22 m barrel vaulted ceiling in a hangar measuring 45.7 m by 73.8 m. 22 tests in total were conducted. The majority of these tests fires burned JP-5 fuel with the remainder burning JP-8. The jet fuel fires ranged in size from .06 m² to 20.9 m² and in heat release rate from 100 kW to approximately 33 MW. The facility was equipped similarly to the Hawaii hangar.

5.15 Vettori Flat Ceiling Experiments

Vettori [81] analyzed a series of 45 experiments conducted at NIST that were intended to compare the effects of different ceiling configurations on the activation times of quick response residential pendent sprinklers. The two ceiling configurations used consisted of an obstructed ceiling, with parallel beams 0.038 m wide by 0.24 m deep placed 0.41 m on center, and a smooth ceiling configuration, in which the beams were covered by a sheet of gypsum board. In addition to the two ceiling configurations, there were also three fire growth rates and three burner locations used – a total of 18 test configurations. The fire growth rate was provided by a computer controlled methane gas burner to mimic a standard t-squared fire growth rate with either a slow, medium, or fast ramp up. The burner was placed in a corner of the room, then against an adjacent wall, and then in a location removed from any wall. Measurements were taken to record sprinkler activation time, temperatures at varying heights and locations within the room, and the ceiling jet velocities at several other locations. A diagram of the test structure is displayed in Figure 5.23.

5.16 VTT Large Hall Tests

The experiments are described in reference [82]. The series consisted three unique fire scenarios with replications for a total of 8 experiments. The experiments were undertaken to study the movement of smoke in a large hall with a sloped ceiling. The tests were conducted inside the VTT Fire Test Hall, with dimensions of 19 m high by 27 m long by 14 m wide. Figure 5.24 shows the important features of the test hall. Figure 5.25 shows detailed plan, side and perspective schematic diagrams of the experimental arrangement. Each test involved a single heptane pool fire, ranging from 2 MW to 4 MW. Figure 5.26 is a photo of a 2 MW fire. Four types of measurements were used in the present evaluation – the hot gas layer temperature and depth, average flame height and the plume temperature. Three vertical arrays of thermocouples, plus two thermocouples in the plume, were compared to model simulation results. The hot gas layer temperature and height were reduced from an average of the three thermocouple arrays using a standard algorithm. The ceiling jet temperature was not considered, because the ceiling in the test hall is not flat, and the model algorithm is not appropriate for these conditions.

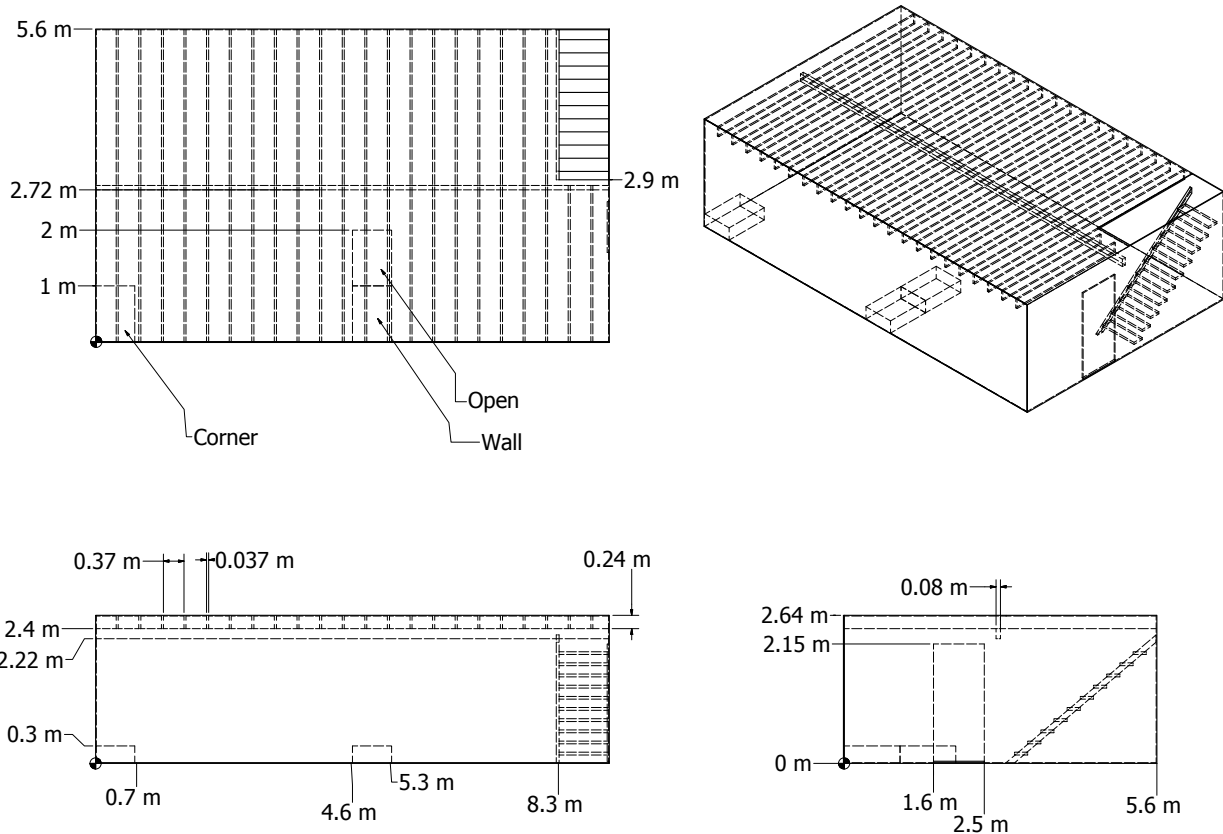


Figure 5.23: Geometry of the Vettori Flat Ceiling compartment.

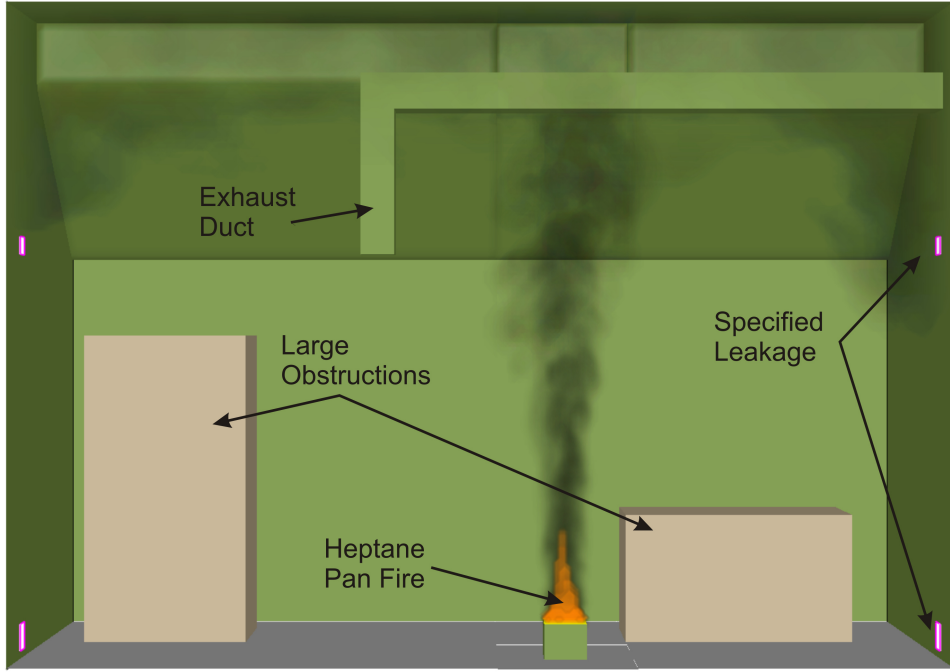


Figure 5.24: Cut-Away View of Case 2 of the VTT Large Hall Tests.

The VTT test report lacks some information needed to model the experiments, so some information was based on private communications with the principal investigator, Simo Hostikka. Details used to conduct the model simulations is presented in reference [64], including information on the fire, the compartment, and the ventilation.

The walls and ceiling of the test hall consist of a 1 mm thick layer of sheet metal on top of a 5 cm layer of mineral wool. The floor was constructed of concrete. The report does not provide thermal properties of these materials. Thermophysical properties of the materials that were used in the simulations are given in table 5.6.

Table 5.6: Thermophysical Properties for VTT Large Hall Tests

Material	Conductivity W/m°C	Specific Heat J/kg°C	Density kg/m ³	Thickness m	Emissivity
Steel ICFMP BE2	54	425	7850	0.001	0.95
Concrete ICFMP BE2	2	900	230	0.15	0.95

In Cases 1 and 2, all doors were closed, and ventilation was restricted to leakage through the building envelope. Precise information on air infiltration during these tests is not available. The scientists who conducted the experiments recommend a leakage area of about 2 m², distributed uniformly throughout the enclosure. By contrast, in Case 3, the doors located in each end wall (Doors 1 and 2, respectively) were open to the external ambient environment. These doors are each 0.8 m wide by 4 m high, and are located such that their centers are 9.3 m from the south wall. The

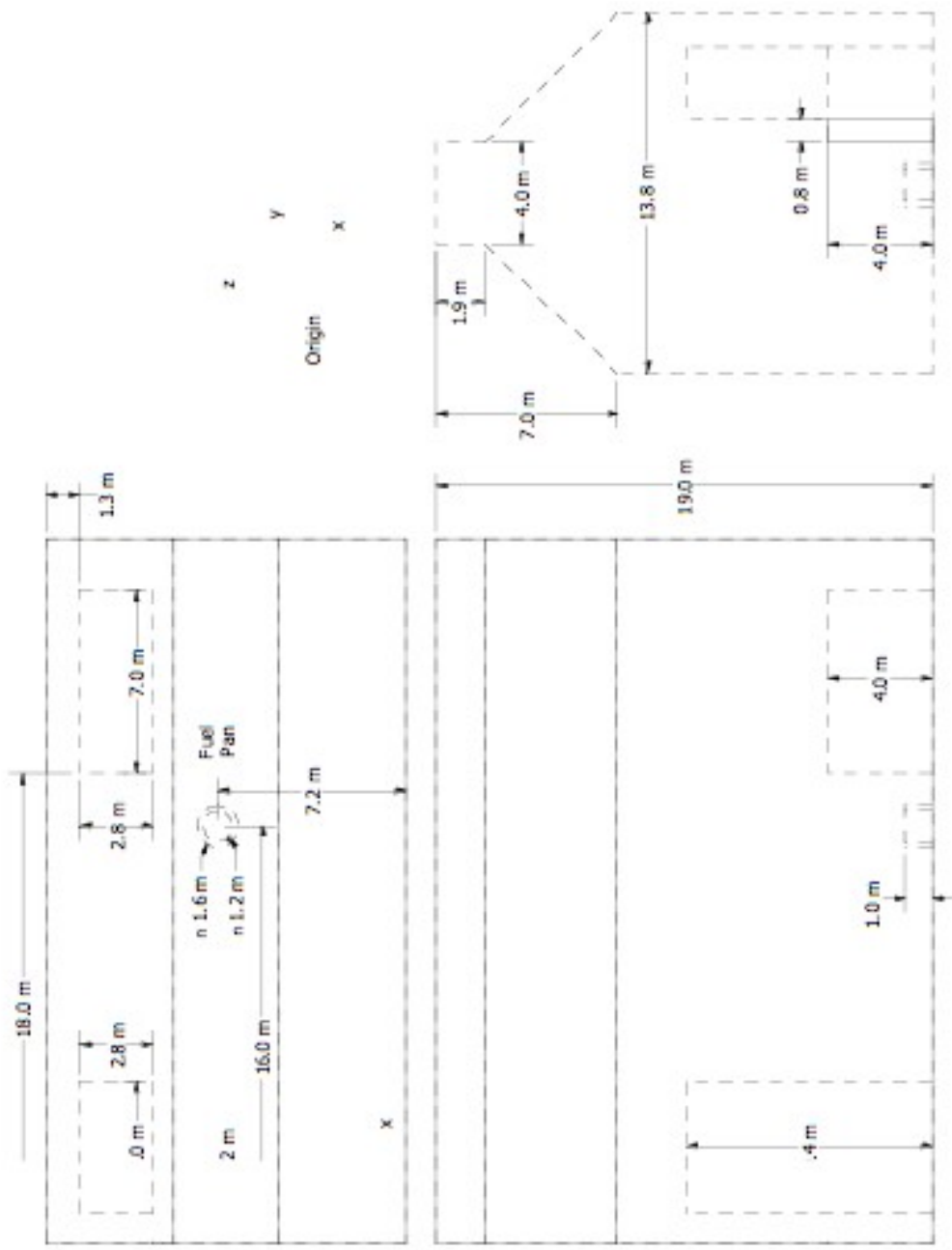


Figure 5.25: Plan, side and perspective schematic drawings of the experimental arrangement of the VTT large hall fire tests, including the fuel pan



Figure 5.26: Photo of a 2 MW heptane fire during the VTT large hall tests. Photo provided by Simo Hostikka, VTT.

test hall had a single mechanical exhaust duct, located in the roof space, running along the center of the building. This duct had a circular section with a diameter of 1 m, and opened horizontally to the hall at a distance of 12 m from the floor and 10.5 m from the west wall. Mechanical exhaust ventilation was operational for Case 3, with a constant volume flow rate of $11 \text{ m}^3/\text{s}$ drawn through the 1 m diameter exhaust duct.

Each test used a single fire source with its center located 16 m from the west wall and 7.4 m from the south wall. For all tests, the fuel was heptane in a circular steel pan that was partially filled with water. The pan had a diameter of 1.17 m for Case 1 and 1.6 m for Cases 2 and 3. In each case, the fuel surface was 1 m above the floor. The trays were placed on load cells, and the HRR was calculated from the mass loss rate. For the three cases, the fuel mass loss rate was averaged from individual replicate tests. In the HRR estimation, the heat of combustion (taken as 44.6 kJ/g) and the combustion efficiency for n-heptane was used. In this report, a combustion efficiency of 0.85 ± 0.12 (or $\pm 14\%$) was used for the VTT pool fire tests [64]. Due to the relatively large value of the uncertainty associated with the combustion efficiency the uncertainty in HRR is dominated by the uncertainty in the combustion efficiency. Uncertainty in the mass loss rate measurement also contributed to the overall uncertainty, and the uncertainty in HRR was estimated as 15 % [64]. Figure 5.27 show the prescribed HRR as a function of time during Cases 1 to 3, respectively. The radiative fraction was assigned a value of 0.35 [64], similar to many smoky hydrocarbons [69]. The relative combined expanded (2σ) uncertainty in this parameter was assigned a value of $\pm 20\%$, which is typical of uncertainty values reported in the literature for this parameter. Further details of the model inputs used for these simulations are included in reference [64].

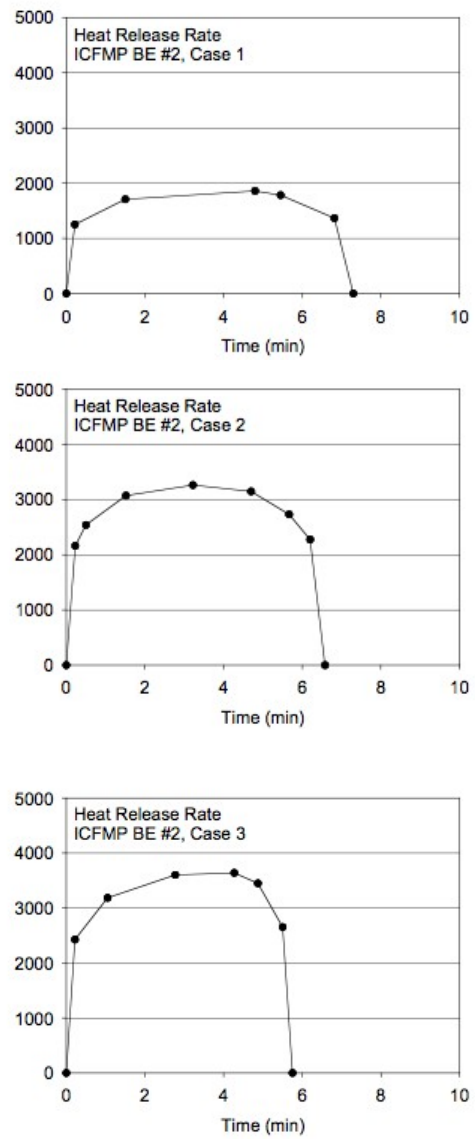


Figure 5.27: Prescribed Heat Release Rate as a Function of Time for VTT Large Hall Tests.

5.17 WTC Spray Burner Test Series

As part of its investigation of the World Trade Center disaster, the Building and Fire Research Laboratory at NIST conducted several series of fire experiments to both gain insight into the observed fire behavior and also to validate FDS for use in reconstructing the fires. The first series of experiments involved a relatively simple compartment with a liquid spray burner and various structural elements with varying amounts of sprayed fire-resistive materials (SFRM). A diagram of the compartment is shown in figure 5.28. A complete description of the experiments can be found in the NIST WTC report NCSTAR 1-5B [83]. The overall enclosure was rectangular, as were the vents and most of the obstructions. The compartment walls and ceiling were made of 2.54 cm thick marinite. The manufacturer provided the thermal properties of the material used in the calculation. The density was 737 kg/m^3 , conductivity 0.12 W/m/K . The specific heat ranged from 1.17 kJ/kg/K at 93°C to 1.42 kJ/kg/K at 425°C . This value was assumed for higher temperatures. The steel used to construct the column and truss flanges was 0.64 cm thick. The density of the steel was assumed to be $7,860 \text{ kg/m}^3$; its specific heat 0.45 kJ/kg/K .

Two fuels were used in the tests. The properties of the fuels were obtained from measurements made on a series of unconfined burns that are referenced in the test report. The first fuel was a blend of heptane isomers, C_7H_{16} . Its soot yield was set at a constant 1.5 %. The second fuel was a mixture (40 % - 60 % by volume) of toluene, C_7H_8 , and heptane. Because FDS only considers the burning of a single hydrocarbon fuel, the mixture was taken to be C_7H_{12} with a soot yield of 11.2 %. The radiative fraction for the heptane blend was 0.44; for the heptane/toluene mixture it was 0.39. The heat release rate of the simulated burner was set to that which was measured in the experiments with the fire placed on the floor at the center of the fire pan.

5.18 Summary of Experiments

Table 5.7 presents a summary of all the experiments described in this chapter in terms of quantities commonly used in fire protection engineering. This “parameter space” outlines the range of applicability of the validation studies performed to date. The parameters are explained below:

Heat Release Rate, \dot{Q} , is the range of peak heat release rates of the fires in the test series.

Fire Diameter, D , is the equivalent diameter of the base of the fire, calculated $D = \sqrt{4A/\pi}$, where A is the area of the base.

Ceiling Height, H , is the distance from floor to ceiling.

Fire Froude Number, \dot{Q}^* , is a useful non-dimensional quantity for plume correlations and flame height estimates.

$$\dot{Q}^* = \frac{\dot{Q}}{\rho_\infty c_p T_\infty \sqrt{g D D^2}} \quad (5.2)$$

It is essentially the ratio of the fuel gas exit velocity and the buoyancy-induced plume velocity. Jet fires are characterized by large Froude numbers. Typical accidental fires have a Froude number near unity.

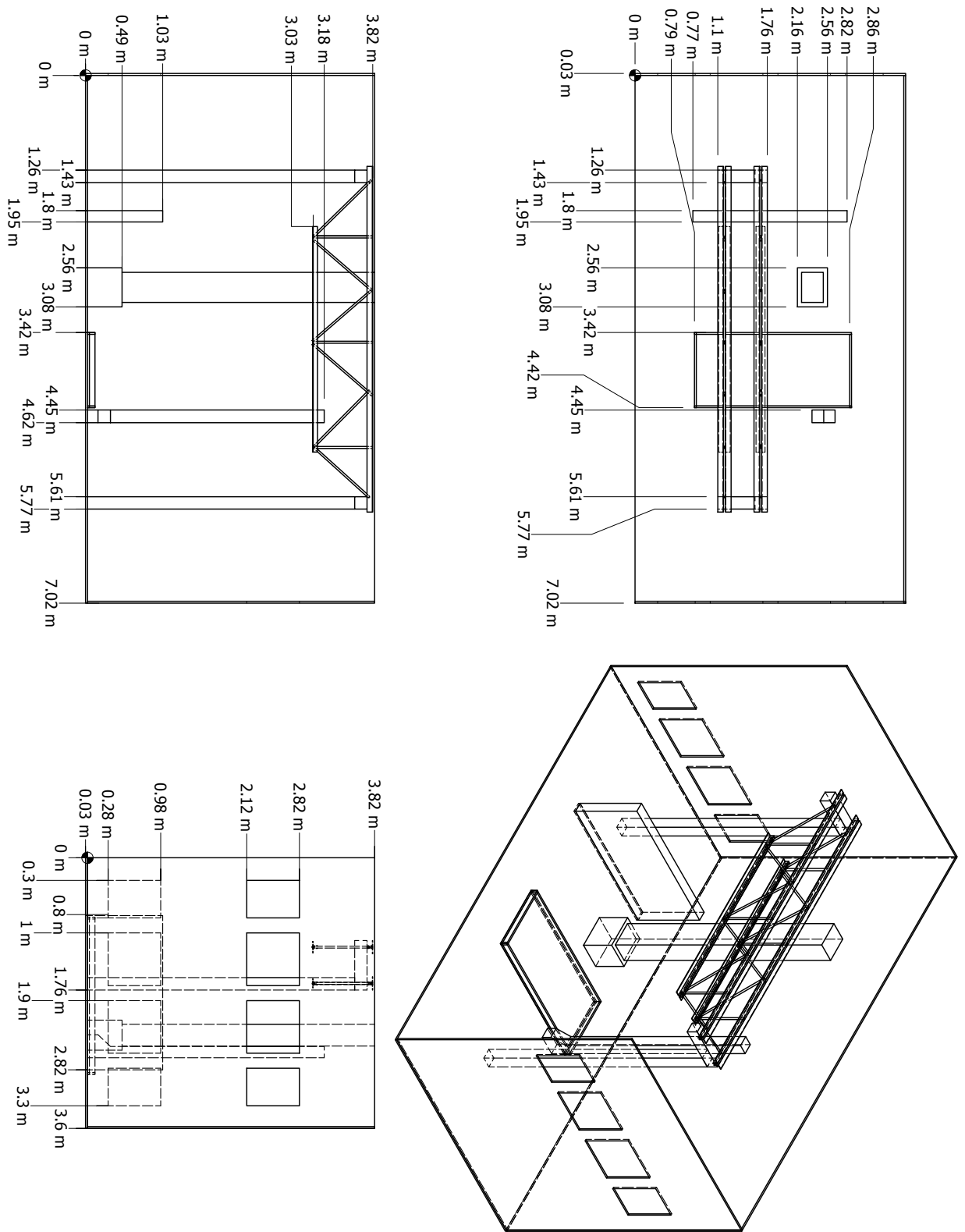


Figure 5.28: Geometry of the WTC Experiments.

Flame Height relative to Ceiling Height, L_f/H , is a convenient way to express the physical size of the fire relative to the size of the room. The height of the visible flame, based on Hesketh's correlation, is estimated by:

$$L_f = D \left(3.7 (\dot{Q}^*)^{2/5} - 1.02 \right) \quad (5.3)$$

Global Equivalence Ratio, ϕ , is the ratio of the mass flux of fuel to the mass flux of oxygen into the compartment, divided by the stoichiometric ratio.

$$\phi = \frac{\dot{m}_f}{r \dot{m}_{O_2}} \equiv \frac{\dot{Q}(\text{kW})}{13,100(\text{kJ/kg}) \dot{m}_{O_2}} \quad ; \quad \dot{m}_{O_2} = \begin{cases} \frac{1}{2} 0.23 A_0 \sqrt{H_0} & : \text{Natural Ventilation} \\ 0.23 \rho \dot{V} & : \text{Mechanical Ventilation} \end{cases} \quad (5.4)$$

Here, r is the stoichiometric ratio, A_0 is the area of the compartment opening, H_0 is the height of the opening, ρ is the density of air, and \dot{V} is the volume flow of air into the compartment. If $\phi < 1$, the compartment is considered "well-ventilated" and if $\phi > 1$, the compartment is considered "under-ventilated."

Compartment Aspect Ratios, W/H and L/H , indicate if the compartment is shaped like a hallway, typical room, or vertical shaft.

Relative Distance along the Ceiling, r_{cj}/H , indicates the distance from the fire plume of a sprinkler, smoke detector, etc., relative to the compartment height, H .

Relative Distance from the Fire, r_{rad}/D , indicates whether a "target" is near or far from the fire.

Table 5.7: Summary of important experimental parameters.

Test Series	\dot{Q} (kW)	D (m)	H (m)	Q^*	L_f/H	ϕ	W/H	L/H	r_{cj}/H	r_{rad}/D
ATF Corridors	50 – 500	0.5	2.4	0.3 – 3.1	0.3 – 1	0.01 – 0.07	0.8	7.1	0.8 – 6	N/A
FM/SNL	470 – 516	0.9	6.1	0.5 – 0.6	0.3	0.2	2.0	3.0	0.2 – 0.3	N/A
LLNL Enclosure	50 – 400	0.6	4.5	0.2 – 1.4	0.1 – 0.4	0.03 – 0.22	0.9	1.3	0.3 – 1.0	N/A
NBS Multi-Room	110	0.3	2.4	1.4	0.4 – 5.2	0.12	1.0	5.1	0.5 – 0.7	0.9 – 2.4
NIST/NRC	350 – 2200	1.0	3.8	0.3 – 1.9	0.4 – 1.1	0.04 – 0.7	1.9	5.7	0.3 – 2.1	2 – 4
Sandia Plume	2025 – 5450	1.0	Open	1.7 – 4.6	Open	Open	Open	Open	N/A	N/A
SP AST	450	0.3	2.4	5.7	1	0.1	1.0	1.5	N/A	N/A
Steckler	31.6 – 158	0.3	2.1	0.7 – 3.5	0.3 – 0.7	0.01 – 0.6	1.3	1.3	N/A	N/A
UL/NFPRF	4400 – 10000	1.0	7.6	3.7 – 8.5	0.8 – 1.1	0	4.9	4.9	0.1 – 2.0	N/A
USN Hawaii	100 – 7700	0.3 – 2.5	15	1.3 – 0.7	0.1 – 0.4	0	4.9	6.5	0 – 1.2	N/A
USN Iceland	100 – 15700	0.3 – 3.4	22	1.3 – 0.6	0.1 – 0.4	0	2.1	3.4	0 – 1.0	N/A
Vettori Flat	1055	0.7	2.6	2.3	1.2	Closed	2.1	3.5	0.8 – 2.9	N/A
VTT Large Hall	1860 – 3640	1.4 – 1.8	19	0.7	0.2	0	1.0	1.4	0 – 0.6	N/A
WTC	965 – 1460	1.0	3.8	0.8 – 1.2	0.7 – 0.9	0.9	1.8	0.1	0.5 – 2	

Chapter 6

Hot Gas Layer Temperature and Depth

CFAST simulated all of the chosen experiments. Details of the comparisons with experimental data, are provided in Appendix A. The results are organized by quantity as follows:

- hot gas layer (HGL) temperature and height
- ceiling jet temperature
- plume temperature
- flame height
- oxygen and carbon dioxide concentration
- smoke concentration
- compartment pressure
- radiation heat flux, total heat flux, and target temperature
- wall heat flux and surface temperature

The measure of model accuracy used throughout this study is related to experimental uncertainty. Reference [64] discusses this issue in detail. In brief, the accuracy of a measurement, for example, a gas temperature, is related to the measurement device, a thermocouple. In addition, the accuracy of the model prediction of the gas temperature is related to the simplified physical description of the fire and the accuracy of the input parameters, especially the specified heat release rate. Ideally, the purpose of a validation study is to determine the accuracy of the model in the absence of any errors related to the measurement of both its inputs and outputs. Because it is impossible to eliminate experimental uncertainty, at the very least a combination of the uncertainty in the measurement of model inputs and output can be used as a yardstick. Dotted lines in figure 6.1 show this combined uncertainty estimate for HGL temperature and layer depth. Corresponding estimates are included for other quantities in later sections. If the numerical prediction falls within the range of uncertainty attributable to both the measurement of the input parameters and the output quantities, it is not possible to further quantify its accuracy. At this stage, it is said that the prediction is within experimental uncertainty.

Note that the calculation of relative difference is based on the temperature rise above ambient, and the layer depth, that is, the distance from the ceiling to where the hot gas layer descends. Where the model over-predicts the HGL temperature or the depth of the HGL, the relative difference is a positive number. This convention is used throughout this report where the model over-predicts the severity of the fire, the relative difference is positive; where it under-predicts, the difference is negative.

Arguably the most frequent question asked about a fire is, How hot did it become? Temperature in the upper layer of a compartment is an obvious indicator to answer this question. Peak temperature, time to peak temperature, or time to reach a chosen temperature tenability limit are typical values of interest. Quality of the prediction (or measurement) of layer interface position is more difficult to quantify. Although observed in a range of experiments, the two-layer assumption is in many ways just a convenience for modeling. In experimental measurements, temperature is typically measured with an array of thermocouples from floor to ceiling. This floor to ceiling temperature profile can then be used to estimate a hot gas layer height and the temperature of the upper and lower gas layers [84] [85] consistent with the two-zone assumption. Appendix A provides details of the calculation.

From a standpoint of hazard, time of descent to a chosen level may be a reasonable criterion (assuming some in the room will then either be forced to crawl beneath the interface to breathe the clean atmosphere near the floor or be forced to breath the upper layer gases). Minimum values may also be used to indicate general agreement. For the single-room tests with furniture or wall-burning, these are appropriate indicators to judge the comparisons between model and experiment. For the more-closely steady-state three- and four-room tests with corridor or the multiple-story building tests, a steady-state average may better characterize the nature of the experiment.

A good prediction of the HGL height is largely a consequence of a good prediction of its temperature because smoke and heat are largely transported together and most numerical models describe the transport of both with the same type of algorithm. Typically, CFAST slightly over-predicts the HGL temperature, most often within experimental uncertainty. Hot gas layer height is typically within experimental uncertainty for well-ventilated tests and near floor level for under-ventilated tests where compartments are closed to the outside. For HGL height, only values from open-door tests are included. For closed-door tests, visual observations typically show that the HGL fills the entire compartment volume from floor to ceiling, inconsistent with the calculated results for the experimental data. Thus, the calculated experimental values of HGL height for closed-door tests are not seen as appropriate for comparison to model results.

6.1 Model / Experiment Comparisons

Figure 6.1 shows a comparison of predicted and measured values for HGL temperature and depth. Appendix A provides individual graphs of model and experimental values and tables of peak values and relative differences.

Following is a summary of the accuracy assessment for the HGL predictions of the test series:

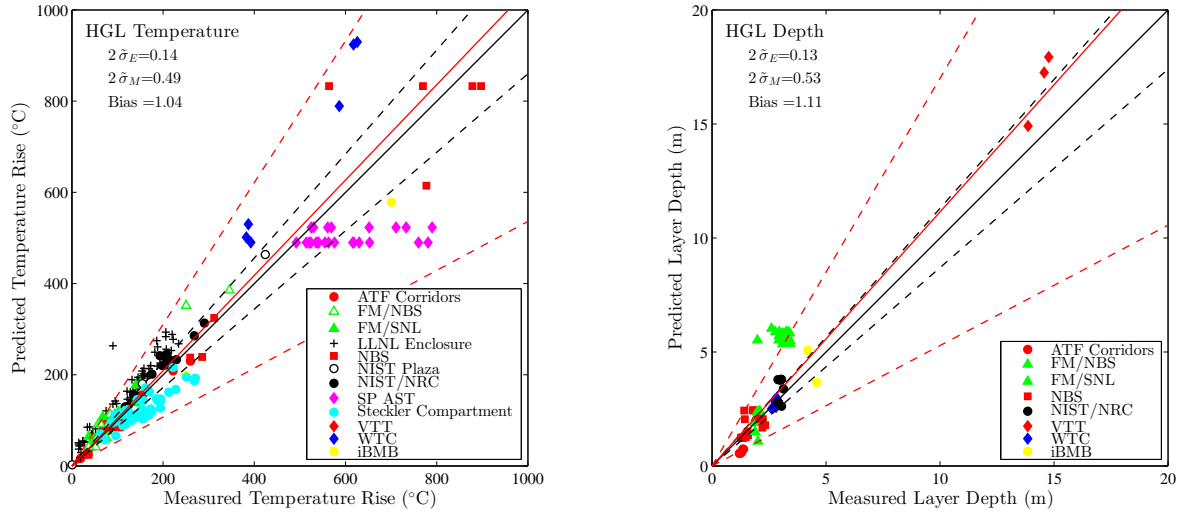


Figure 6.1: Comparison of Measured and Predicted HGL Temperature and Height.

NBS Single Room Tests with Furniture

For two of the four tests (Tests F1 and F6, tests with a single furniture item in the compartment), the HGL temperature and depth for these tests were calculated separately for two different thermocouple arrays, one located in the front of the compartment and one in the rear. For the other two tests (tests W1 and W2, tests with furniture and a wood wall surface), a single thermocouple array was available.

For the single-room tests, predicted temperatures and layer interface position show obvious similarities to the measured values (see, for example, figure 6.2). Peak values occurred at similar times with comparable rise and fall for most comparisons. Interface height for the single-room with wall-burning is a notable exception. Unlike the model prediction, the experimental measurement did not show the rise and fall in concert with the temperature measurement. Peak values were typically higher for upper layer temperature and lower for lower layer temperature and layer interface position.

For the furniture tests, the agreement ranges from a relative difference of -43% to 31%. The agreement is quite different for the two arrays in each test. Table 6.1 shows the relative differences for tests F1 and F6. For both the layer temperature and layer depth, the difference between the model and experiment changes depending on the measurement location. In the same test (F1) the values are well within experimental uncertainty at one location and outside for the other. For test F6, the differences are greater. For these tests with a post-flashover fire in a small compartment, the assumption of a uniform upper layer may be questionable. Still, curve shape for the experimental data and model predictions is quite similar.

VTT Large Hall Test Series

The HGL temperature and depth were calculated from the averaged gas temperatures from three vertical thermocouple arrays. Ten thermocouples in each vertical array, spaced 2 m apart in the

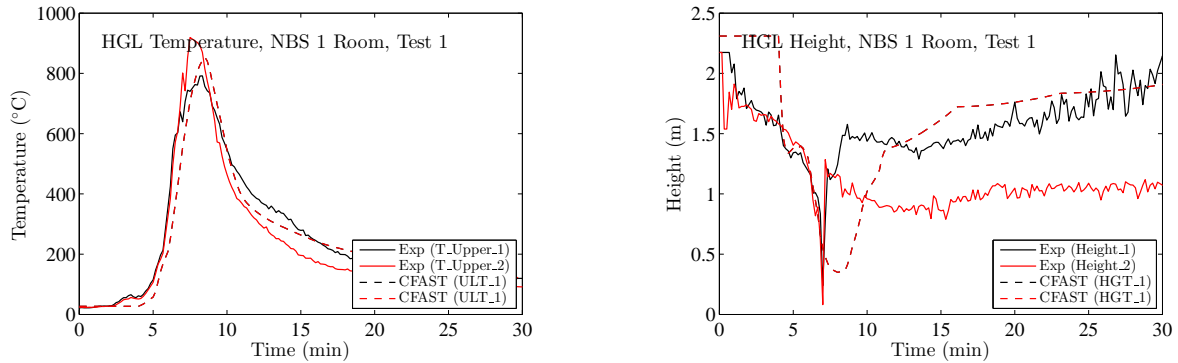


Figure 6.2: Measured and Predicted HGL Temperature and Height for a Single Compartment Test.

Table 6.1: Relative Difference for HGL Temperature and Depth for Two Measurement Locations in Two Single-Room Tests

Test	Location	Temperature %	Layer Depth %
F1	A	-4	-1
	B	-18	-8
F6	A	31	-8
	B	-16	-43

lower two-thirds of the hall, and 1 m apart near the ceiling were used to determine layer temperatures and depth.

CFAST predicts the HGL temperature and height near experimental uncertainty for all three tests, with relative differences ranging from 6 % to 10 %, depending on the test. Relative differences are shown in figure 6.1.

NIST/NRC Test Series

The NIST/NRC series consisted of 15 liquid spray fire tests with different heat release rates, pan locations, and ventilation conditions. Gas temperatures were measured using seven floor-to-ceiling thermocouple arrays (or “trees”) distributed throughout the compartment. The average hot gas layer temperature and height were calculated using thermocouple Trees 1, 2, 3, 5, 6 and 7. Tree 4 was not used because one of its thermocouples malfunctioned during most of the experiments.

A few observations about the simulations:

- In the closed-door tests, the HGL layer descended all the way to the floor. However, the reduction method used on the measured temperatures (see reference [85]) does not account for the formation of a single layer and, therefore, does not indicate that the layer dropped all the way to the floor, rather just to the position of the lowest temperature measurement point. This is not a flaw in the measurements, but rather that the data reduction method only applies to tests where two distinct layers are present, i.e., in the open door tests.
- The HGL reduction method produces spurious results in the first few minutes of each test because no clear layer has yet formed.

CFAST predicts the HGL temperature to within experimental uncertainty for all of the closed-door tests. Relative differences for the open-door tests are somewhat higher, ranging from 9 % for Test 15 to 24 % for Test 18. CFAST predicts HGL height to within experimental uncertainty for the open-door tests.

FM/SNL Test Series

Tests 4, 5, and 21 from the FM/SNL test series are selected for comparison. The hot gas layer temperature and height are calculated using the standard method. The thermocouple arrays that are referred to as Sectors 1, 2 and 3 are averaged (with an equal weighting for each) for Tests 4 and 5. For Test 21, only Sectors 1 and 3 are used, as Sector 2 falls within the smoke plume.

Note the following:

- The experimental HGL heights are somewhat noisy because of the effect of ventilation ducts in the upper layer. The corresponding predicted HGL heights are consistently lower than experimental measurements, typically approaching floor level by the end of the test. This is likely a combination of the calculation technique for the experimental measurements and rules for flow from mechanical vents in the CFAST model.
- The ventilation was turned off after 9 minutes in Test 5, the effect of which was a slight increase in the measured HGL temperature.

CFAST predicts the HGL temperature well within experimental uncertainty for Tests 4 and 5, but overpredicts for Test 21. This is likely because of the configuration of the fire in the test, with the fire inside a cabinet in the fire compartment. This complex geometry leads to an interaction between the fire and the confining cabinet that a zone model cannot simulate.

iBMB Compartment Tests

CFAST predicts the HGL temperature and height somewhat outside experimental uncertainty with some discrepancy in the shapes of the curves. It is not clear whether this is related to the measurement or the model. For the cable fire test (Test 4), this is likely because of the complicated geometry within the compartment that includes a partial height wall that affects both plume entrainment and radiative heat transfer from the fire to surroundings.

NBS Multi-Room Test Series

This series of experiments consists of two relatively small rooms connected by a long corridor. The fire is located in one of the rooms. Eight vertical arrays of thermocouples are positioned throughout the test space: one in the burn room, one near the door of the burn room, three in the corridor, one in the exit to the outside at the far end of the corridor, one near the door of the other or “target” room, and one inside the target room. Four of the eight arrays have been selected for comparison with model prediction: the array in the burn room (BR), the array in the middle of the corridor (5.5 m from the BR), the array at the far end of the corridor (11.6 m from the BR), and the array in the target room (TR). In Tests 100A and 100O, the target room is closed, in which case the array in the exit (EXI) doorway is used. The test director reduced the layer information individually for the eight thermocouple arrays using an alternative method. These results are included in the original data sets. However, for the current validation study, the selected TC trees were reduced using the method common to all the experiments considered.

CFAST predicts the HGL temperature and depth to within experimental uncertainty for many of the measurement locations in the three tests considered, averaging within 14% for the HGL temperature and 21% for the HGL depth. The discrepancies in various locations appear to be attributable to experimental, rather than model, error. In particular, the calculation of HGL temperature and height are quite sensitive to the measured temperature profile, which in these tests was determined with bare-bead thermocouples that are subject to quite high uncertainties. Wide spacing of the thermocouples also leads to higher uncertainty in HGL height.

Calculations of HGL temperature and depth in rooms remote from the fire tend to higher relative differences than those closer to the fire. This is likely a combination of the simplified single representative layer temperature inherent in zone models (temperature in the long corridor of this test series varied from one end of the compartment to the other), calculation of flow through doorways based on a correlation based on the pressure difference between the connected compartments, and unknown leakage from each the compartments that would effect these pressure differences.

FM Four Room Including Corridor Test Series

This series of experiments has a burn room connected to a long corridor with two smaller compartments at the far end of the corridor. Six vertical arrays of thermocouples (one in most com-

parts and three in the corridor) were used to estimate layer temperature and depth. In general, CFAST over predicts layer temperature and depth closer to the fire with a general trend towards under prediction at locations more remote from the fire; at times within experimental uncertainty but with significant over prediction at other locations. Relative differences averaged within 14 % for HGL temperature and within 21 % for HGL depth.

NIST Seven-story Hotel Tests

These tests were conducted in a seven story hotel with multiple rooms on each floor and a stairwell connecting all floors. Layer temperatures are available for comparison directly from the data. Relative differences comparing model and experiment are well within experimental uncertainty except on the seventh floor. While the relative difference for this location was quite large (292 %, this represents a 2 °C over prediction by the model.

6.2 Summary

Following is a summary of the accuracy assessment for the HGL predictions. The two-zone assumption inherent in CFAST, modeled as a series of ordinary differential equations that describe mass and energy conservation of flows in a multiple-compartment structure typically provide appropriate prediction of gas layer temperature and layer height for the applications studied.

- The CFAST predictions of the HGL temperature and height are, with a few exceptions, within or close to experimental uncertainty. On average, predicted HGL temperature is within 14 % and HGL depth is within 21 % of experimental measurements. The CFAST predictions are typical of those found in other studies where the HGL temperature is typically somewhat over-predicted and HGL height somewhat lower (HGL depth somewhat thicker) than experimental measurements. These differences are likely attributable to simplifications in the model dealing with mixing between the layers, entrainment in the fire plume, and flow through vents.
- Calculation of HGL temperature and height has higher uncertainty in rooms remote from the fire compared to those in the fire compartment. Most likely, this is due to a combination of the simplified vent flow predictions (based on idealized Bernoulli flow) and the assumption of constant compartment surface thermal properties that are assumed independent of temperature.

Chapter 7

Fire Plumes, Ceiling Jets, and Device Activation

7.1 Flame Height

Flame height is recorded by visual observations, photographs, or video footage. Videos from the NIST/NRC test series and photographs from the VTT Large Hall Test Series are available. It is difficult to precisely measure the flame height, but the photos and videos allow one to make estimates accurate to within a pan diameter.

VTT Large Hall Test Series

The height of the visible flame in the photographs has been estimated to be between 2.4 and 3 pan diameters (3.8 m to 4.8 m). From the CFAST calculations, the estimated flame height is 4.3 m.

NIST/NRC Test Series

CFAST estimates the peak flame height to be 2.8 m, consistent with the roughly 3 m flame height observed through the doorway during the test. The test series was not designed to record accurate measurements of flame height.

NIST/Navy High Bay Hangar Test Series

For the 9 Iceland tests, CFAST predicts flame height within 25 % of the experimentally reported values, with the largest relative differences for the smaller heat release rate fires. Uncertainty in the flame height measurements for the experiments was reported to be ± 0.5 m, approaching 30 % of the experimental values for the lower heat release rate fires.

7.2 Plume Temperature

As with the ceiling jet, CFAST includes a specific plume temperature model based on the McCaffrey plume [86, 87] to account for presence of higher gas temperatures near a target located

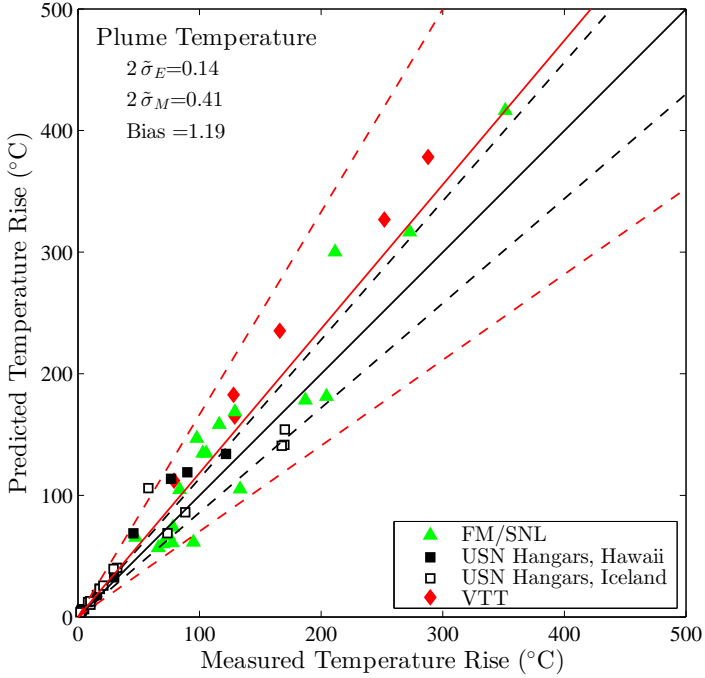


Figure 7.1: Comparison of Measured and Predicted Plume Centerline Temperature.

at the centerline of the fire plume. the correlation has been subjected to extensive validation efforts by McCaffrey [86] and others [23] and shown to provide predictions within about 30 % of a wide range of experimental results [23]. In the model, this increased temperature has the effect of increasing the convective heat transfer to the target. Only two of the six test series (VTT and FM/SNL) included measurements of plume centerline temperature.

Figure 7.1 shows a comparison of predicted and measured values for plume temperature. Appendix A provides individual graphs of model and experimental values. All of the comparisons are to the surrounding gas temperature predicted by CFAST. Comparisons to the target surface temperature or target center temperature would be expected to have a smaller relative difference since all the predictions of surrounding gas temperature are higher than experimental measurements. Following is a summary of the predictions in the two test series.

VTT Test Series

With one exception, CFAST predicts plume temperature within experimental uncertainty for the experiments in this test series. The predictions average within 10 % of the experimental measurements.

FM/SNL Test Series

For the tests in this test series, predictions are near experimental uncertainty (averaging within 13 % of experimental measurements). This does not include results from test 21 since this test was a fire inside an electrical equipment cabinet that did not form a well-defined plume within the larger compartment.

NIST / Navy High Bay Hangar Test Series

Predictions for the high bay tests average within 30 %. With a wide range of fire sizes (from 1.4 MW to 33 MW), this test series provides a broad evaluation of the underlying correlations used in the model. The two tests with the highest relative difference are the lowest heat release rate tests. With all plume temperature measurements made at a height of more than 22 m, a higher uncertainty for the lowest heat release rate tests is understandable.

7.3 Ceiling Jets

CFAST includes an algorithm to account for the presence of the higher gas temperatures near the ceiling surfaces in compartments involved in a fire. In the model, this increased temperature has the effect of increasing the convective heat transfer to ceiling surfaces. The temperature and velocity of the ceiling jet are also available from the model by placing a heat detector at the specified location. The ceiling jet algorithm is based on the model by Cooper [88], with details described in the CFAST Technical Reference Guide [2]. The algorithm predicts gas temperature and velocity under a flat, unconstrained ceiling above a fire source. Only two of the six test series (NIST/NRC and FM/SNL) involved relatively large flat ceilings.

Figure 7.2 shows a comparison of predicted and measured values for ceiling jet temperature. Appendix A provides individual graphs of model and experimental values. Following is a summary of the accuracy assessment for the ceiling jet predictions in the two test series.

NIST/NRC Test Series

The thermocouple nearest the ceiling in Tree 7, located towards the back of the compartment, has been chosen as a surrogate for the ceiling jet temperature. This location was well removed from the fire plume so that plume effects would not be evident, but closer to the wall surfaces so that the assumption of an unconfined ceiling inherent in the typical ceiling jet correlations that wall effects may impact the comparison. Still, CFAST predicts ceiling jet temperature well within experimental uncertainty for all but one of the tests in the series, with an average relative difference of 5 %. For these tests, the fire source was sufficiently large (relative to the compartment size) such that a well-defined ceiling jet was evident in temperature measurements near ceiling level.

FM/SNL Test Series

With fire sizes comparable to the smaller fire sizes used in the tests in NIST/NRC test series and compartment volumes significantly larger, measured temperature rise near the ceiling in the FM/SNL tests was below 100 °C in all three tests. Relative differences averaged within 19 % of

t

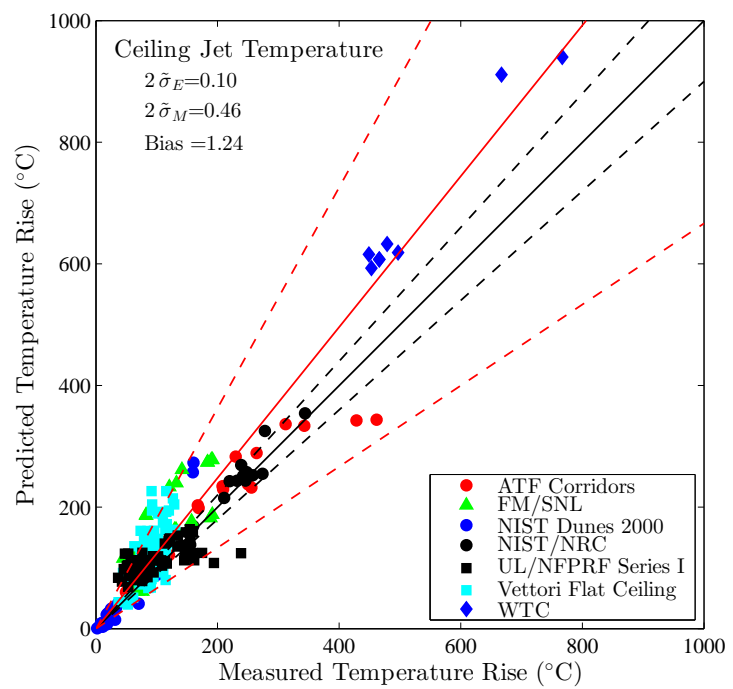


Figure 7.2: Comparison of Measured and Predicted Ceiling Jet Temperature.

experimental measurements. Hot gas layer temperatures for these tests were below 70 °C . CFAST consistently predicts higher ceiling jet temperatures in the FM/SNL tests compared to experimental measurements. With a larger compartment relative to the fire size, the ceiling jet for the FM/SNL tests is not nearly as well-developed as those in the NIST/NRC tests. The difference between the experimental ceiling jet temperature and HGL temperature for the FM/SNL tests is less than half that observed in the NIST/NRC tests. While the over-prediction of ceiling jet temperature could be considered conservative for some applications, for scenarios involving sprinkler or heat detector activation, the increased temperature in the ceiling jet would lead to shorter estimates of activation times for the simulated sprinkler or heat detector.

7.4 Device Activation

Smoke detector, heat detector, and sprinkler activations are all treated similarly in CFAST. Device activation is modeled using temperatures and velocities from the ceiling jet. For rooms without a fire (which do not have a ceiling jet), the upper layer temperature (and a default velocity of 0.1 m/s) is used. Devices are described with a characteristic activation temperature and response time index (RTI). The RTI a measure of the sensor's sensitivity to temperature change (thermal inertia). For heat detectors and sprinklers, the activation temperature and RTI values are part of the device specification. For smoke detectors, a temperature rise of 10 °C and RTI of 5 (m s)^{1/2} were used, consistent with values in NUREG 1805 [89]. With these inputs, the characteristic detector temperature is modeled using the differential equation [90]

$$\frac{dT_L}{dt} = \frac{\sqrt{v(t)}}{RTI} (T_g(t) - T_L(t)), \quad T_L(0) = T_g(0) \quad (7.1)$$

where T_L and T_g are the link and gas temperatures, v is the gas velocity, and RTI .

Figure 7.3 shows a comparison of predicted and measured values for activation times. Appendix A provides individual graphs of model and experimental values. Following is a summary of predictions in the test series.

7.5 Summary

Based on the model physics and comparisons of model predictions with experimental measurements, CFAST provides appropriate calculations of flame height for the following reasons:

- The correlation used in CFAST to predict plume temperature is well-suited for this application and has been subjected to extensive comparisons with experimental results.
- CFAST provides predictions consistent with visual observation for available data in this validation exercise.

Based on the model physics and comparisons of model predictions with experimental measurements, the use of CFAST to predict plume temperature requires caution for the following reasons:

- The correlation used in CFAST to predict plume temperature is well-suited for this application and has been subjected to extensive validation efforts.

t

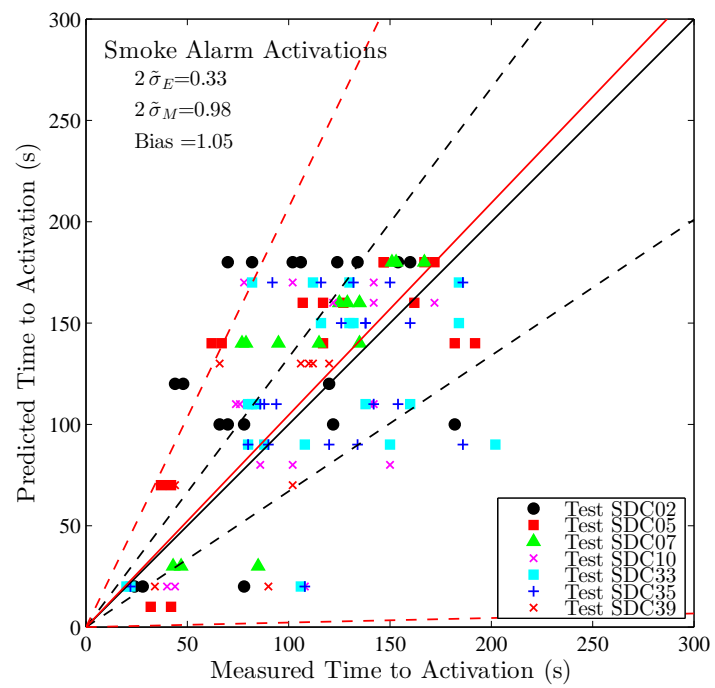
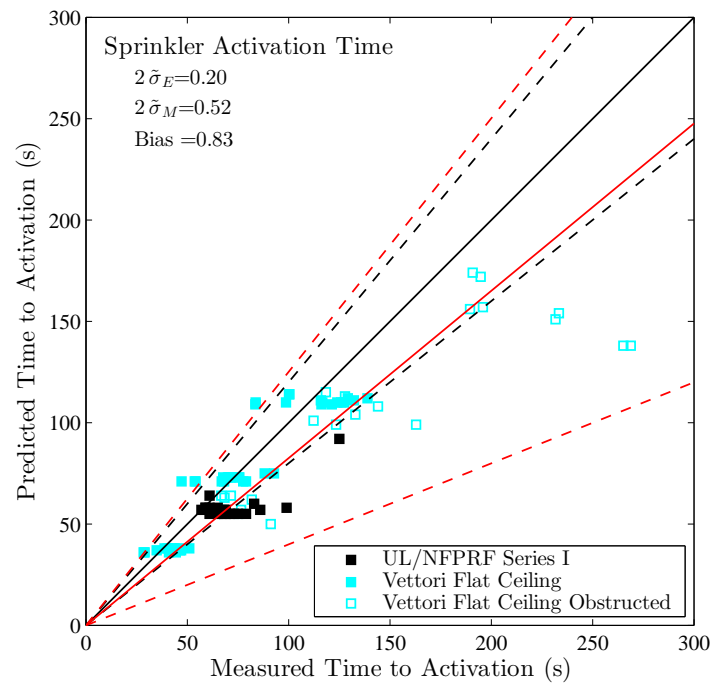


Figure 7.3: Comparison of Measured and Predicted Ceiling Jet Temperature.

- CFAST tends to over-predict plume temperatures comparing experimental measurements to gas temperature predictions by the model. Comparisons to target surface or center temperature (which may be appropriate for unshielded thermocouple measurements in experiments) show closer agreement.
- 90 % of the predictions by CFAST are within 43 % of experimental measurements, higher than the estimated experimental uncertainty in this validation exercise, but this is largely driven by a few individual tests. User's should take this higher uncertainty into account when using predictions from the model.

Based on the model physics and comparisons of model predictions with experimental measurements, CFAST provides appropriate calculations of ceiling jet temperature for the following reasons:

- For tests with a well-defined ceiling jet layer beneath flat ceilings, CFAST predicts ceiling jet temperatures well-within experimental uncertainty.
- For tests with a less well-defined ceiling jet layer, CFAST over-predicts the ceiling jet temperature. For the tests studied, over-predictions were noted when the HGL temperature was below 70 °C.

Chapter 8

Gas Species and Smoke

CFAST simulates a fire as a mass of fuel that burns at a prescribed pyrolysis rate and releases both energy and combustion products. CFAST calculates species production based on user-defined production yields, and both the pyrolysis rate and the resulting energy and species generation may be limited by the oxygen available for combustion. When sufficient oxygen is available for combustion, the heat release rate for a constrained fire is the same as for an unconstrained fire. Mass and species concentrations, assumed to be homogeneous throughout each layer, are tracked by the model as gases flow through openings in a structure to other compartments in the structure or to the outdoors.

The fire chemistry scheme in CFAST is essentially a species balance from user-prescribed species yields and the oxygen available for combustion. Once generated, it is a matter of book-keeping to track the mass of species throughout the various control volumes in a simulated building. It does, however, provide a check of the flow algorithms within the model. Since the major species (CO and CO_2) are generated only by the fire, the relative accuracy of the predicted values throughout multiple rooms of a structure should be comparable.

8.1 Oxygen and CO_2

Gas sampling data are available from a number of the experimental tests. Figure 8.1 shows a comparison of predicted and measured values for oxygen and carbon dioxide concentrations, along with a summary of the relative difference for the tests.

CFAST predicts the upper-layer concentrations of oxygen and carbon dioxide within an average of 22 % of experimental values. Details for individual test series are discussed below.

NBS Single Room Tests with Furniture

For the single-room tests with furniture, the predicted concentrations are lower than those measured experimentally (with an average relative difference of 22 % for oxygen). This is probably due to the treatment of oxygen limited burning. In CFAST, the burning rate simply decreases as the oxygen level decreases. A user prescribed lower limit determines the point below which burning will not take place. This parameter could be finessed to provide better agreement with the experiment. For the present comparisons, it was always left at the default value. Since this parameter impacts the

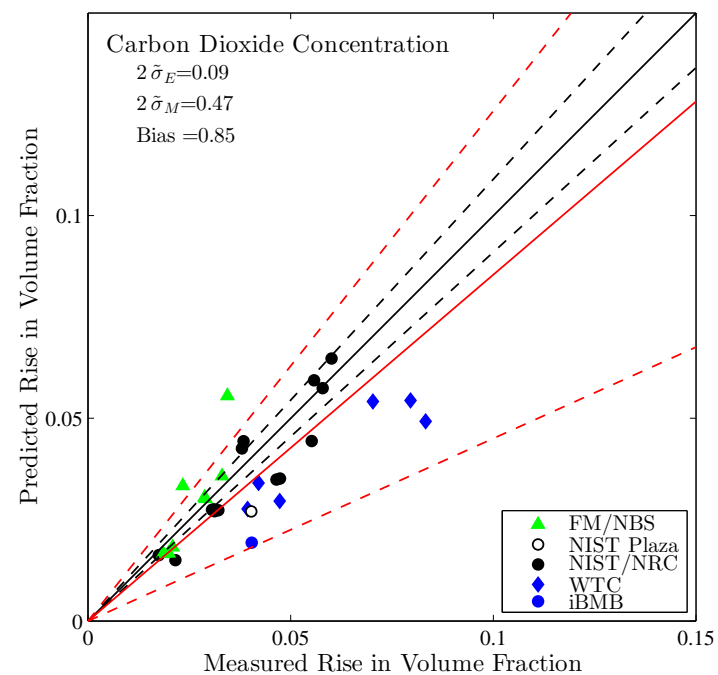
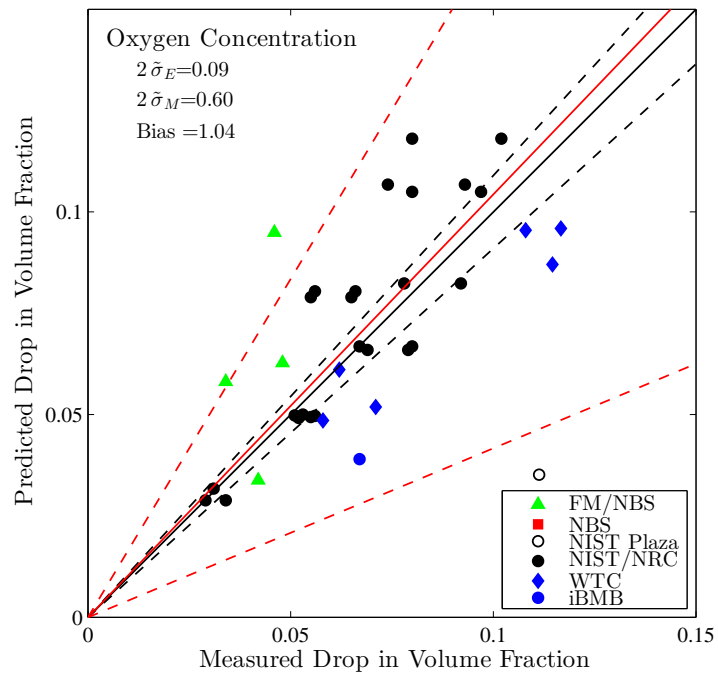


Figure 8.1: Comparison of Measured and Predicted Oxygen Concentration and Carbon Dioxide Concentration.

overall combustion chemistry in CFAST and the generation of all species, it would impact both oxygen and carbon dioxide.

In addition, species concentrations measured for large fires in small spaces can show considerable spatial variation within the upper layer of the fire compartment [91]. For such under-ventilated fires, the representation of the species concentration in a hot gas layer by a single representative average value may not be valid. For example, two measurement locations in test F6 show an underprediction in one measurement location and an overprediction in the other.

NIST/NRC Tests

Relative differences for both oxygen and carbon dioxide are typically higher for the closed door tests than for the open door tests (see figure 8.1). Tests 4, 10, and 16 were closed-door tests with the mechanical ventilation system on. A higher relative difference for these tests are likely because of a non-uniform gas layer in the experiments with higher oxygen concentration near the mechanical ventilation inlet and lower concentrations remote from the inlet. In CFAST, the flow from the mechanical ventilation system is assumed to completely mix with the gases in the appropriate gas layer of a compartment. For other tests, the reasons for a higher relative difference are not clear. Replicate tests are seen to typically compare quite well, with a difference of about 2 % typical.

Table 8.1: Relative Difference for Oxygen and Carbon Dioxide in Open and Closed Door Tests in a Single Compartment

Vent	Oxygen %	Carbon Dioxide %
Open Door	7	13
Closed Door	20	15

iBMB Cable Fire Test

CFAST under predicts oxygen and carbon dioxide concentrations by 58 % and 66 %, respectively.

FM Four Room Including Corridor Test Series

For these four compartment tests, the end of test values of the gas concentrations agree far better than the peak values. With the underlying assumption of all zone fire models of a uniform concentration of gas species throughout a control volume, it is assumed that the point measurement is the bulk concentration of the entire upper layer. In reality, some vertical distribution not unlike the temperature profile exists for the gas concentration as well.

Since this measurement point is near the lower edge of the upper layer for a significant time, it should underestimate the bulk concentration until the layer is large in volume and well mixed. Still, the relative differences for these tests are larger than the NIST/NRC tests, averaging 54 % for oxygen and 22 % for carbon dioxide.

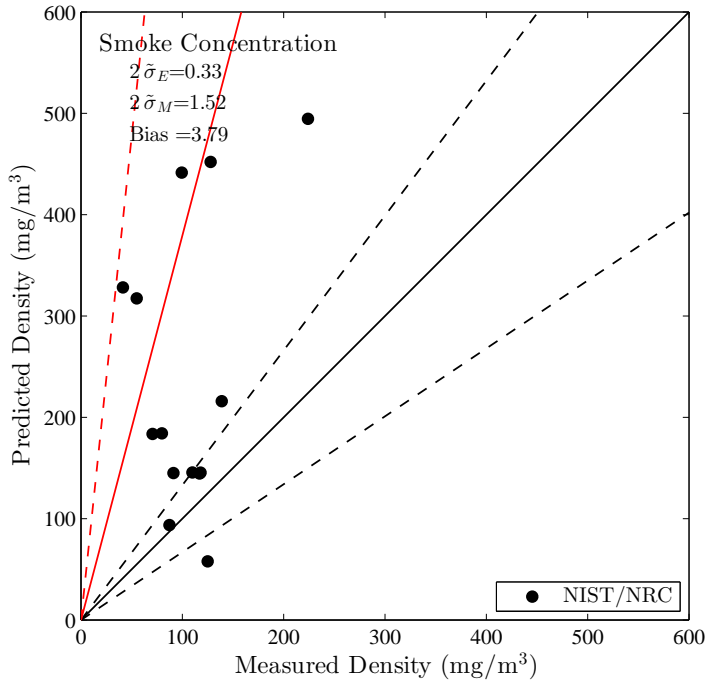


Figure 8.2: Comparison of Measured and Predicted Smoke Concentration.

NIST Seven-story Hotel Tests

For the multiple-story building test, predicted values for CO₂, CO, and O₂ are lower than measured experimentally. Both the lower burning rate limit as well as leakage in the 100 year-old structure probably contributed to the differences between the experiments and model. In addition, values for species yields were simply literature values since no test data were available.

8.2 NIST/NRC Test Series, Smoke

CFAST treats smoke like all other combustion products, with an overall mass balance dependent on interrelated user-specified species yields for major combustion species. To model smoke movement, the user prescribes the smoke yield relative to the yield of carbon monoxide. A simple combustion chemistry scheme in the model then determines the smoke particulate concentration in the form of an optical density. Figure 8.2 shows a comparison of predicted and measured values for smoke concentration along with a summary of the relative difference for the tests.

Only the NIST/NRC test series has been used to assess predictions of smoke concentration. For these tests, the smoke yield was specified as one of the test parameters. There are two obvious trends in the results. First, the predicted concentrations are within or near experimental uncertainties in the open-door tests. Second, the predicted concentrations are roughly three to five times the measured concentrations in the closed-door tests. The experimental uncertainty for these mea-

surements has been estimated to be 33 %. The closed-door tests cannot be explained from the experimental uncertainty.

The difference between model and experiment is far more pronounced in the closed-door tests. Given that the oxygen and carbon dioxide predictions are no worse (and indeed even better) in the closed-door tests, there is reason to believe either that the smoke is not transported with the other exhaust gases or the specified smoke yield, developed from free-burning experiments, is not appropriate for the closed-door tests. These qualitative differences between the open- and closed-door tests are consistent with the FDS predictions (see reference [92]).

8.3 Summary

Based on the model physics and comparisons of model predictions with experimental measurements, CFAST calculations of oxygen and carbon dioxide concentration are seen as appropriate with the following comments:

- CFAST uses a simple user-specified combustion chemistry scheme based on a prescribed pyrolysis rate and species yields that is appropriate for the applications studied.
- CFAST predicts the major gas species to within 22 % of experimental measurements.
- For large fires in small compartments or where mixing within a compartment may be important, local species concentration may vary considerably from a bulk average value. Thus higher uncertainty can be expected for predictions of species concentrations in these scenarios.

Use of CFAST calculations of smoke concentration require additional care for the following reasons:

- CFAST is capable of transporting smoke throughout a compartment, assuming that the production rate is known and its transport properties are comparable to gaseous exhaust products.
- CFAST typically over-predicts the smoke concentration in all of the NIST/NRC tests, with the exception of Test 17. Predicted concentrations for open-door tests are within experimental uncertainties, but those for closed-door tests are far higher. No firm conclusions can be drawn from this single data set. The measurements in the closed-door experiments are inconsistent with basic conservation of mass arguments, or there is a fundamental change in the combustion process as the fire becomes oxygen-starved.

Chapter 9

Pressure

Comparisons between measurement and prediction of compartment pressure for the NIST/NRC test series and two of the NBS furniture tests are shown in of Appendix A. Figure 9.1 shows a comparison of predicted and measured values for compartment pressure, along with a summary of the relative difference for the tests.

For those tests in which the door to the compartment is open, the magnitude of the pressures are only a few Pascals; however, when the door is closed, the over-pressures are several hundred Pascals. For both the open- and closed-door tests, CFAST predicts the pressure to within experimental uncertainty with exceptions. The most notable exception is Test 16, which involved a large (2.3 MW) fire with the door closed and the ventilation on. By contrast, Test 10 involved a 1.2 MW fire with comparable geometry and ventilation. There is considerable uncertainty in the magnitude of both the supply and return mass flow rates for Test 16. Compared to Test 16, Test 10 involves a greater measured supply velocity and a lesser measured exhaust velocity. This is probably the result of the higher pressure caused by the larger fire in Test 16. CFAST does not adjust the ventilation rate based on the compartment pressure until a specified cutoff pressure is reached. This is also the most likely explanation for the over-prediction of compartment pressure in Test 16.

In general, prediction of pressure in CFAST in closed compartments is critically dependent on correct specification of the leakage from the compartment. Compartments are rarely entirely sealed, and small changes in the leakage area can produce significant changes in the predicted over-pressure.

By comparison, the large relative differences for the two NBS compartment tests with furniture and wall-burning are qualitatively different than the NIST/NRC outlier. For these two tests, the difference between model and experiment are on the order of 2 Pa rather than the more than 100 Pa of the NIST/NRC test. Qualitatively, the comparison between model and experiment for the NBS tests show similar curve shapes but with a notable single spike in the experimental measurements which particularly effects the comparison of peak values.

Based on the model physics and comparisons of model predictions with experimental measurements, CFAST calculations of pressure are seen as appropriate for the tests considered with the following reasons:

- With exceptions, CFAST predicts compartment pressures within experimental uncertainty.
- Prediction of compartment pressure for closed-door tests is critically dependent on correct specification of the leakage from the compartment.

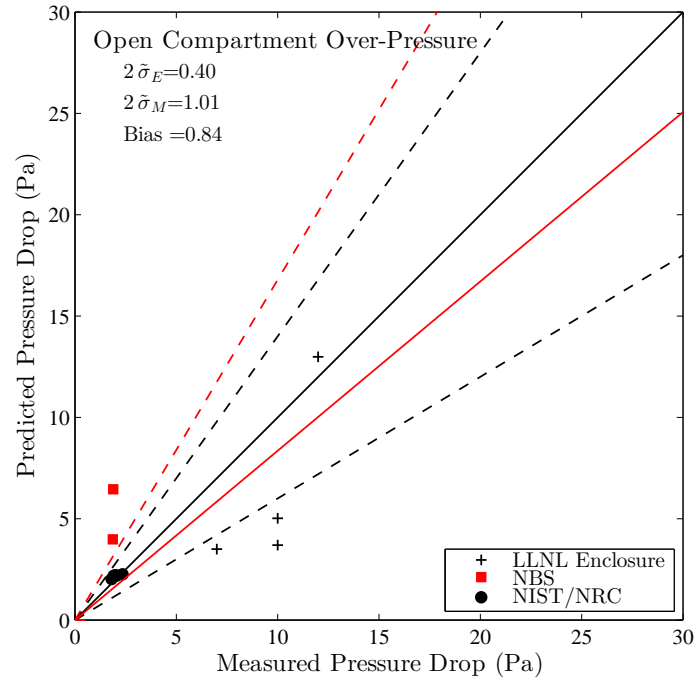
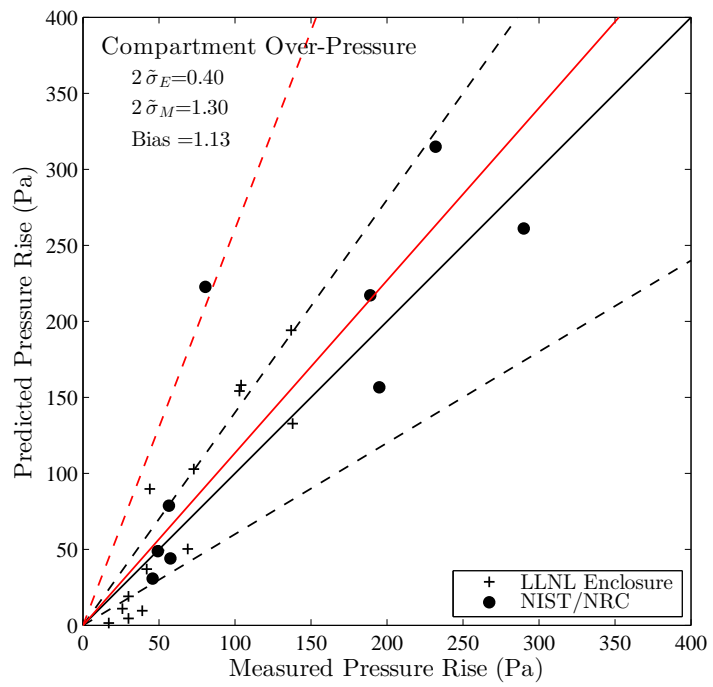


Figure 9.1: Comparison of Measured and Predicted Compartment Pressure.

Chapter 10

Heat Flux and Surface Temperature

10.1 NIST/NRC Test Series, Cables

Target temperature and heat flux data are available from the NIST/NRC test series. In the NIST/NRC tests, the targets are different types of cables in various configurations: horizontal, vertical, in trays, or free-hanging. Figure 10.1 shows a comparison of predicted and measured values for radiation, total heat flux, and target temperature, along with a summary of the relative difference for the tests.

Appendix A provides nearly 200 comparisons of heat flux and surface temperature on four different cables. The following trends are notable comparing CFAST predictions to experimental measurements:

- Overall, the comparisons of target flux and temperature show larger relative differences than other quantities. This is to be expected since the target flux and temperature are inherently local quantities.
- The difference between predicted and measured cable surface temperatures is often within experimental uncertainty, with exceptions. Total target flux and target surface temperature predictions average within 2 % of experimental values. However, there is considerable spread in the relative differences. Ignoring the sign of the relative difference, total target flux and target temperature average within 22 % and 20 %, respectively. Accurate prediction of the surface temperature of the cable should indicate that the flux to the target (a combination of radiation from the fire, surrounding surfaces, and the gas layers, along with convection from the surrounding gas) should be correspondingly accurate. For the NIST/NRC tests, the cable surface temperature predictions show lower relative difference overall compared to the total heat flux and (particularly) the radiative heat flux.
- Total heat flux to targets is typically predicted to within an average difference of 2 %. Predictions for Cables D (horizontal) and G (vertical) are notable exceptions, with higher uncertainties.
- Radiative heat flux to targets is typically over-predicted compared to experimental measurements, with higher values for closed-door tests. For the closed-door tests, this may be a function of the over-prediction of the smoke concentration, which leads to the radiation contribution from the hot gas layer being a larger fraction of the total heat flux compared to the experimental values.

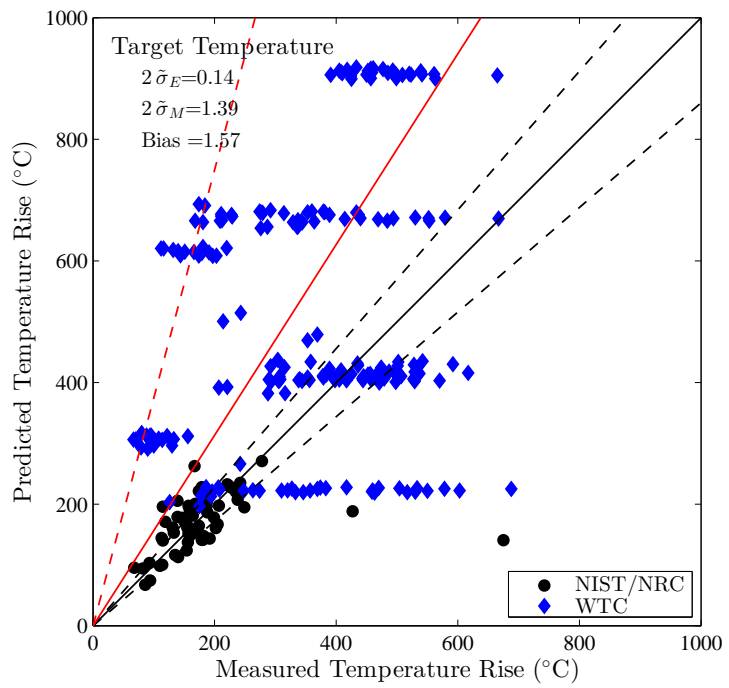
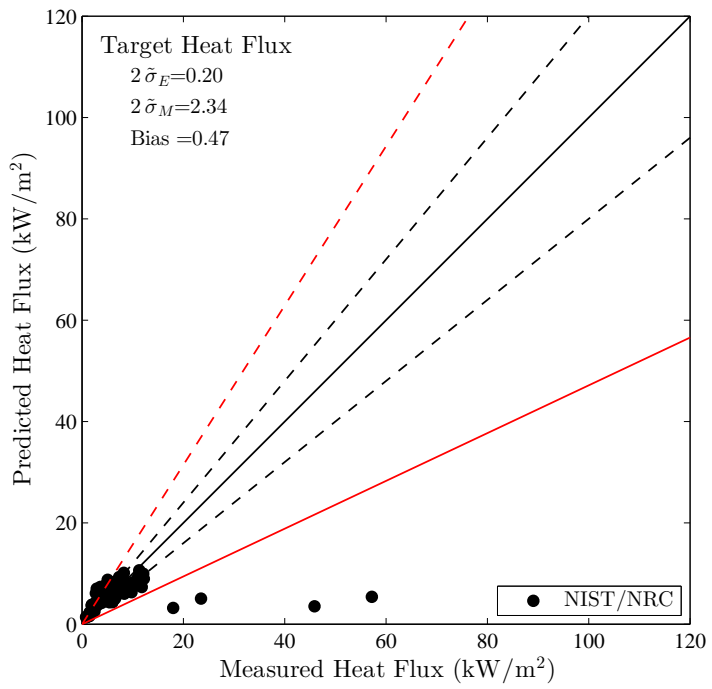


Figure 10.1: Comparisons of Measured and Predicted Heat Flux to Targets and Target Temperature

- For many of the experiments, the convective heat flux component, taken to be the difference between the total heat flux and the radiative heat flux is seen to be higher than the values typically measured in fire experiments.

10.2 NIST/NRC Test Series, Compartment Walls, Floor and Ceiling

Thirty-six heat flux gauges were positioned at various locations on all four walls of the compartment, plus the ceiling and floor. Comparisons between measured and predicted heat fluxes and surface temperatures are shown on the following pages for a selected number of locations. Over half of the measurement points are in roughly the same relative location to the fire and hence the measurements and predictions are similar. For this reason, data for the east and north walls are shown because the data from the south and west walls are comparable. Data from the south wall is used in cases where the corresponding instrument on the north wall failed, or in cases where the fire is positioned close to the south wall. For each test, eight locations are used for comparison, two on the long (mainly north) wall, two on the short (east) wall, two on the floor, and two on the ceiling. Of the two locations for each panel, one is considered in the far-field, relatively remote from the fire; one is in the near-field, relatively close to the fire. How close or far varies from test to test, depending on the availability of working flux gauges. The two short wall locations are equally remote from the fire; thus, one location is in the lower layer, one in the upper.

Figure 10.1 shows a comparison of predicted and measured values for radiation, total heat flux for the tests.

CFAST predicts the heat flux and surface temperature of the compartment walls to within 121 % and 21 %, respectively. The high value for heat flux is due to the way CFAST calculates flux to targets. The calculation of heat flux to a target in CFAST is done separately for the front face and rear face of the target. For target completely within a compartment, these two values are typically similar. For target on a compartment surface, the rear surface is assumed to radiate to ambient conditions. Thus, considering only the front face in the comparison should lead to a significant indicated overprediction of the heat flux. The predicted surface temperature is predicted far closer to experimental conditions than the surface heat flux indicating the actual heat flux is likely better than indicated by this front-face only comparison. Still, there is considerable scatter in the data indicating a higher uncertainty in prediction of heat flux and temperature to surfaces like those observed in heat flux and temperature to targets.

Typically, CFAST over-predicts the far-field fluxes and temperatures and under-predicts the near-field measurements. This is understandable, given that any two-zone model predicts an average representative value of gas temperature in the upper and lower regions of a compartment. Thus, the values predicted by CFAST should be an average of values near the fire and those farther away.

However, differences for the ceiling and (particularly) floor fluxes and temperatures are higher, with a more pronounced difference between the near-field and far-field comparisons. In addition to the limitations of the two-zone assumption, calculations of the flux to ceiling and floor surfaces are further confounded by the simple point-source calculation of radiation exchange in CFAST for the fire source. In CFAST, the fire is assumed to be a point source of energy located at the base

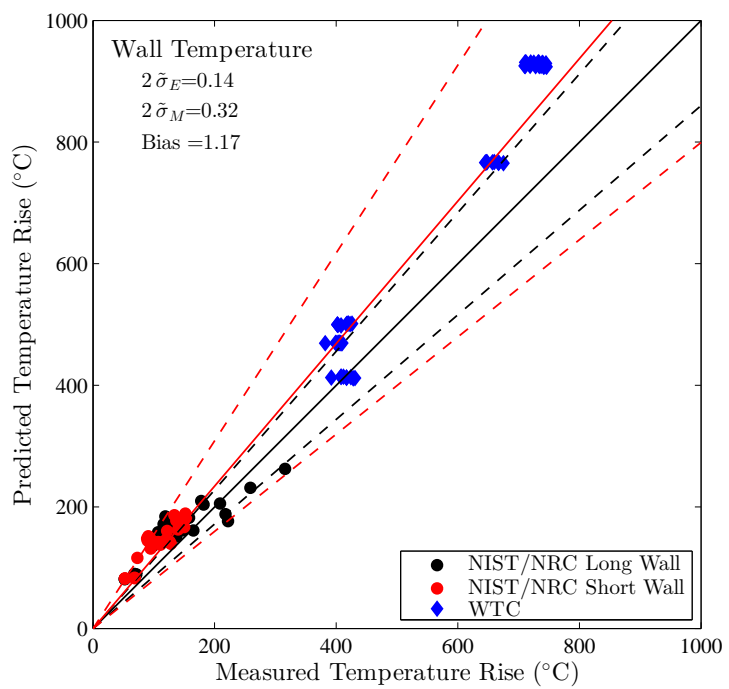
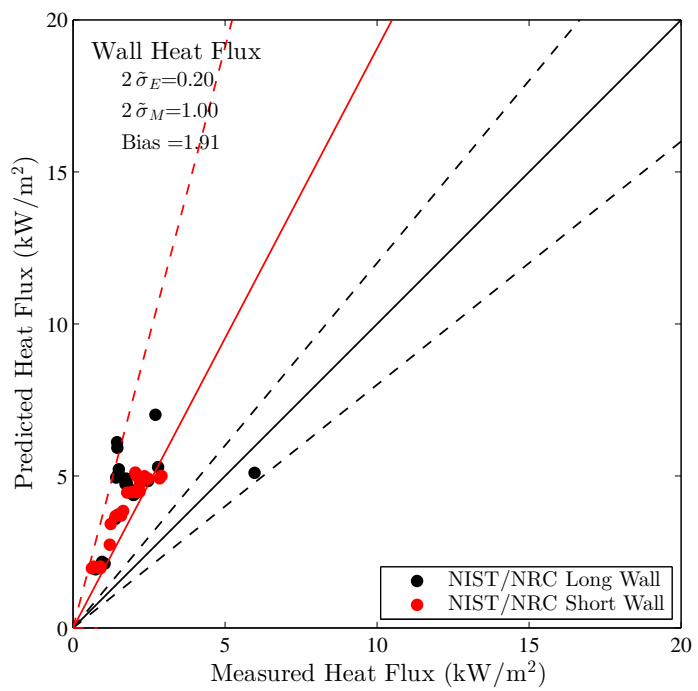


Figure 10.2: Comparisons of Measured and Predicted Heat Flux to Compartment Surfaces and Surface Temperature

of the fire rather than a three-dimensional flame surface radiating to surroundings. With the fire typically at the floor surface, this makes the calculation of flux to the floor surface inherently less accurate than for other surfaces.

10.3 Summary

Use of CFAST for heat flux and temperature requires caution for the following reasons:

- Prediction of heat flux to targets and target surface temperature is largely dependent on local conditions surrounding the target. Like any two-zone model, CFAST predicts an average representative value of gas temperature in the upper and lower regions of a compartment. In addition, CFAST does not directly predict plume temperature or its effects on targets that may be within a fire plume. Thus, CFAST can be expected to under-predict values near a fire source, and over-predict values for targets remote from a fire.
- Cable target surface temperature predictions are often within experimental uncertainty, with exceptions, particularly for Cables F and G.
- Total heat flux to targets is typically predicted to within about 30 %.
- Radiative heat flux to targets is typically over-predicted compared to experimental measurements, with higher relative difference values for closed-door tests.
- CFAST is capable of predicting the surface temperature of a wall, assuming that its composition is fairly uniform and its thermal properties are well-characterized. Predictions are typically within 10 % to 30 %. Generally, CFAST over-predicts the far-field fluxes and temperatures, and under-predicts the near-field measurements. This is consistent with the single representative layer temperature assumed by zone fire models.
- CFAST predictions of floor heat flux and temperature are more problematic because of the simple point-source calculation of radiative exchange between the fire and compartment surfaces.

Chapter 11

Summary and Conclusions

How to best quantify the comparisons between model predictions and experiments is not obvious. The necessary and perceived level of agreement for any variable is dependent upon both the typical use of the variable in a given simulation, the nature of the experiment, and the context of the comparison in relation to other comparisons being made. For instance, the user may be interested in the time it takes to reach a certain temperature in the room, but have little or no interest in peak temperature for experiments that quickly reach a steady-state value. Insufficient experimental data and understanding of how to compare the numerous variables in a complex fire model prevent a complete validation of the model.

A true validation of a model would involve proper statistical treatment of all the inputs and outputs of the model with appropriate experimental data to allow comparisons over the full range of the model. Thus, the comparisons of the differences between model predictions and experimental data discussed here are intentionally simple and vary from test to test and from variable to variable due to the changing nature of the tests and typical use of different variables.

Table 11.1 summarizes the comparisons in this report.

Four of the quantities were seen to require additional care when using the model to evaluate the given quantity. This typically indicates limitations in the use of the model. A few notes on the comparisons are appropriate:

- CFAST typically predicts plume temperature near to experimental uncertainty, but tends to under-predict temperatures nearer to the fire source and over-predict temperatures farther away.
- CFAST typically over-predicts smoke concentration. Predicted concentrations for open-door tests are within experimental uncertainties, but those for closed-door tests are far higher.
- With exceptions, CFAST predicts cable surface temperatures within experimental uncertainties. Total heat flux to targets is typically predicted to within about 30 %, and often under-predicted. Radiative heat flux to targets is typically over-predicted compared to experimental measurements, with higher relative difference values for closed-door tests. Care should be taken in predicting localized conditions (such as target temperature and heat flux) because of inherent limitations in all zone fire models.
- Predictions of compartment surface temperature and heat flux are typically within 10 % to 30 %. Generally, CFAST over-predicts the far-field fluxes and temperatures and under-

Table 11.1: Summary of Model Comparisons

Quantity	Number of Datasets	Number of Points	$2\tilde{\sigma}_E$	$2\tilde{\sigma}_M$	Bias
HGL Temperature	12	244	0.14	0.49	1.04
HGL Temperature: Forced Ventilation	7	92	0.14	0.39	1.26
HGL Temperature: Natural Ventilation	9	128	0.14	0.45	0.99
HGL Temperature: No Ventilation	3	22	0.14	0.78	1.38
HGL Depth	8	87	0.13	0.53	1.11
HGL Depth: Open Compartments	7	53	0.13	0.45	0.98
HGL Depth: Closed Compartments	4	34	0.13	0.50	1.44
Ceiling Jet Temperature	7	291	0.10	0.46	1.24
Plume Temperature	4	51	0.14	0.41	1.19
Oxygen Concentration	6	40	0.09	0.60	1.04
Carbon Dioxide Concentration	5	31	0.09	0.47	0.85
Smoke Concentration	1	15	0.33	1.52	3.79
Compartment Over-Pressure	2	23	0.40	1.30	1.13
Open Compartment Over-Pressure	3	12	0.40	1.01	0.84
Target Temperature	2	265	0.14	1.39	1.57
Wall Temperature	3	110	0.14	0.32	1.17
Ceiling Temperature	2	184	0.14	0.47	0.99
Floor Temperature	1	26	0.14	0.92	1.40
Target Heat Flux	1	100	0.20	2.34	0.47
Wall Heat Flux	2	44	0.20	1.00	1.91
Ceiling Heat Flux	2	41	0.20	0.84	1.13
Floor Heat Flux	2	36	0.20	0.62	1.32
Smoke Alarm Activations	7	125	0.33	0.98	1.05
Sprinkler Activation Time	3	89	0.20	0.52	0.83

predicts the near-field measurements. This is consistent with the single representative layer temperature assumed by zone fire models.

CFAST predictions in this validation study were consistent with numerous earlier studies, which show that the use of the model is appropriate in a range of fire scenarios. The CFAST model has been subjected to extensive evaluation studies by NIST and others. Although differences between the model and the experiments were evident in these studies, most differences can be explained by limitations of the model as well as of the experiments. Like all predictive models, the best predictions come with a clear understanding of the limitations of the model and the inputs provided to perform the calculations.

References

- [1] American Society for Testing and Materials, West Conshohocken, Pennsylvania. *ASTM E 1355-04, Standard Guide for Evaluating the Predictive Capabilities of Deterministic Fire Models*, 2004.
- [2] R. D. Peacock, G. P. Forney, and P. A. Reneke. CFAST – Consolidated Model of Fire Growth and Smoke Transport (Version 6): Technical Reference Guide. Special Publication 1026, National Institute of Standards and Technology, Gaithersburg, Maryland, July 2011.
- [3] EPRI/NRC-RES Fire PRA Methodology for Nuclear Power Facilities: Volume 2: Detailed Methodology. Technical Report EPRI TR-1011989 and NUREG/CR-6850, Electric Power Research Institute (EPRI), Palo Alto, CA, and U.S. Nuclear Regulatory Commission, Office of Nuclear Regulatory Research (RES), Rockville, MD, 2005.
- [4] R. D. Peacock, W. W. Jones, P. A. Reneke, and G. P. Forney. CFAST – Consolidated Model of Fire Growth and Smoke Transport (Version 6): User’s Guide. Special Publication 1041, National Institute of Standards and Technology, Gaithersburg, Maryland, December 2005.
- [5] Verification and Validation of Selected Fire Models for Nuclear Power Plant Applications, Volume 5: Consolidated Fire and Smoke Transport Model (CFAST),. NUREG 1824, U. S. Nuclear Regulatory Commission, Office of Nuclear Regulatory Research, Rockville, MD, 2007.
- [6] The Institute of Electrical and Electronics Engineers. *IEEE Standard for Software Quality Assurance Plans*, IEEE Std 730-2002 edition, 2002.
- [7] Verification and Validation of Selected Fire Models for Nuclear Power Plant Applications, Volume 1: Main Report. NUREG 1824, U. S. Nuclear Regulatory Commission, Office of Nuclear Regulatory Research, Rockville, MD, 2007.
- [8] K. E. Brenan, S. L. Campbell, and L. R. Petzold. *Numerical Solution of Initial-Value Problems in Differential-Algebraic Equations*. Elsevier Science Publishing, New York, 1989.
- [9] G. P. Forney. Computing Radiative Heat Transfer Occurring in a Zone Fire Model. NISTIR 4709, National Institute of Standards and Technology, 1991.
- [10] N. A. Dempsey, P. J. Pagni, and R. B. Williamson. Compartment Fire Experiments: Comparison With Models. *Fire Safety Journal*, 25(3):187, 1995.

- [11] International Conference of Building Officials, Whittier, CA. *1997 Uniform Building Code*, 1997.
- [12] W. M. Pitts, E. Braun, R. D. Peacock, H. E. Mitler, E. L. Johnsson, P. A. Reneke, and L. G. Blevins. Temperature Uncertainties for Bare-Bead and Aspirated Thermocouple Measurements in Fire Environments. In *Thermal Measurements: The Foundation of Fire Standards*, Special Technical Publication 1427, West Conshohocken, PA, 2001. American Society for Testing and Materials.
- [13] Y. He and V. Beck. Smoke Spread Experiment in a Multi-Storey Building and Computer Modeling. *Fire Safety Journal*, 28(2):139, 1997.
- [14] M. Luo, Y. He, and V. Beck. Comparison of Existing Fire Model Predictions With Experimental Results From Real Fire Scenarios. *Journal of Applied Fire Science*, 6(4):357, 1996/1997.
- [15] G. M. Poole, E. J. Weckman, and A. B. Strong. Fire Growth Rates in Structural Fires. NISTIR 5499, National Institute of Standards and Technology, 1994.
- [16] J. Bailey and P. Tatem. Validation of Fire/Smoke Spread Model (CFAST) Using Ex-USS SHADWELL Internal Ship Conflagration Control (ISCC) Fire Tests. Technical Report NRL/MR/6180-95-7781, Naval Research Laboratory, 1995.
- [17] J. L. Bailey, P. A. Tatem, W. W. Jones, and G. P. Forney. Development of an Algorithm to Predict Vertical Heat Transfer Through Ceiling/Floor Conduction. *Fire Technology*, 34(2):139, 1998.
- [18] S. Deal. A Review of Four Compartment Fires with Four Compartment Fire Models. In *Proceedings of the Annual Meeting of the Fire Retardant Chemicals Association*, volume Fire Safety Developments and Testing, pages 33–51, Ponte Verde Beach, Florida, October 21-24 1990. Fire Retardant Chemicals Association.
- [19] L. Y. Cooper and G. P. Forney. The Consolidated Compartment Fire Model (CCFM) Computer Application CCFM-VENTS – Part I: Physical Reference Guide. NISTIR 4342, National Institute of Standards and Technology, 1990.
- [20] H. E. Mitler and J. A. Rockett. Users' Guide to FIRST, A Comprehensive Single-Room Fire Model. NBSIR 87-3595, National Institute of Standards and Technology, September 1987.
- [21] H. E. Nelson. FPETOOL: Fire Protection Engineering Tools for Hazard Estimation. NISTIR 4380, National Institute of Standards and Technology, 1990.
- [22] W. W. Jones and R. D. Peacock. Technical Reference Guide for FAST Version 18. Technical Note 1262, National Institute of Standards and Technology, 1989.
- [23] W. D. Davis. Comparison of Algorithms to Calculate Plume Centerline Temperature and Ceiling Jet Temperature With Experiments. *Journal of Fire Protection Engineering*, 12:9, 2002.

- [24] W. W. Jones and R. D. Peacock. Refinement and Experimental Verification of a Model for Fire Growth and Smoke Transport. In T. Wakamatsu, Y. Hasemi, A. Sekizawa, P. G. Seeger, P. J. Pagni, and C. E. Grant, editors, *Fire Safety Science. Proceedings. 2nd International Symposium*, pages 897–906, Tokyo, Japan, June 13-17 1988. International Association for Fire Safety Science, Hemisphere Publishing Corporation.
- [25] R. S. Levine and H. E. Nelson. Full Scale Simulation of a Fatal Fire and Comparison of Results with Two Multiroom Models. NISTIR 90-4168, National Institute of Standards and Technology, 1990.
- [26] D. Q. Duong. The Accuracy of Computer Fire Models: Some Comparisons with Experimental Data from Australia. *Fire Safety Journal*, 16:415, 1990.
- [27] T. Tanaka. Model of Multiroom Fire Spread. *Fire Science and Technology*, 3(2):105–121, 1983.
- [28] W. Chow. Predicability of Flashover by Zone Models. *Journal of Fire Sciences*, 16:335, September/October 1988.
- [29] M. Luo, Y. He, and V. Beck. Application of Field Model and Two-Zone Model to Flashover Fires in a Full-Scale Multi-Room Single Level Building. *Fire Safety Journal*, 29:1, 1997.
- [30] P. Collier. Fire in a Residential Building: Comparisons Between Experimental Data and a Fire Zone Model. *Fire Technology*, 32:195, August/September 1996.
- [31] D. White, C. Beyler, J. Scheffrey, and F. Williams. Modeling the Impact of Post-Flashover Shipboard Fires on Adjacent Spaces. *Journal of Fire Protection Engineering*, 10, 2000.
- [32] R. D. Peacock, P. A. Reneke, R. W. Bukowski, and V. Babrauskas. Defining Flashover for Fire Hazard Calculations. *Fire Safety Journal*, 32(4):331–345, 1999.
- [33] V. Babrauskas, R. D. Peacock, and P. A. Reneke. Defining Flashover for Fire Hazard Calculations: Part II. *Fire Safety Journal*, 38:613–622, 2003.
- [34] V. Babrauskas. Upholstered Furniture Room Fires—Measurements, Comparison with Furniture Calorimeter Data, and Flashover Predictions. *Journal of Fire Sciences*, 2(1):5–19, January/February 1984.
- [35] S. Deal and C. Beyler. Correlating Preflashover Room Fire Temperatures. *Journal of Fire Protection Engineering*, 2(2):33–48, 1990.
- [36] P. H. Thomas. Testing Products and Materials for Their Contribution to Flashover in Rooms. *Fire and Materials*, 5:103–111, 1981.
- [37] B. J. McCaffrey, J. G. Quintiere, and M. F. Harkleroad. Estimating Room Temperatures and the Likelihood of Flashover Using Fire Test Data Correlations. *Fire Technology*, 17(2):98–119, 1981.
- [38] B. Hägglund. Estimating Flashover Potential in Residential Rooms. FOA Rapport C 202369-A3, Forsvarets Forkningsanstalt, 1980.

- [39] W. W. Jones. Multicompartment Model for the Spread of Fire, Smoke and Toxic Gases. *Fire Safety Journal*, 9(1):172, 1985.
- [40] J. A. Rockett and M. Morita. The NBS Harvard VI Multi-room Fire Simulation. *Fire Science and Technology*, 5(2):159–164, 1985.
- [41] R. W. Bukowski. Modeling a Backdraft Incident: The 62 Watts Street (New York) Fire. *Fire Engineers Journal*, 56(185):14–17, 1996.
- [42] W. Chow. Preliminary Studies of a Large Fire in Hong Kong. *Journal of Applied Fire Science*, 6(3):243–268, 1996/1997.
- [43] R. W. Bukowski. Analysis of the Happyland Social Club Fire with HAZARD I. *Fire and Arson Investigator*, 42:36, 1992.
- [44] J. Floyd. Comparison of CFAST and FDS for Fire Simulation With the HDR T51 and T52 Tests. NISTIR 6866, National Institute of Standards and Technology, 2002.
- [45] K.B. McGrattan, S. Hostikka, J.E. Floyd, H.R. Baum, and R.G. Rehm. Fire Dynamics Simulator (Version 5), Technical Reference Guide. NIST Special Publication 1018-5, National Institute of Standards and Technology, Gaithersburg, Maryland, October 2007.
- [46] G. Lui and W. Chow. A Short Note on Experimental Verification of Zone Models with an Electric Heater. *International Journal on Engineering Performance-Based Fire Codes*, 5:30, 2003.
- [47] W. Chow. Studies on Closed Chamber Fires. *Journal of Fire Sciences*, 13:89, 1995.
- [48] W. Chow. Experimental Evaluation of the Zone Models CFAST, FAST and CCFM.VENTS. *Journal of Applied Fire Science*, 2:307, 1992-1993.
- [49] M. Altinakar, A. Weatherhill, and P. Nasch. Use of a Zone Model in Predicting Fire and Smoke Propagation in Tunnels. In J. R. Gillard, editor, *9th International Symposium on Aerodynamics and Ventilation of Vehicle Tunnels*, pages 623–639, Aosta Valley, Italy, October 6-8 1997. BHR Group.
- [50] R. D. Peacock, J. D. Averill, D. Madrzykowski, D. W. Stroup, P. A. Reneke, and R. W. Bukowski. Fire Safety of Passenger Trains; Phase III: Evaluation of Fire Hazard Analysis Using Full-Scale Passenger Rail Car Tests. NISTIR 6563, National Institute of Standards and Technology, 2004.
- [51] J. Hoover and P. A. Tatem. Application of CFAST to Shipboard Fire Modeling. Part 3. Guidelines for Users. NRL/ML 6180-01-8550, Naval Research Laboratory, 2001.
- [52] J. L. Bailey, G. P. Forney, P. A. Tatem, and W. W. Jones. Development and Validation of Corridor Flow Submodel for CFAST. *Journal of Fire Protection Engineering*, 12:139, 2002.
- [53] W. Chow. Use of Zone Models on Simulating Compartmental Fires With Forced Ventilation. *Fire and Materials*, 14:466, 1995.

- [54] M. Luo. One Zone or Two Zones in the Room of Fire Origin During Fires? *Journal of Fire Sciences*, 15:240, 1997.
- [55] D. Madrzykowski and R. Vettori. A Sprinkler Fire Suppression Algorithm for the GSA Engineering Fire Assessment System. NISTIR 4833, National Institute of Standards and Technology, 1992.
- [56] W. Chow. Performance of Sprinkler in Atria. *Journal of Fire Sciences*, 14:466, 1996.
- [57] K. Matsuyama, T. Wakamatsu, and K. Harada. Systematic Experiments of Room and Corridor Smoke Filling for Use in Calibration of Zone and CFD Fire Models. NISTIR 6588, National Institute of Standards and Technology, 2000.
- [58] D.T. Sheppard and B.W. Klein. Burn Tests in Two Story Structure with Hallways. Technical report, ATF Laboratories, Ammendale, Maryland, 2009.
- [59] G. Heskestad and J. P. Hill. Experimental Fires in Multiroom/Corridor Enclosures. NBS-GCR 86-502, National Institute of Standards and Technology, 1986.
- [60] R. D. Peacock, S. Davis, and B. T. Lee. Experimental Data Set for the Accuracy Assessment of Room Fire Models. NBSIR 88-3752, National Bureau of Standards, 1988.
- [61] S. P. Nowlen. Enclosure Environment Characterization Testing for the Base line Validation of Computer Fire Simulation Codes. Technical Report NUREG/CR-4681, SAND86-1296, Sandia National Laboratories, Albuquerque, NM, 1987.
- [62] A Summary of Nuclear Power Plant Fire Safety Research at Sandia National Laboratories 1975 - 1987. Technical report, Sandia National Laboratories, Albuquerque, NM, 1989.
- [63] W. Klein-Helßling and M. Röwenkamp. Evaluation of Fire Models for Nuclear Power Plant Applications: Fuel Pool Fire Inside a Compartment. Technical report, Gesellschaft für Anlagen-und Reaktorsicherheit (GRS), Köln, Germany, May 2005.
- [64] Verification and Validation of Selected Fire Models for Nuclear Power Plant Applications, Volume 2: Experimental Uncertainty. NUREG 1824, U. S. Nuclear Regulatory Commission, Office of Nuclear Regulatory Research, Rockville, MD, 2007.
- [65] O. Riese and D. Hosser. Evaluation of Fire Model for Nuclear Power Plant Applications: Flame SPread in Cable Tray Fires. Draft Version Revision 1, Gesellschaft für Anlagen-und Reaktorsicherheit (GRS), June 2004.
- [66] K.L. Foote. 1986 LLNL Enclosure Fire Tests Data Report. Technical Report UCID-21236, Lawrence Livermore National Laboratory, August 1987.
- [67] B. T. Lee. Effect of Wall and Room Surfaces on the Rates of Heat, Smoke, and Carbon Monoxide Production in a Park Lodging Bedroom Fire. NBSIR 85-2998, National Bureau of Standards, 1985.
- [68] Fire Modeling Code Comparison. TR 108875, Electric Power Research Institute (EPRI), Palo Alto, CA.

- [69] A. Hamins, M. Klassen, J. Gore, and T. Kashiwagi. Estimate of Flame Radiance via a Single Location Measurement in Liquid Pool Fires. *Combustion and Flame*, 86:223–228, 1991.
- [70] R.W. Bukowski, R.D. Peacock, J.D. Averill, T.G. Cleary, N.P. Bryner, W.D. Walton, P.A. Reneke, and E.D. Kuligowski. Performance of Home Smoke Alarms Analysis of the Response of Several Available Technologies in Residential Fire Settings. NIST Technical Note 1455-1, National Institute of Standards and Technology, Gaithersburg, Maryland, February 2008.
- [71] J. H. Klote. Fire Experiments of Zoned Smoke Control at the Plaza Hotel in Washington, DC. NISTIR 90-4253, National Institute of Standards and Technology, 1990.
- [72] J. H. Klote and Jr. Fothergill, J. W. *Design of Smoke Control Systems for Buildings*. American Society of Heating, Refrigerating, and Air-Conditioning Engineers, Inc, 1983.
- [73] J. H. Klote. Project Plan for Full Scale Smoke Movement and Smoke Control Tests. NBSIR 88-3800, National Bureau of Standards, 1988.
- [74] A. Hamins, A. Maranghides, E. L. Johnsson, M. K. Donnelly, J. C. Yang, G. W. Mullholland, and R. L. Anleitner. Report of Experimental Results for the International Fire Model Benchmarking and Validation Exercise #3. Special Publication 1013-1, National Institute of Standards and Technology, 2005.
- [75] A. Hamins, A. Maranghides, and G. W. Mullholland. The Global Combustion Behavior of 1 MW to 3 MW Hydrocarbon Spray Fires Burning in an Open Environment. NISTIR 7013, National Institute of Standards and Technology, 2003.
- [76] U. Wickström, R. Jansson, and H. Tuovinen. Verification fire tests on using the adiabatic surface temperature for predicting heat transfer. Technical Report 2009:19, SP Technical Research Institute of Sweden, Böras, Sweden, 2009.
- [77] K. D Steckler, J. G. Quintiere, and W. J. Rinkinen. Flow Induced by Fire in a Compartment. NBSIR 82-2520, National Bureau of Standards, 1982.
- [78] D.T. Sheppard and D.R. Steppan. Sprinkler, Heat & Smoke Vent, Draft Curtain Project – Phase 1 Scoping Tests. Technical report, Underwriters Laboratories, Northbrook, Illinois, May 1997.
- [79] J. E. Gott, D. L. Lowe, K. A. Notarianni, and W. D. Davis. Analysis of High Bay Hangar Facilities for Fire Detector Sensitivity and Placement. Technical Note 1423, National Institute of Standards and Technology, Gaithersburg, Maryland, February 1997.
- [80] W. D. Davis, K. A. Notarianni, and P. Z. Tapper. An Algorithm for Calculating the Plume Centerline Temperature in the Presence of a Hot Upper Layer. *Journal of Fire Protection Engineering*, 10(3):23–31, 2000.
- [81] R. Vettori. Effect of an Obstructed Ceiling on the Activation Time of a Residential Sprinkler. NISTIR 6253, National Institute of Standards and Technology, Gaithersburg, Maryland, November 1998.

- [82] S. Hostikka, M. Kokkala, and J. Vaari. Experimental Study of the Localized Room Fires, NFDC2 Test Series. VTT Research Notes 2104, VTT Building and Transport, 2001.
- [83] A. Hamins, A. Maranghides, K.B. McGrattan, E. Johnsson, T. Ohlemiller, M. Donnelly, J. Yang, G. Mulholland, K. Prasad, S. Kukuck, R. Anleitner, and T. McAllister. Federal Building and Fire Safety Investigation of the World Trade Center Disaster: Experiments and Modeling of Structural Steel Elements Exposed to Fire. NIST NCSTAR 1-5B, National Institute of Standards and Technology, Gaithersburg, Maryland, September 2005.
- [84] M.L. Janssens and H.C. Tran. Data Reduction of Room Tests for Zone Model Validation. *Journal of Fire Sciences*, 10:528–555, 1992.
- [85] K.B. McGrattan and G. P. Forney. Fire Dynamics Simulator (Version 4), User's Guide. NISTIR 7013, National Institute of Standards and Technology, June 2003.
- [86] H.R. Baum and B. J. McCaffrey. Fire Induced Flow Field: Theory and Experiment. In T. Wakamatsu, Y. Hasemi, A. Sekizawa, and P. G. Seeger, editors, *Fire Safety Science. Proceedings. 2nd International Symposium*, pages 129–148, Tokyo, Japan, June 13-17 1989. International Association for Fire Safety Science, Hemisphere Publishing Corporation.
- [87] B. J. McCaffrey. Momentum Implications for Buoyant Diffusion Flames. *Combustion and Flame*, 52:149, 1983.
- [88] L. Y. Cooper. Fire-Plume-Generated Ceiling Jet Characteristics and Convective Heat Transfer to Ceiling and Wall Surfaces in a Two-Layer Zone-Type Fire Environment. NISTIR 4705, National Institute of Standards and Technology, 1991.
- [89] Fire Dynamics tools (FDTs), Quantitative Fire Hazard Analysis Methods for the U.S. Nuclear Regulatory Commission Fire Protection Inspection Program. NUREG 1805, U. S. Nuclear Regulatory Commission, Office of Nuclear Regulatory Research, Rockville, MD, 2004.
- [90] G. Hesketh and H. F. Smith. Investigation of a New Sprinkler Sensitivity Approval Test: the Plunge Test. Technical Report 22485 2937, Factory Mutual Research Corporation, Norwood, MA, 1976.
- [91] M. Bundy, A. Hamins, E. L. Johnsson, C. K. Kim, G. H. Ko, and D. B. Lenhart. Measurements of Heat and Combustion Products in Reduced-Scale Ventilation-Limited Compartment Fires. Technical Note 1483, National Institute of Standards and Technology, July 2007.
- [92] Verification and Validation of Selected Fire Models for Nuclear Power Plant Applications, Volume 7: FDS. NUREG 1824, U. S. Nuclear Regulatory Commission, Office of Nuclear Regulatory Research, Rockville, MD, 2007.
- [93] Y. He, A. Fernando, and M. Luo. Determination of Interface Height from Measured Parameter Profile in Enclosure Fire Experiment. *Fire Safety Journal*, 31:19–38, 1998.

Appendix A

Calculation of Layer Height and the Average Upper and Lower Layer Temperatures

Fire protection engineers often need to estimate the location of the interface between the hot, smoke-laden upper layer and the cooler lower layer in a burning compartment. Zone fire models such as CFAST compute this quantity directly, along with the average temperature of the upper and lower layers. In an experimental test or a computational fluid dynamics (CFD) model like FDS [45], there are not two distinct zones, but rather a continuous profile of temperature. Nevertheless, methods have been developed to estimate layer height and average temperatures from a continuous vertical profile of temperature. One such method [84] is as follows: Consider a continuous function $T(z)$ defining temperature T as a function of height above the floor z , where $z = 0$ is the floor and $z = H$ is the ceiling. Define T_u as the upper layer temperature, T_l as the lower layer temperature, and z_{int} as the interface height. Compute the quantities:

$$(H - z_{int}) T_u + z_{int} T_l = \int_0^H T(z) dz = I_1 \quad (\text{A.1})$$

$$(H - z_{int}) \frac{1}{T_u} + z_{int} \frac{1}{T_l} = \int_0^H \frac{1}{T(z)} dz = I_2 \quad (\text{A.2})$$

Solve for z_{int} :

$$z_{int} = \frac{T_l(I_1 I_2 - H^2)}{I_1 + I_2 T_l^2 - 2 T_l H} \quad (\text{A.3})$$

Let T_l be the temperature in the lowest mesh cell and, using Simpson's Rule, perform the numerical integration of I_1 and I_2 . T_u is defined as the average upper layer temperature via

$$(H - z_{int}) T_u = \int_{z_{int}}^H T(z) dz \quad (\text{A.4})$$

For experimental test data or CFD model output, the integral function of temperature as a function of height can be estimated empirically from a number of discrete data points. Further discussion of similar procedures can be found in Ref. [93].

Appendix B

Model / Experiment Comparison Graphs

B.1 FM Four Room Including Corridor Test Series

This data set describes a series of tests conducted in a multiple room configuration with more complex gas burner fires than the previous data set. This study [59] was included because, in many ways, it is similar to the smoke movement study performed at NBS [60], and permits comparisons between two different laboratories. In addition, it expands upon that data set by providing larger a time-varying gas burner fires in a room-corridor configuration. Fire size was about up to 1 MW with a total volume of 200 m³. This study was performed to collect data allowing for variations in fire source, ventilation, and geometry in a multi-compartment structure, especially for situations with closed doors.

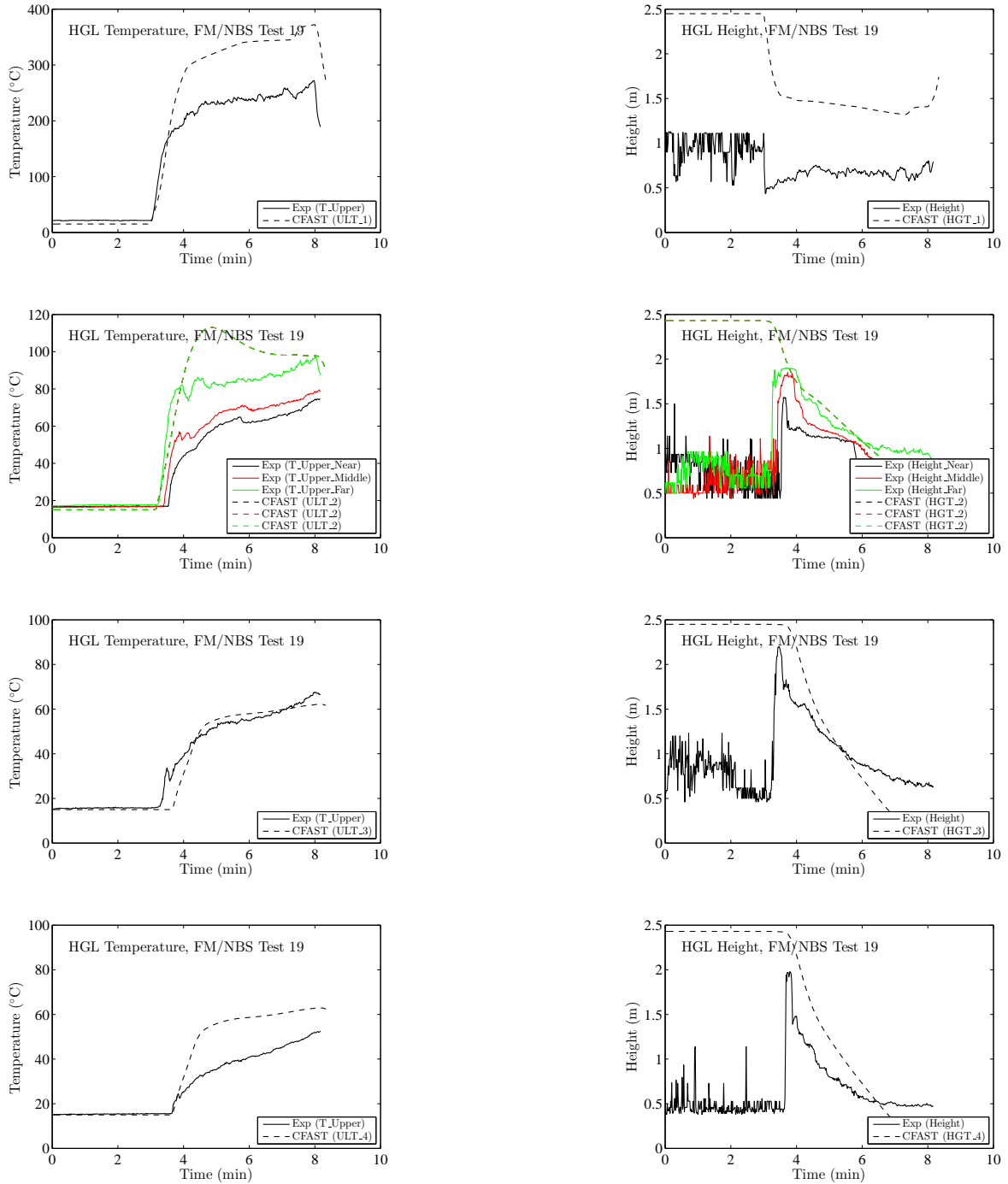


Figure B.1: Hot Gas Layer Temperature and Height for the FM/NBS Four Compartment Test 19.

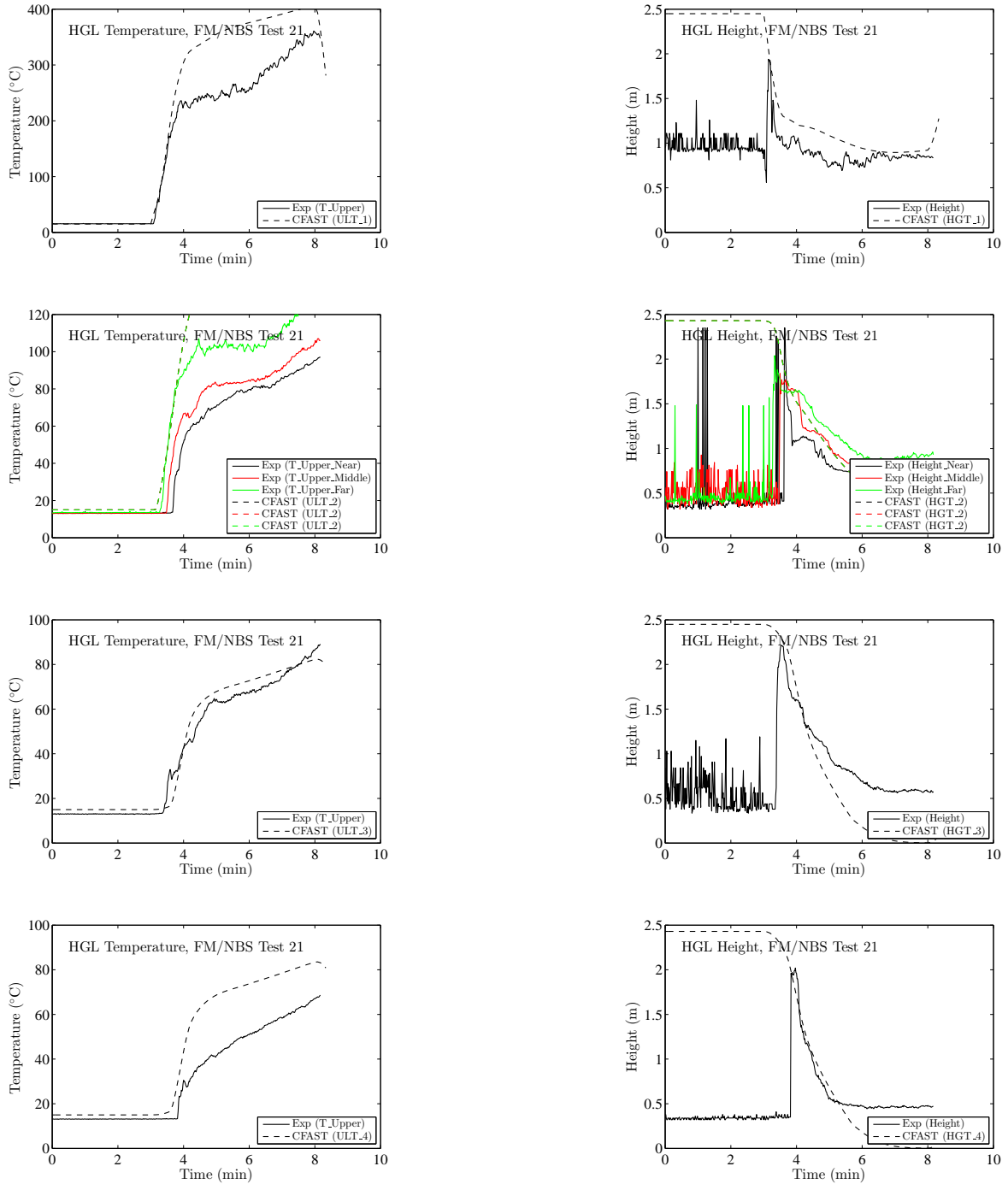


Figure B.2: Hot Gas Layer Temperature and Height for the FM/NBS Four Compartment Test 21.

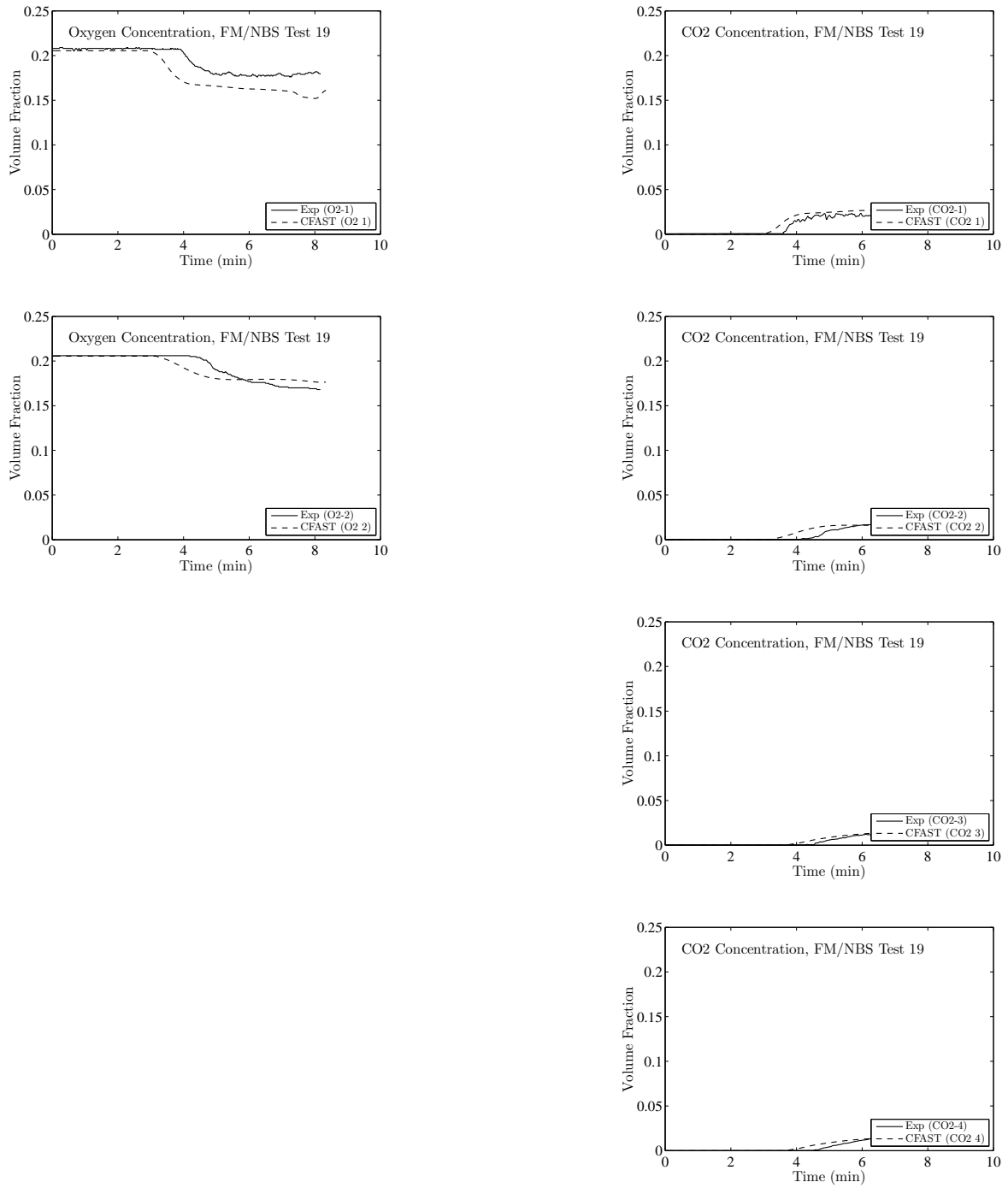


Figure B.3: Oxygen and Carbon Dioxide Concentration for the FM/NBS Test 19.

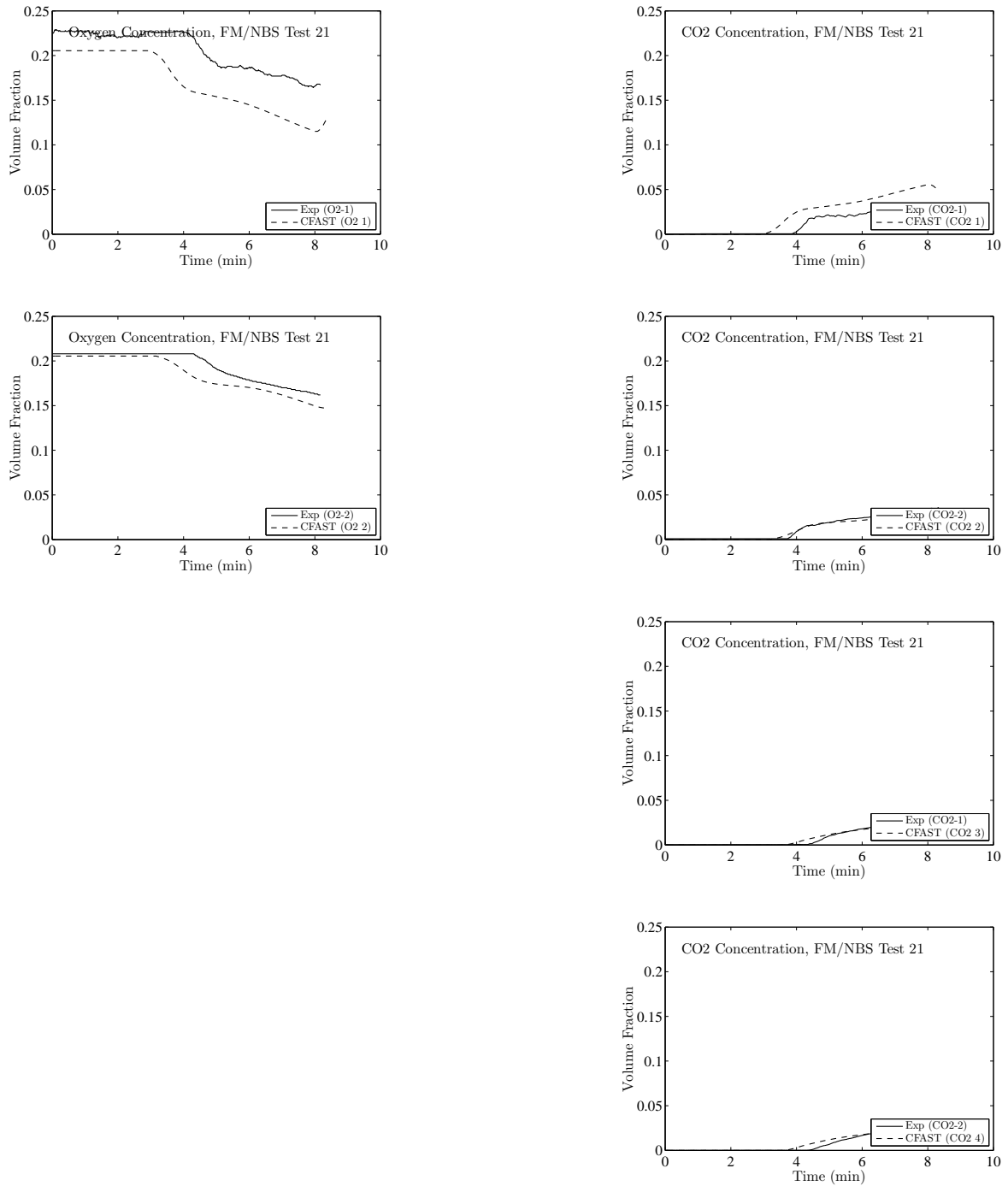


Figure B.4: Oxygen and Carbon Dioxide Concentration for the FM/NBS Test 21.

B.2 FM/SNL Test Series

The Factory Mutual and Sandia National Laboratories (FM/SNL) Test Series was a series of 25 fire tests conducted in 1985 for the NRC by Factory Mutual Research Corporation (FMRC), under the direction of Sandia National Laboratories (SNL). The primary purpose of these tests was to provide data with which to validate computer models for various types of NPP compartments. The experiments were conducted in an enclosure measuring 18 m x 12 m x 6 m, constructed at the FMRC fire test facility in Rhode Island. The FM/SNL test series is described in detail, including the types and locations of measurement devices, as well as some results in References [61, 62].

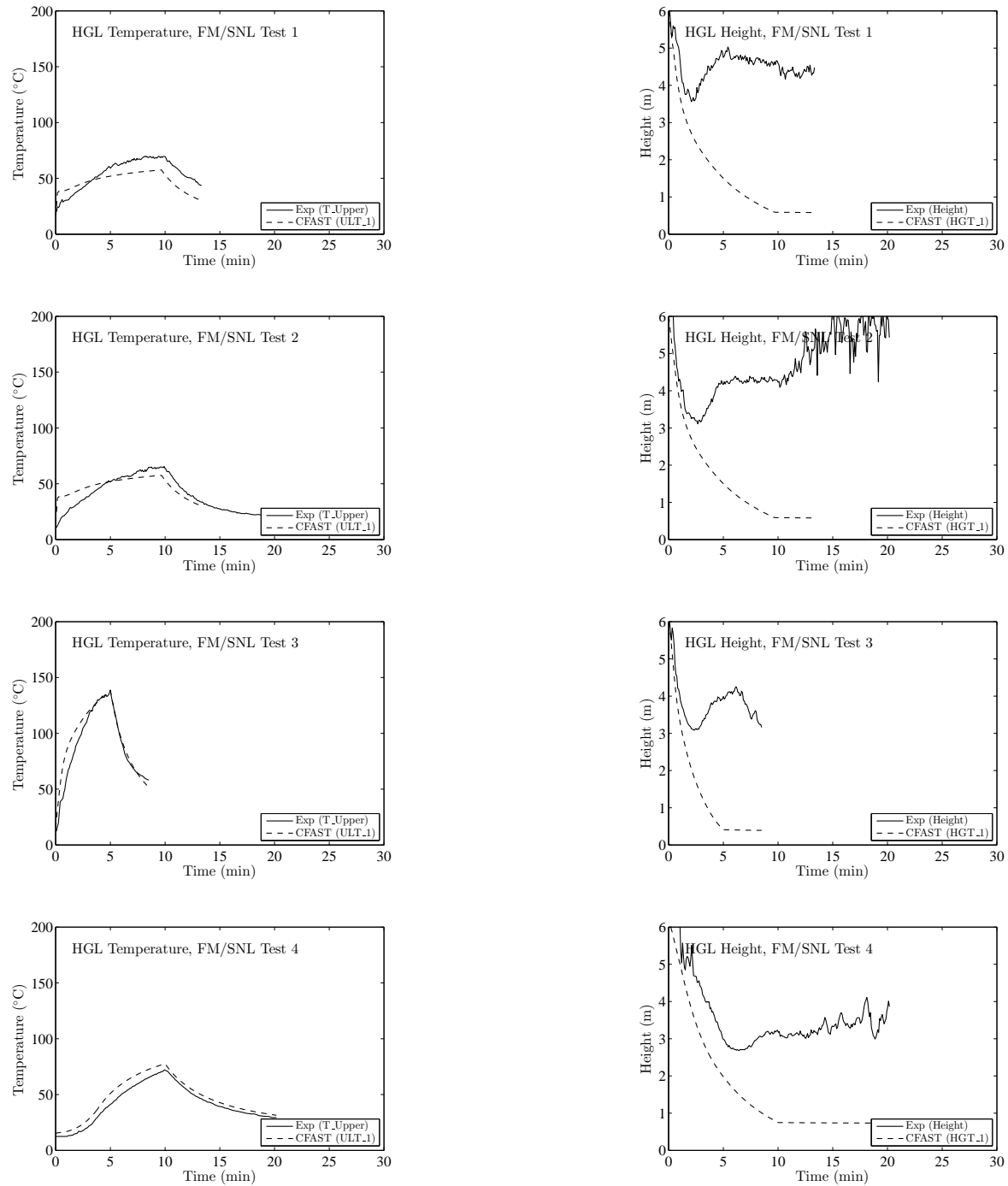


Figure B.5: Hot Gas Layer Temperature and Height for the FM/SNL Tests.

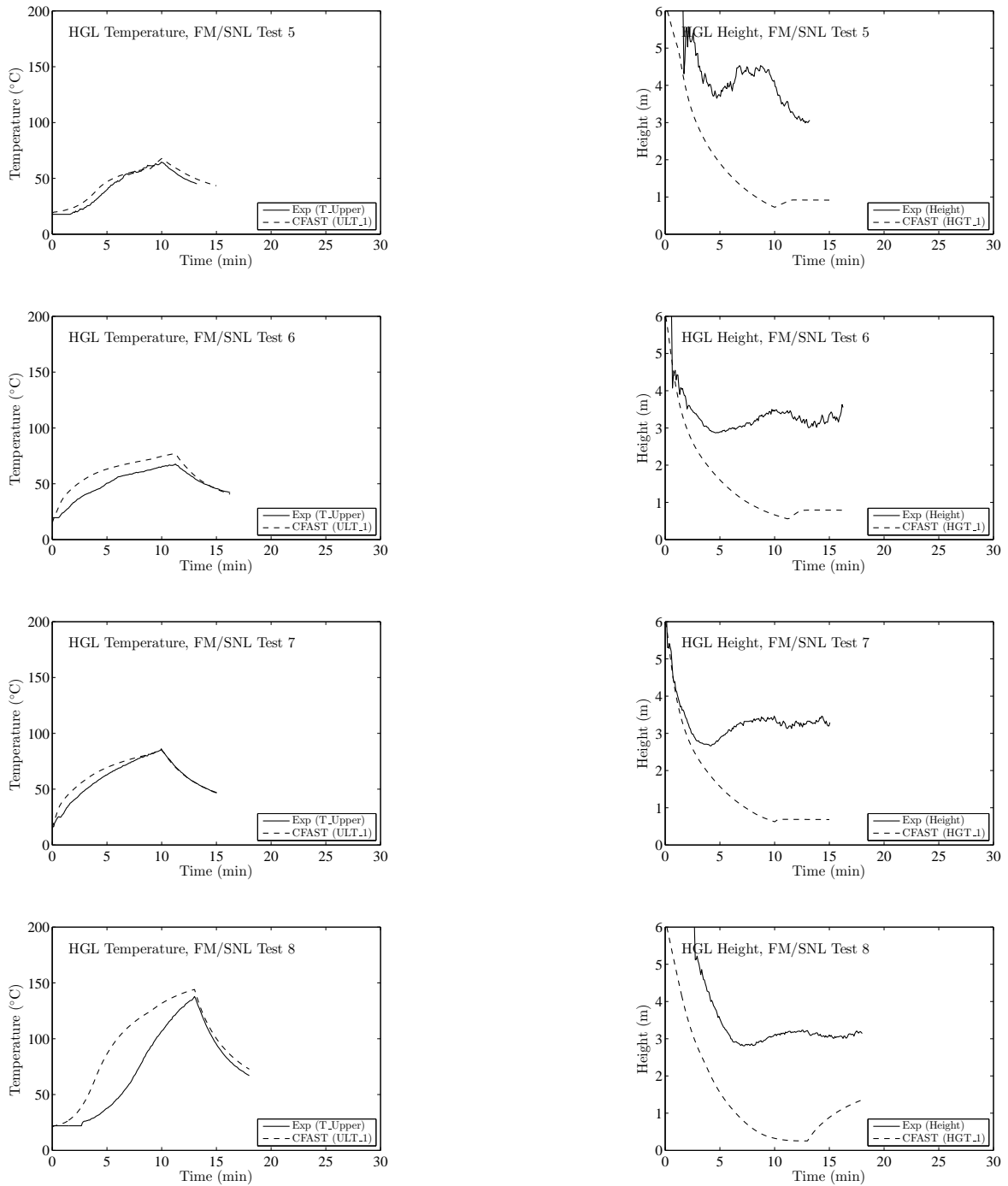


Figure B.6: Hot Gas Layer Temperature and Height for the FM/SNL Tests.

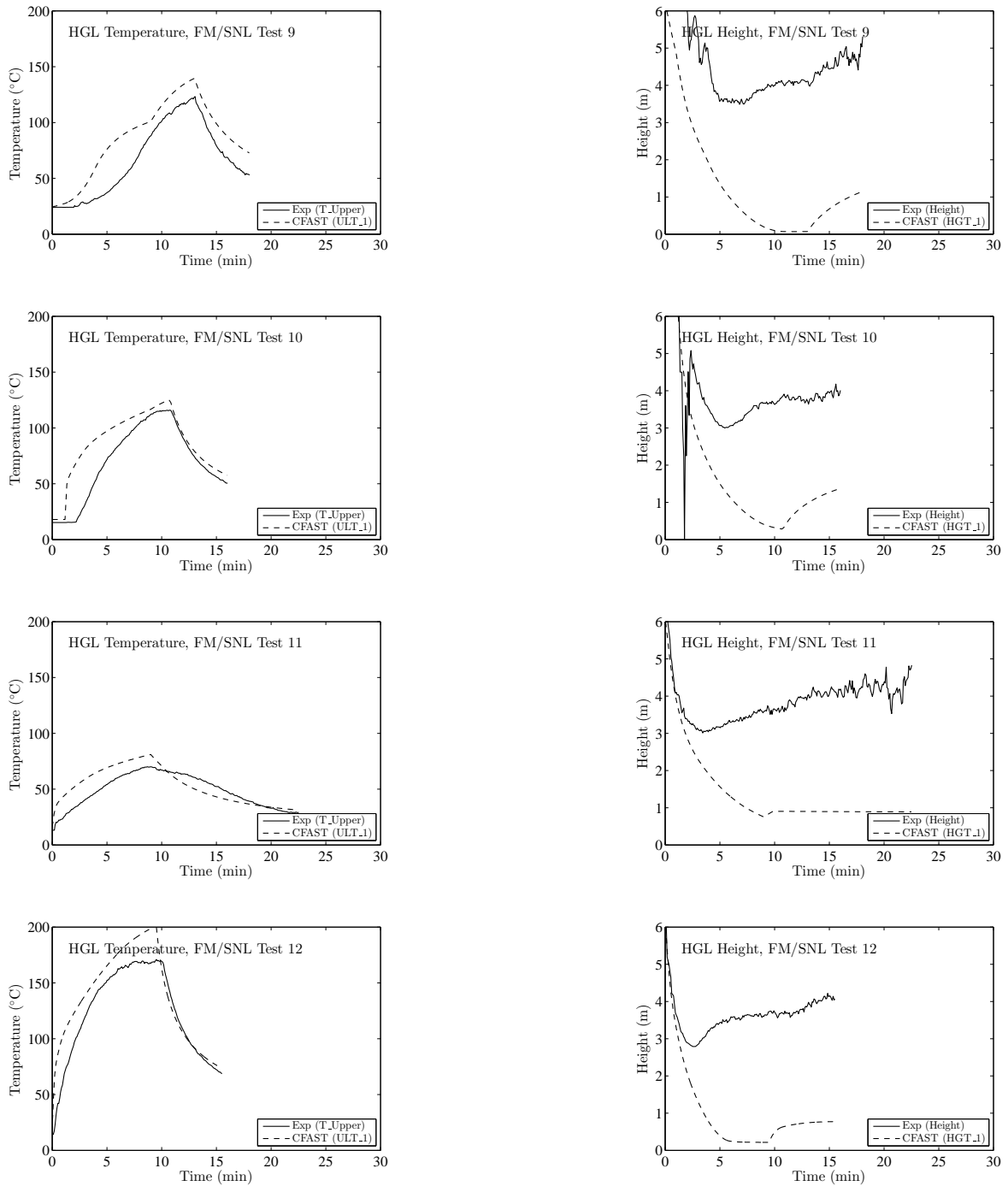


Figure B.7: Hot Gas Layer Temperature and Height for the FM/SNL Tests.

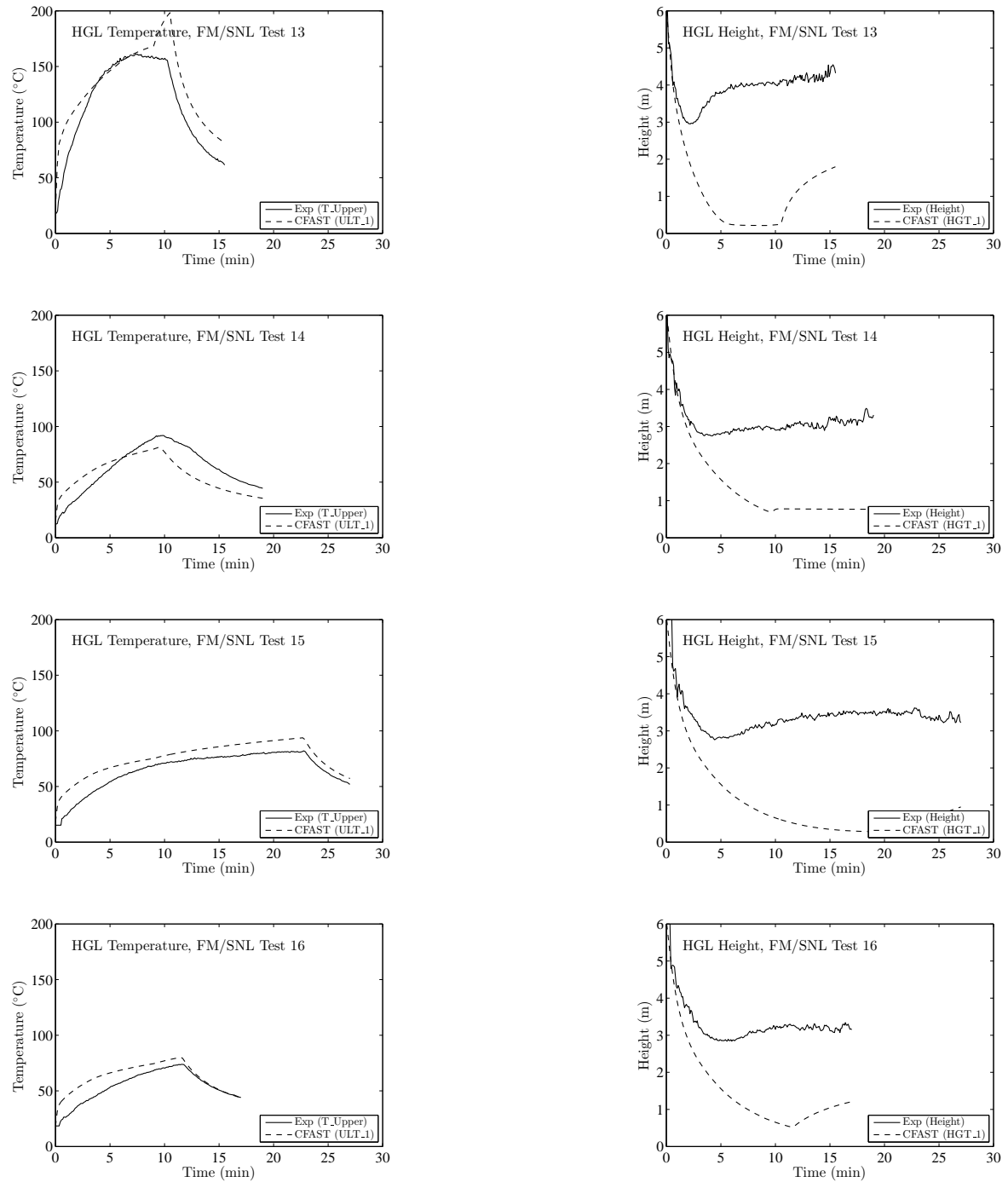


Figure B.8: Hot Gas Layer Temperature and Height for the FM/SNL Tests.

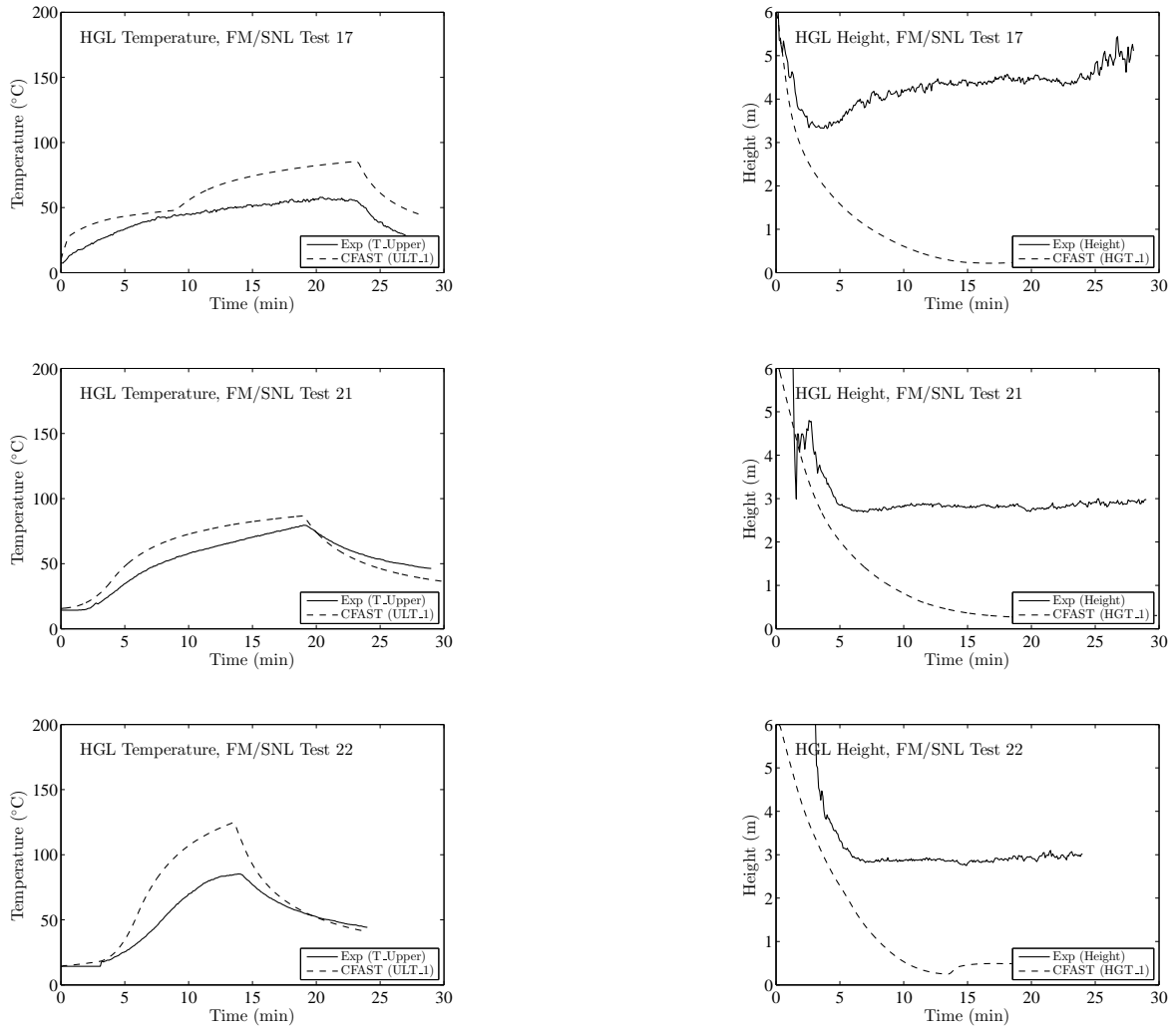


Figure B.9: Hot Gas Layer Temperature and Height for the FM/SNL Tests.

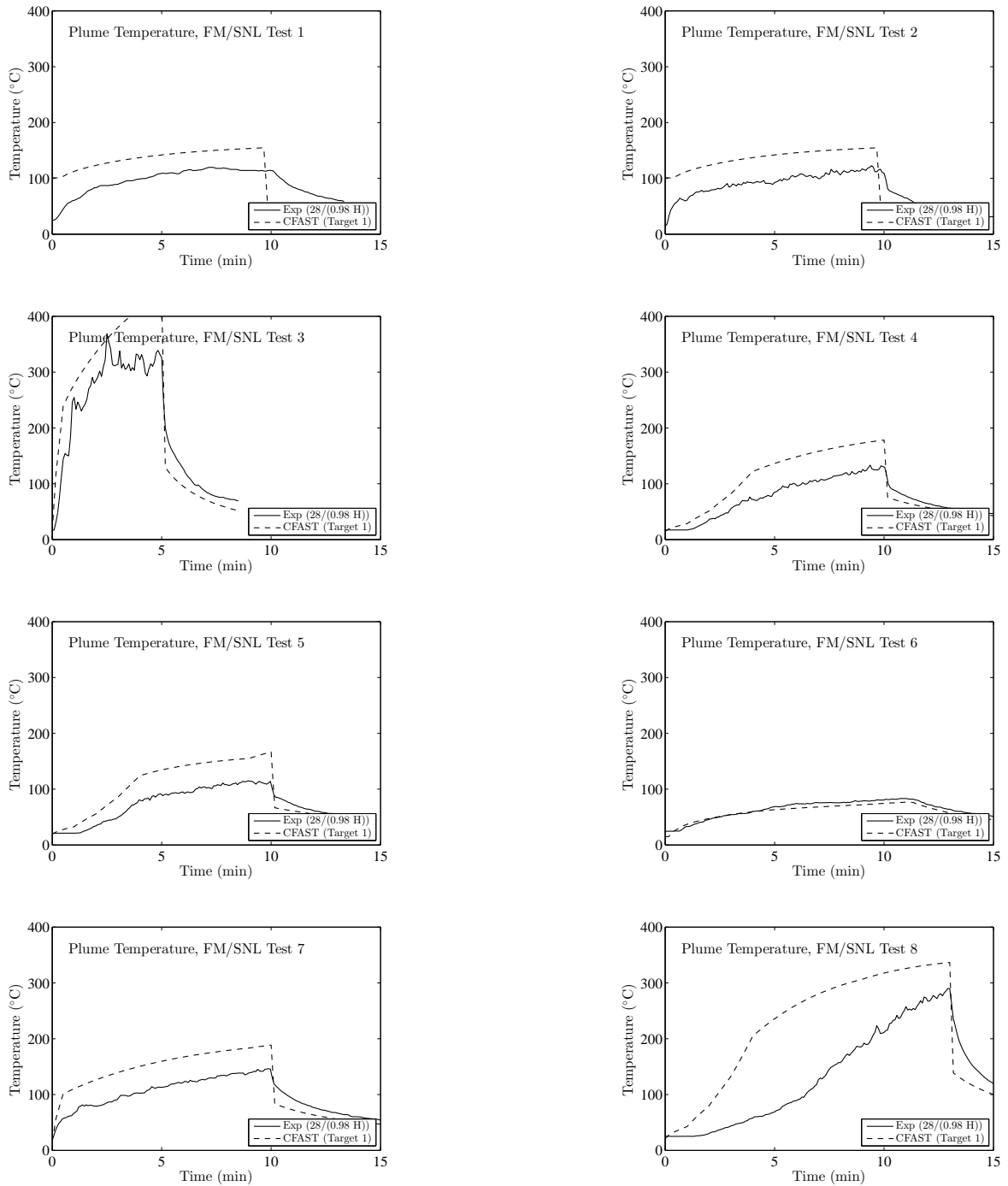


Figure B.10: Predicted Plume Centerline Temperature for the FM/SNL Tests.

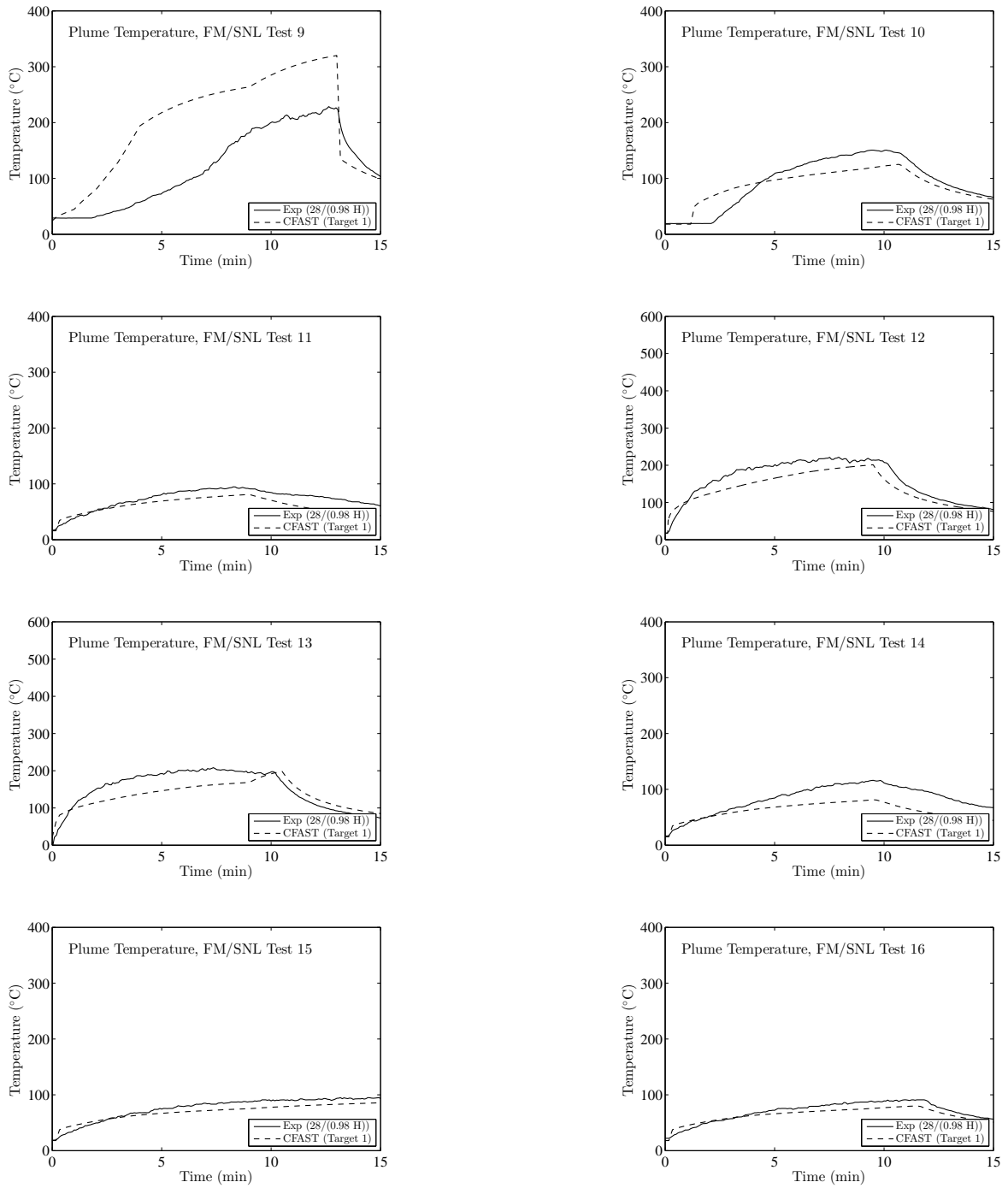


Figure B.11: Predicted Plume Centerline Temperature for the FM/SNL Tests.

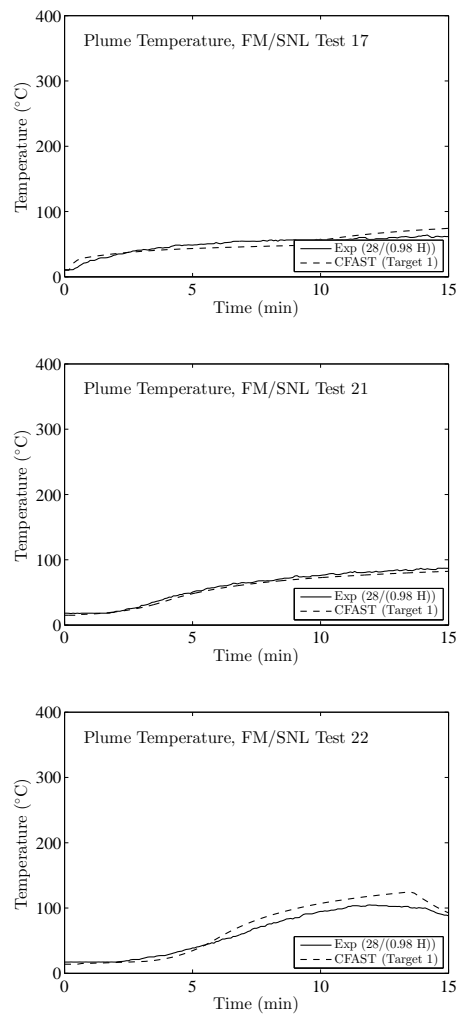


Figure B.12: Predicted Plume Centerline Temperature for the FM/SNL Tests.

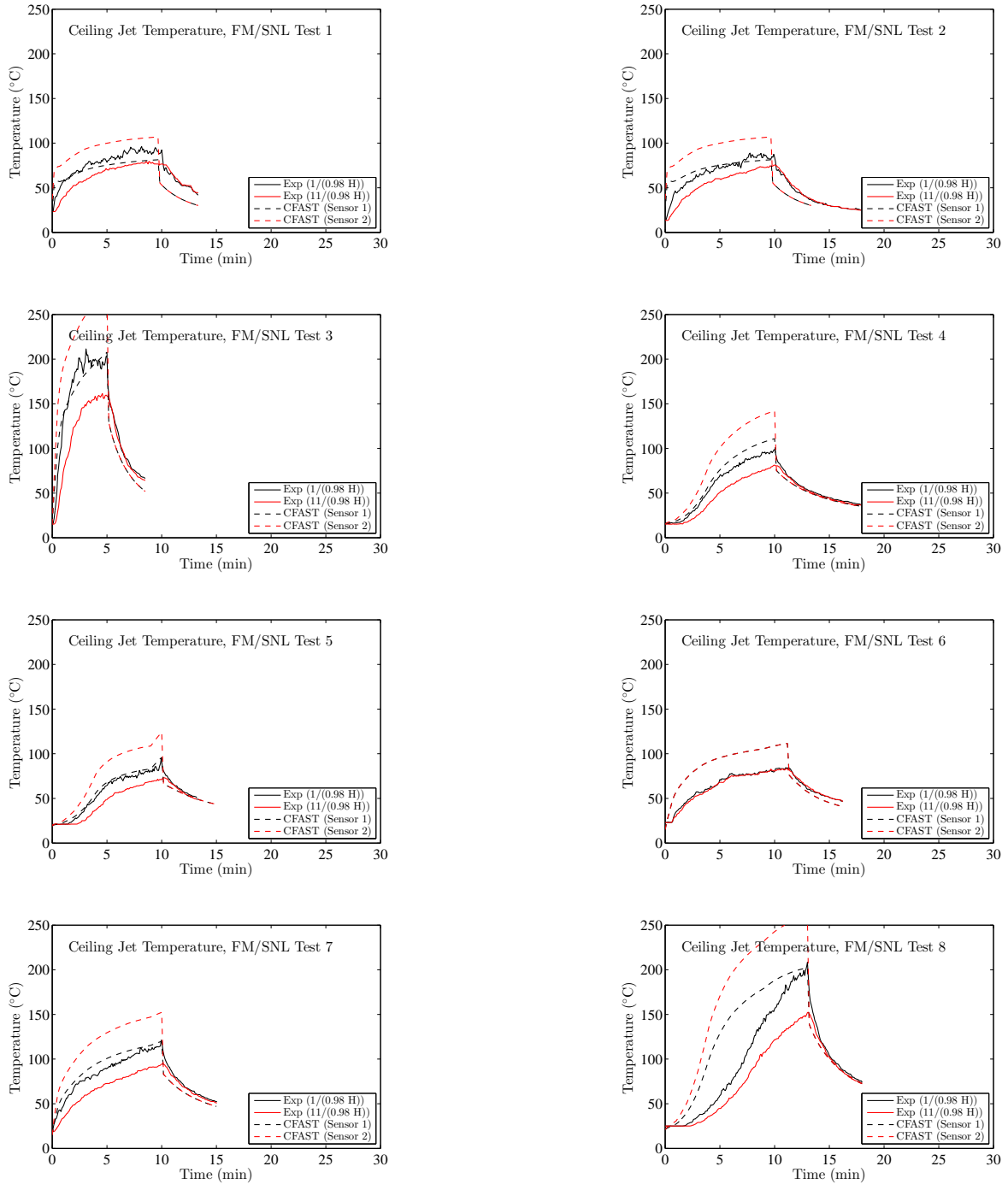


Figure B.13: Predicted Plume Centerline Temperature for the FM/SNL Tests.

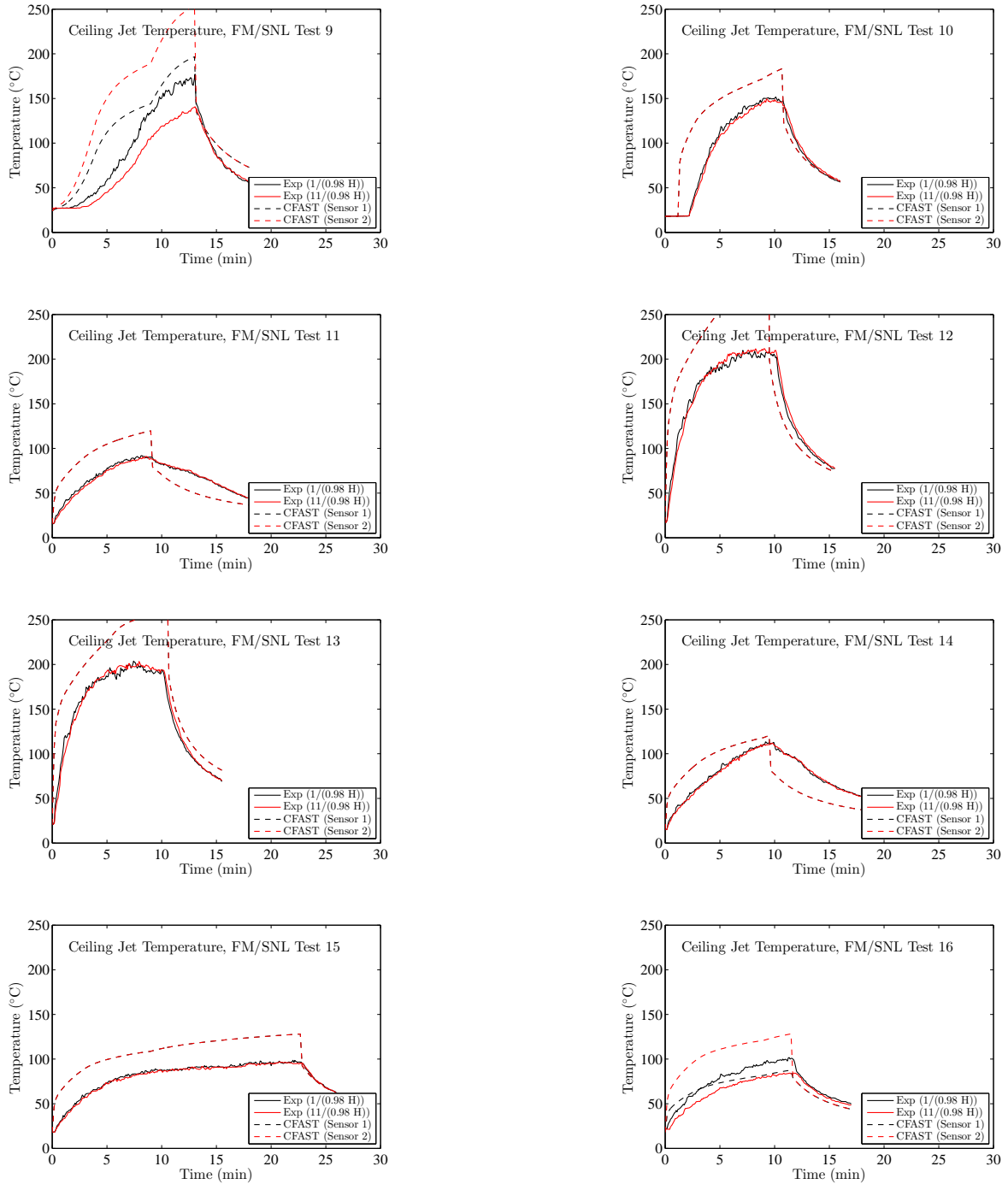


Figure B.14: Predicted Plume Centerline Temperature for the FM/SNL Tests.

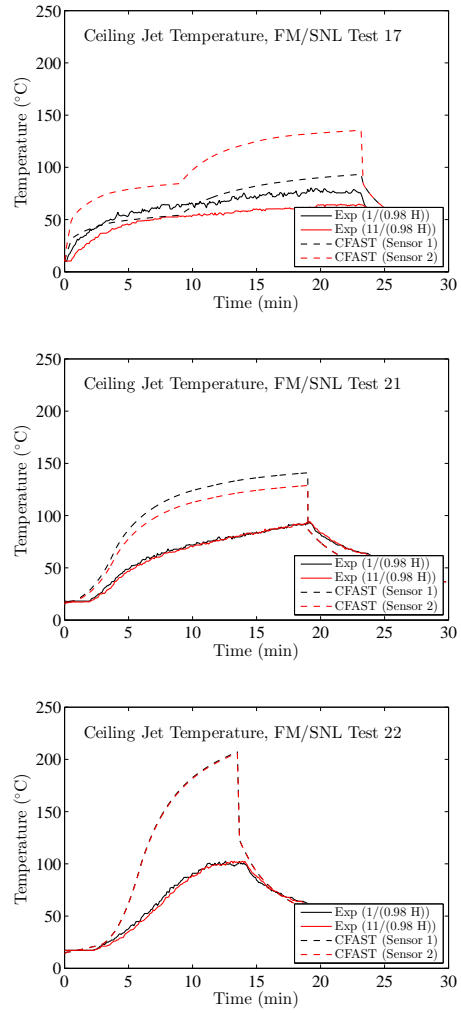


Figure B.15: Predicted Plume Centerline Temperature for the FM/SNL Tests.

B.3 iBMB Compartment Tests

A series of small compartment kerosene pool fire experiments, conducted at the Institut für Baustoffe, Massivbau und Brandschutz (iBMB) of Braunschweig University of Technology in Germany in 2004 [63]. The results from Test 1 were considered here. These experiments involved relatively large fires in a relatively small (3.6 m x 3.6 m x 5.7 m) concrete enclosure.

A second series of fire experiments in 2004, conducted under the International Collaborative Fire Model Project (ICFMP) involved realistically routed cable trays inside the same concrete enclosure at iBMB [65]. The compartment was configured slightly differently with a ceiling height of 5.6 m. Six types of measurements conducted during the test series were used in the evaluation conducted here, including the HGL temperature and depth, oxygen gas concentration, the temperature of targets and compartment surfaces, and heat flux.

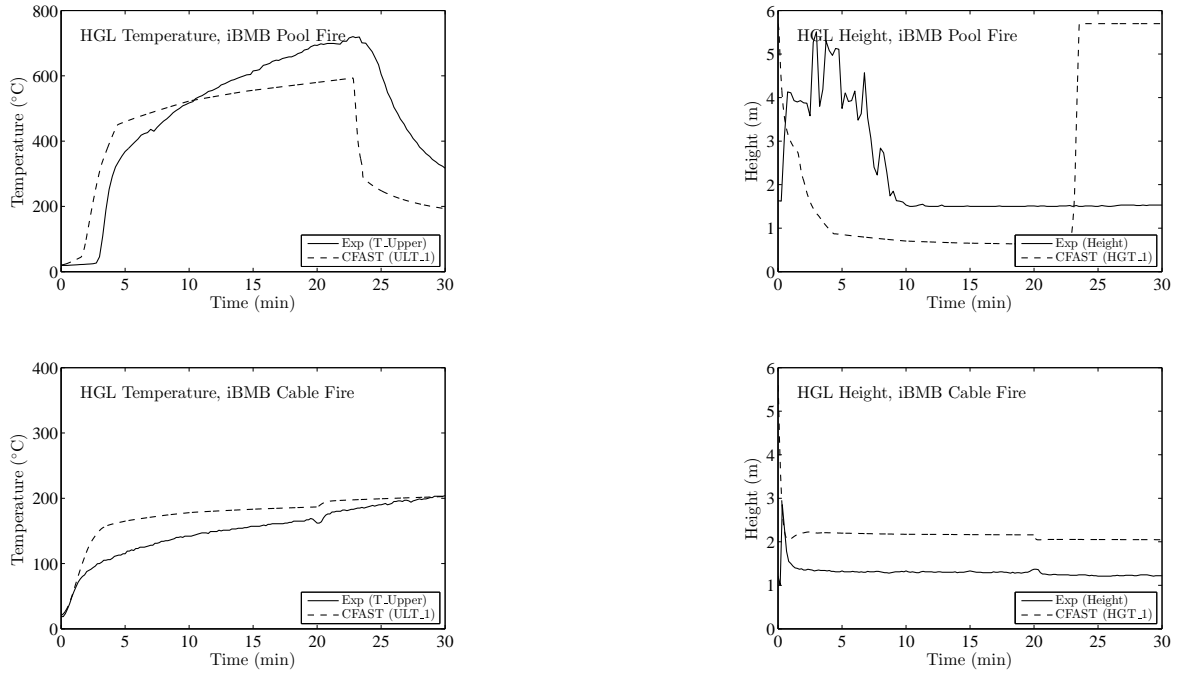


Figure B.16: Predicted HGL Temperature and Height for the iBMB Single Compartment Tests.

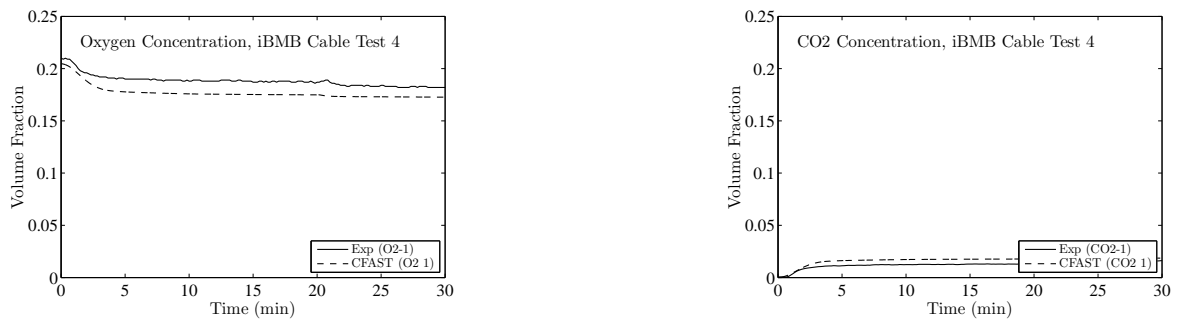
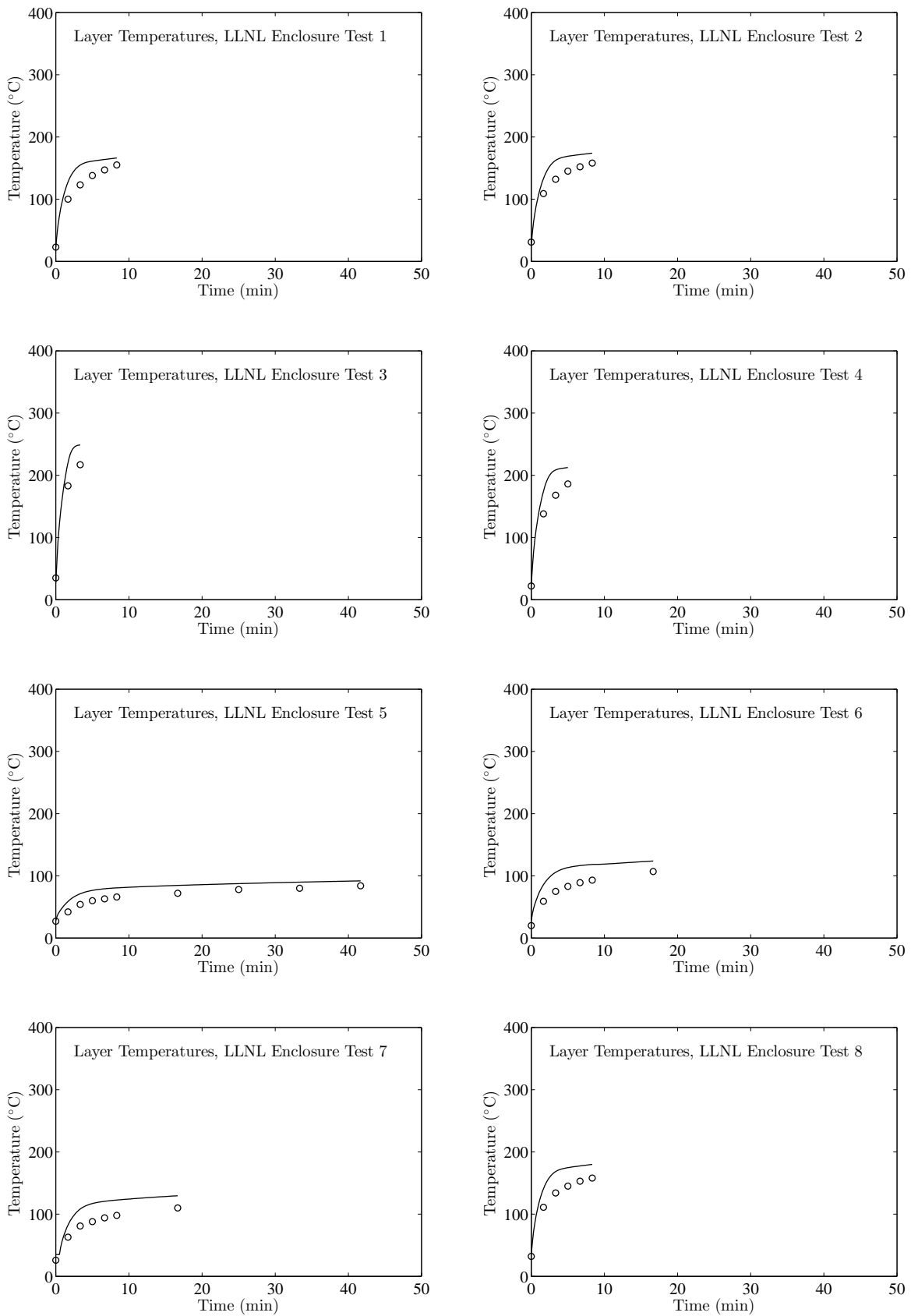


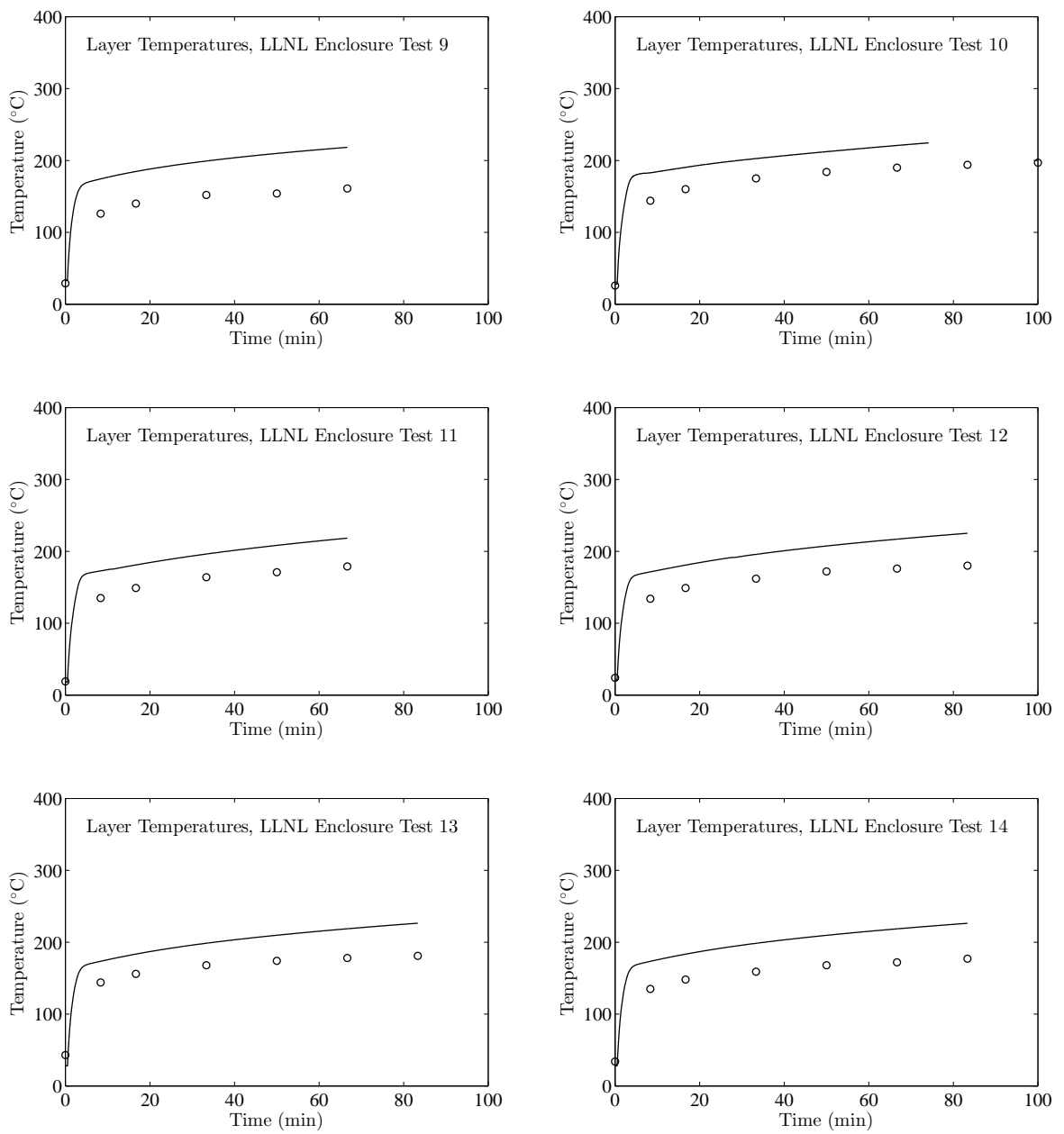
Figure B.17: Predicted Oxygen and Carbon Dioxide for the iBMB Cable Test 5.

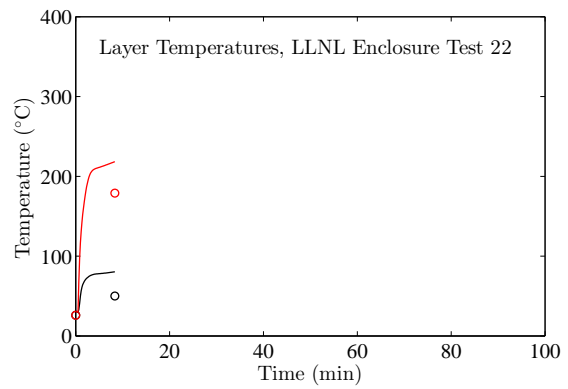
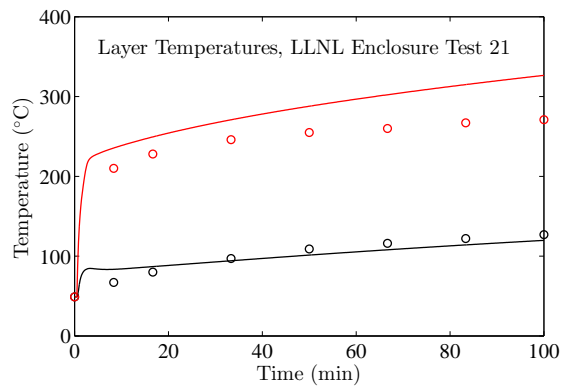
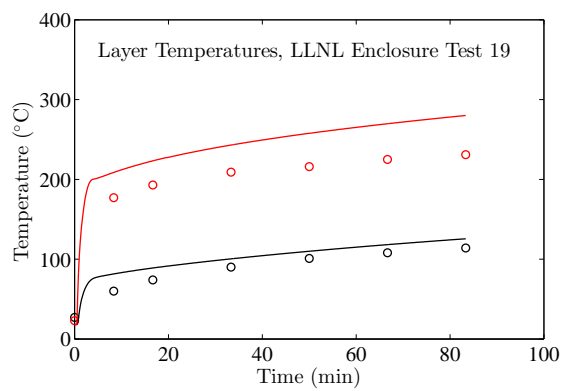
B.4 LLNL Enclosure Series

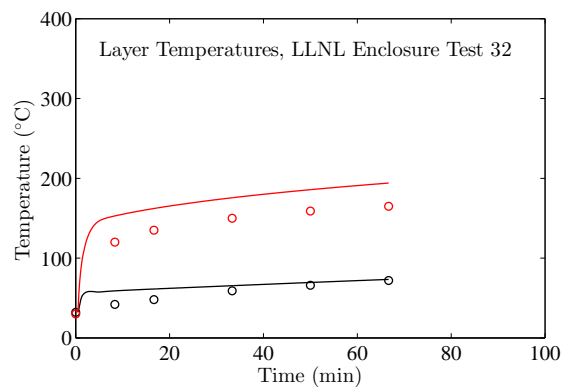
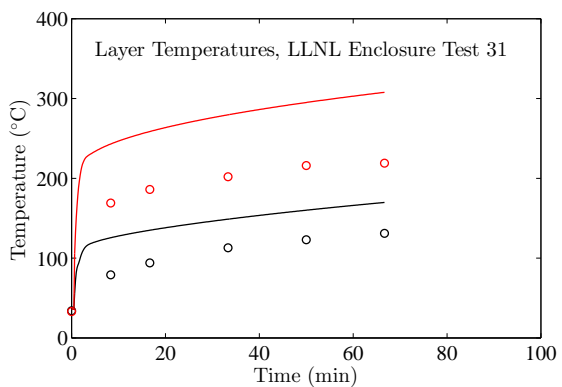
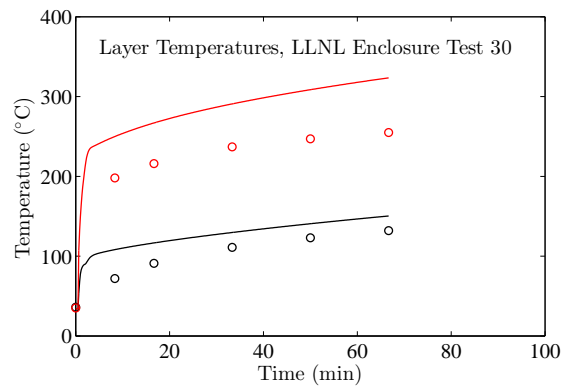
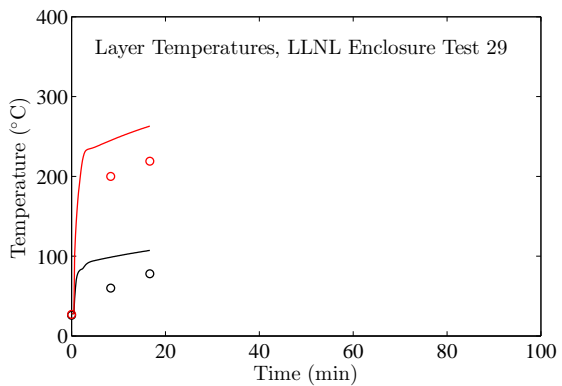
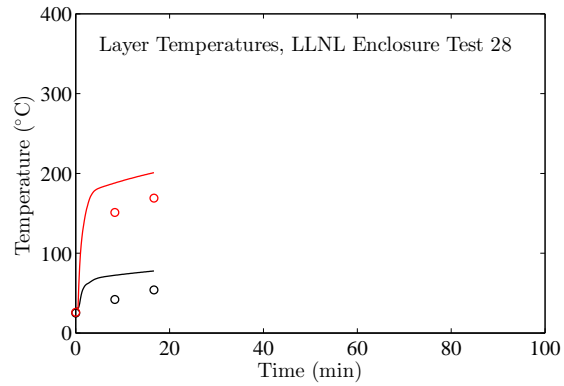
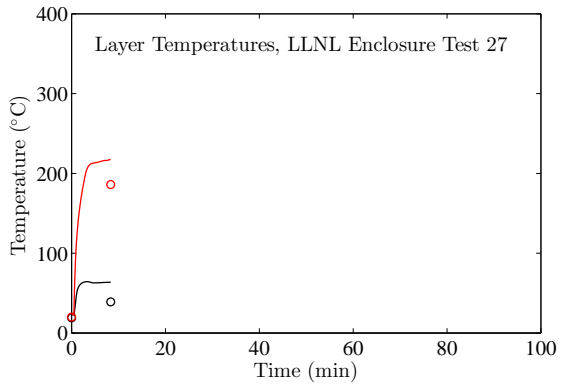
The plots on the following pages compare predicted and measured layer temperatures from the LLNL Enclosure test series. In the experiments, fifteen thermocouples were evenly spaced from floor to ceiling on either side of the burner. The measured temperatures were reported as averages of the lower, middle, and upper five TCs. Some of the experiments were conducted with a separated plenum space in the top one-third of the overall compartment (Tests 17-60). In these cases, the upper five TCs are a measure of the average plenum temperature.

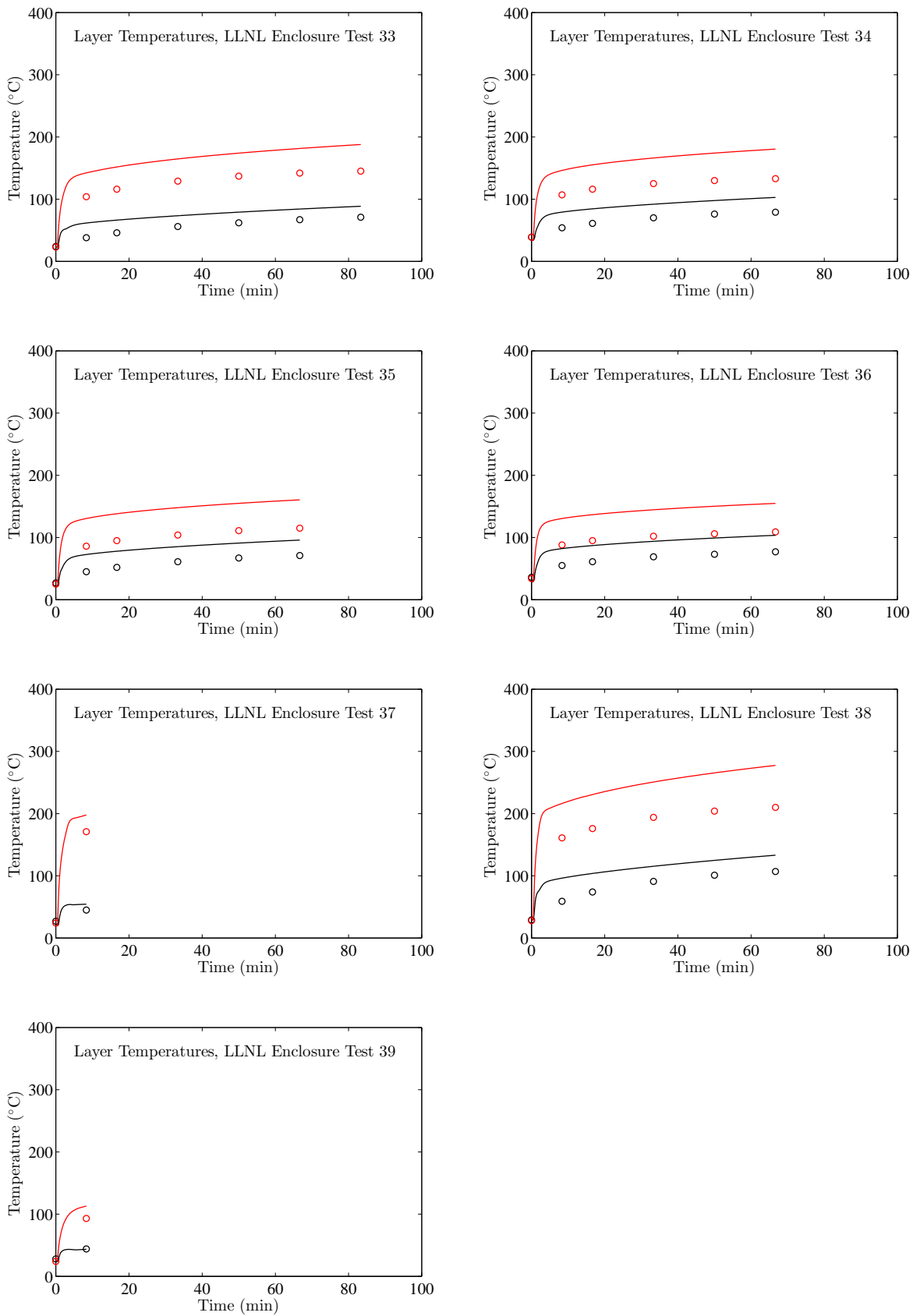
In the figures on the following pages, the black circles represent the average of the five uppermost TC measurements. The lines represent the simulation. The red circles represent the average of the middle five TC measurements. For the plenum tests, these TCs are located immediately beneath the plenum and their average temperature is typically greater than that of the plenum. Note that in a number of tests, the fuel flow was stopped or the fire self-extinguished. The simulations last only as long as the reported measurements.

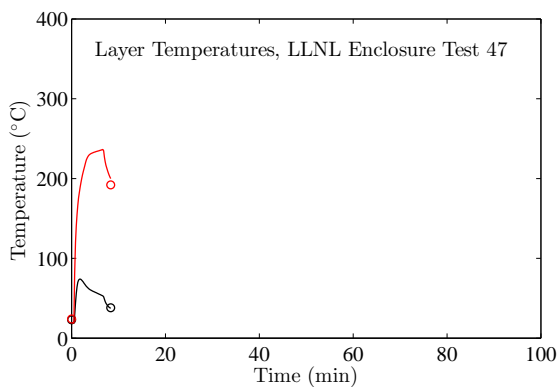
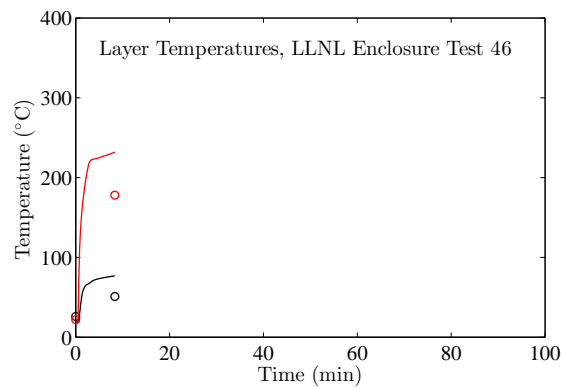
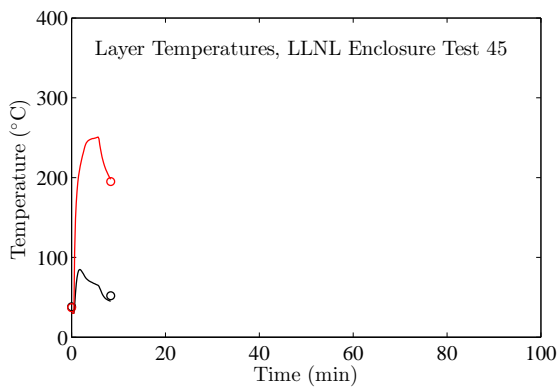
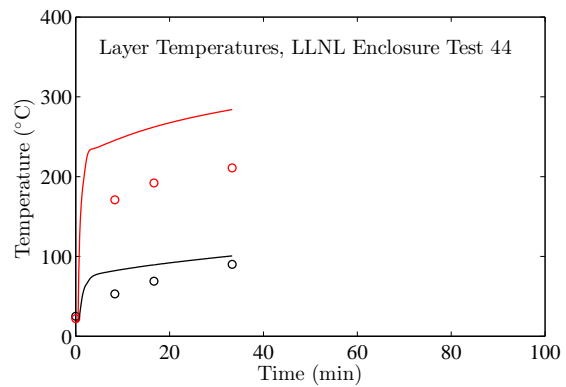
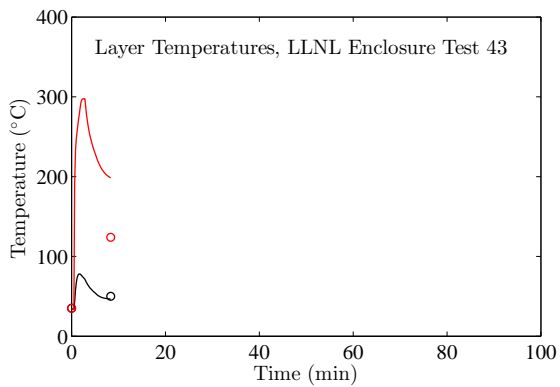
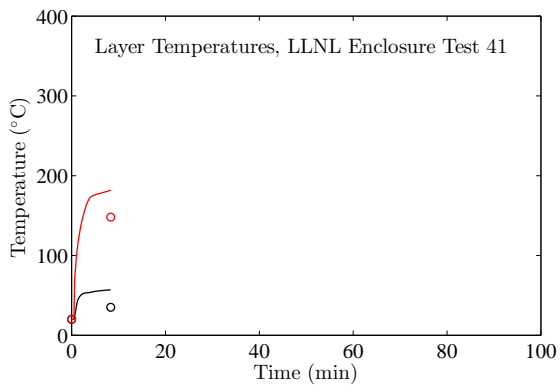


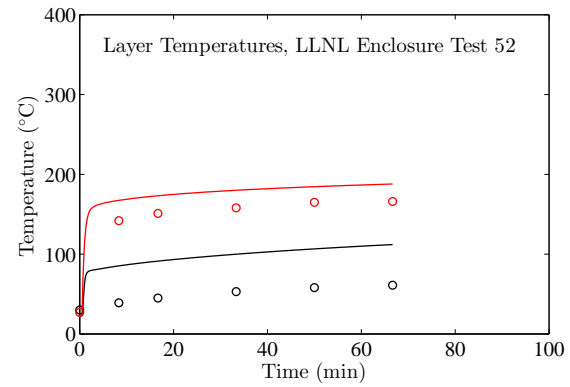
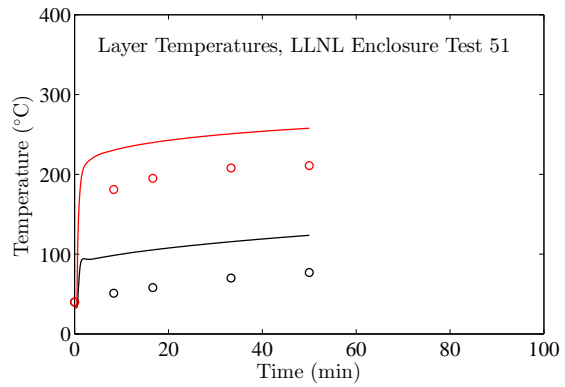
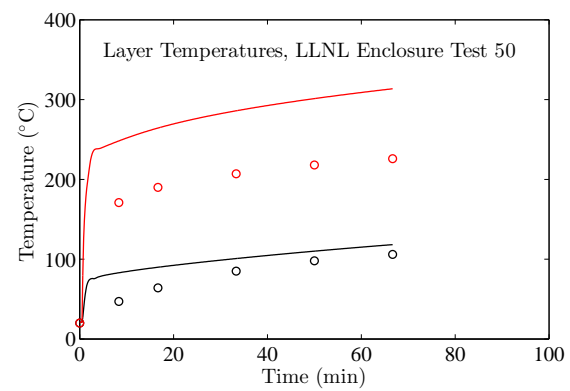
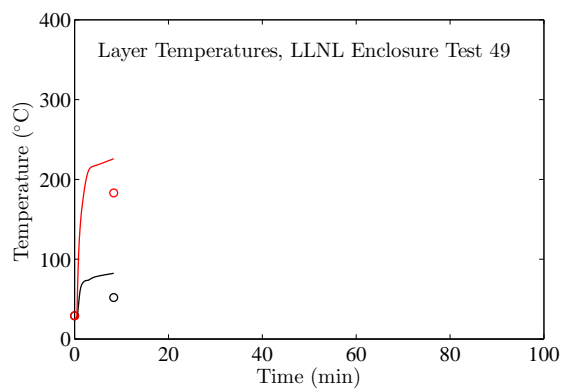


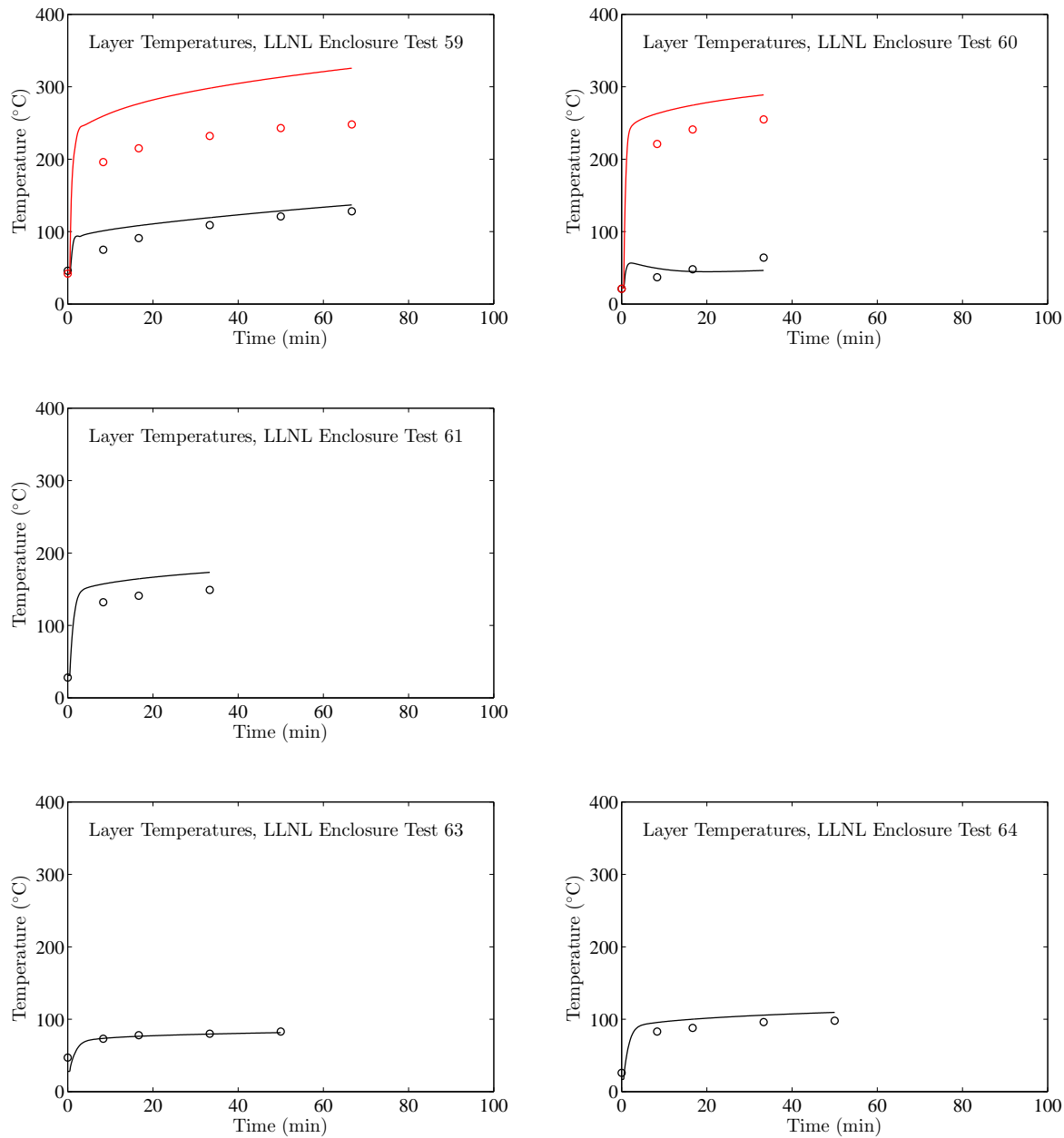












B.5 NBS Single Room Tests with Furniture

These data describe a series of room fire tests using upholstered furniture items in a room of fixed size but with varying opening sizes and shapes [34] conducted by the National Bureau of Standards (NBS, former name of NIST). It was selected for its well characterized and realistic fuel sources in a simple single-room geometry. In addition, the wide variation in opening size should provide challenges for current zone fire models. Peak fire size was about 2.9 MW with a total room volume of 21 m^3 . A series of four single-room fire tests were conducted using upholstered furniture items for comparison with their free burning behavior, previously determined in a furniture calorimeter. The experiments were conducted in a single room enclosure; ventilation to the room was provided by window openings of varying sizes. The room was equipped with an instrumented exhaust collection system outside the window opening.

A second similar test series also utilized a single-room fire test with furniture as the fire source [67]. It expanded upon the first data set by adding the phenomenon of wall burning. Peak fire size was about 7 MW. The room size was similar to the first test series.

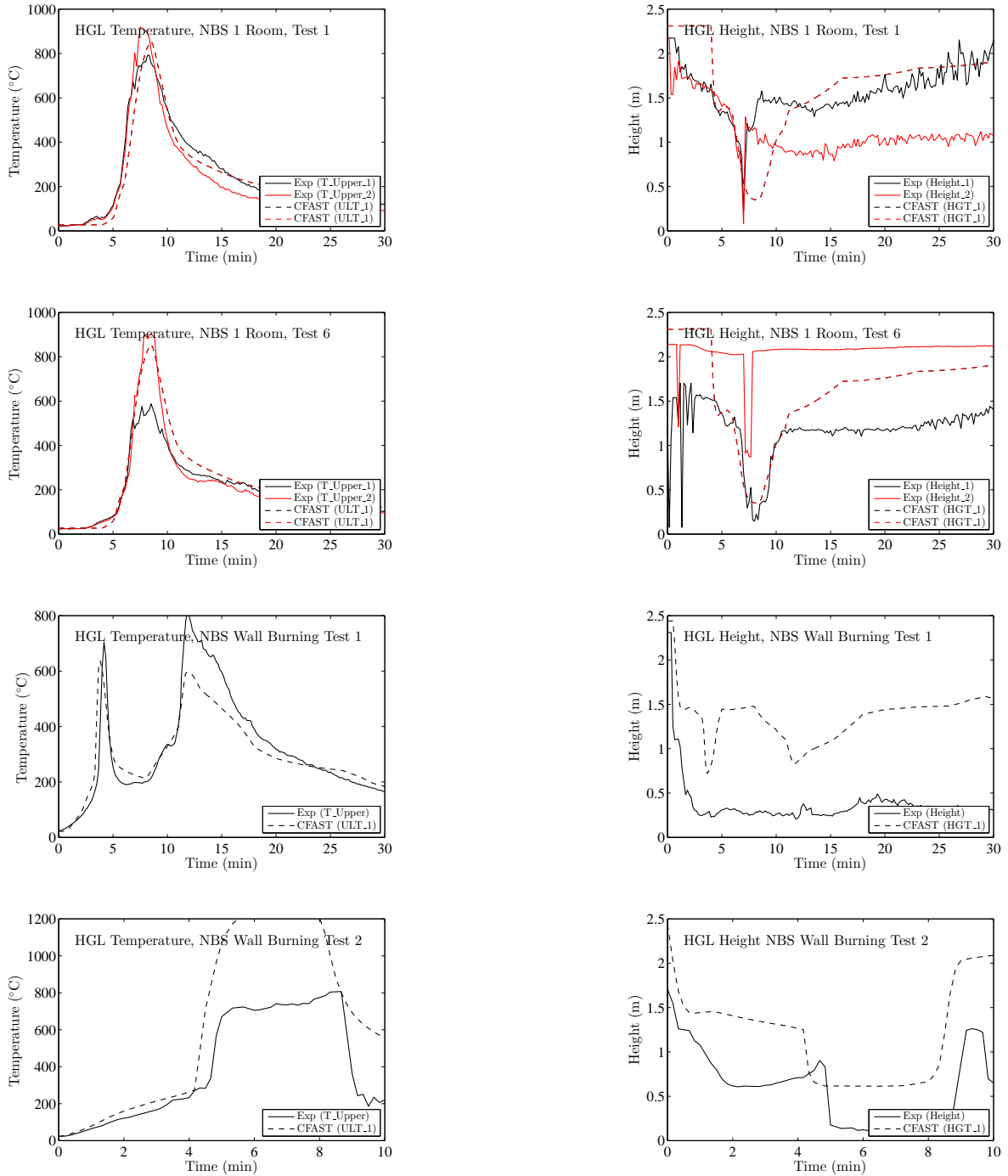


Figure B.18: Predicted HGL Temperature and Height for the NBS Single Compartment Tests.

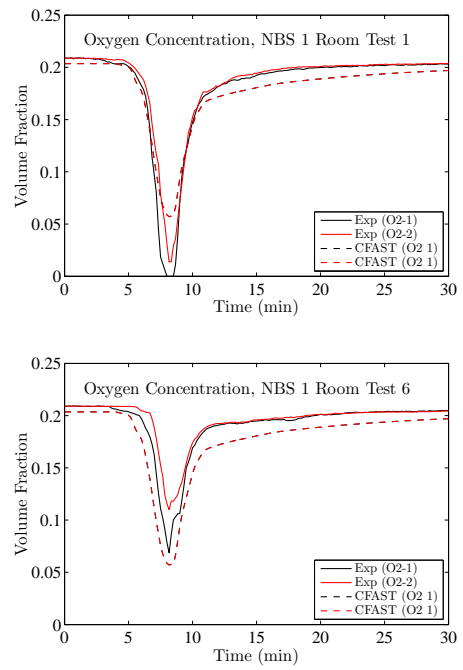


Figure B.19: Predicted Oxygen Concentration for the NBS Single Compartment Tests.

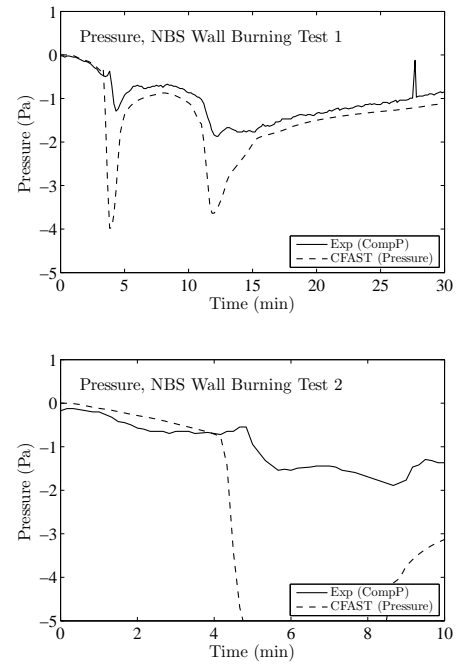


Figure B.20: Predicted Compartment Pressure for the NBS Single Compartment Tests.

B.6 NBS Multi-Compartment Test Series

The National Bureau of Standards (NBS, former name of NIST) Multi-Compartment Test Series consisted of 45 fire tests representing 9 different sets of conditions were conducted in a three-room suite. The experiments were conducted in 1985 and are described in detail in reference [60]. The suite consisted of two relatively small rooms, connected via a relatively long corridor. Total volume of the structure was approximately 100 m². The fire source, a gas burner, was located against the rear wall of one of the small compartments . Fire tests of 100 kW, 300 kW and 500 kW were conducted. For the current study, three 100 kW fire experiments have been used, including Test 100A from Set 1, Test 100O from Set 2, and Test 100Z from Set 4. For the NBS Multi-room series, Tests 100A, 100O and 100Z were selected for study, because they were constructively used in a previous validation study [[68], and because these tests had the steadiest values of measured heat release rate during the steady burning period. The selected data are also available in Reference [68].

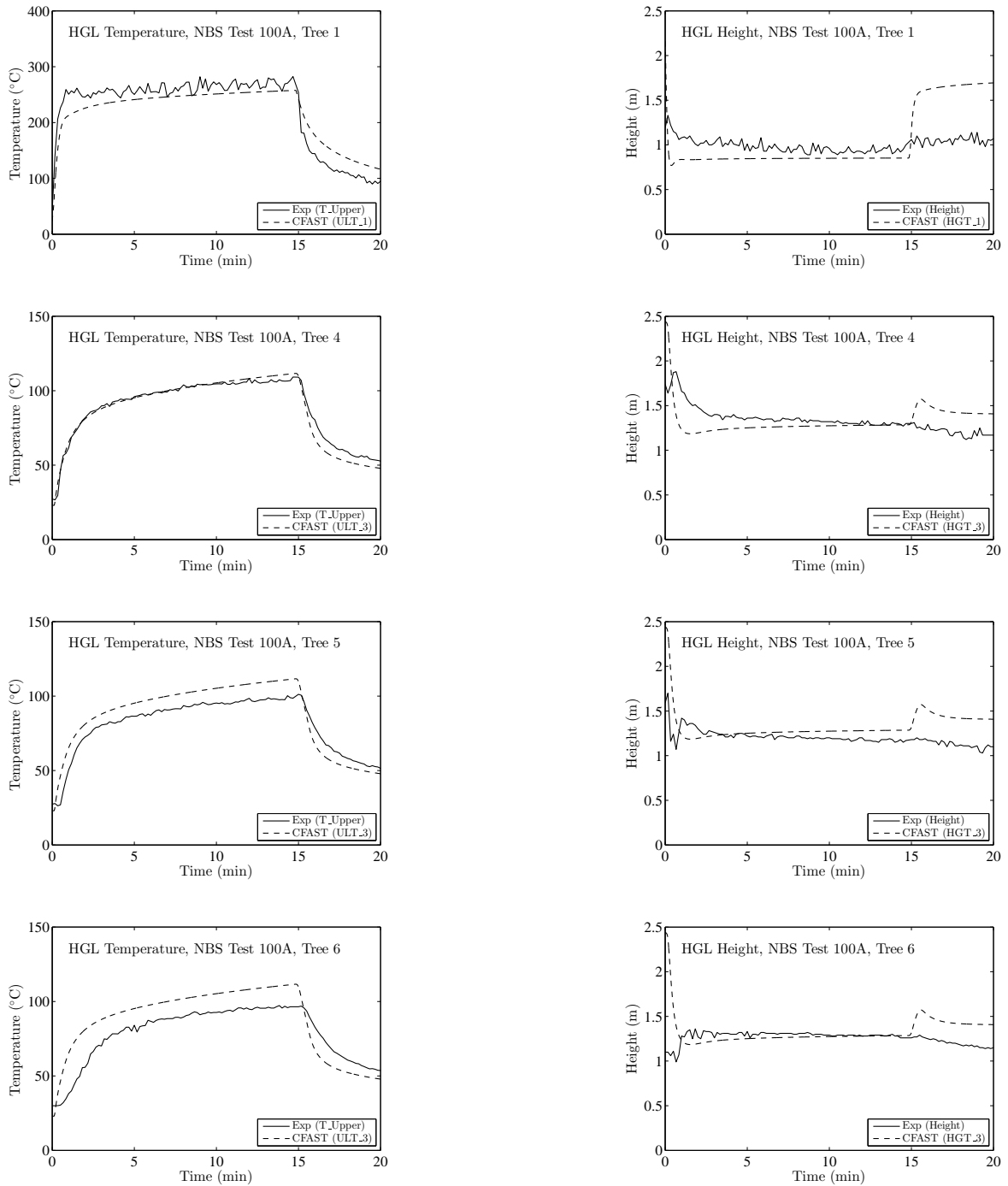


Figure B.21: Hot Gas Layer Temperature and Height for the NBS Multi-Room Test 100A.

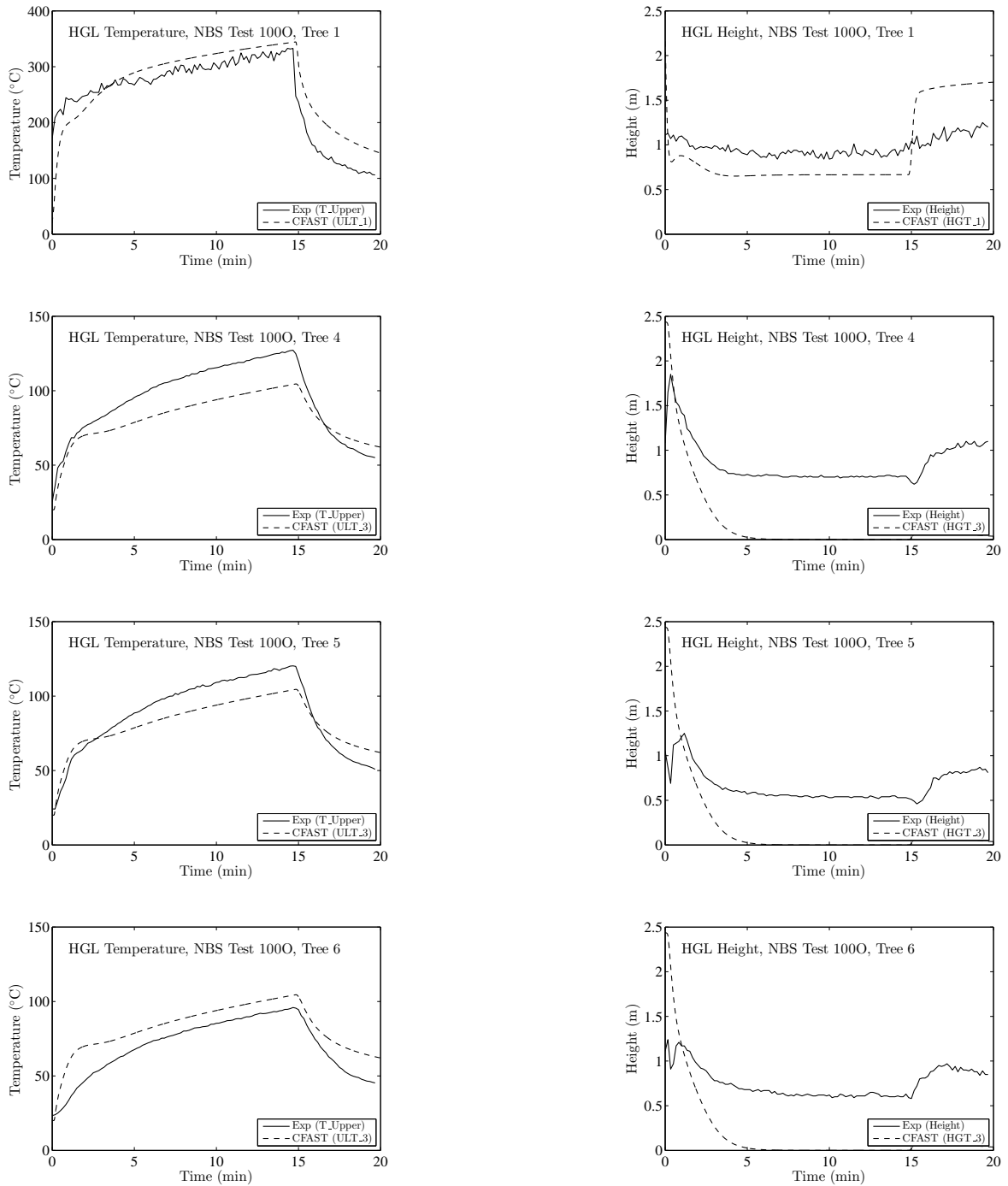


Figure B.22: Hot Gas Layer Temperature and Height for the NBS Multi-Room Test 100O.

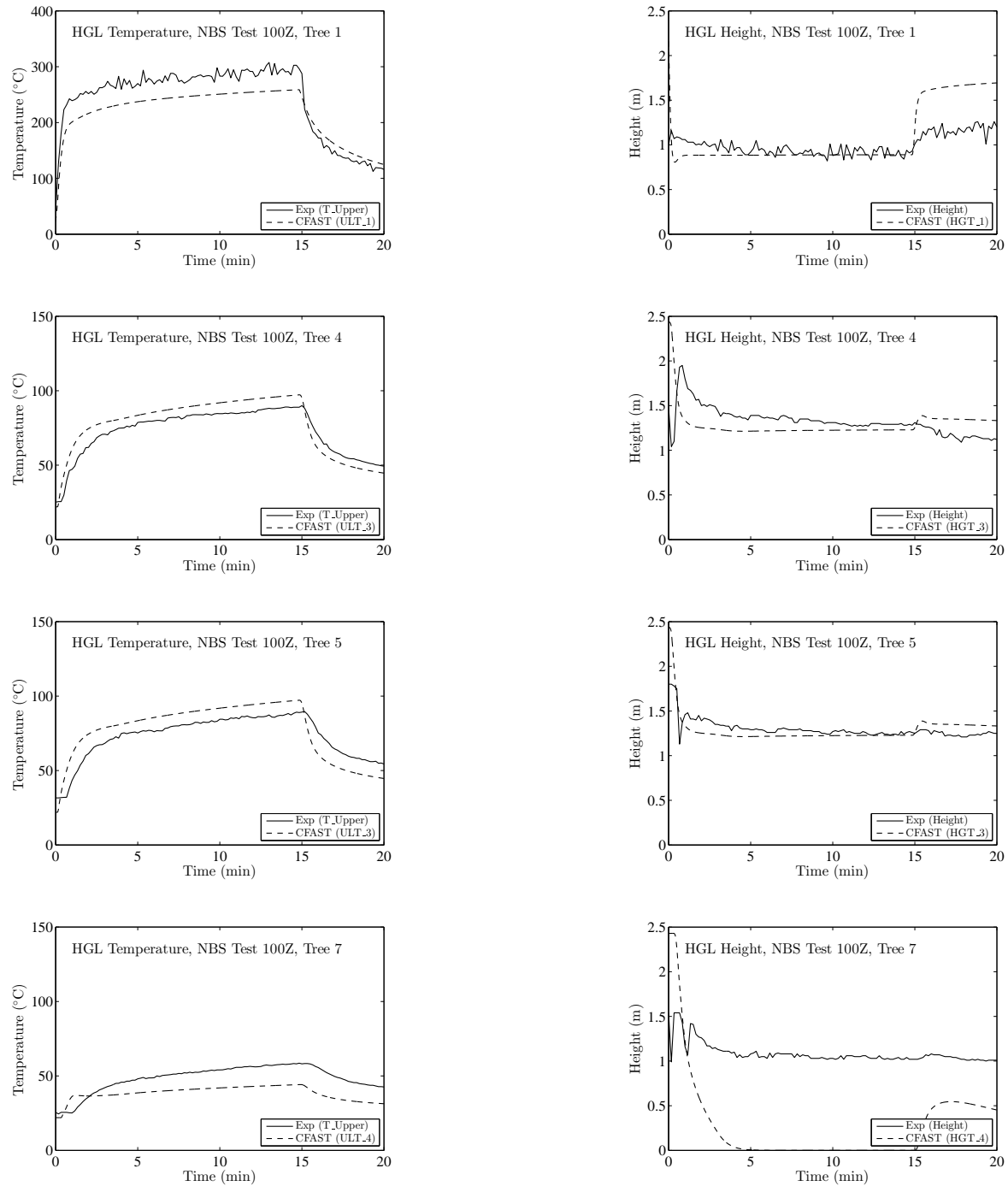
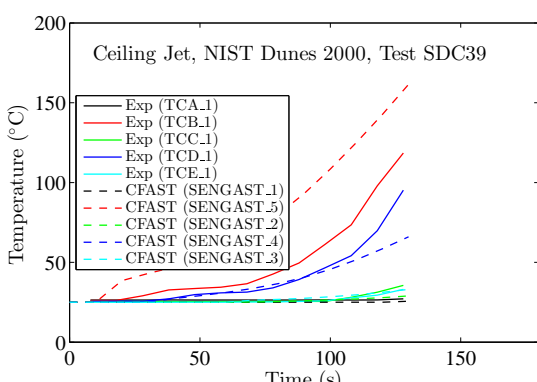
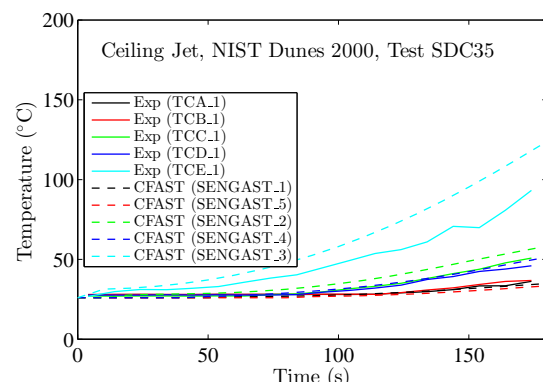
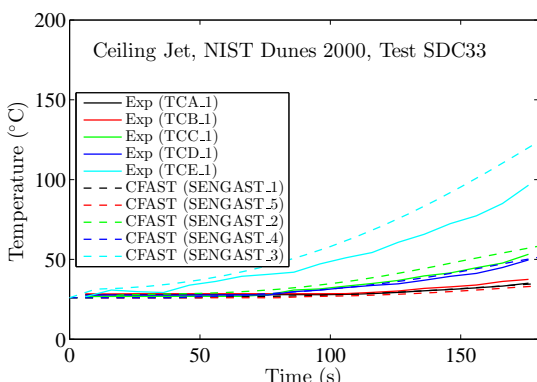
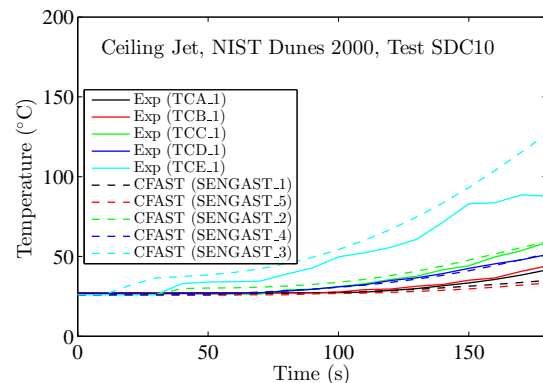
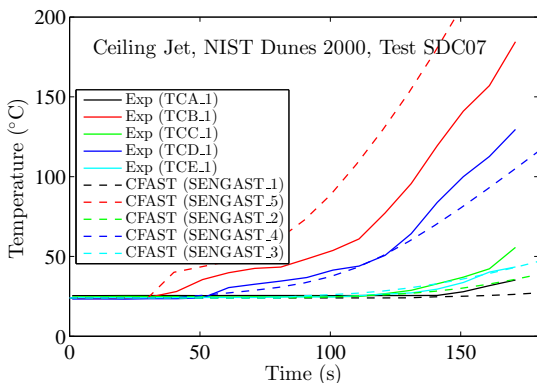
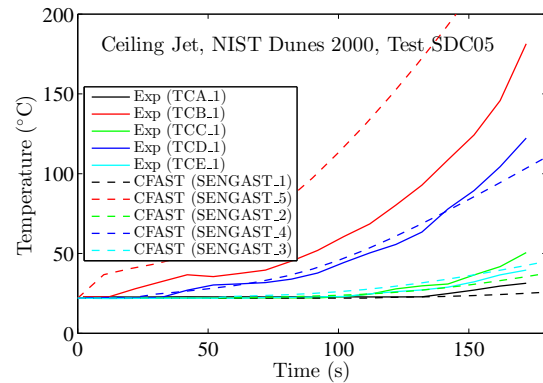
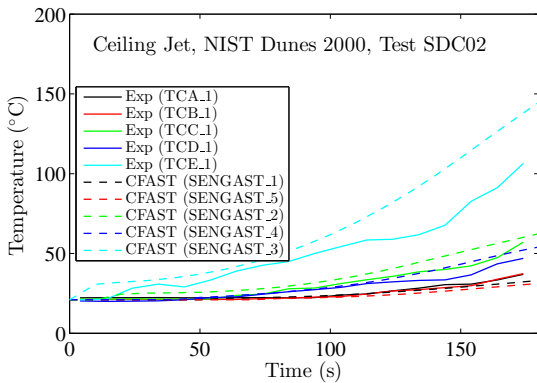


Figure B.23: Hot Gas Layer Temperature and Height for the NBS Multi-Room Test 100Z.

B.7 NIST Dunes 2000 Experiments

The primary purpose of the NIST Dunes 2000 experiments was to measure smoke alarm activation times in residential settings. In the single-story manufactured home tests that were selected for validation, five smoke alarm measurement stations (A-E) were located in different areas of the manufactured home. Included is a scatterplot of measured and predicted smoke alarm activation time. Thermocouple trees were also located at each measurement station. The highest thermocouple in the tree can be compared to ceiling jet temperature predictions. The plots on the following page show the measured and predicted ceiling jet temperatures for the five measurement stations in each test.



B.8 NIST Seven-story Hotel Tests

By far the most complex test, this data set is part of a series of full-scale experiments conducted to evaluate zoned smoke control systems, with and without stairwell pressurization [71]. It was conducted in a seven story hotel with multiple rooms on each floor and a stairwell connecting all floors. This data set was chosen because it would challenge the scope of most current fire models. Measured temperatures and pressure differences between the rooms and floors of the building are extensive and consistent. Peak fire size was 3 MW with a total building volume of 140 000 m³. The hotel was a masonry structure consisting of two wings, one three stories and the other seven stories tall. The fires were set on the second floor of the seven-story wing.

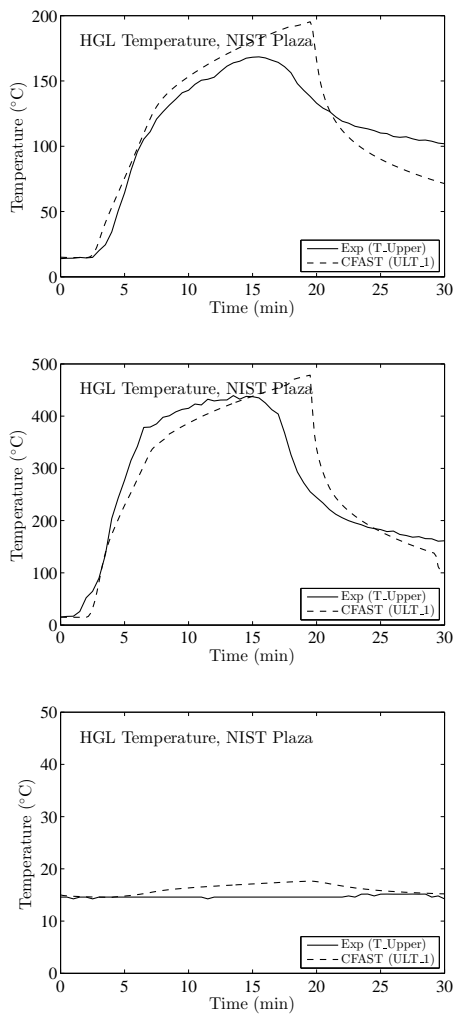


Figure B.24: Predicted HGL Temperature and Height for the Seven-Story Hotel Test 7.

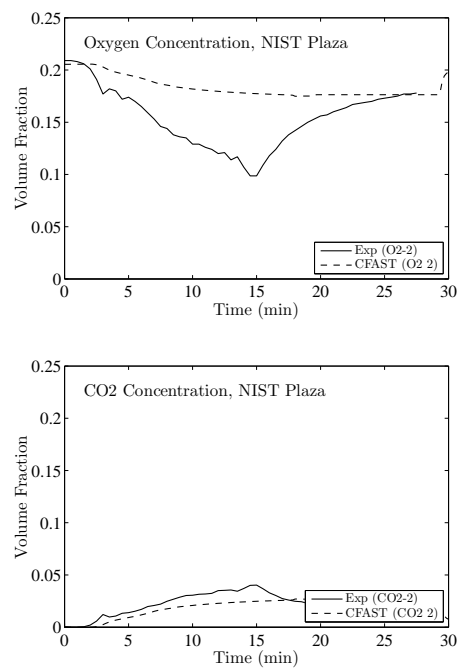


Figure B.25: Predicted Oxygen and Carbon Dioxide for the Seven-Story Hotel Test 7.

B.9 NIST/NRC Test Series

These experiments, sponsored by the US NRC and conducted at NIST, consisted of 15 large-scale experiments performed in June 2003. All 15 tests were included in the validation study. The experiments are documented in Ref. [74]. The fire sizes ranged from 350 kW to 2.2 MW in a compartment with dimensions 21.7 m by 7.1 m by 3.8 m high, designed to represent a compartment in a nuclear power plant containing power and control cables. The room had one door and a simple mechanical ventilation system. Ventilation conditions, the fire size, and fire location were varied. Numerous measurements (approximately 350 per test) were made.

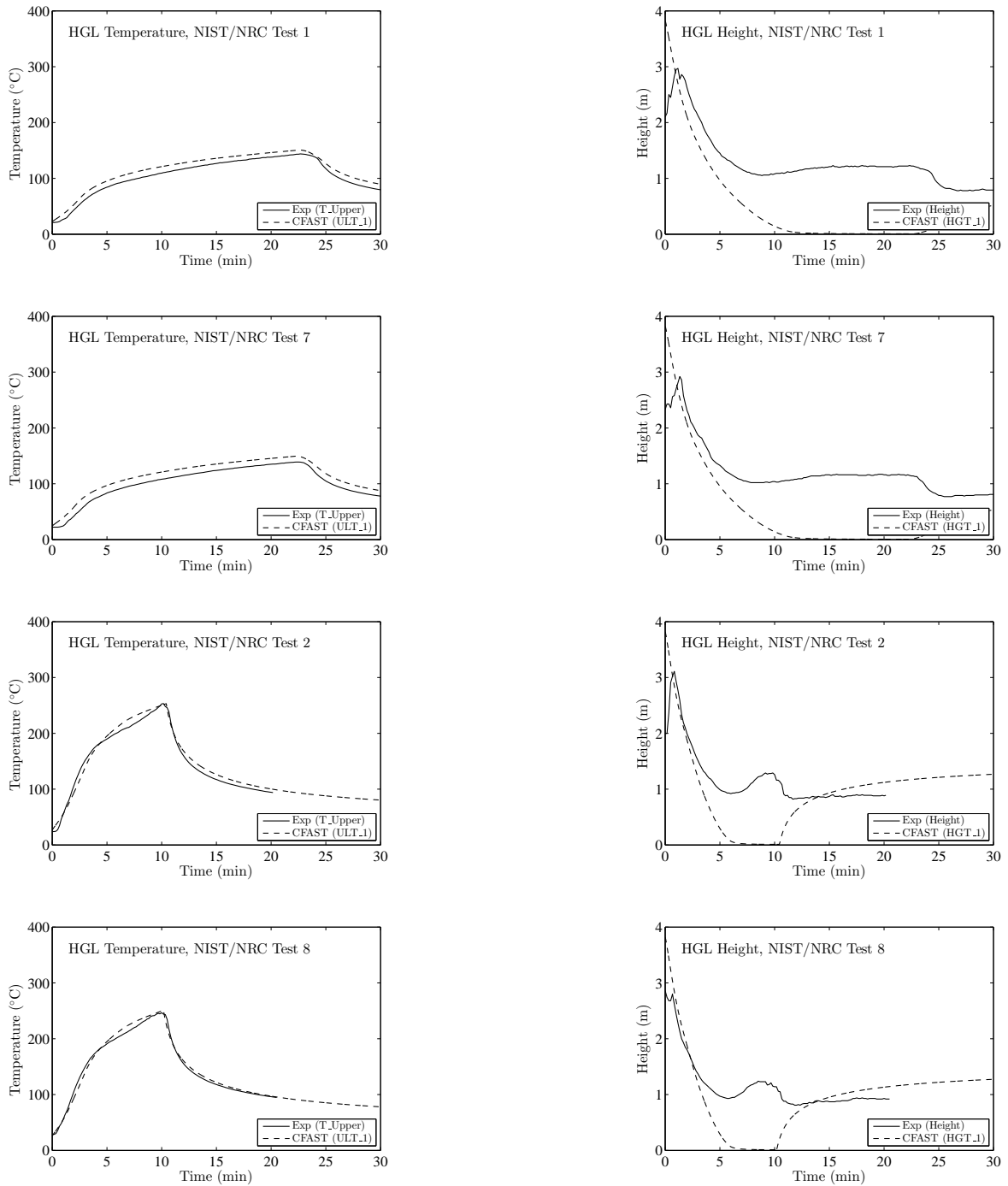


Figure B.26: Predicted HGL Temperature and Height for the NIST/NRC Tests 1, 7, 2 and 8.

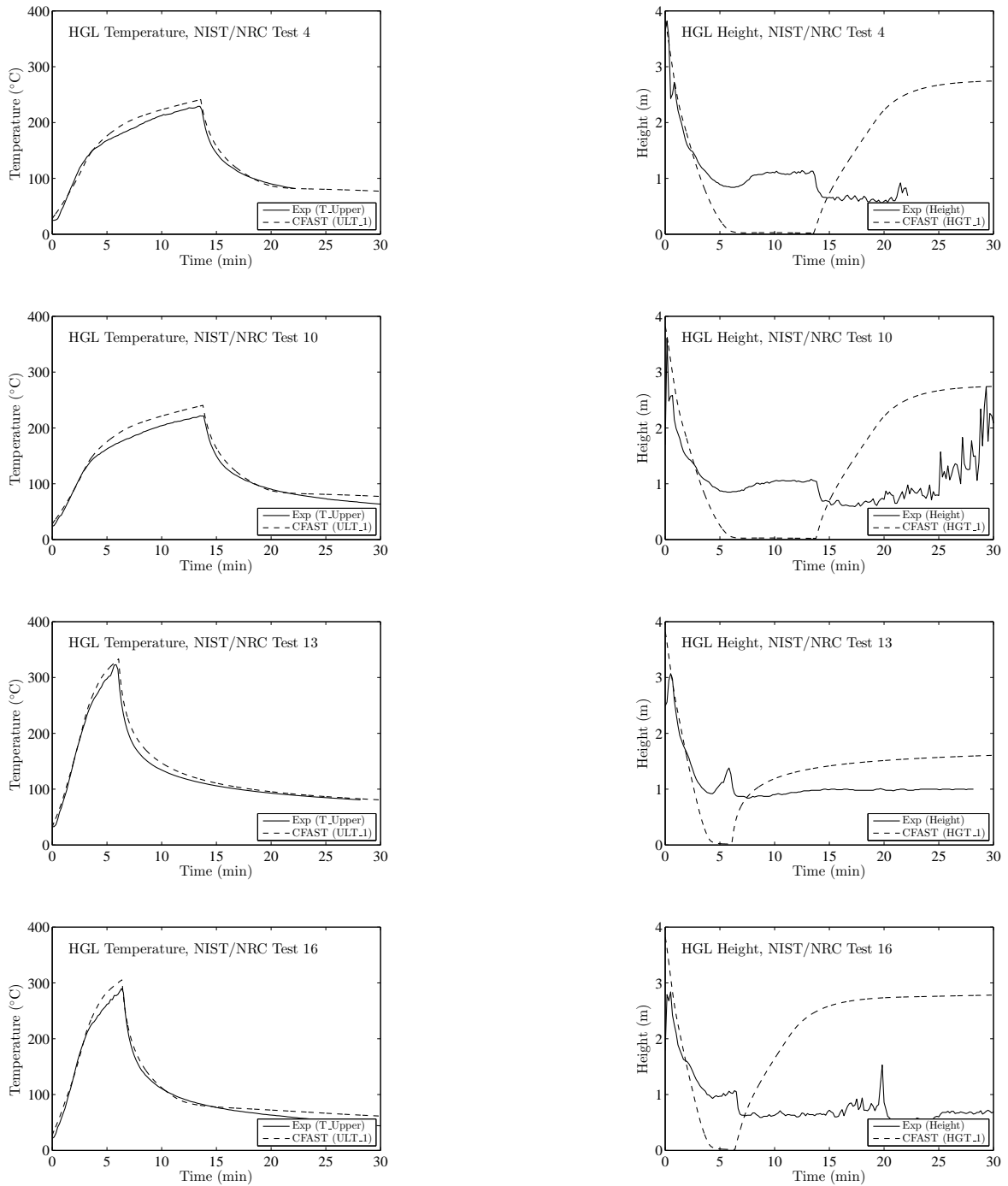
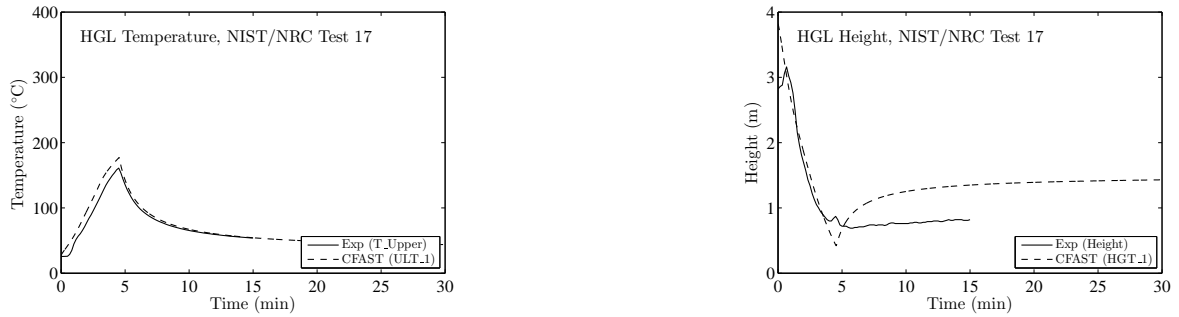


Figure B.27: Predicted HGL Temperature and Height for the NIST/NRC Tests 4, 10, 13 and 16.



Open Door Tests to follow

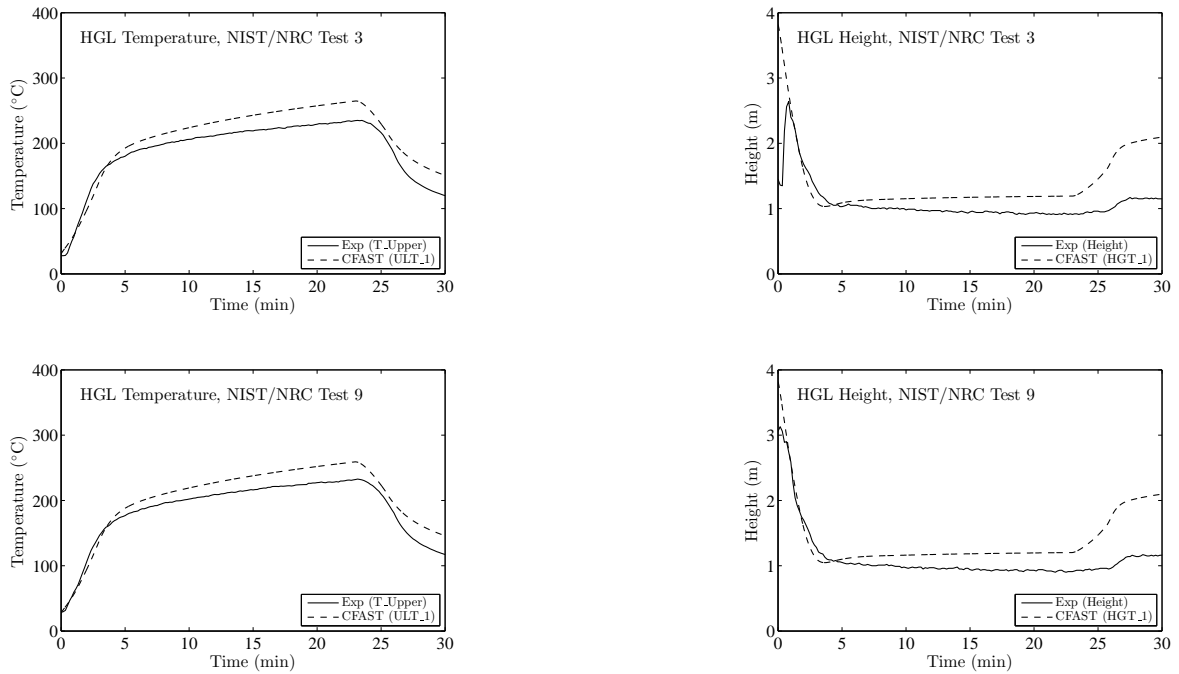


Figure B.28: Predicted HGL Temperature and Height for the NIST/NRC Tests 17, 3 and 9.

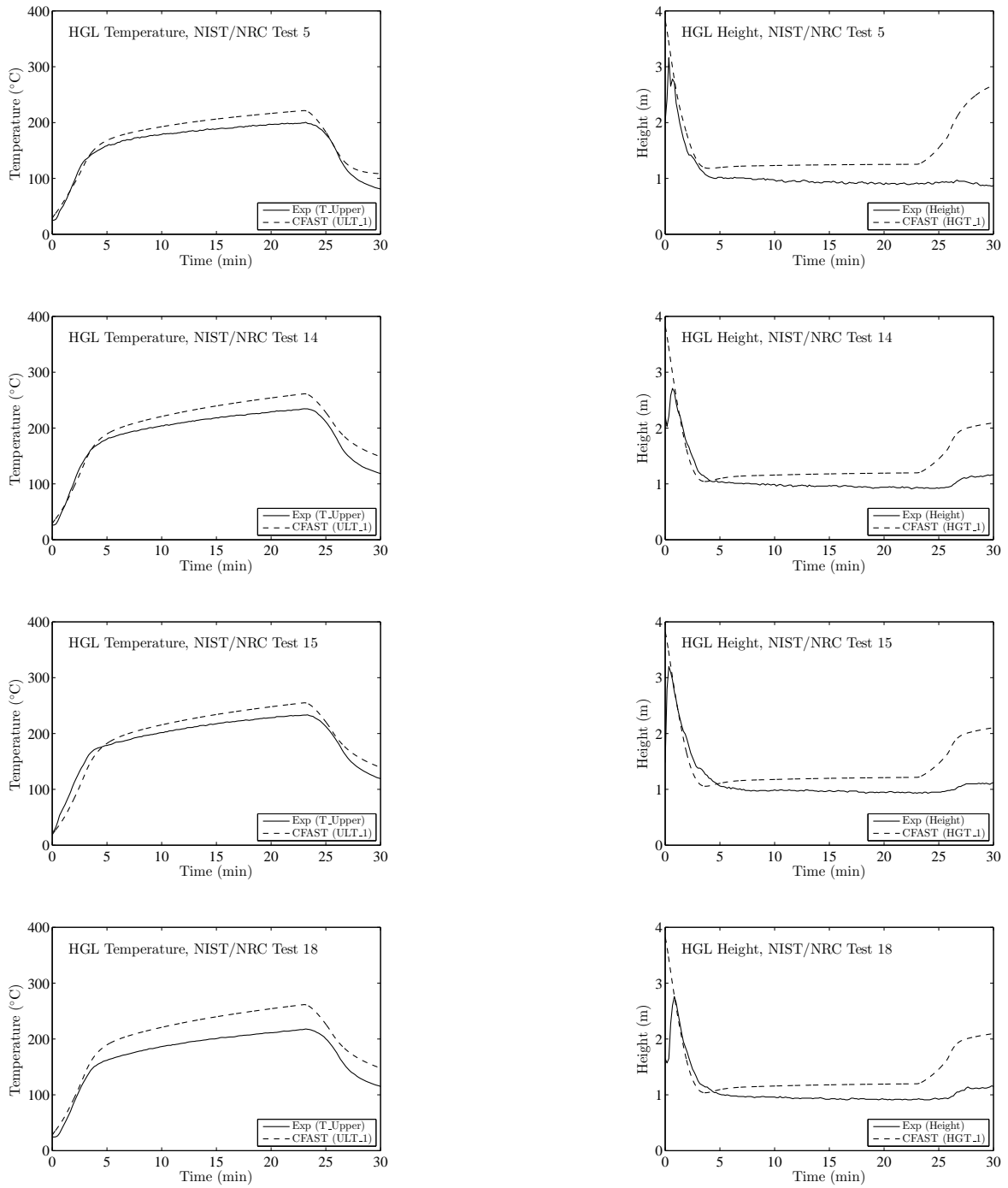


Figure B.29: Predicted HGL Temperature and Height for the NIST/NRC Tests 5, 14, 15 and 18.

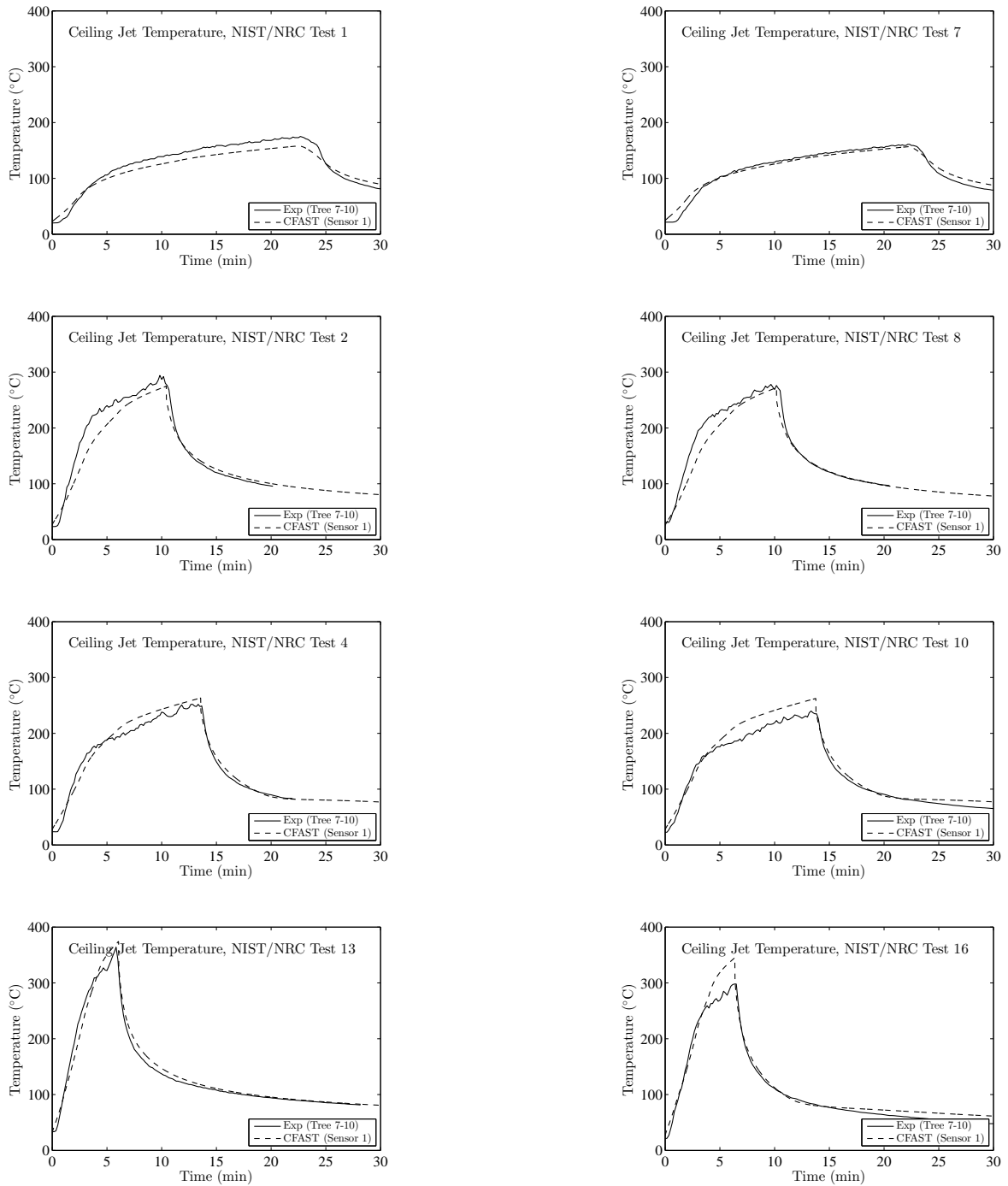


Figure B.30: Ceiling Jet Temperature for the NIST/NRC Series, Closed Door Tests.

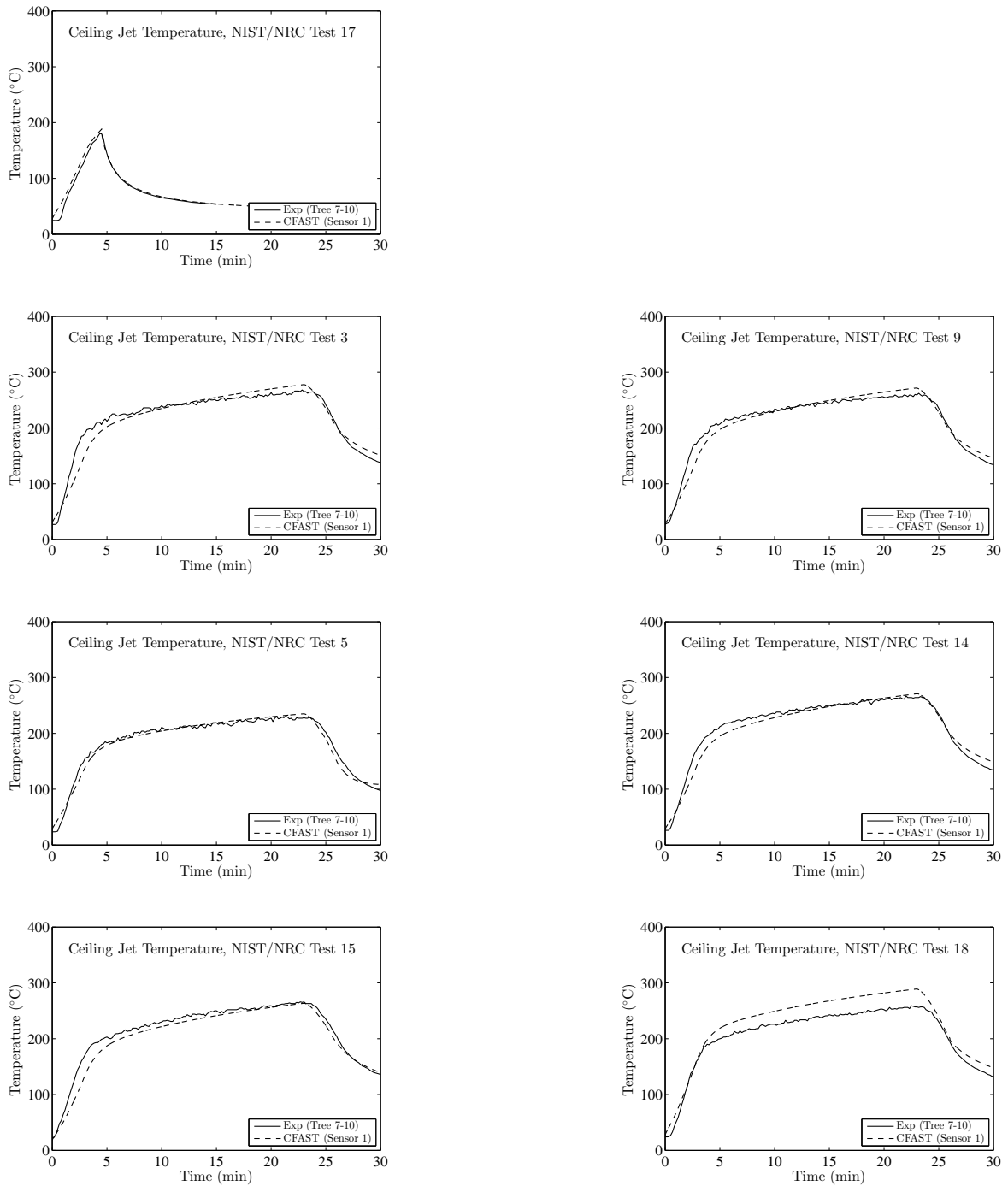


Figure B.31: Ceiling Jet Temperature for the NIST/NRC Series, Open Door Tests.

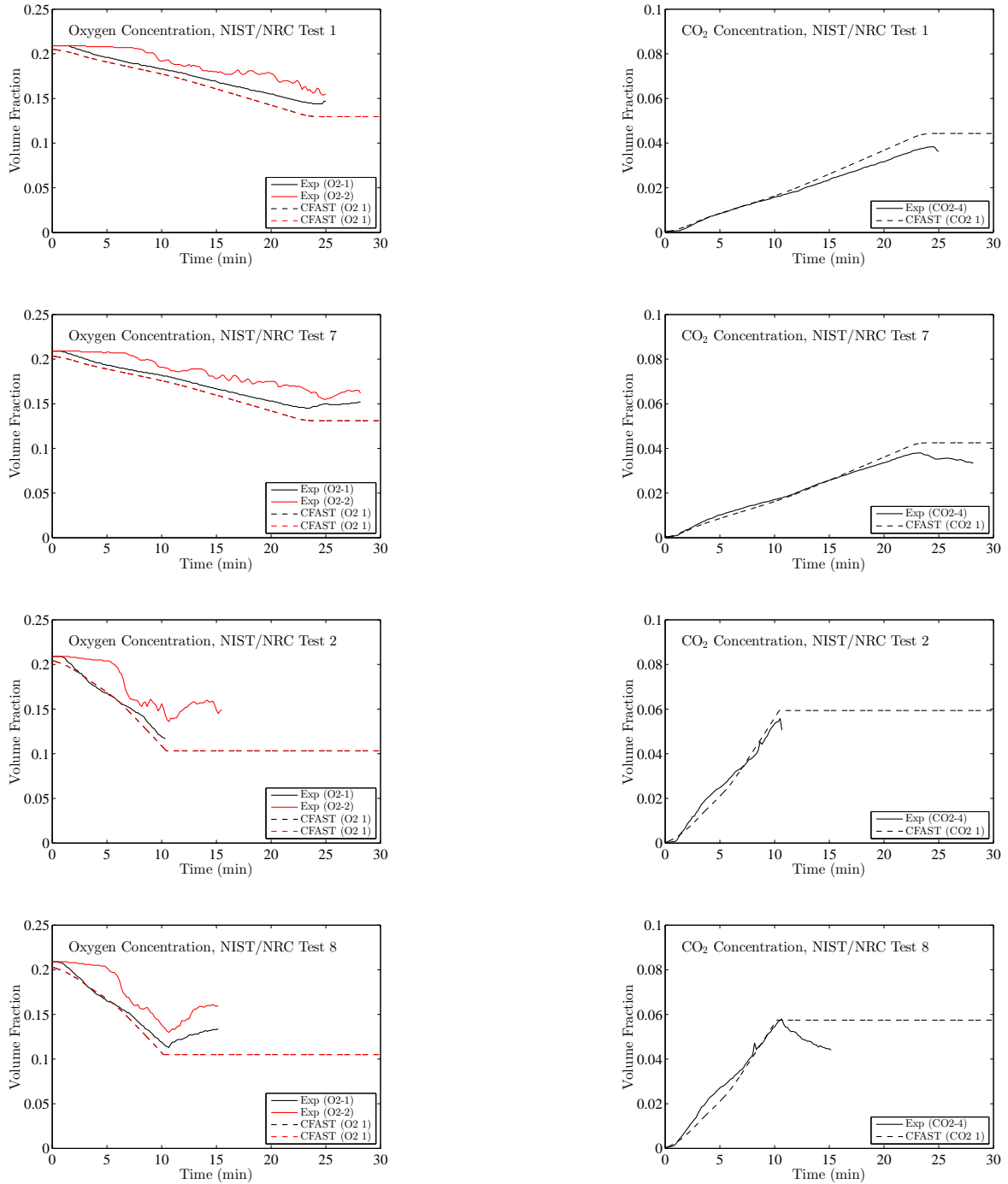


Figure B.32: Predicted Oxygen and Carbon Dioxide for the NIST/NRC Tests 1, 7, 2 and 8.

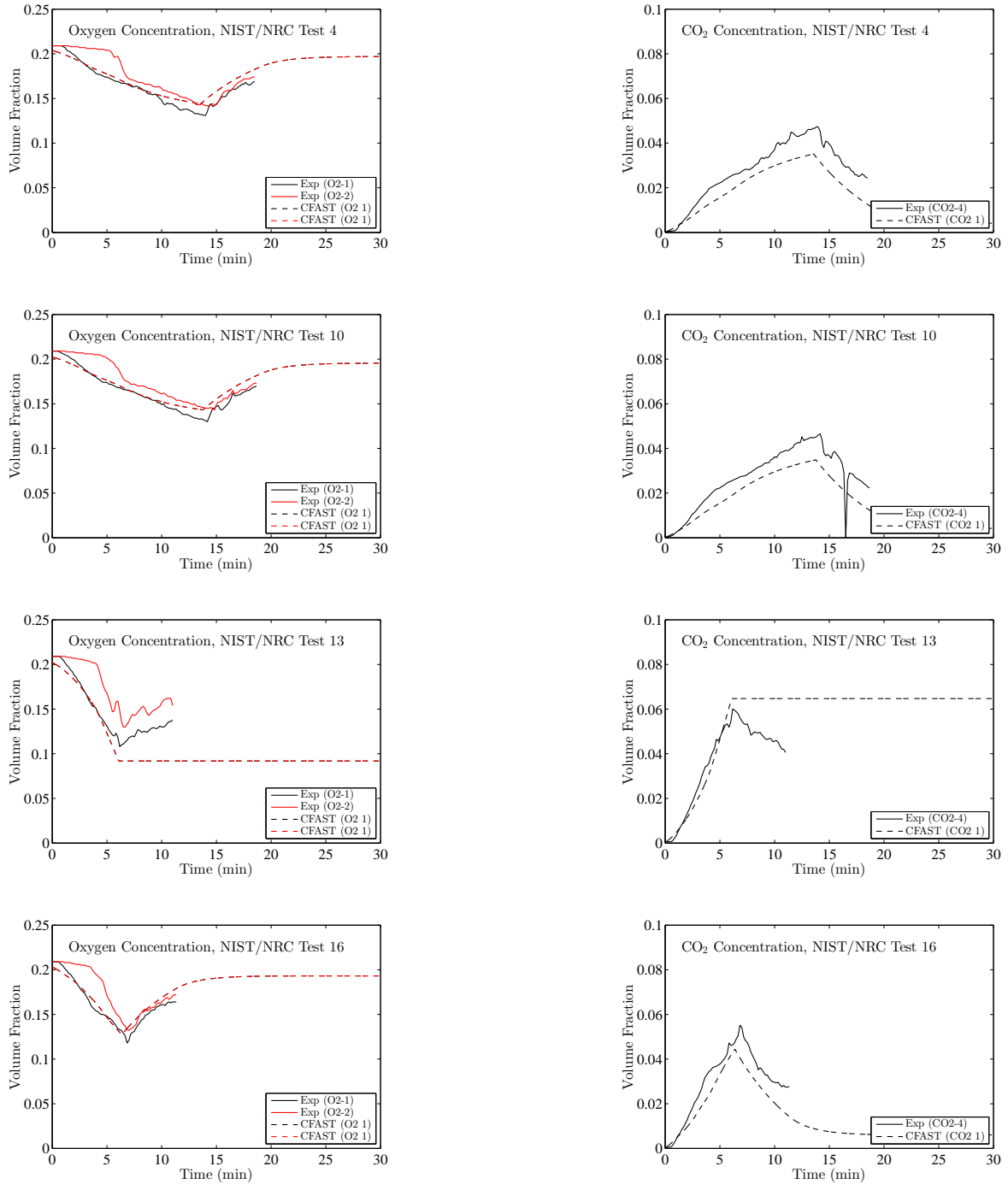
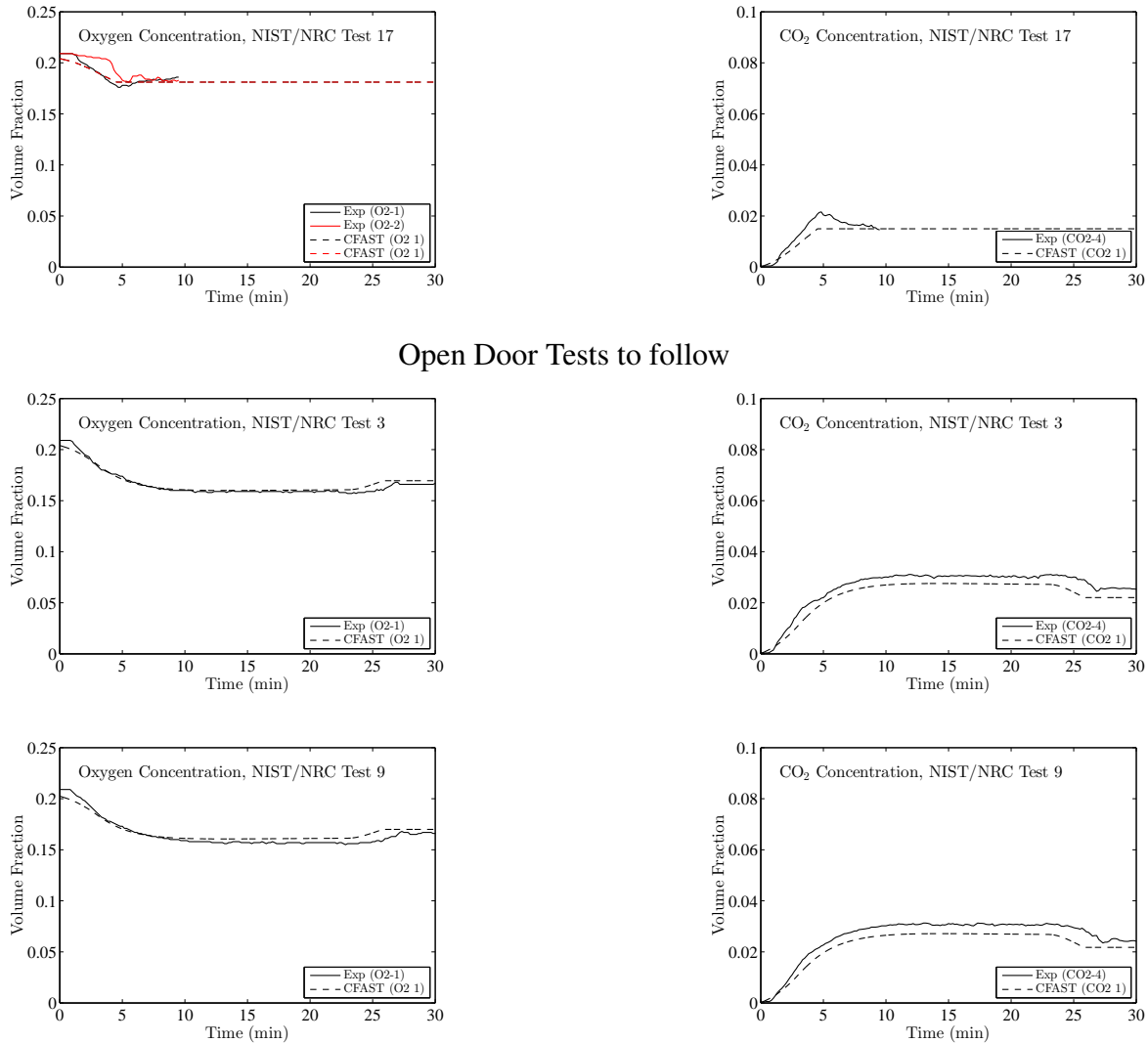


Figure B.33: Predicted Oxygen and Carbon Dioxide for the NIST/NRC Tests 4, 10, 13 and 16.



Open Door Tests to follow

Figure B.34: Predicted Oxygen and Carbon Dioxide for the NIST/NRC Tests 17, 3, and 9.

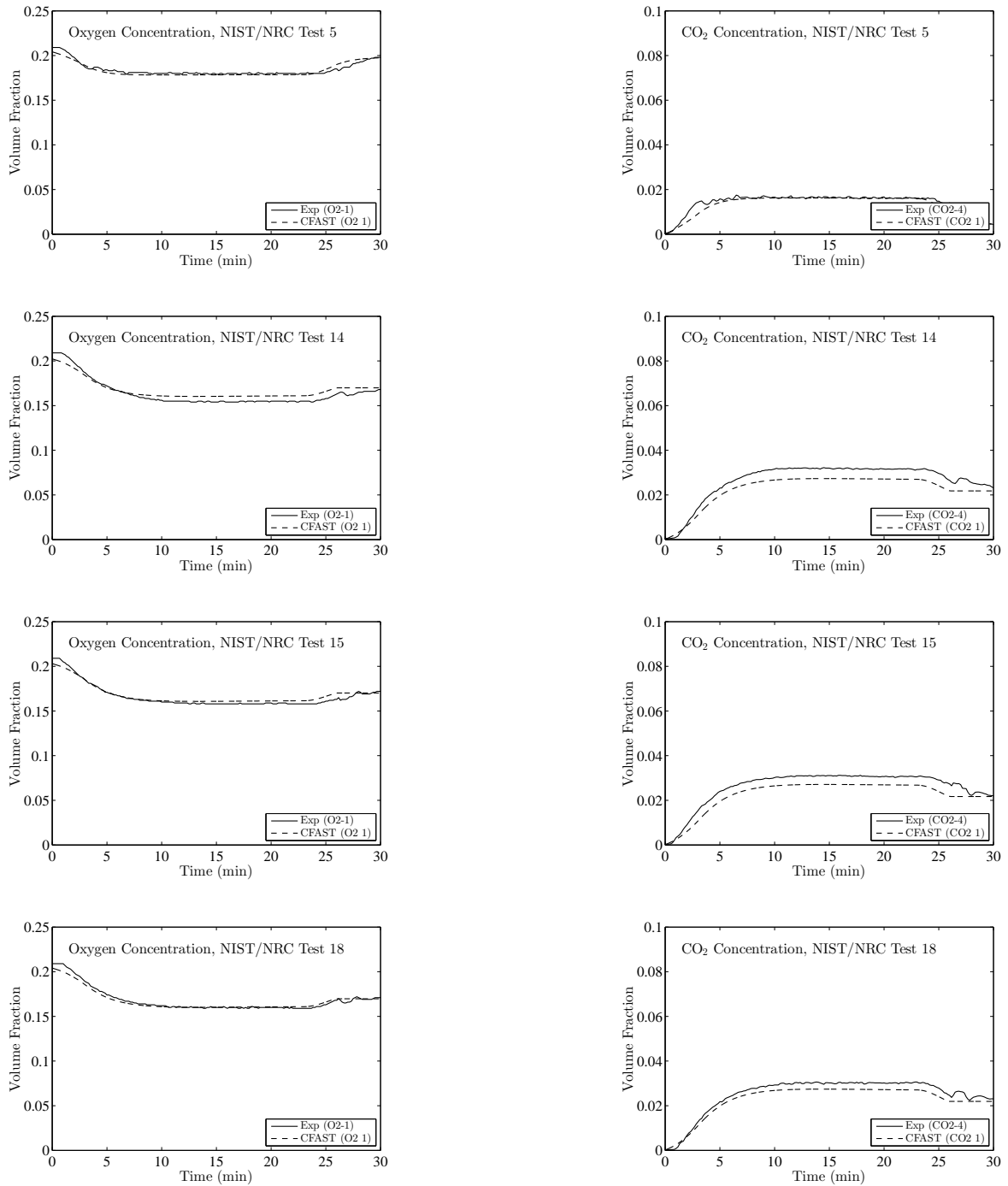


Figure B.35: Predicted Oxygen and Carbon Dioxide for the NIST/NRC Tests 5, 14, 15 and 18.

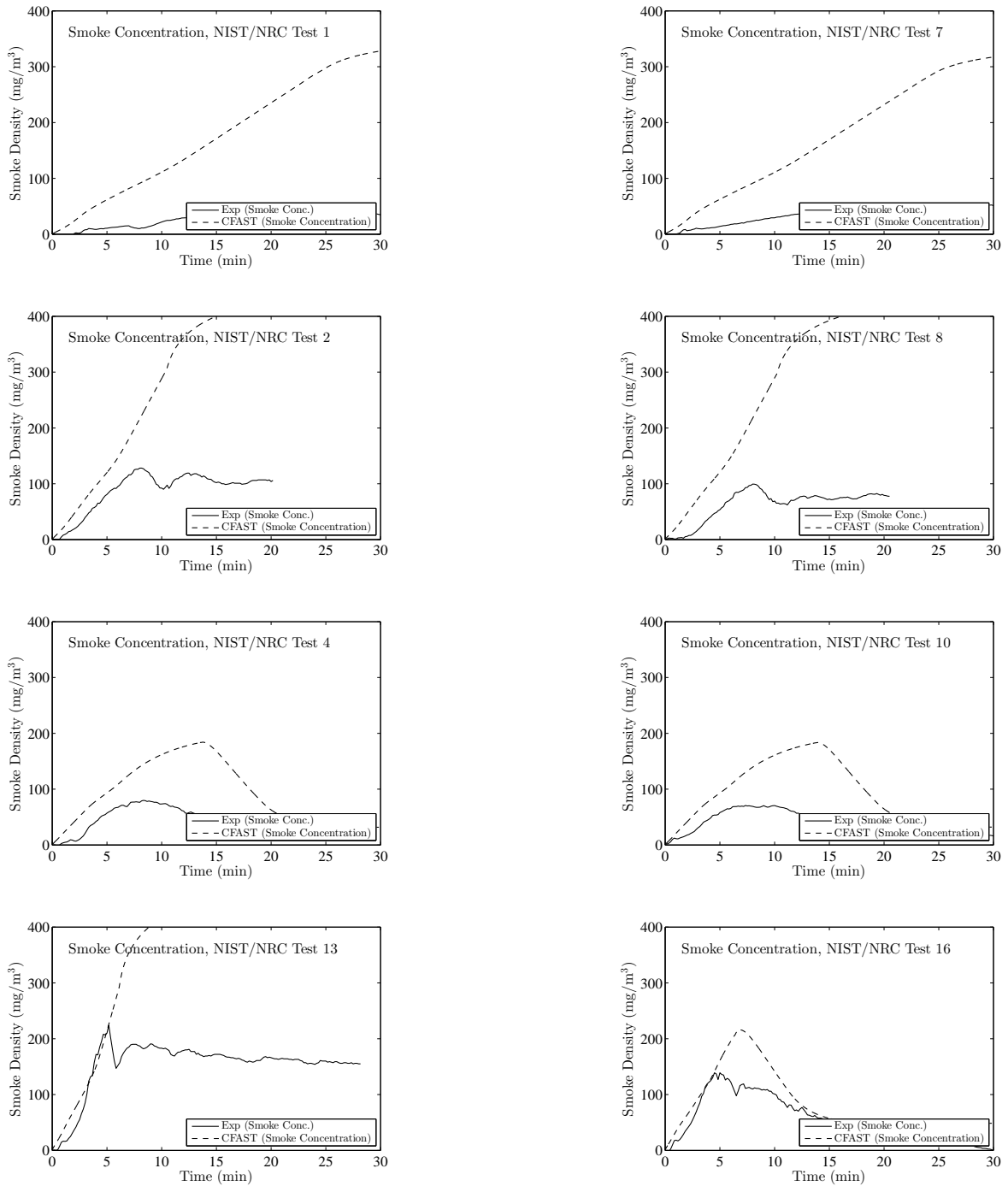


Figure B.36: Smoke Concentration for the NIST/NRC Series, Closed Door Tests.

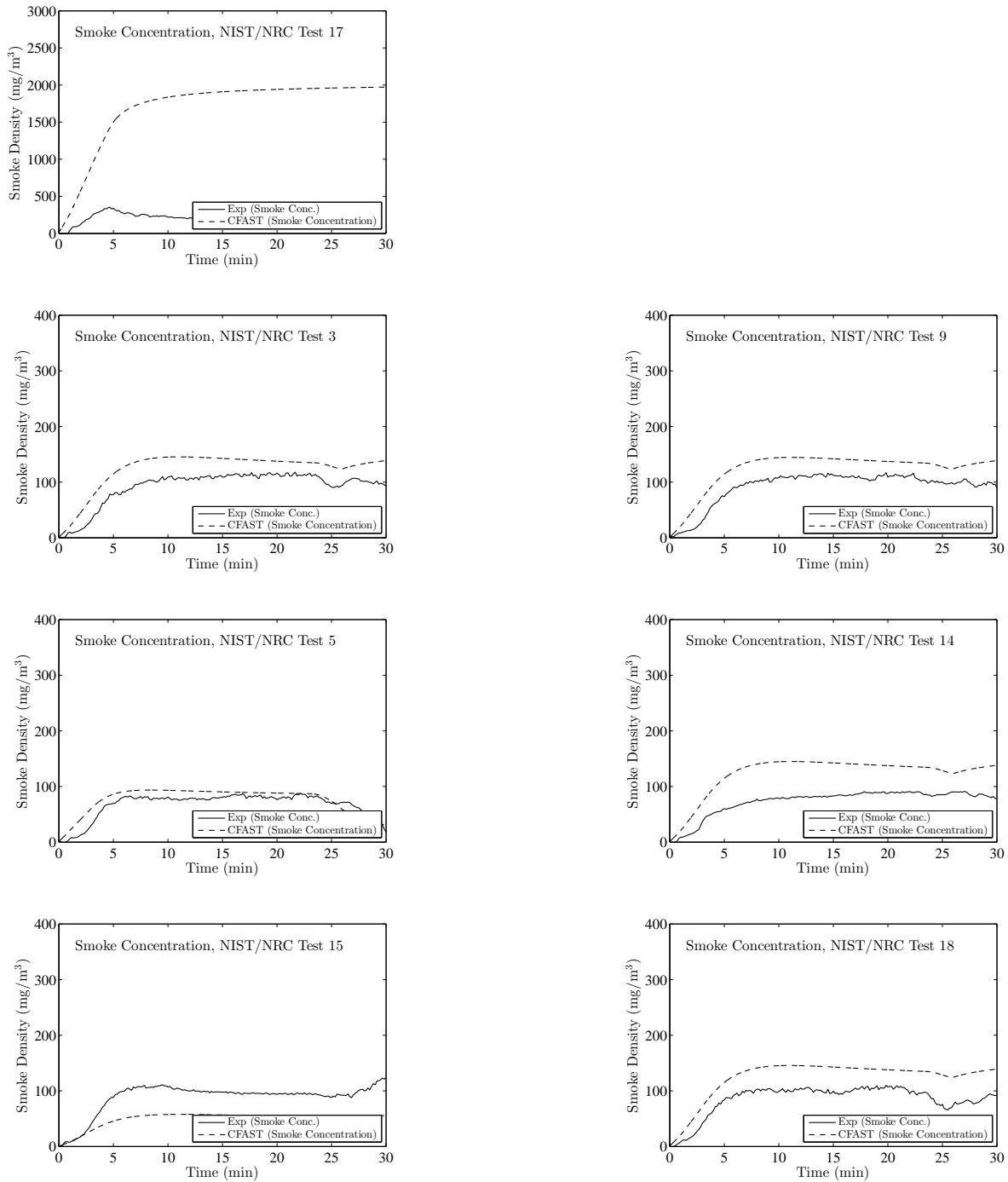


Figure B.37: Smoke Concentration for the NIST/NRC Series, Open Door Tests.

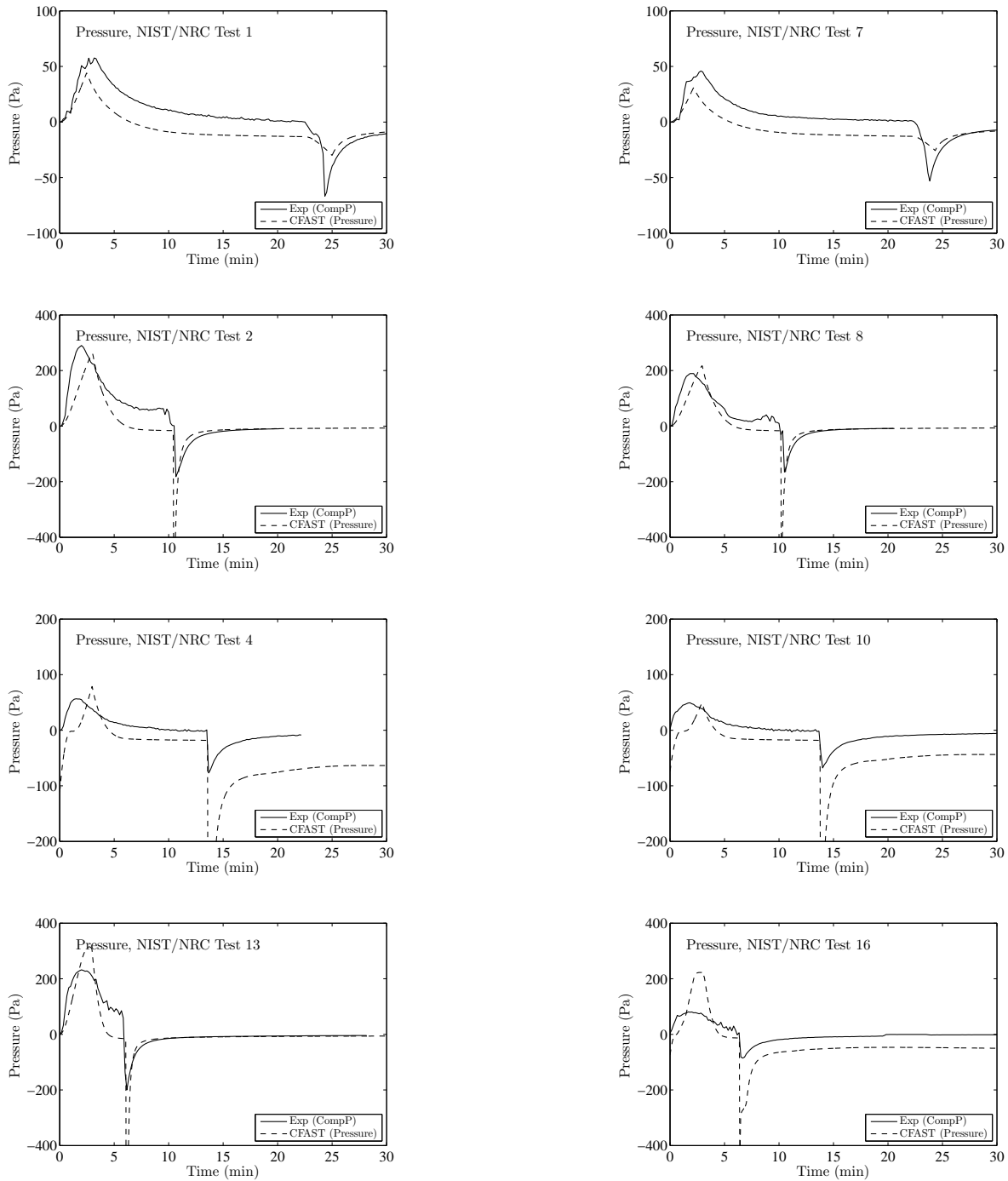


Figure B.38: Compartment Pressures for the NIST/NRC Series, Closed Door Tests.

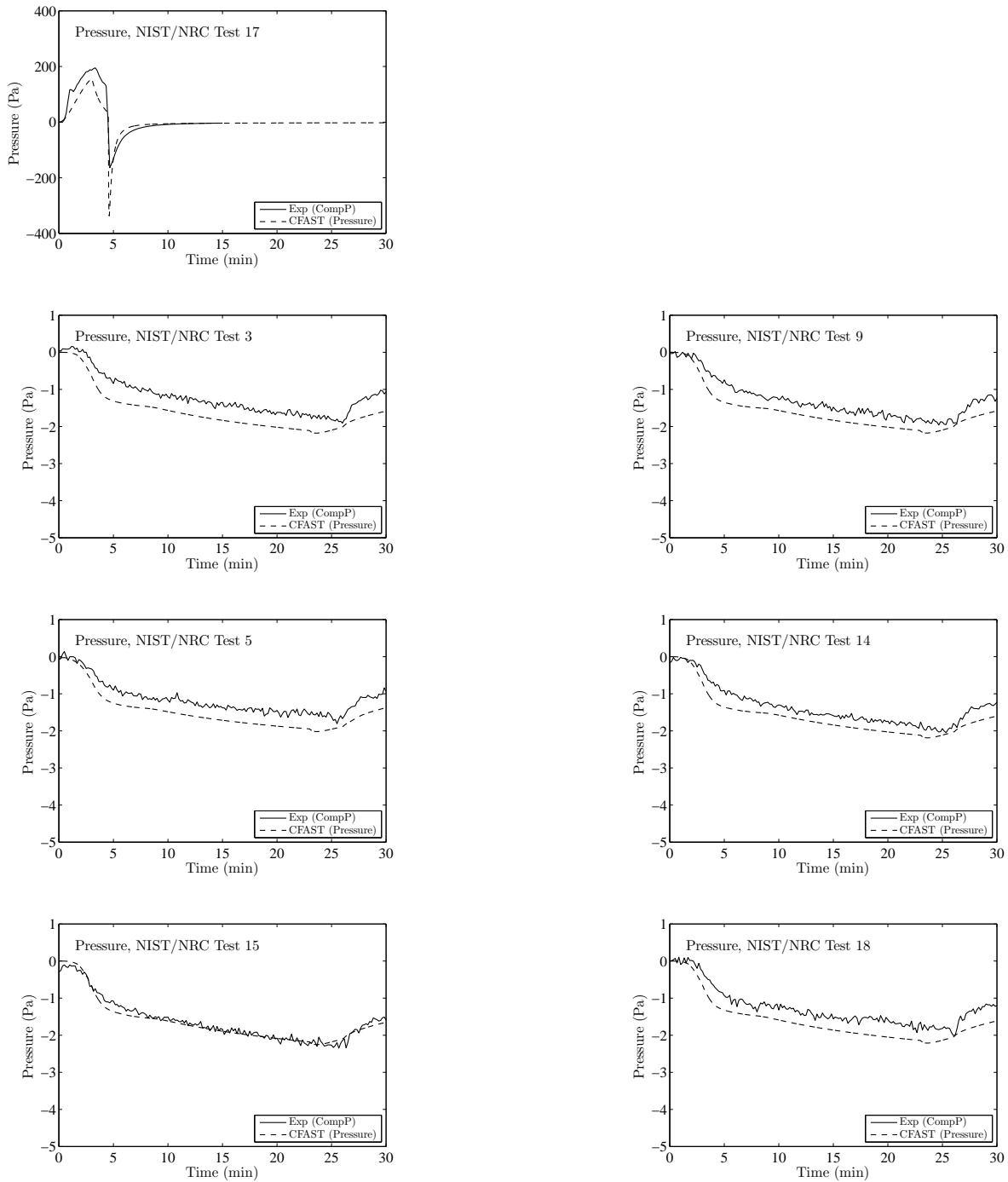


Figure B.39: Compartment Pressures for the NIST/NRC Series, Open Door Tests.

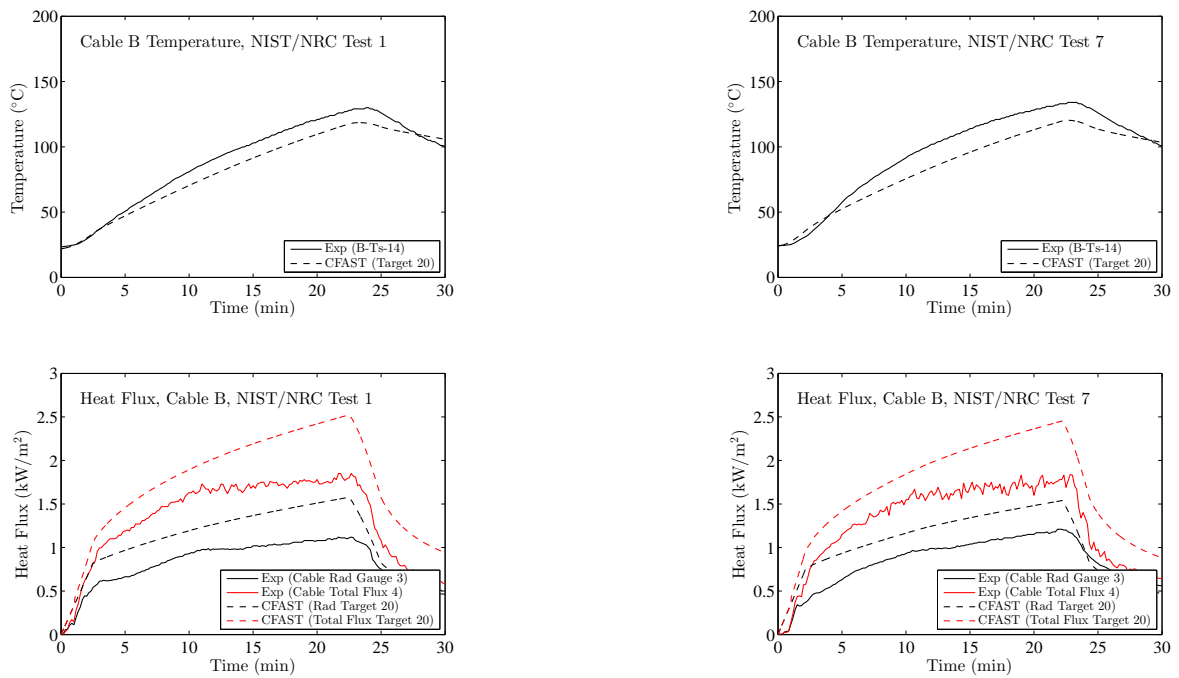


Figure B.40: NIST/NRC Series, Cable B Temperature and Heat Flux, Replicate Tests 1 and 7.

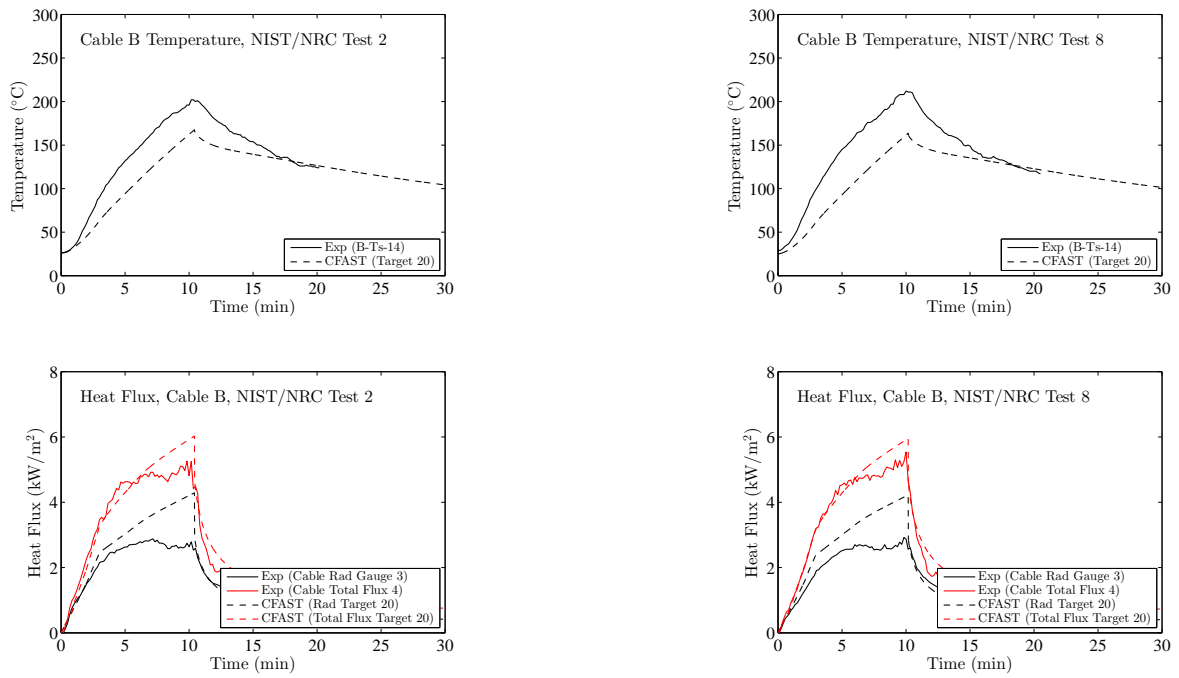


Figure B.41: NIST/NRC Series, Cable B Temperature and Heat Flux, Replicate Tests 2 and 8.

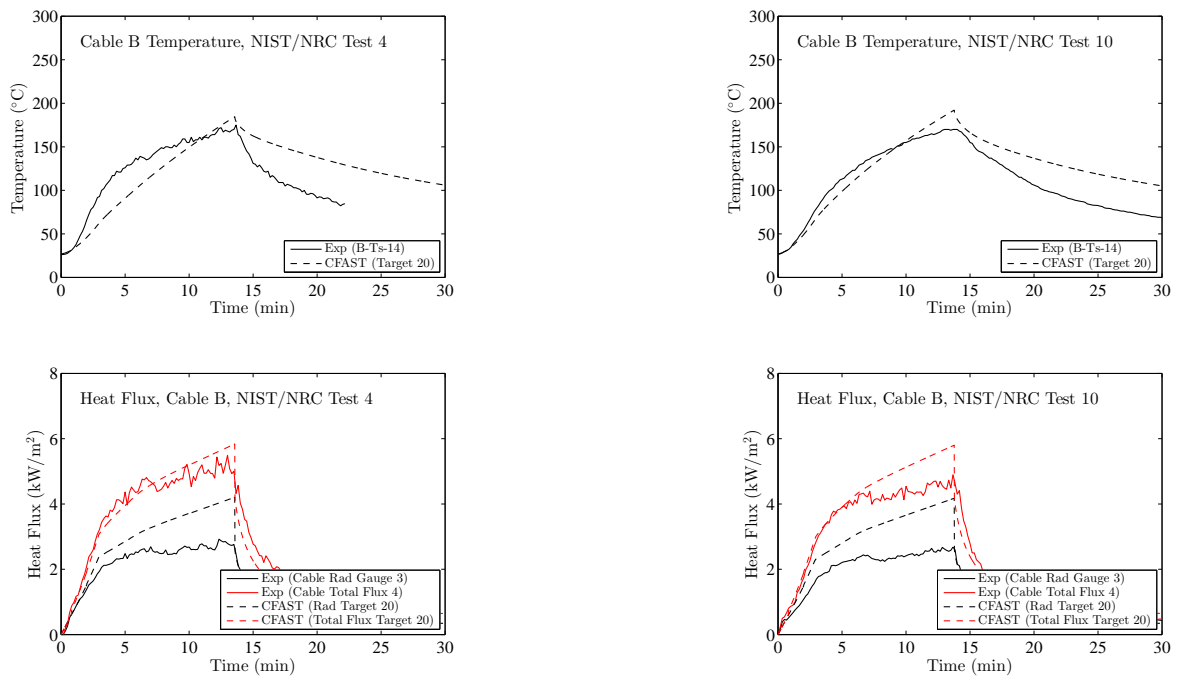


Figure B.42: NIST/NRC Series, Cable B Temperature and Heat Flux, Replicate Tests 4 and 10.

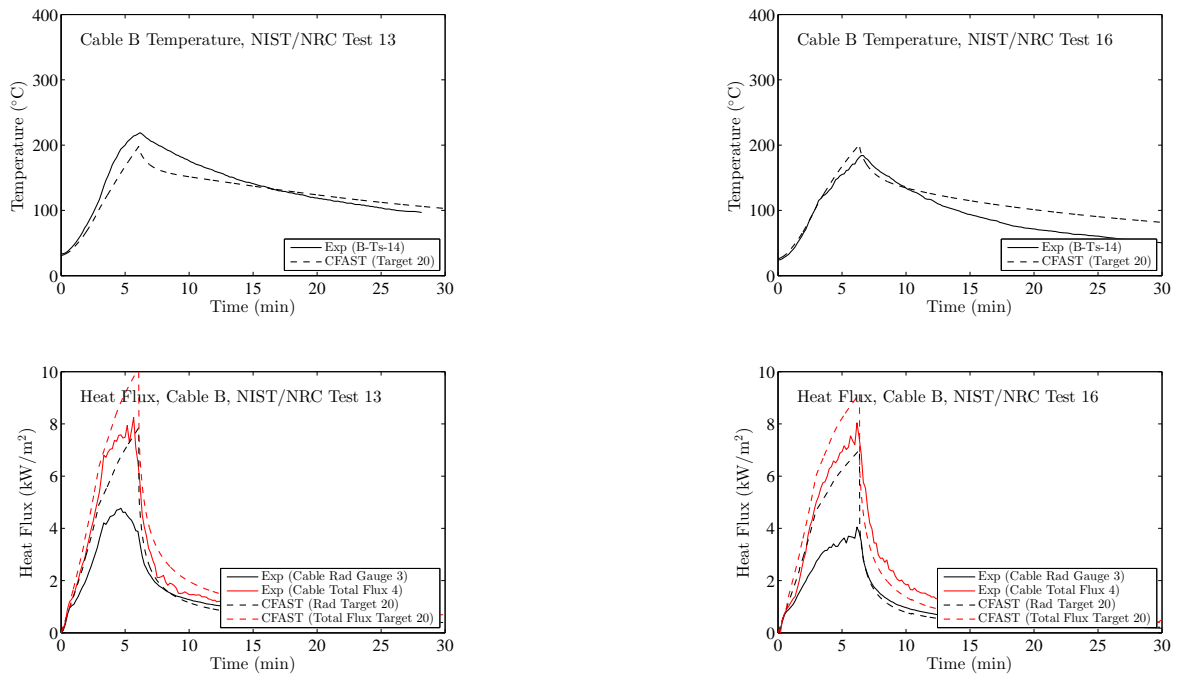


Figure B.43: NIST/NRC Series, Cable B Temperature and Heat Flux, Replicate Tests 13 and 16.

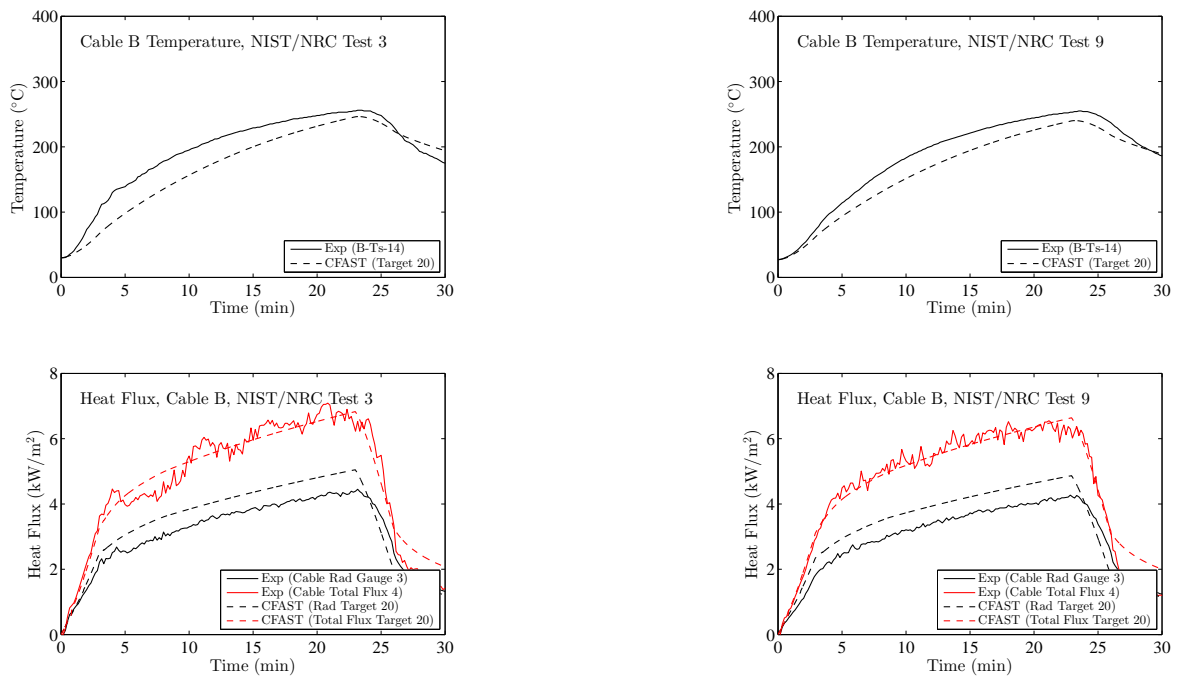


Figure B.44: NIST/NRC Series, Cable B Temperature and Heat Flux, Replicate Tests 3 and 9.

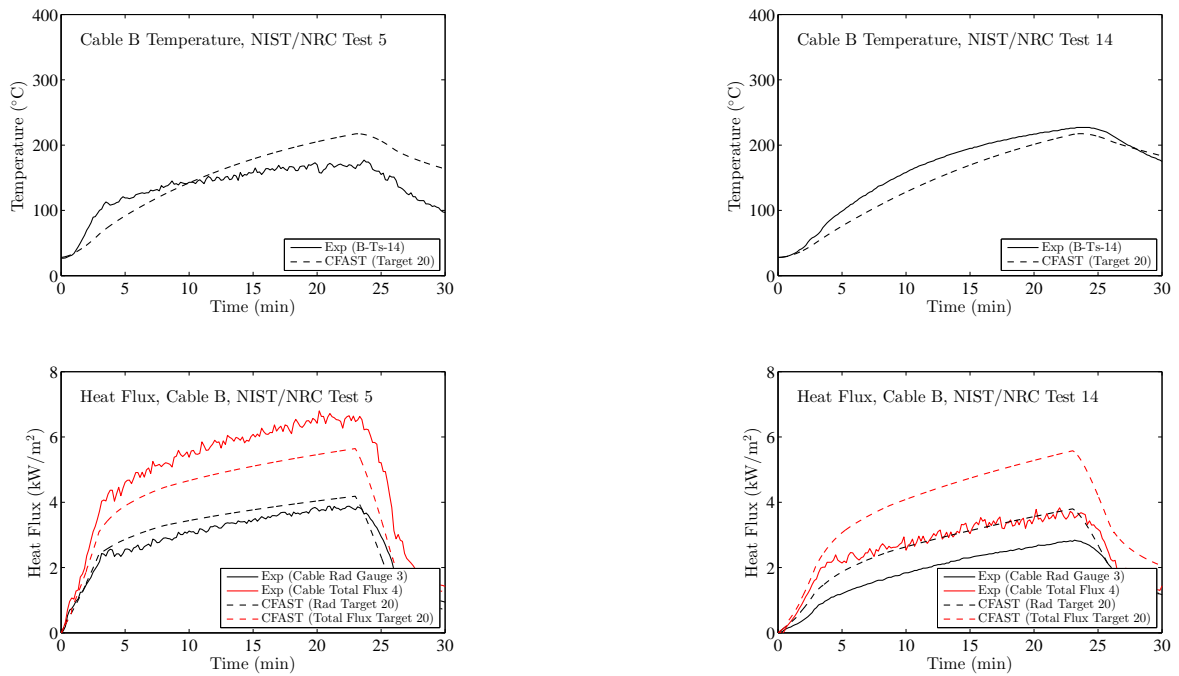


Figure B.45: NIST/NRC Series, Cable B Temperature and Heat Flux, Replicate Tests 5 and 14.

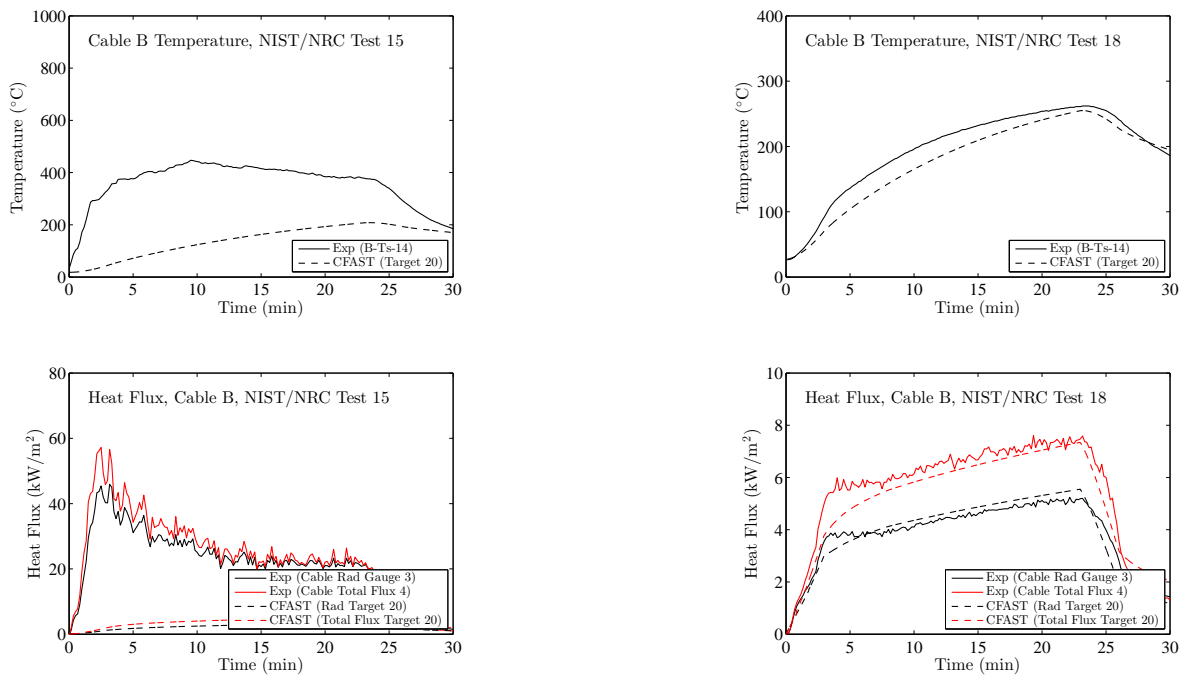


Figure B.46: NIST/NRC Series, Cable B Temperature and Heat Flux, Replicate Tests 15 and 18.

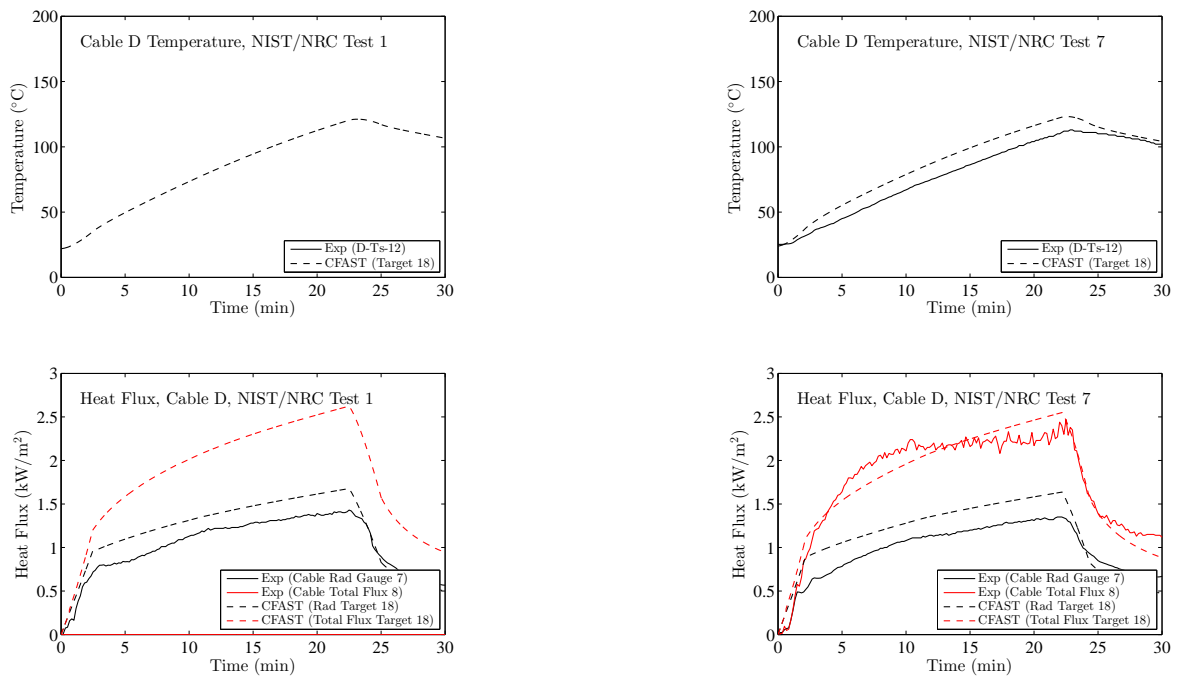


Figure B.47: NIST/NRC Series, Cable D Temperature and Heat Flux, Replicate Tests 1 and 7.

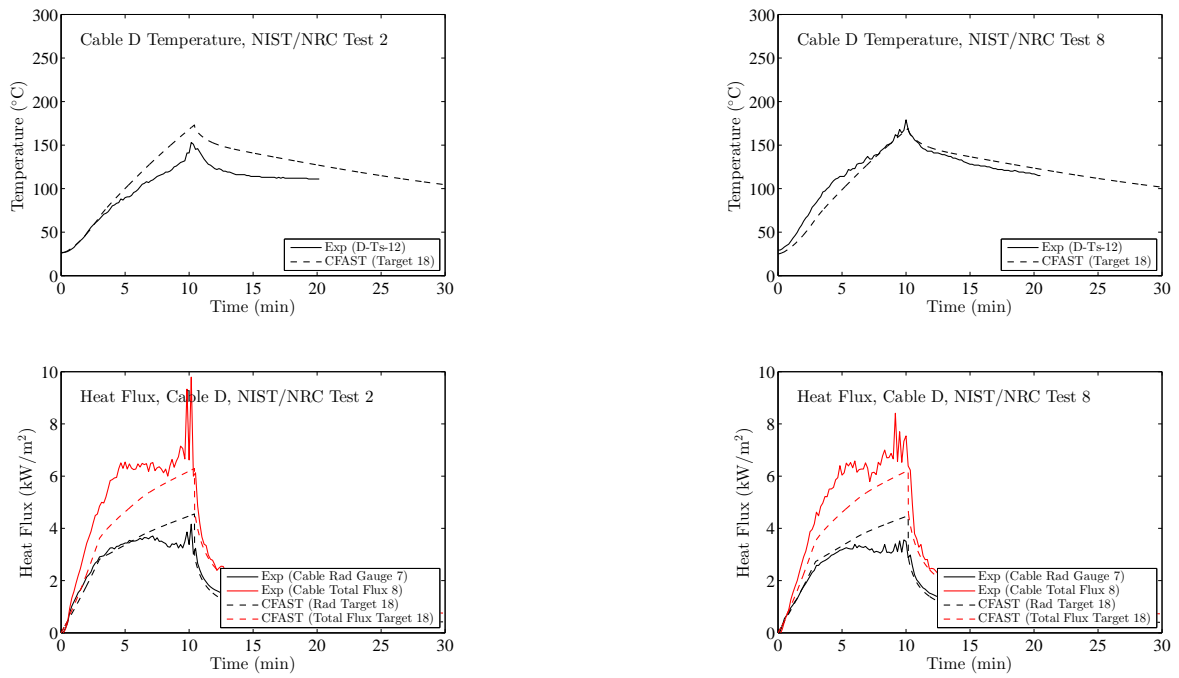


Figure B.48: NIST/NRC Series, Cable D Temperature and Heat Flux, Replicate Tests 2 and 8.

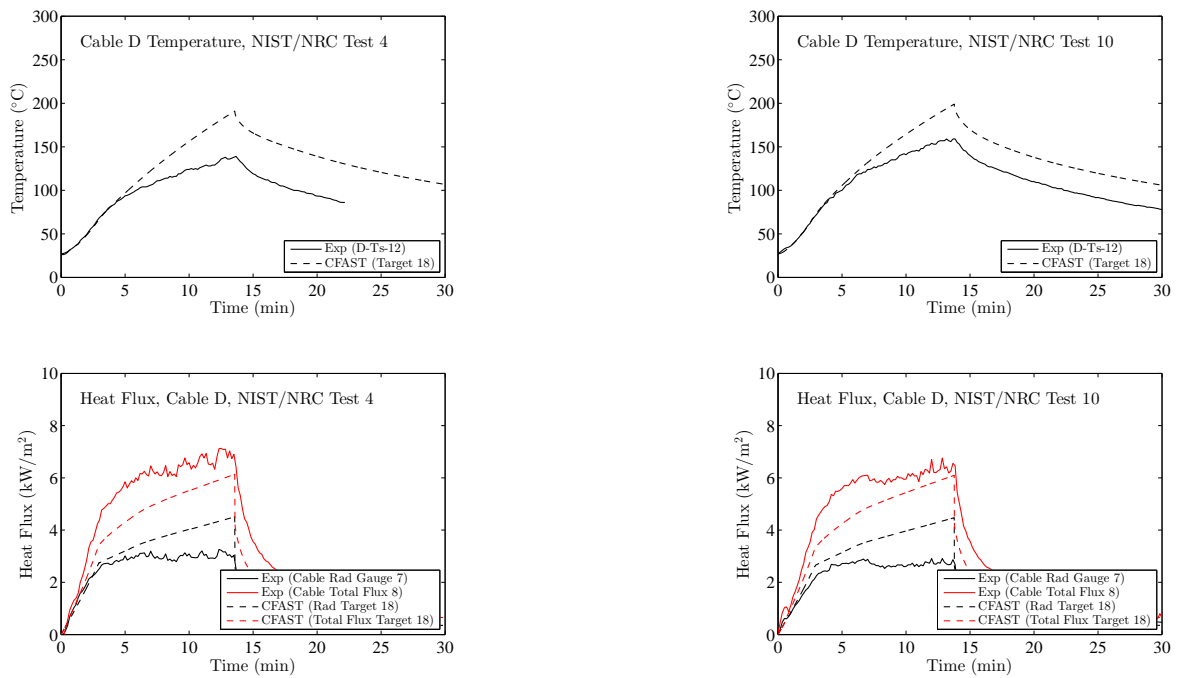


Figure B.49: NIST/NRC Series, Cable D Temperature and Heat Flux, Replicate Tests 4 and 10.

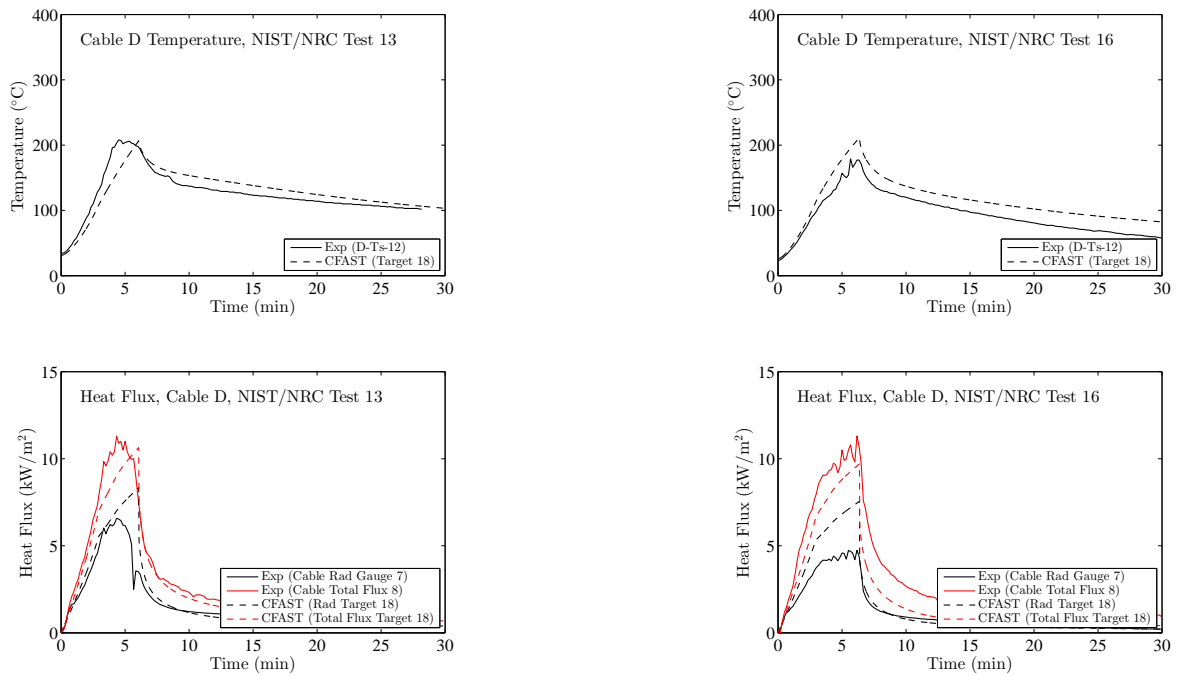


Figure B.50: NIST/NRC Series, Cable D Temperature and Heat Flux, Replicate Tests 13 and 16.

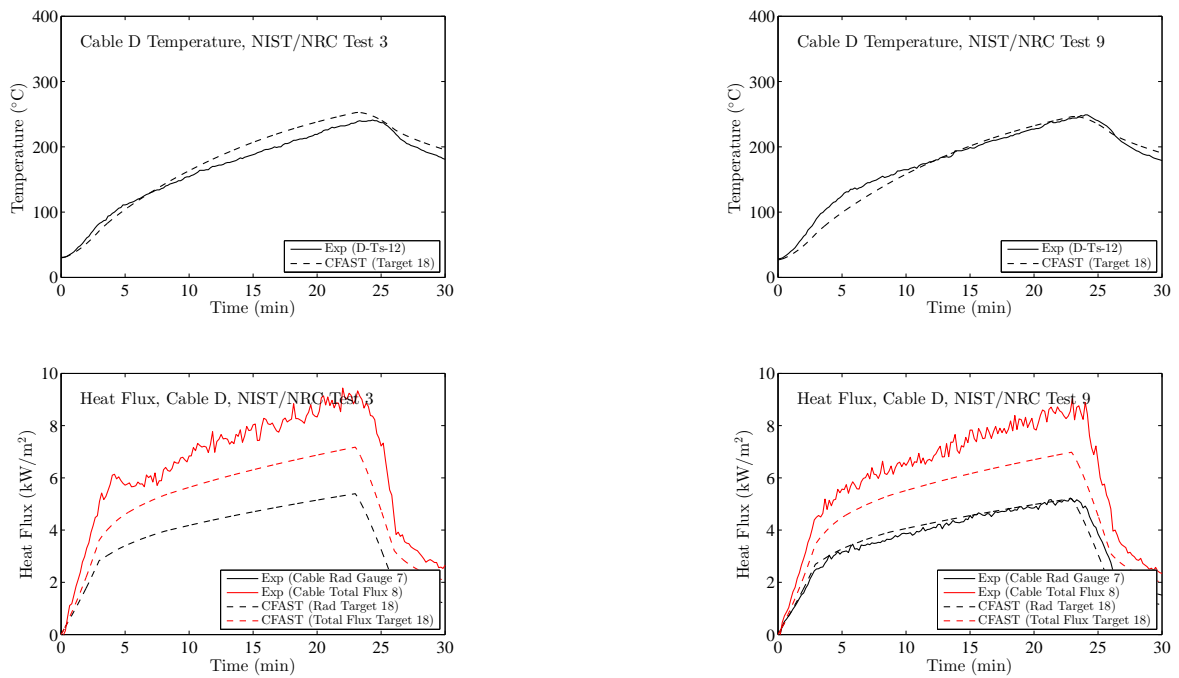


Figure B.51: NIST/NRC Series, Cable D Temperature and Heat Flux, Replicate Tests 3 and 9.

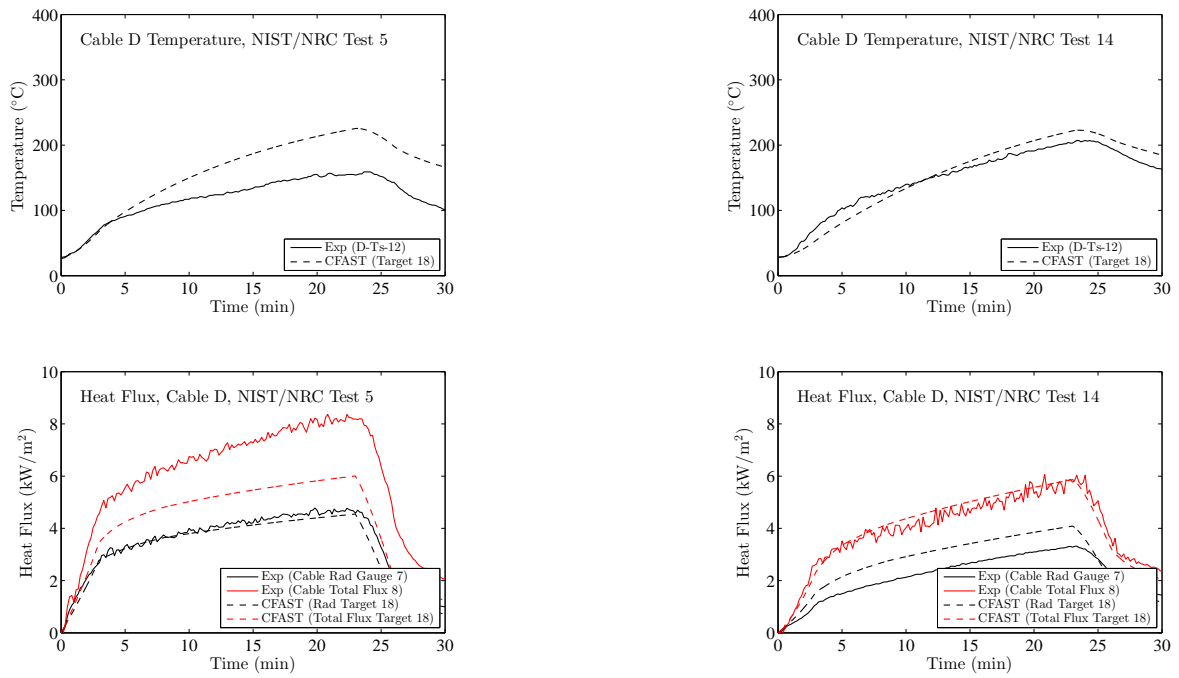


Figure B.52: NIST/NRC Series, Cable D Temperature and Heat Flux, Replicate Tests 5 and 14.

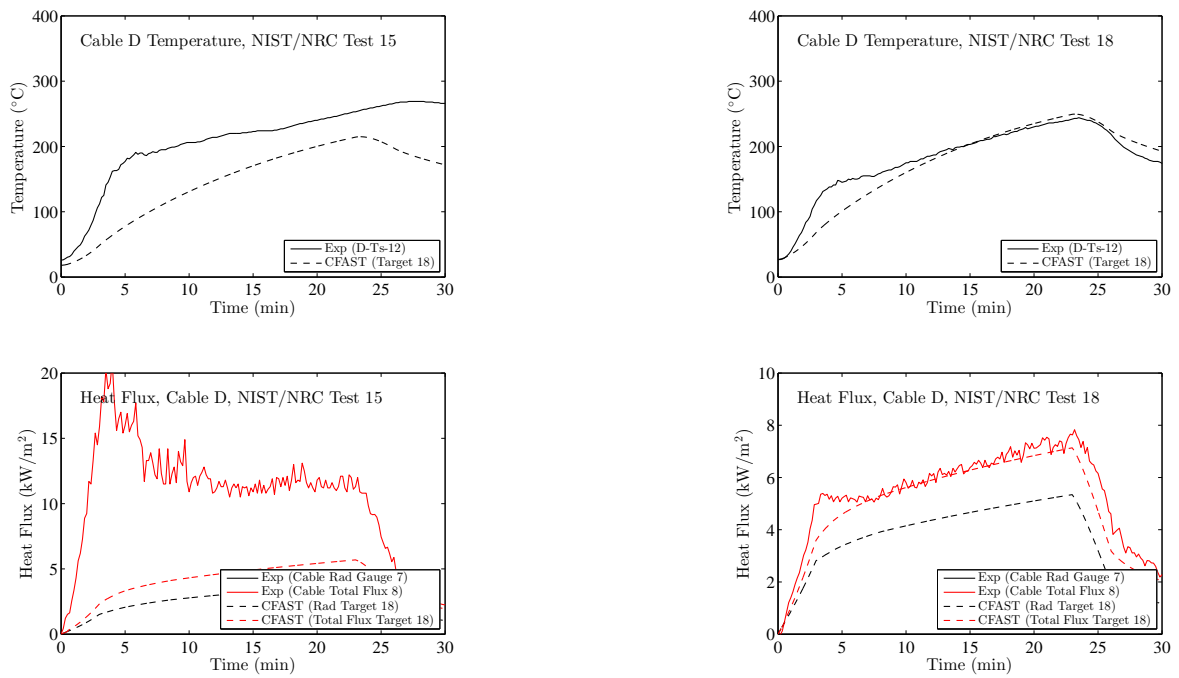


Figure B.53: NIST/NRC Series, Cable D Temperature and Heat Flux, Replicate Tests 15 and 18.

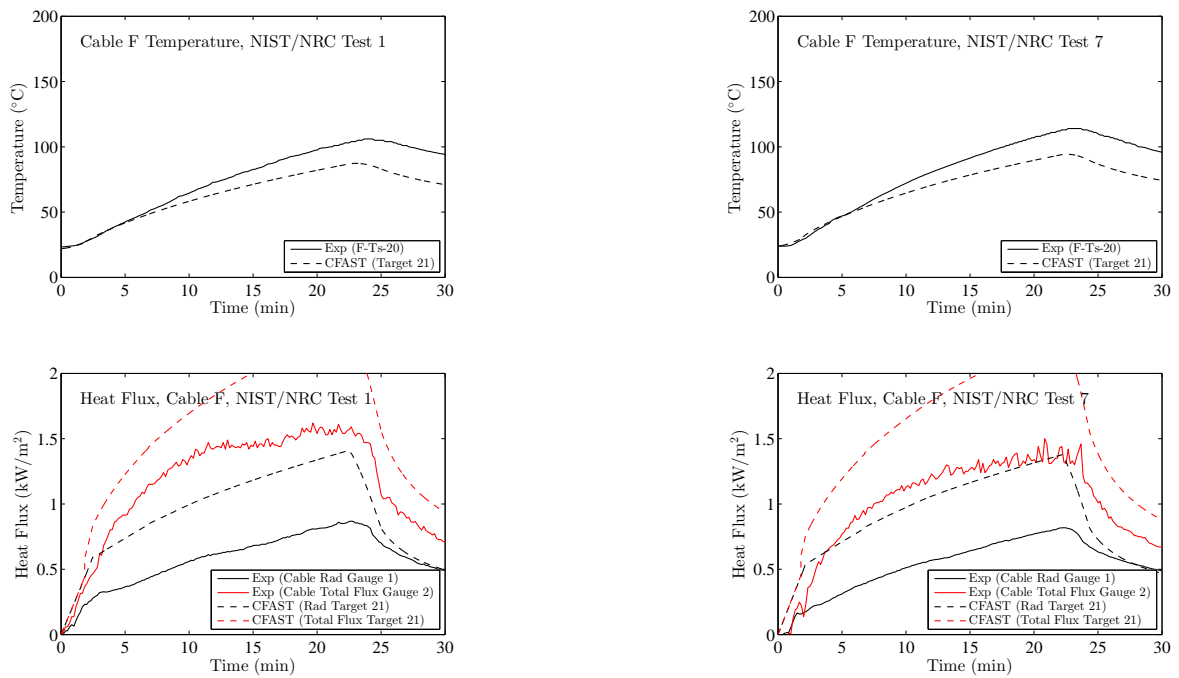


Figure B.54: NIST/NRC Series, Cable F Temperature and Heat Flux, Replicate Tests 1 and 7.

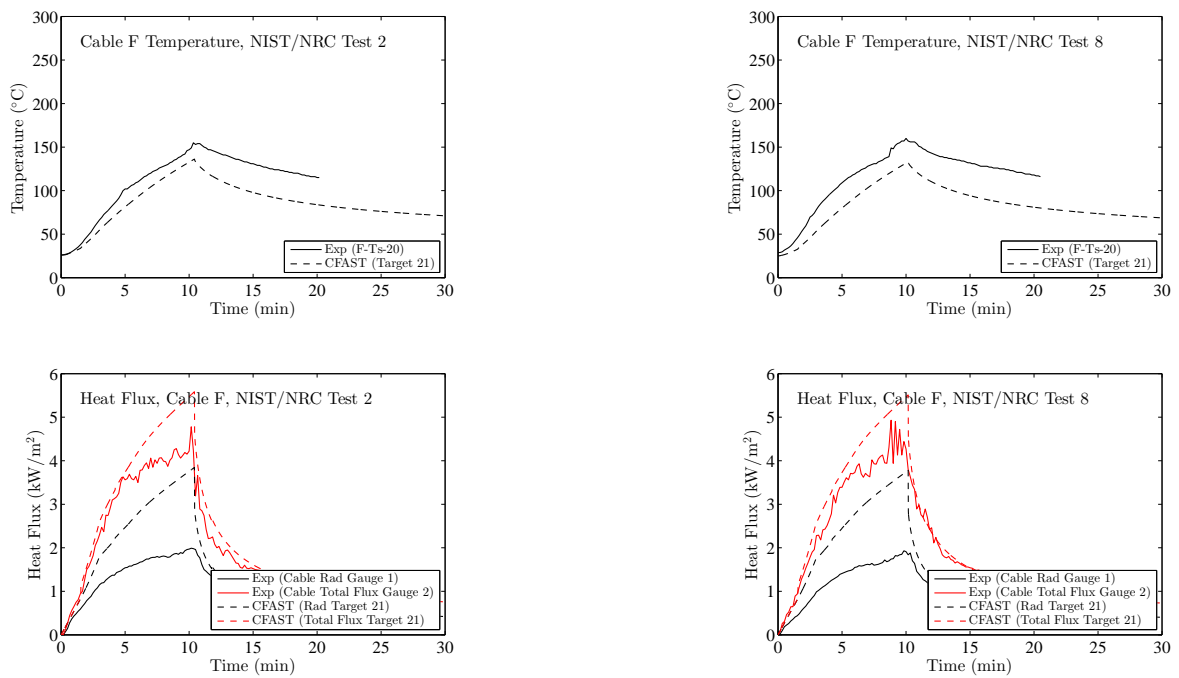


Figure B.55: NIST/NRC Series, Cable F Temperature and Heat Flux, Replicate Tests 2 and 8.

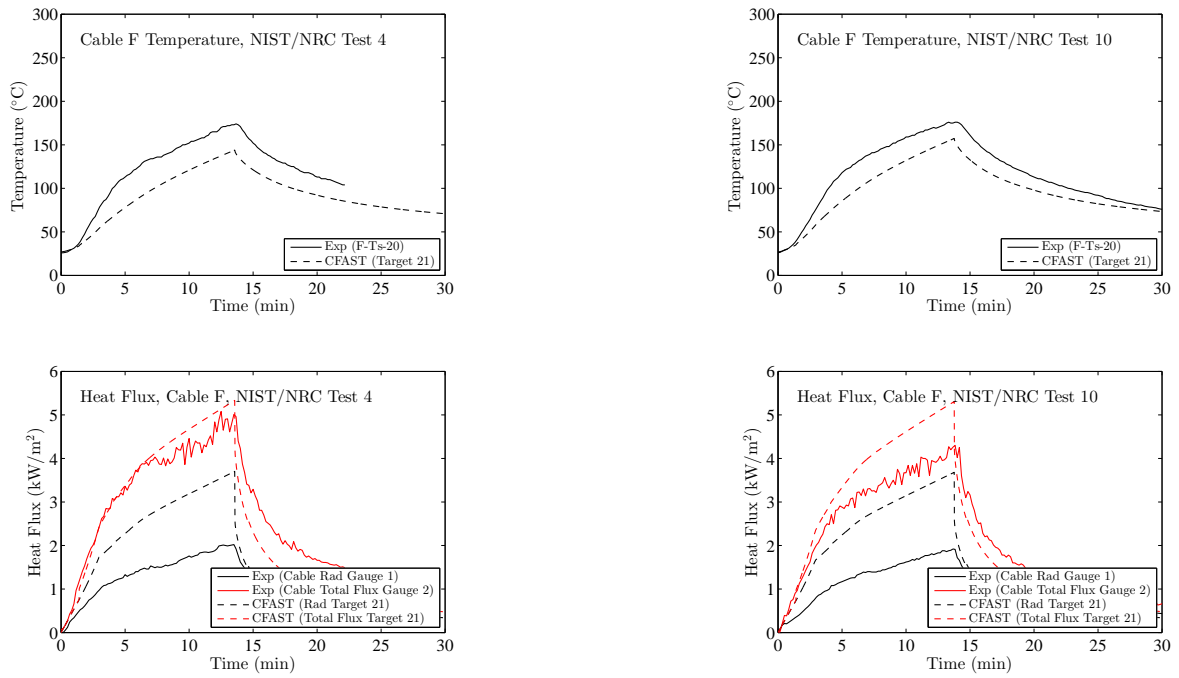


Figure B.56: NIST/NRC Series, Cable F Temperature and Heat Flux, Replicate Tests 4 and 10.

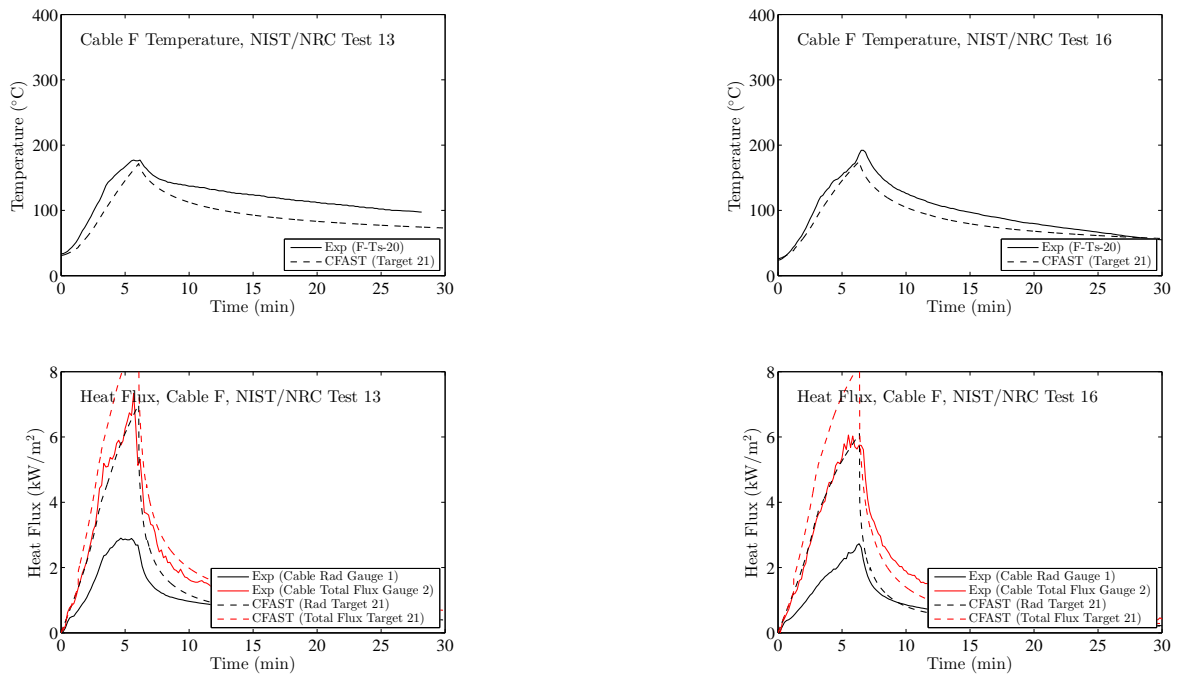


Figure B.57: NIST/NRC Series, Cable F Temperature and Heat Flux, Replicate Tests 13 and 16.

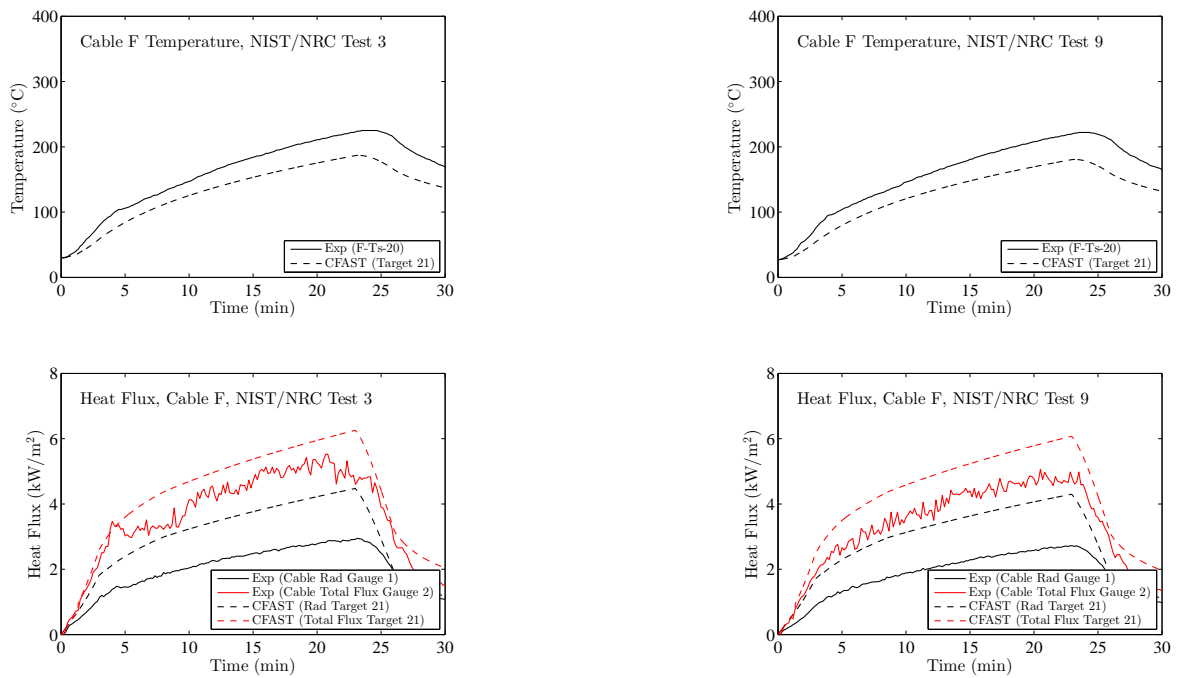


Figure B.58: NIST/NRC Series, Cable F Temperature and Heat Flux, Replicate Tests 3 and 9.

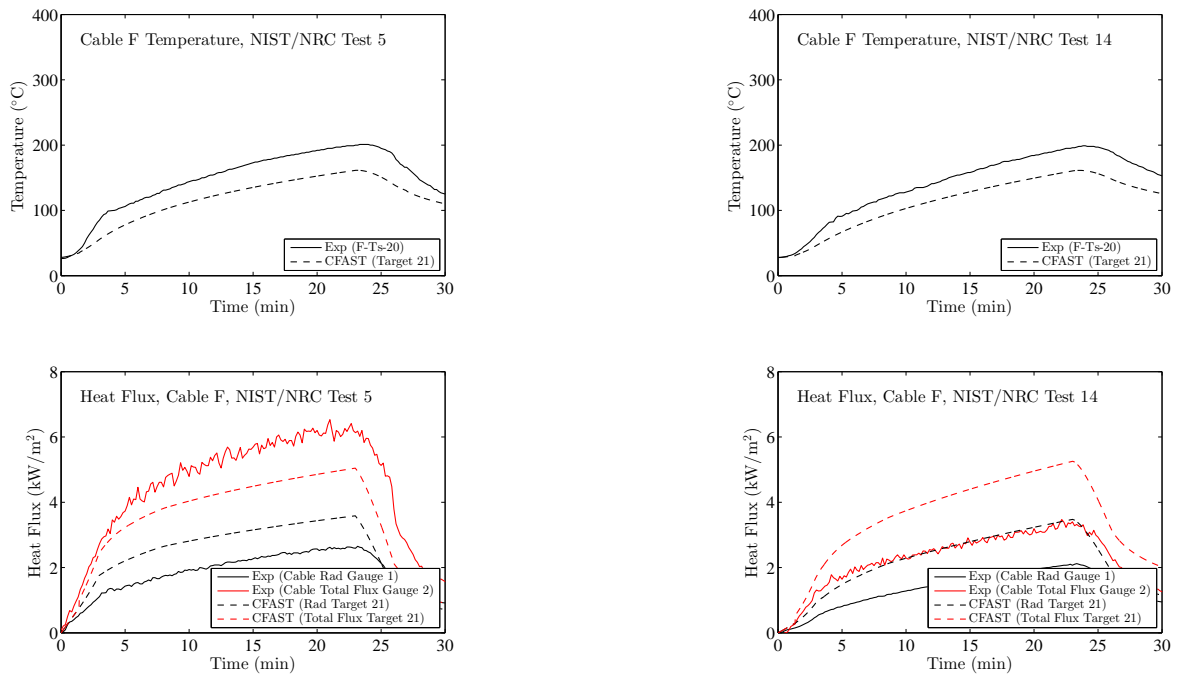


Figure B.59: NIST/NRC Series, Cable F Temperature and Heat Flux, Replicate Tests 5 and 14.

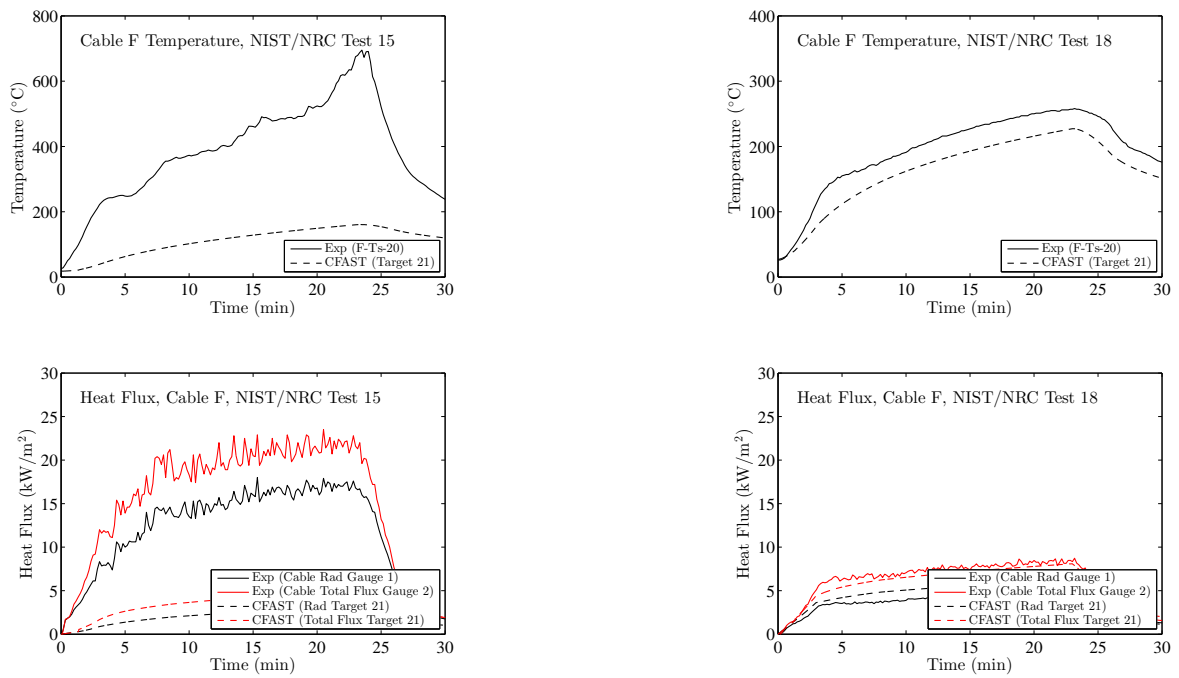


Figure B.60: NIST/NRC Series, Cable F Temperature and Heat Flux, Replicate Tests 15 and 18.

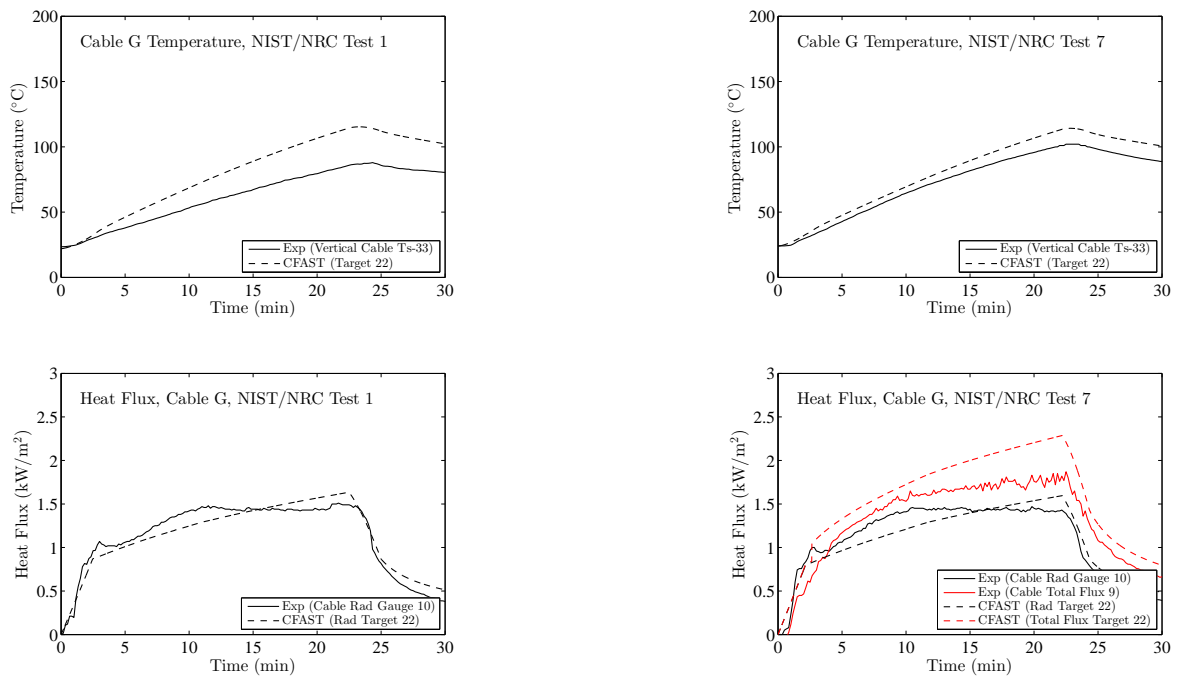


Figure B.61: NIST/NRC Series, Cable G Temperature and Heat Flux, Replicate Tests 1 and 7.

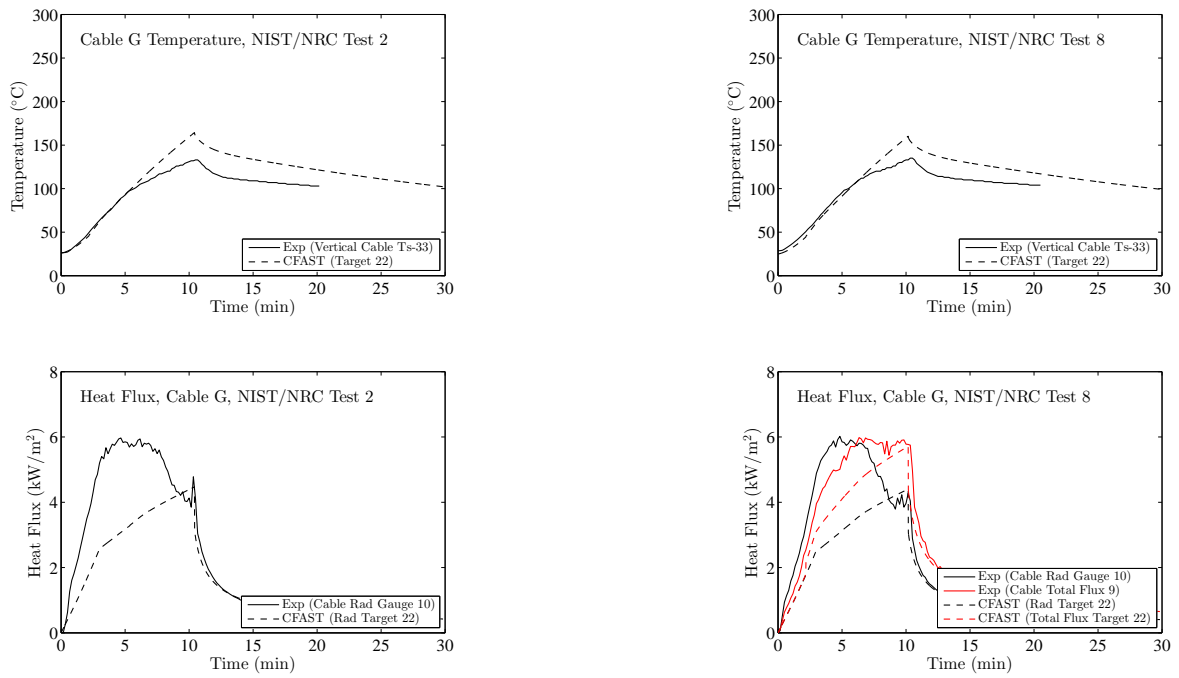


Figure B.62: NIST/NRC Series, Cable G Temperature and Heat Flux, Replicate Tests 2 and 8.

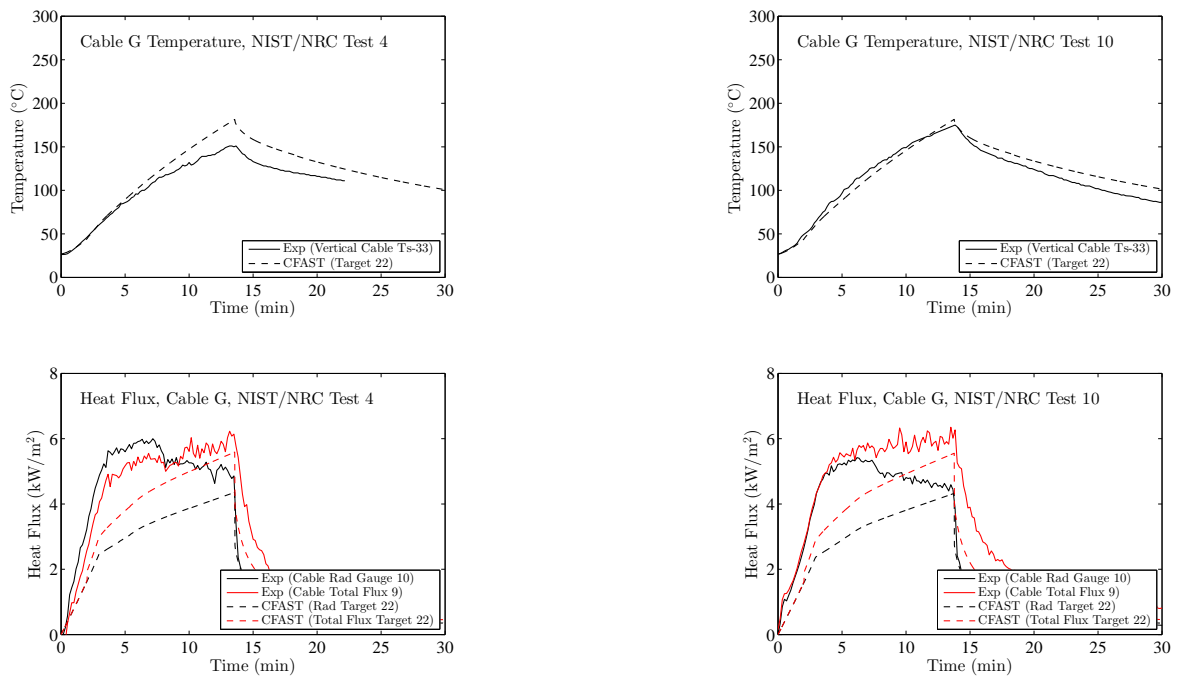


Figure B.63: NIST/NRC Series, Cable G Temperature and Heat Flux, Replicate Tests 4 and 10.

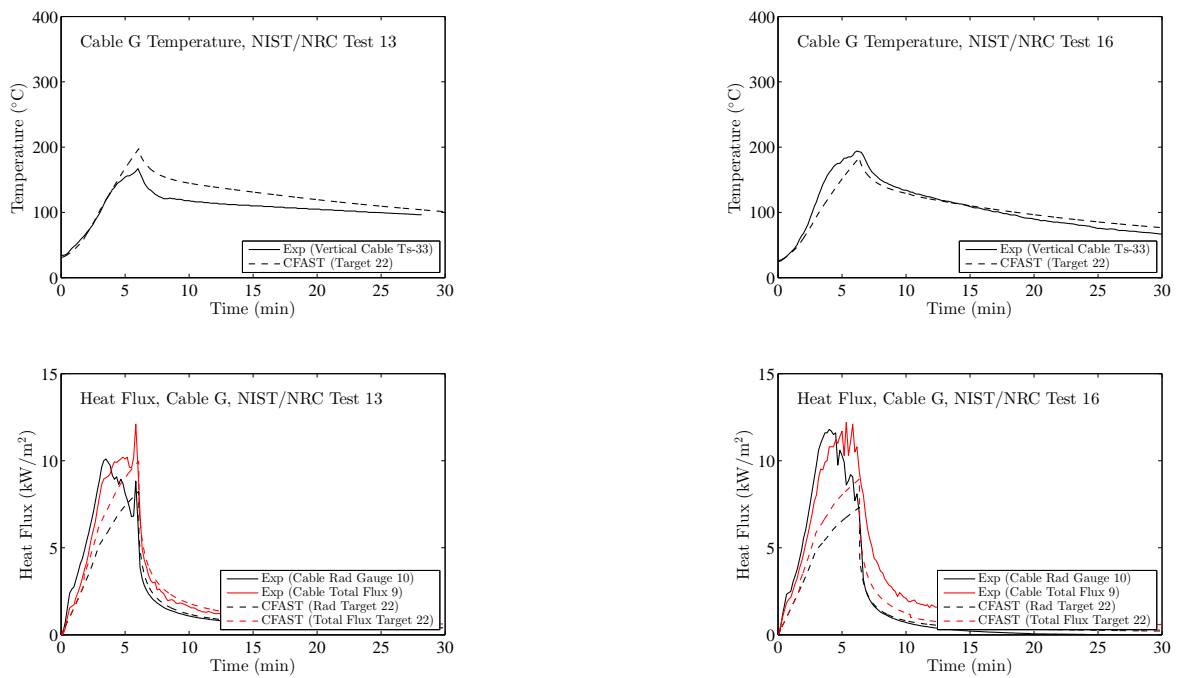


Figure B.64: NIST/NRC Series, Cable G Temperature and Heat Flux, Replicate Tests 13 and 16.

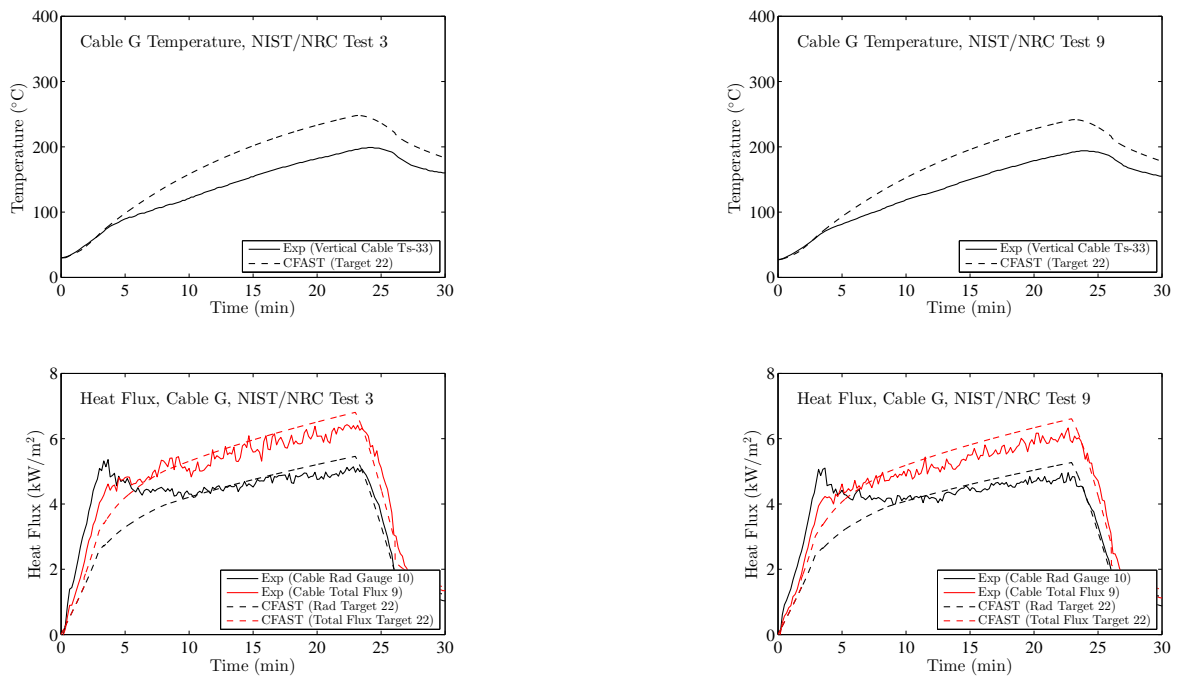


Figure B.65: NIST/NRC Series, Cable G Temperature and Heat Flux, Replicate Tests 3 and 9.

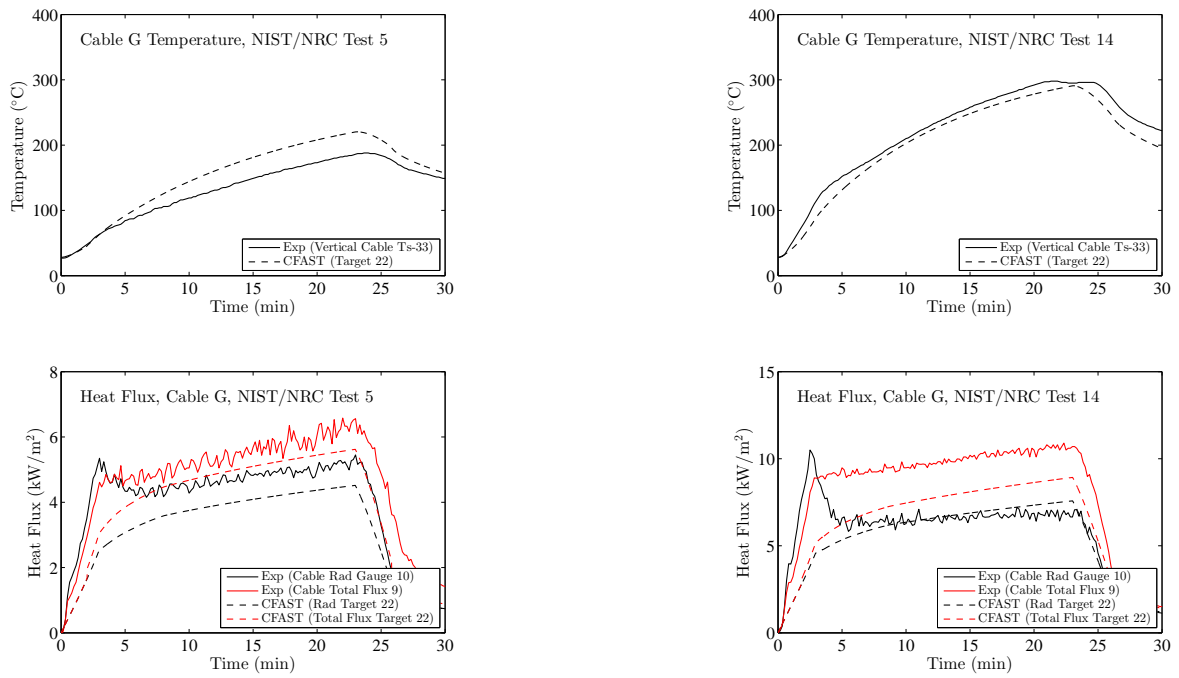


Figure B.66: NIST/NRC Series, Cable G Temperature and Heat Flux, Replicate Tests 5 and 14.

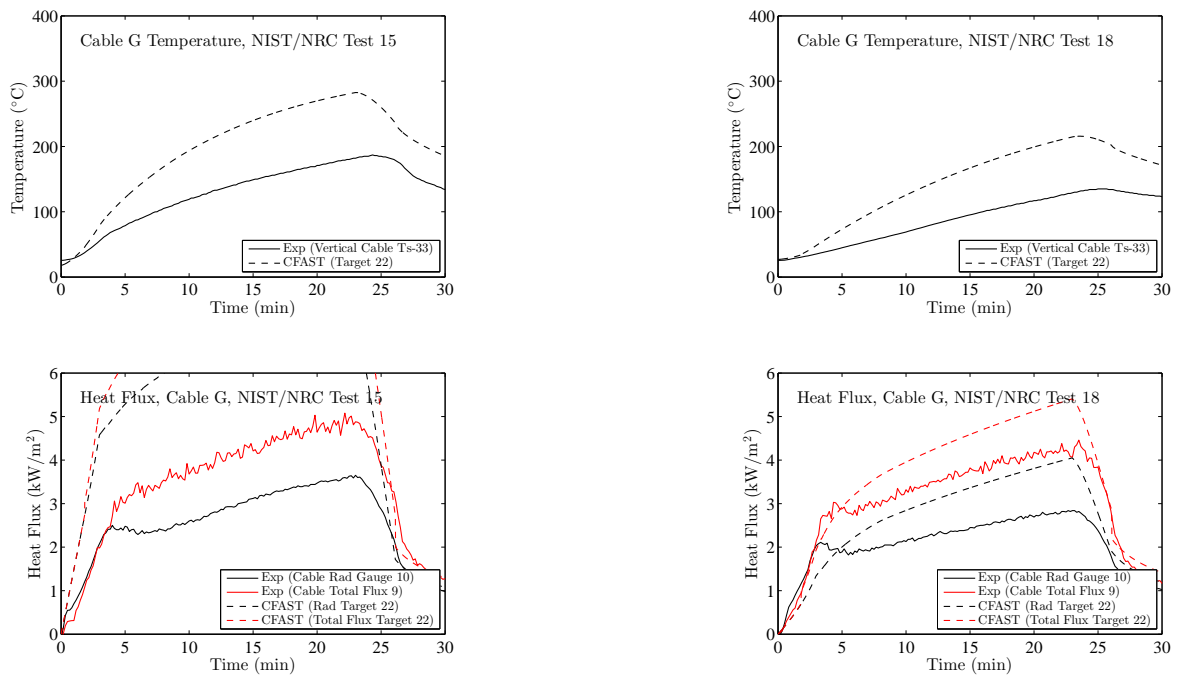


Figure B.67: NIST/NRC Series, Cable G Temperature and Heat Flux, Replicate Tests 15 and 18.

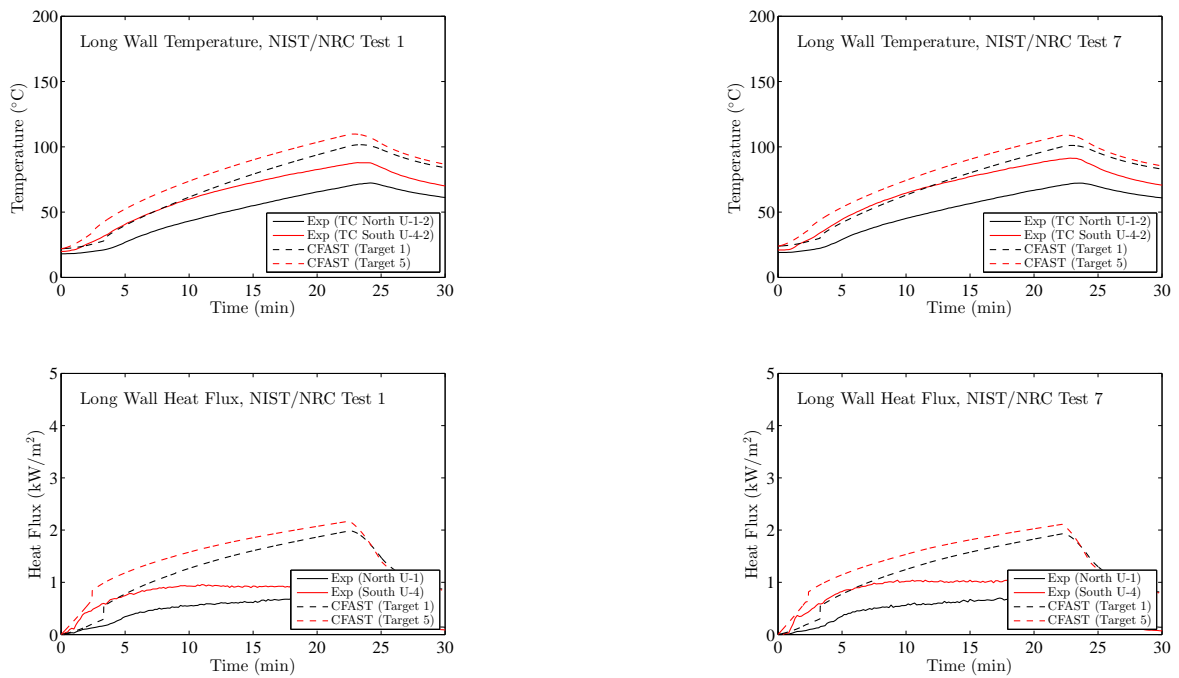


Figure B.68: NIST/NRC Series, Long Wall Temperature and Heat Flux, Replicate Tests 1 and 7.

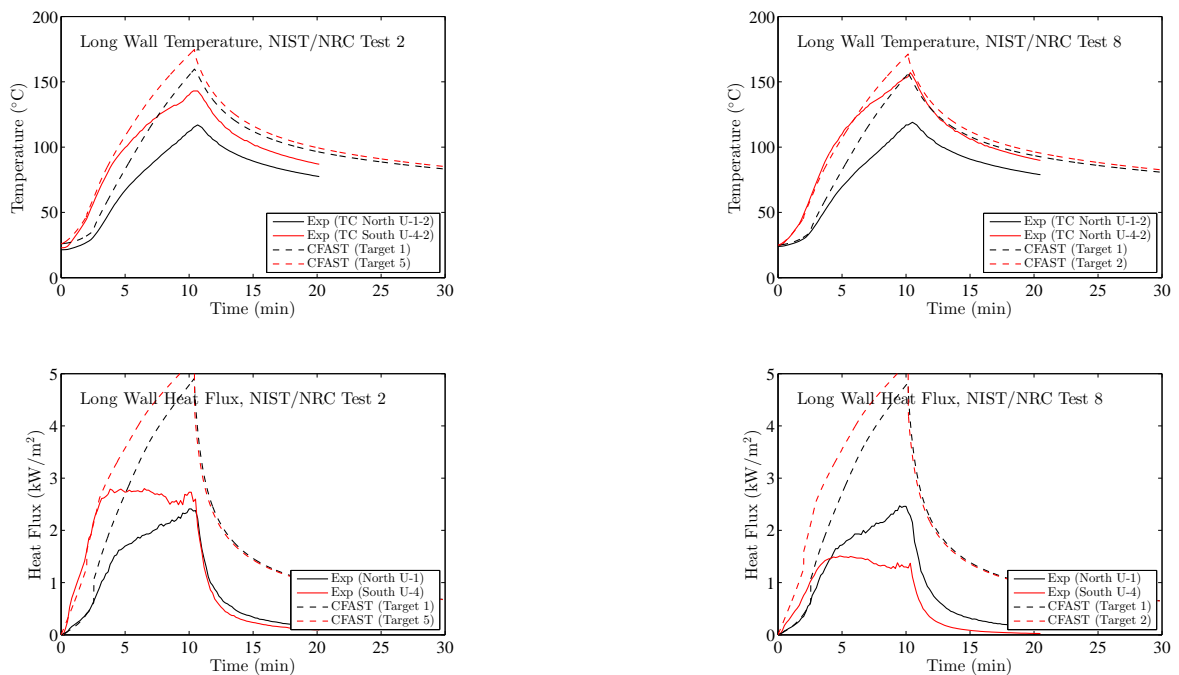


Figure B.69: NIST/NRC Series, Long Wall Temperature and Heat Flux, Replicate Tests 2 and 8.

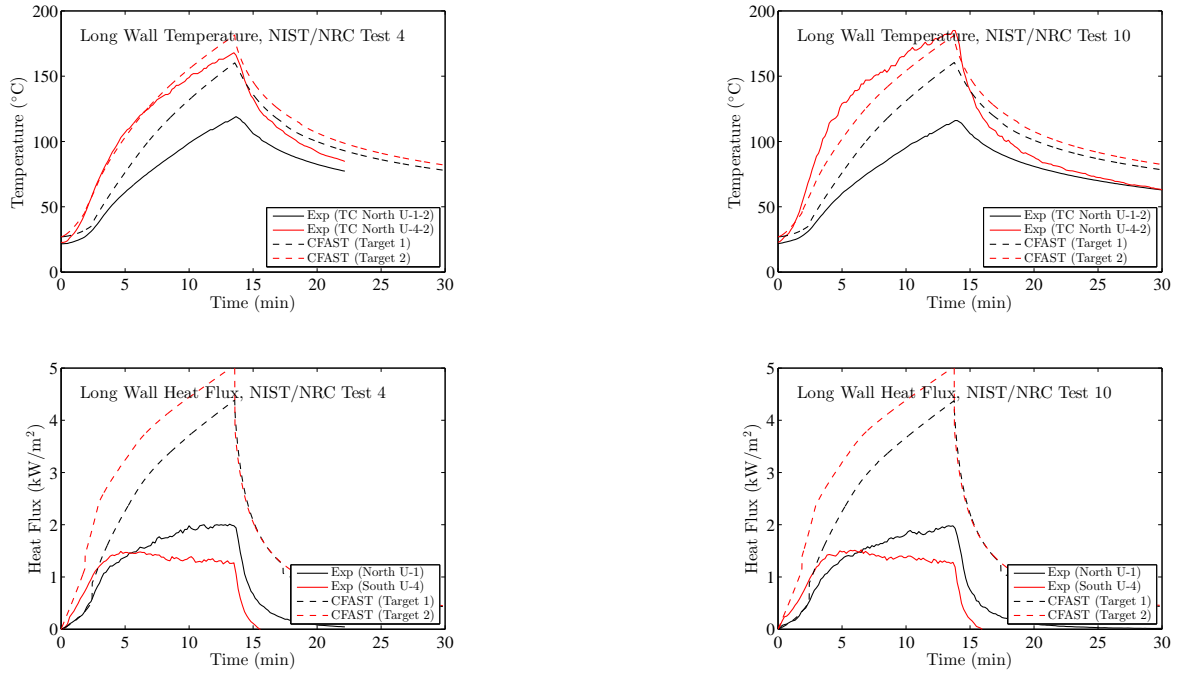
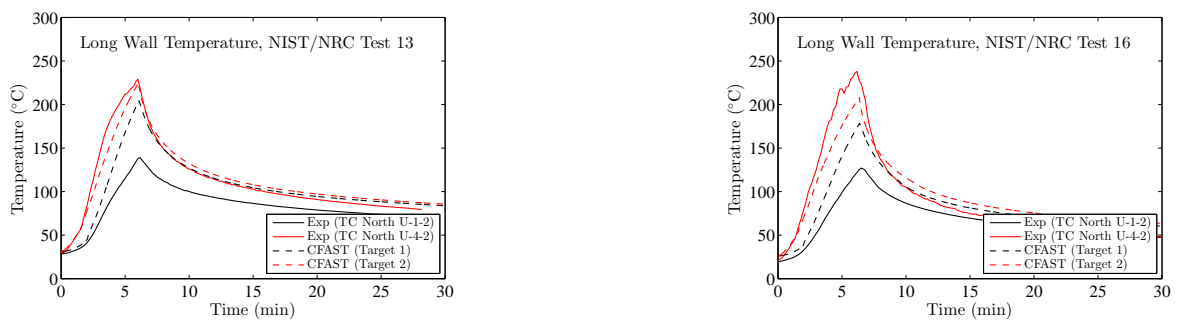


Figure B.70: NIST/NRC Series, Long Wall Temperature and Heat Flux, Replicate Tests 4 and 10.



Experimental Heat Flux Data Not Available

Experimental Heat Flux Data Not Available

Figure B.71: NIST/NRC Series, Long Wall Temperature and Heat Flux, Replicate Tests 13 and 16.

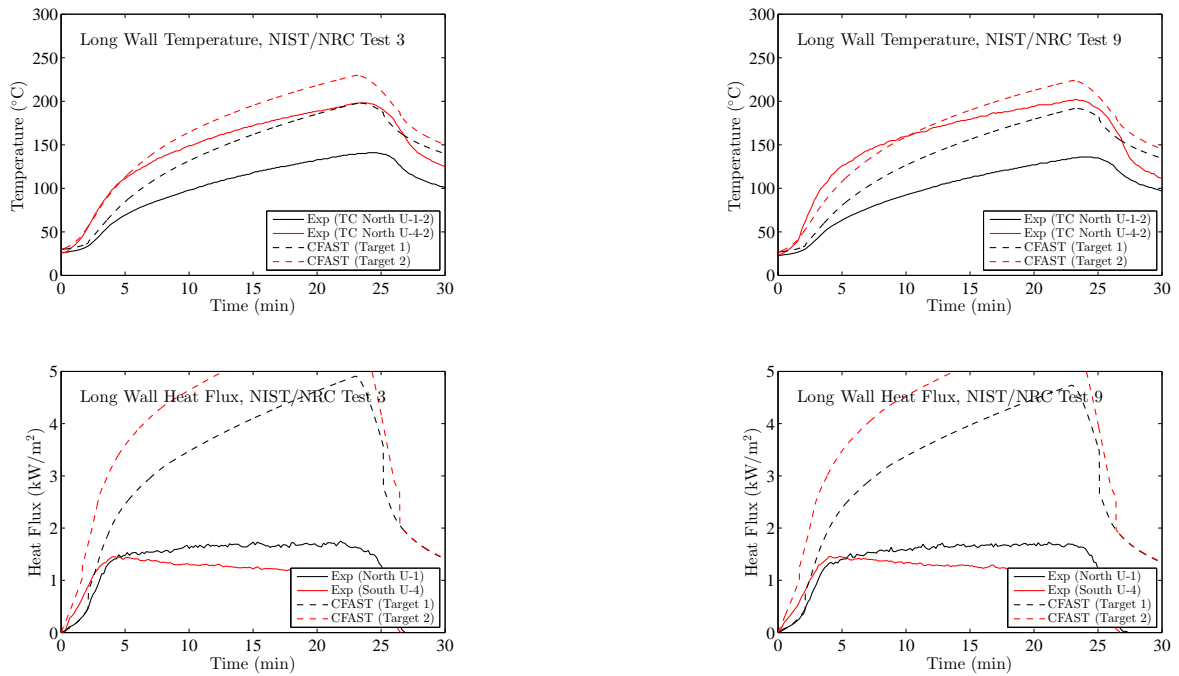


Figure B.72: NIST/NRC Series, Long Wall Temperature and Heat Flux, Replicate Tests 3 and 9.

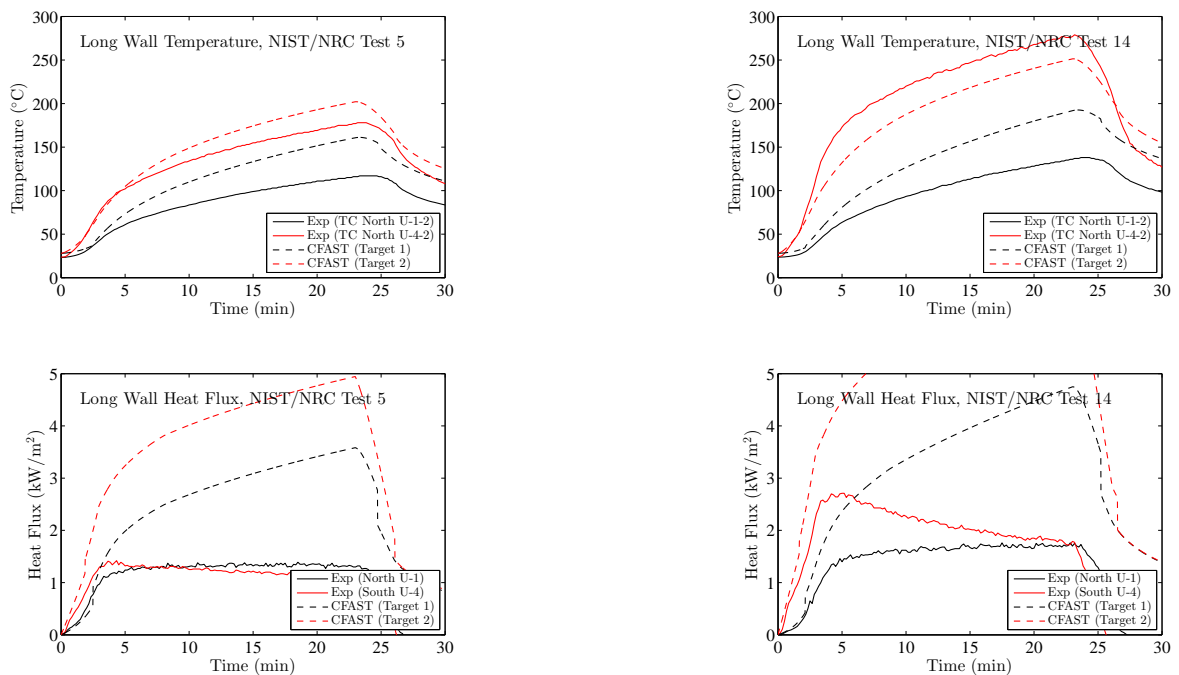


Figure B.73: NIST/NRC Series, Long Wall Temperature and Heat Flux, Replicate Tests 5 and 14.

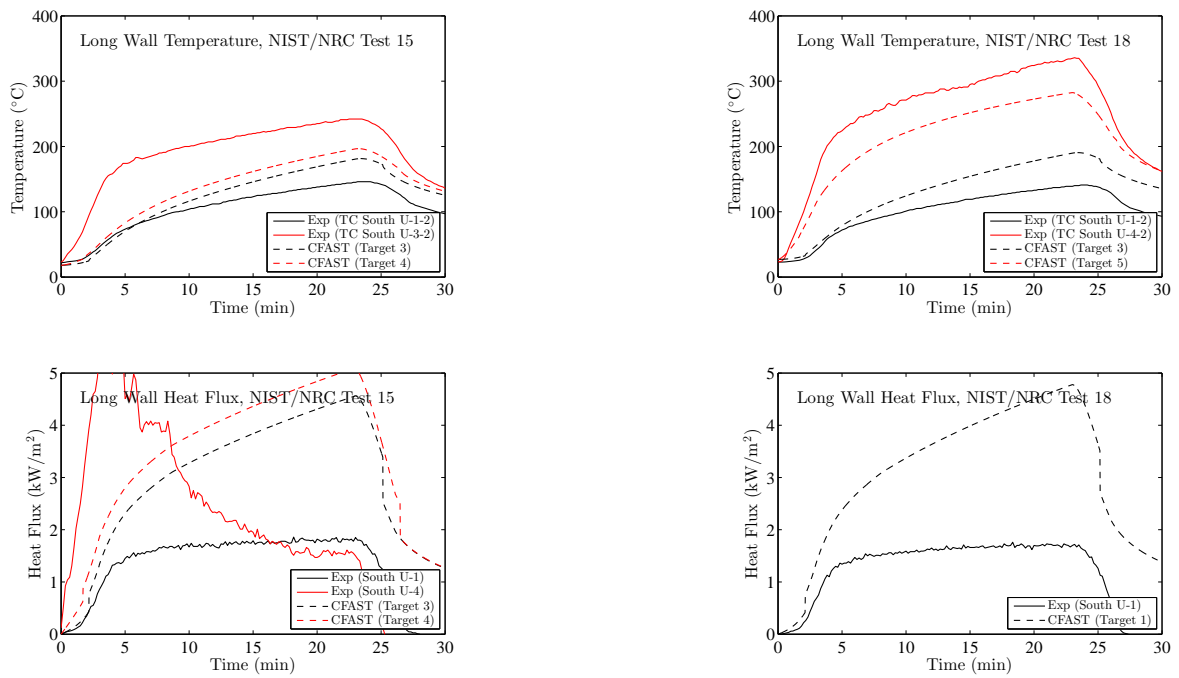


Figure B.74: NIST/NRC Series, Long Wall Temperature and Heat Flux, Replicate Tests 15 and 18.

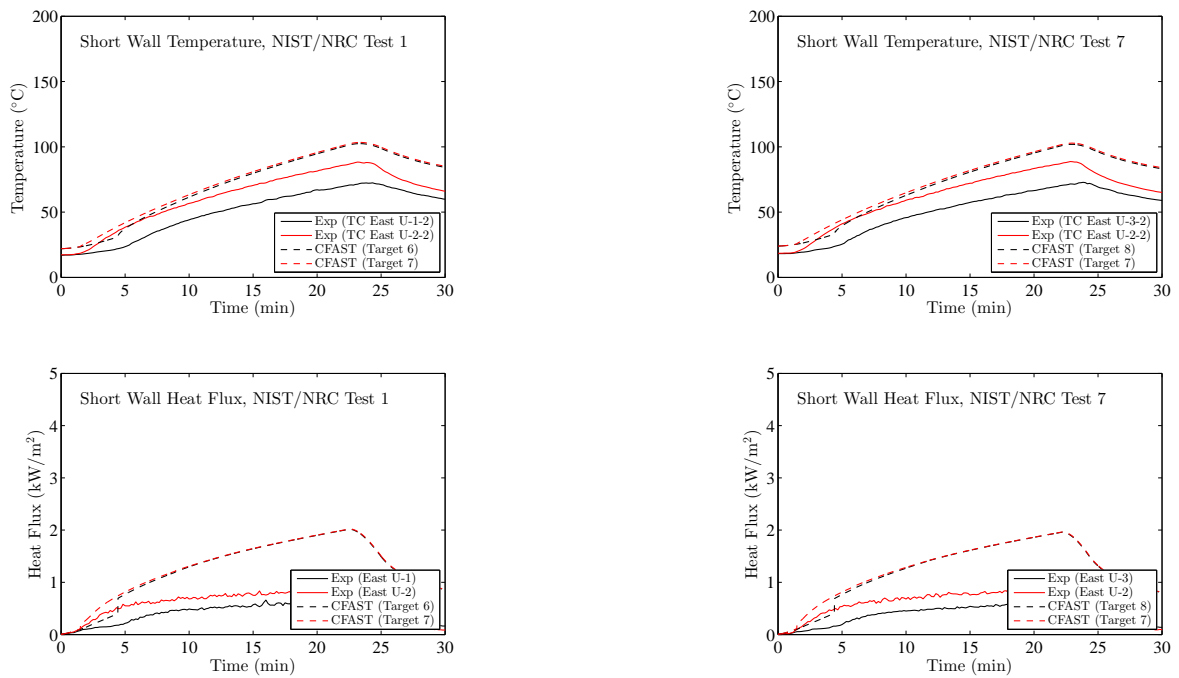


Figure B.75: NIST/NRC Series, Short Wall Temperature and Heat Flux, Replicate Tests 1 and 7.

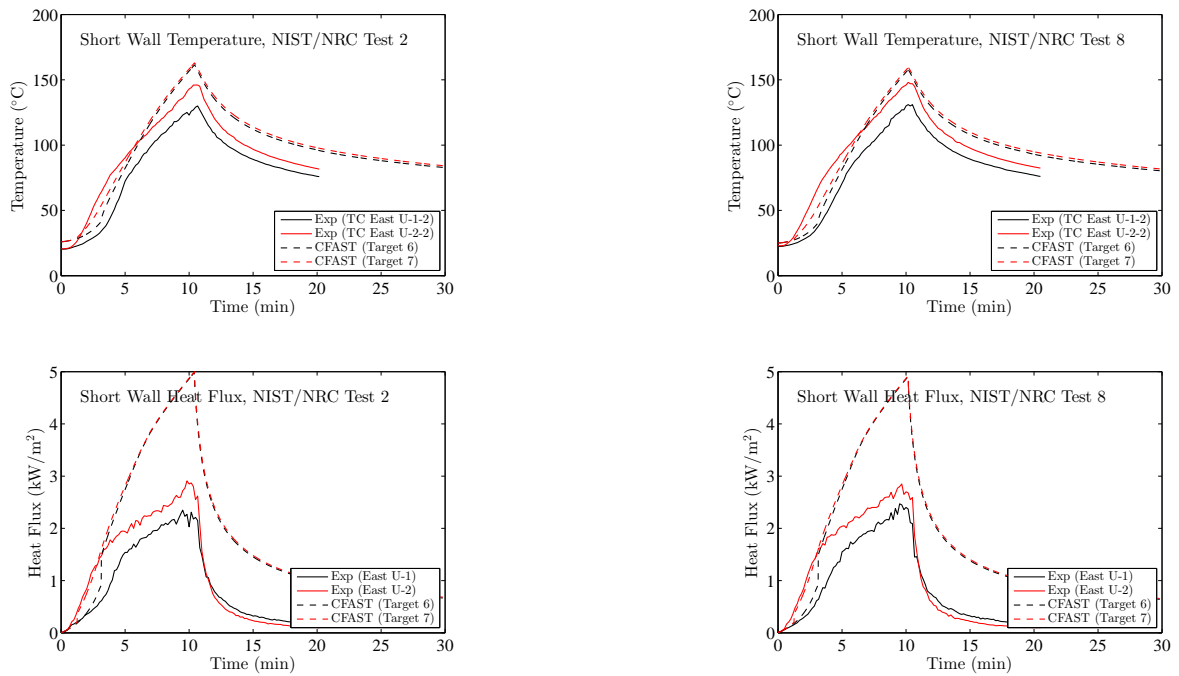


Figure B.76: NIST/NRC Series, Short Wall Temperature and Heat Flux, Replicate Tests 2 and 8.

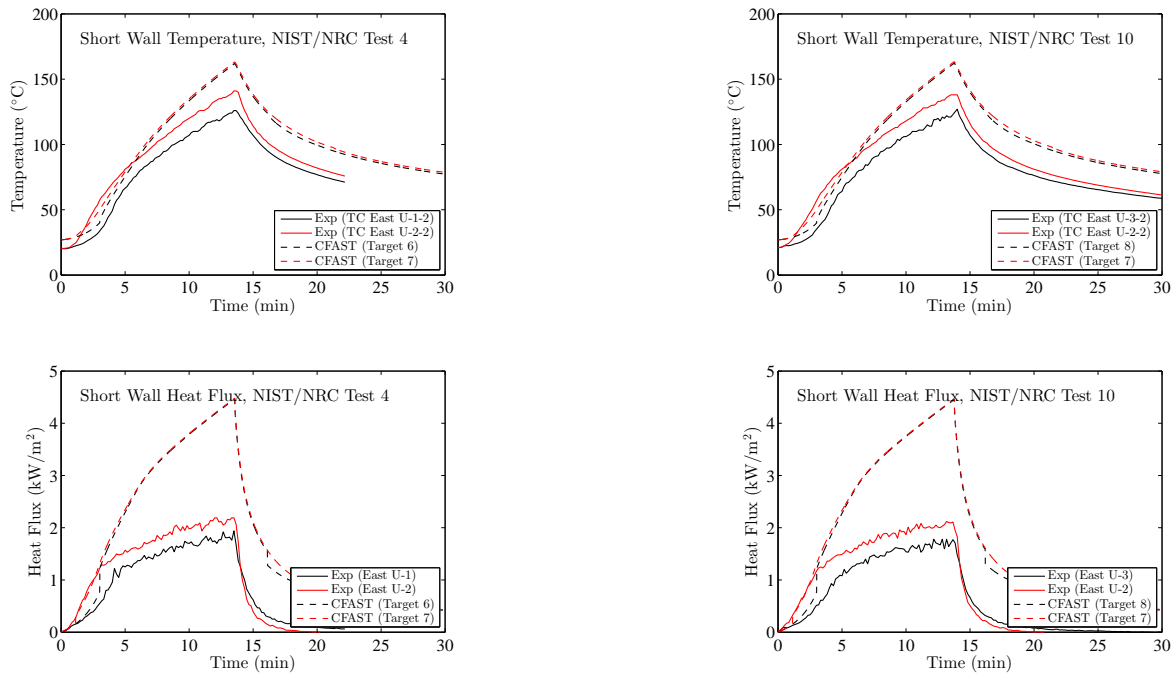
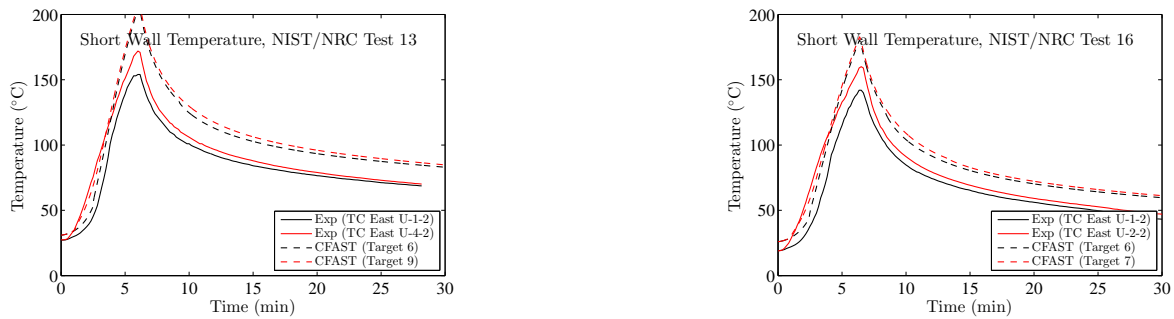


Figure B.77: NIST/NRC Series, Short Wall Temperature and Heat Flux, Replicate Tests 4 and 10.



Experimental Heat Flux Data Not Available

Experimental Heat Flux Data Not Available

Figure B.78: NIST/NRC Series, Short Wall Temperature and Heat Flux, Replicate Tests 13 and 16.

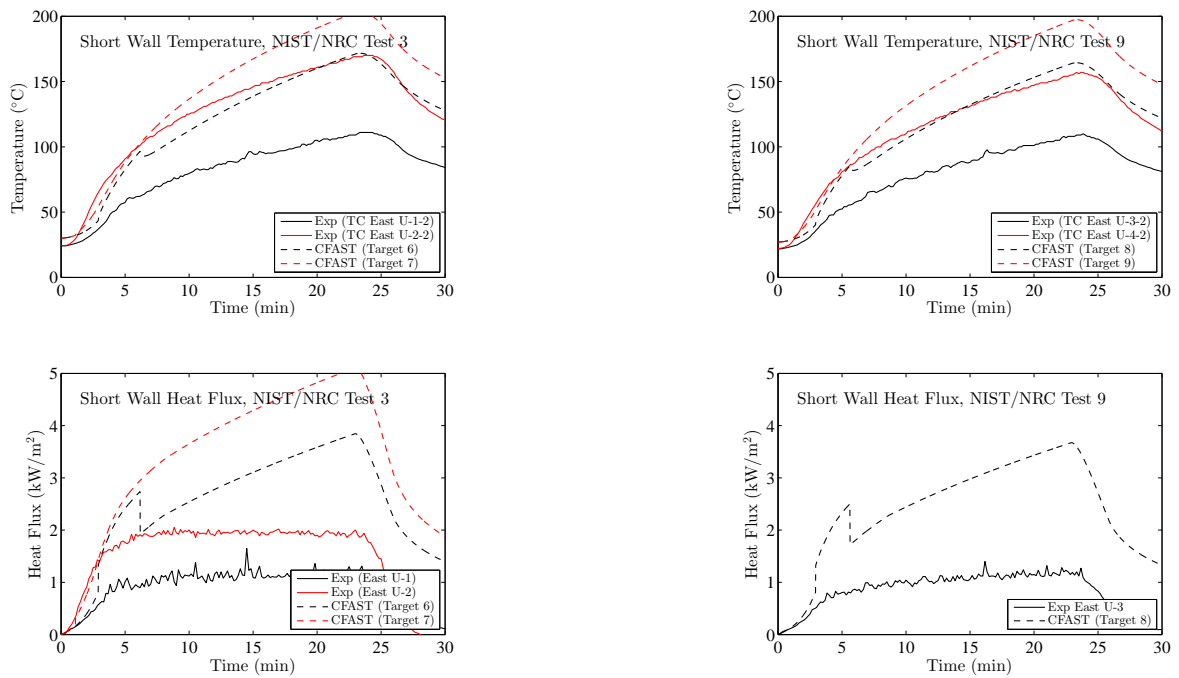


Figure B.79: NIST/NRC Series, Short Wall Temperature and Heat Flux, Replicate Tests 3 and 9.

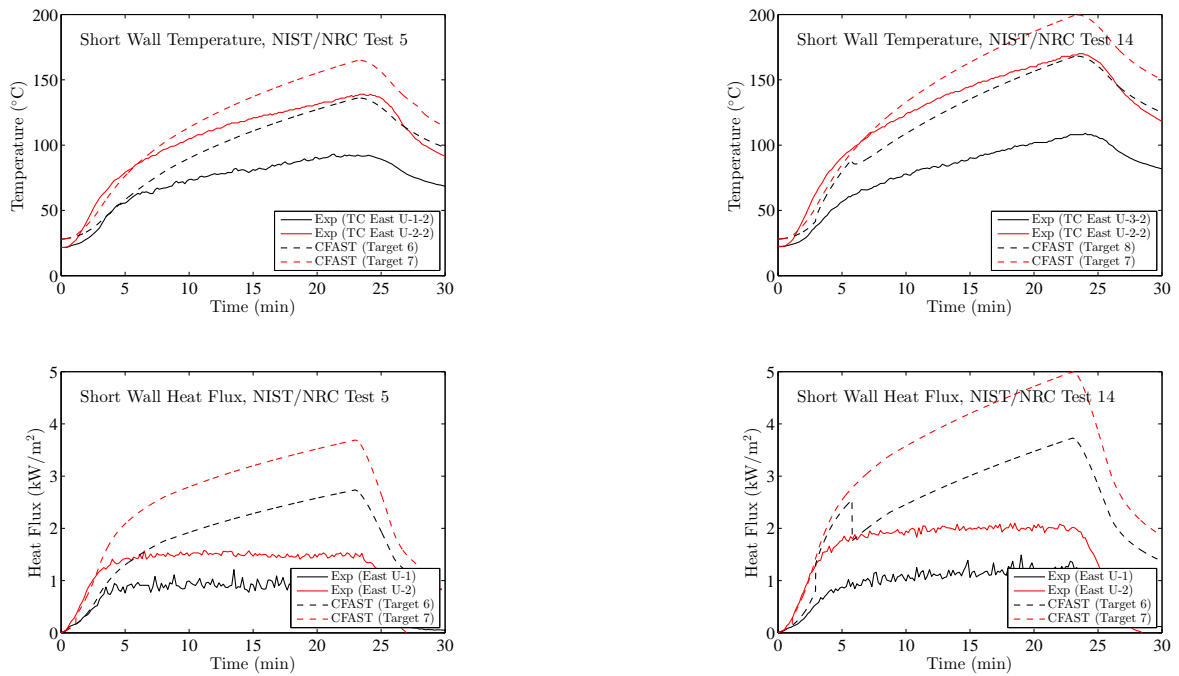
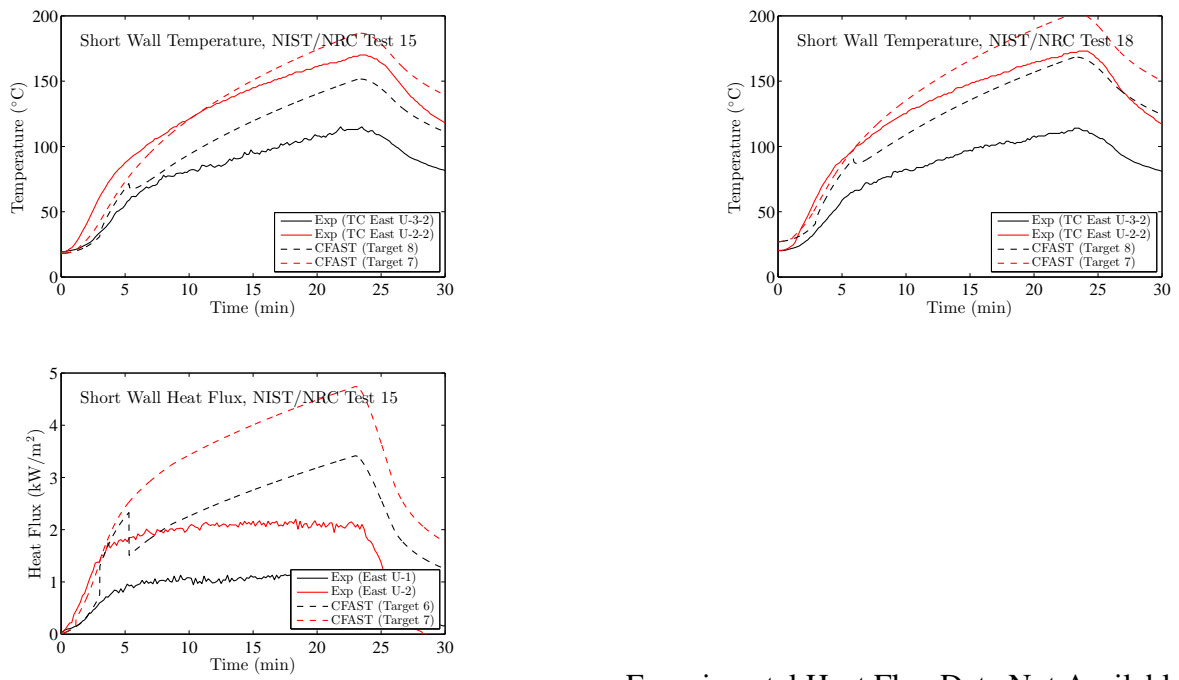


Figure B.80: NIST/NRC Series, Short Wall Temperature and Heat Flux, Replicate Tests 5 and 14.



Experimental Heat Flux Data Not Available

Figure B.81: NIST/NRC Series, Short Wall Temperature and Heat Flux, Replicate Tests 15 and 18.

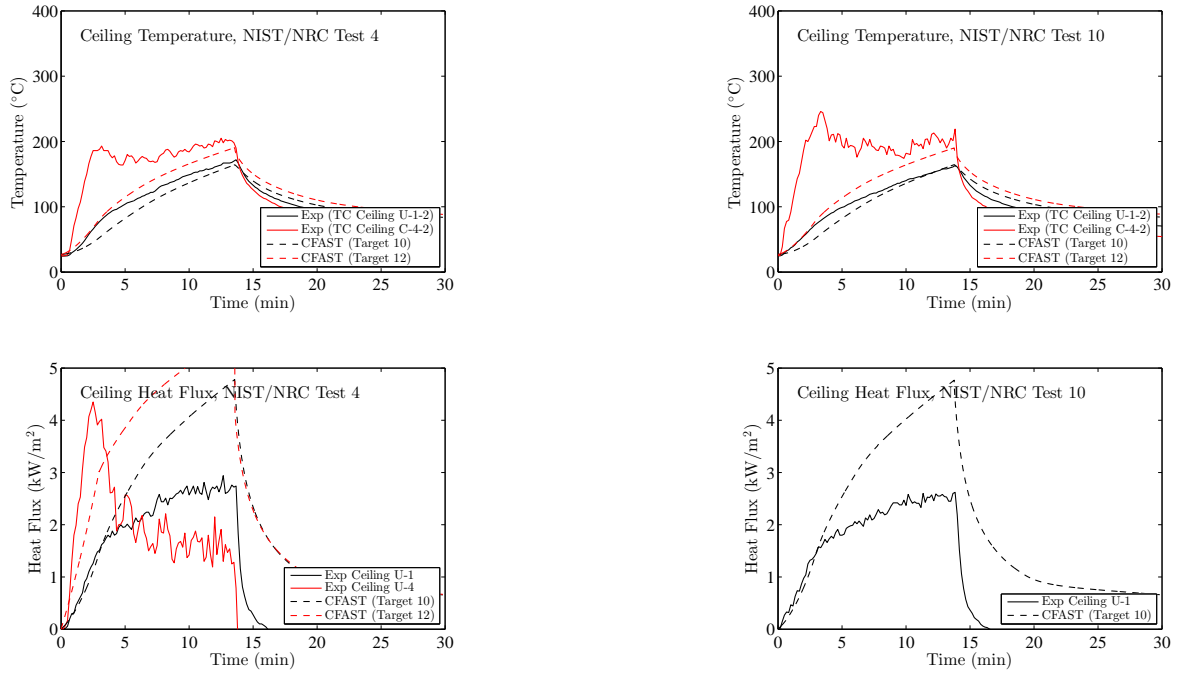
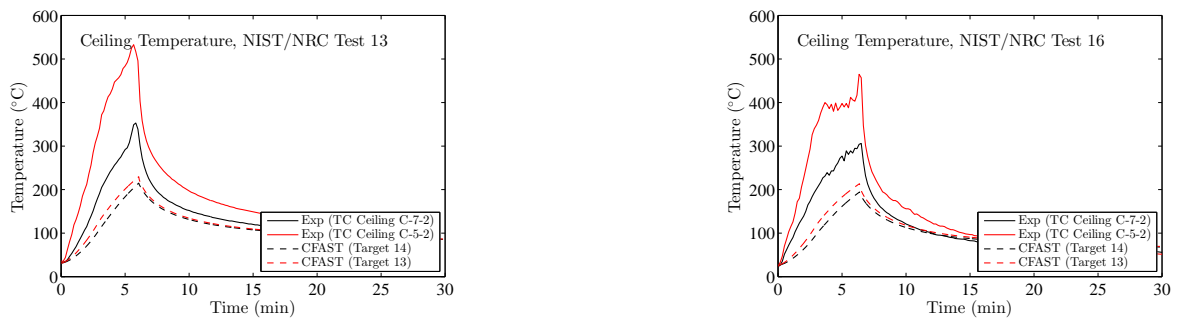


Figure B.82: NIST/NRC Series, Ceiling Temperature and Heat Flux, Replicate Tests 4 and 10.



Experimental Heat Flux Data Not Available

Experimental Heat Flux Data Not Available

Figure B.83: NIST/NRC Series, Ceiling Temperature and Heat Flux, Replicate Tests 13 and 16.

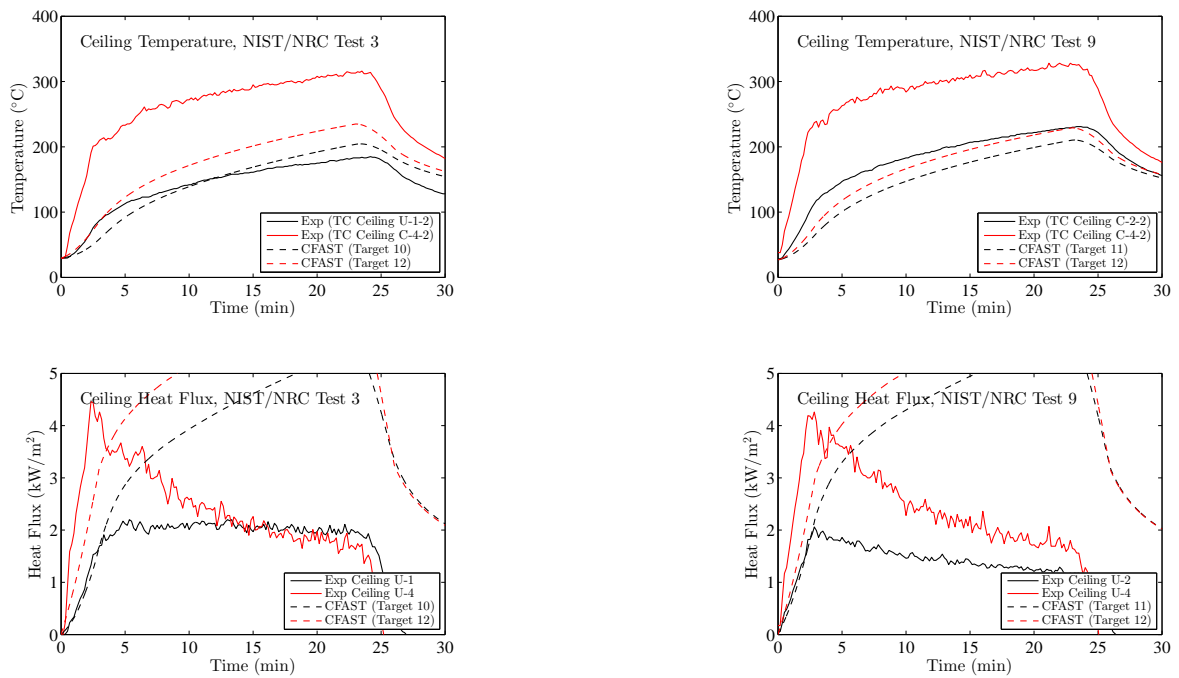


Figure B.84: NIST/NRC Series, Ceiling Temperature and Heat Flux, Replicate Tests 3 and 9.

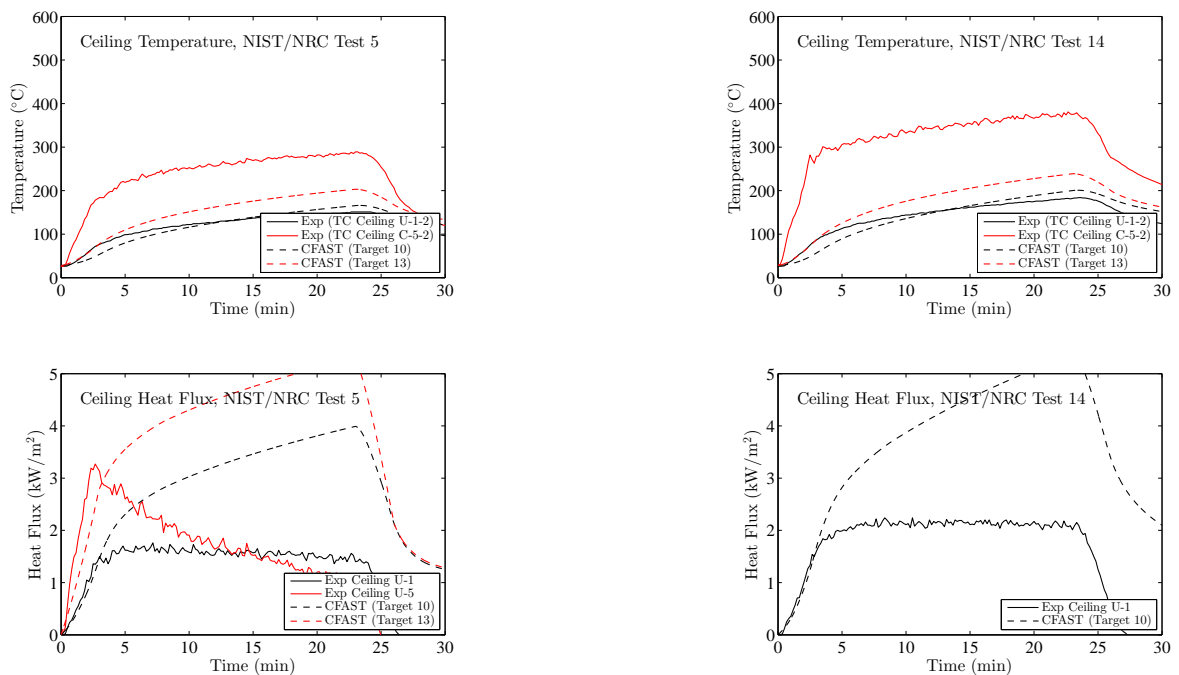
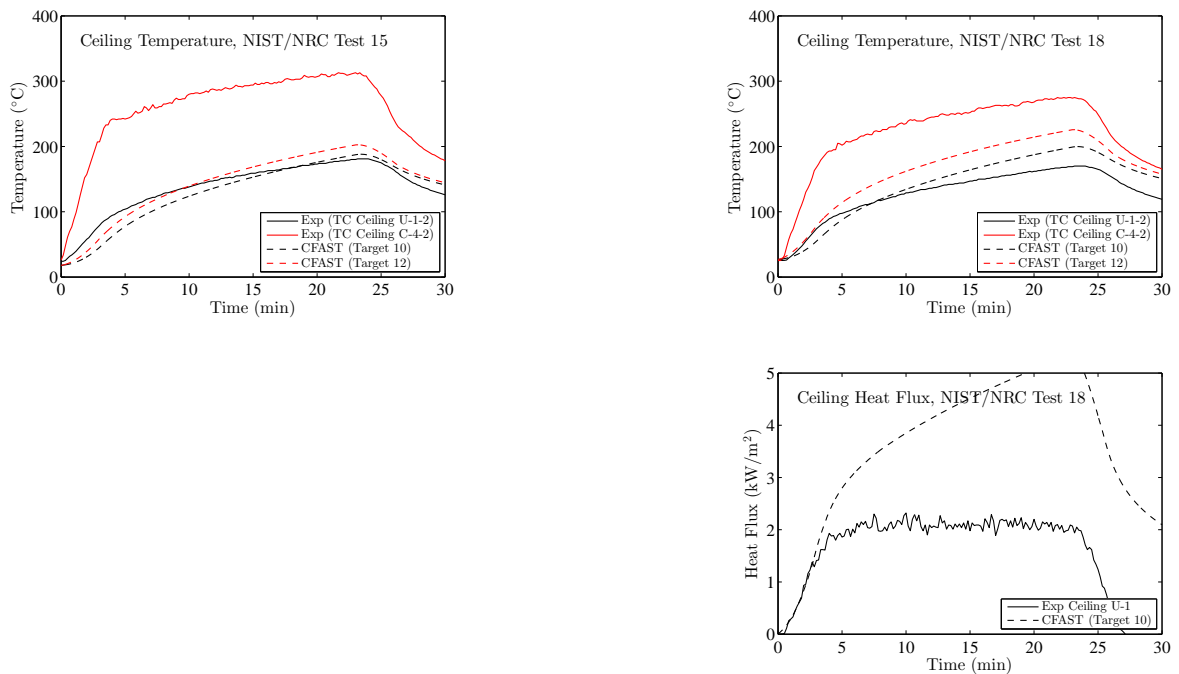


Figure B.85: NIST/NRC Series, Ceiling Temperature and Heat Flux, Replicate Tests 5 and 14.



Experimental Heat Flux Data Not Available

Figure B.86: NIST/NRC Series, Ceiling Temperature and Heat Flux, Replicate Tests 15 and 18.

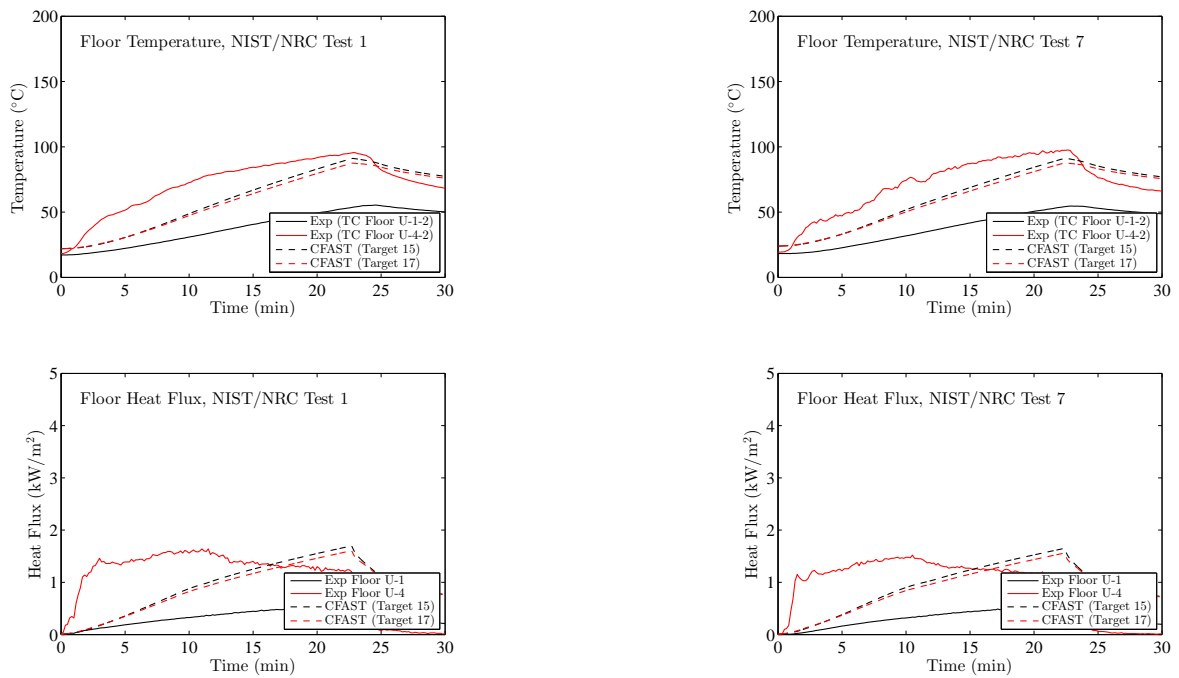


Figure B.87: NIST/NRC Series, Floor Temperature and Heat Flux, Replicate Tests 1 and 7.

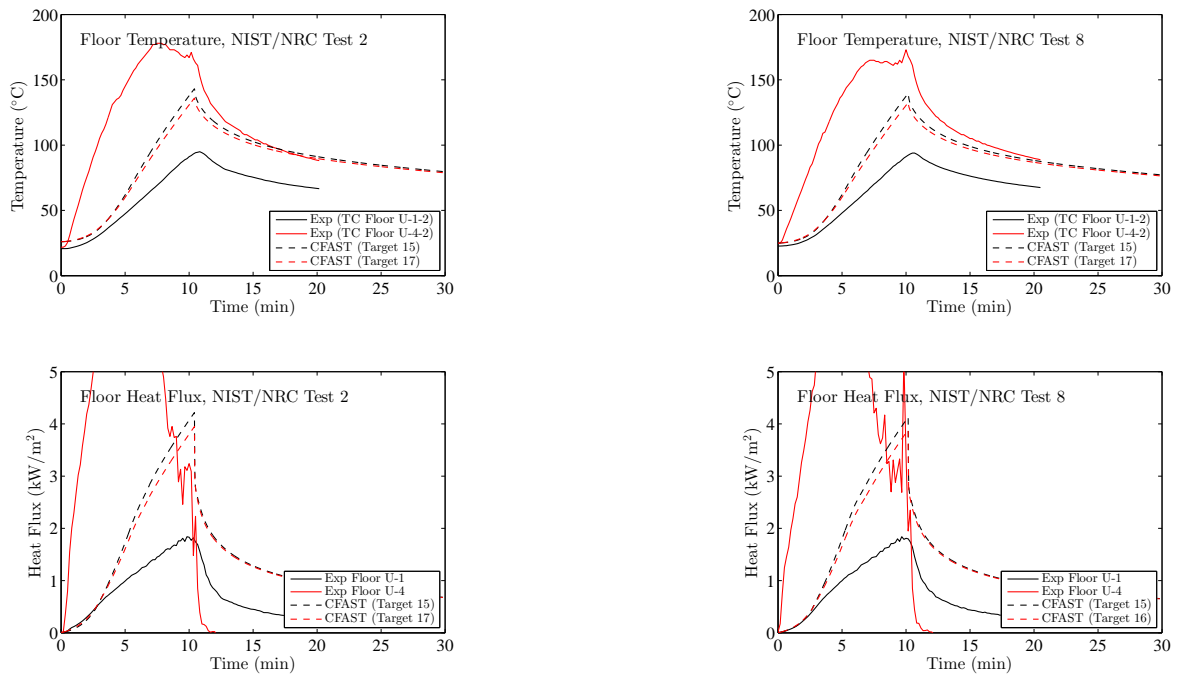


Figure B.88: NIST/NRC Series, Floor Temperature and Heat Flux, Replicate Tests 2 and 8.

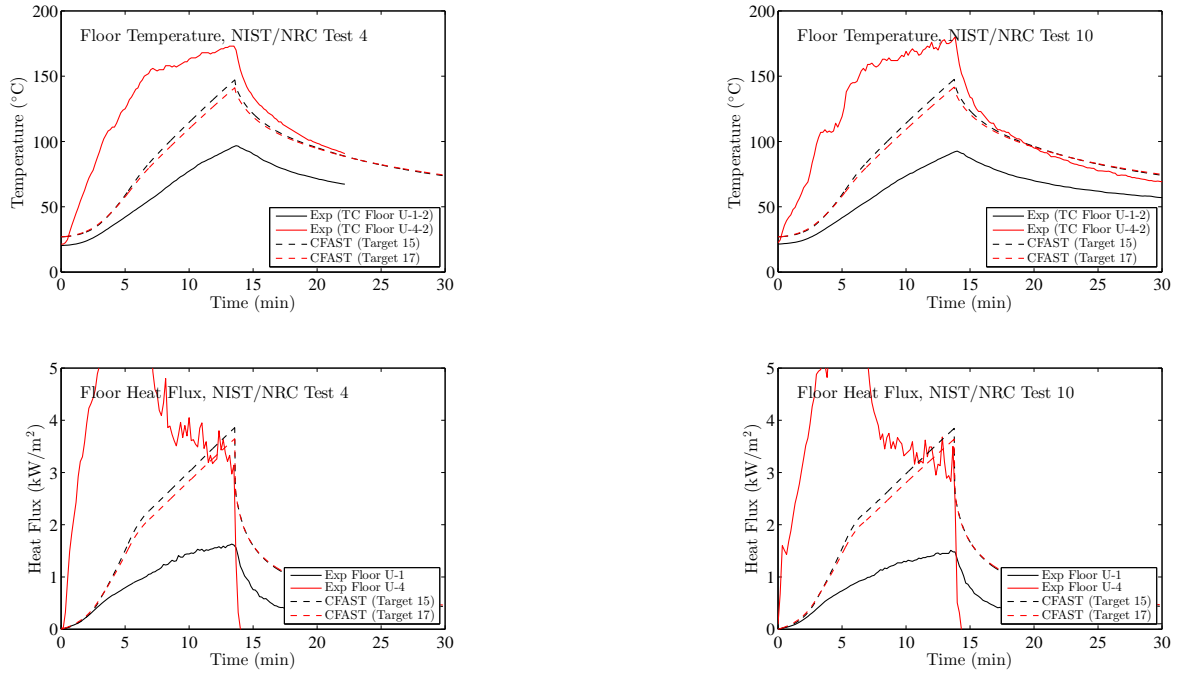
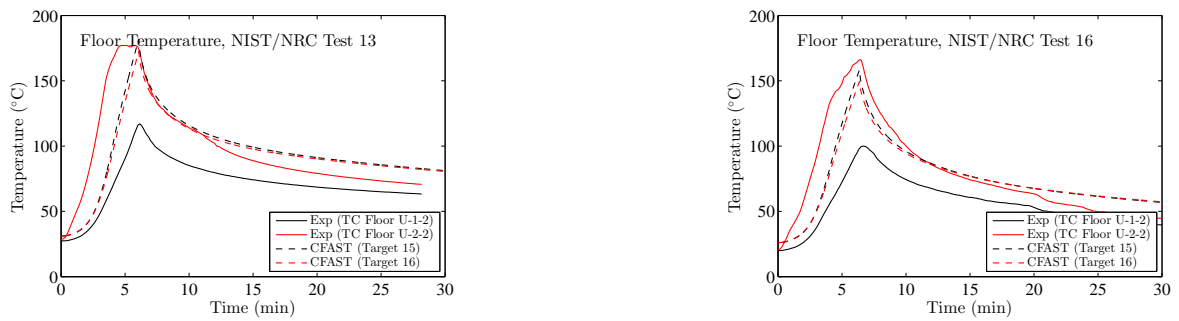


Figure B.89: NIST/NRC Series, Floor Temperature and Heat Flux, Replicate Tests 4 and 10.



Experimental Heat Flux Data Not Available

Experimental Heat Flux Data Not Available

Figure B.90: NIST/NRC Series, Floor Temperature and Heat Flux, Replicate Tests 13 and 16.

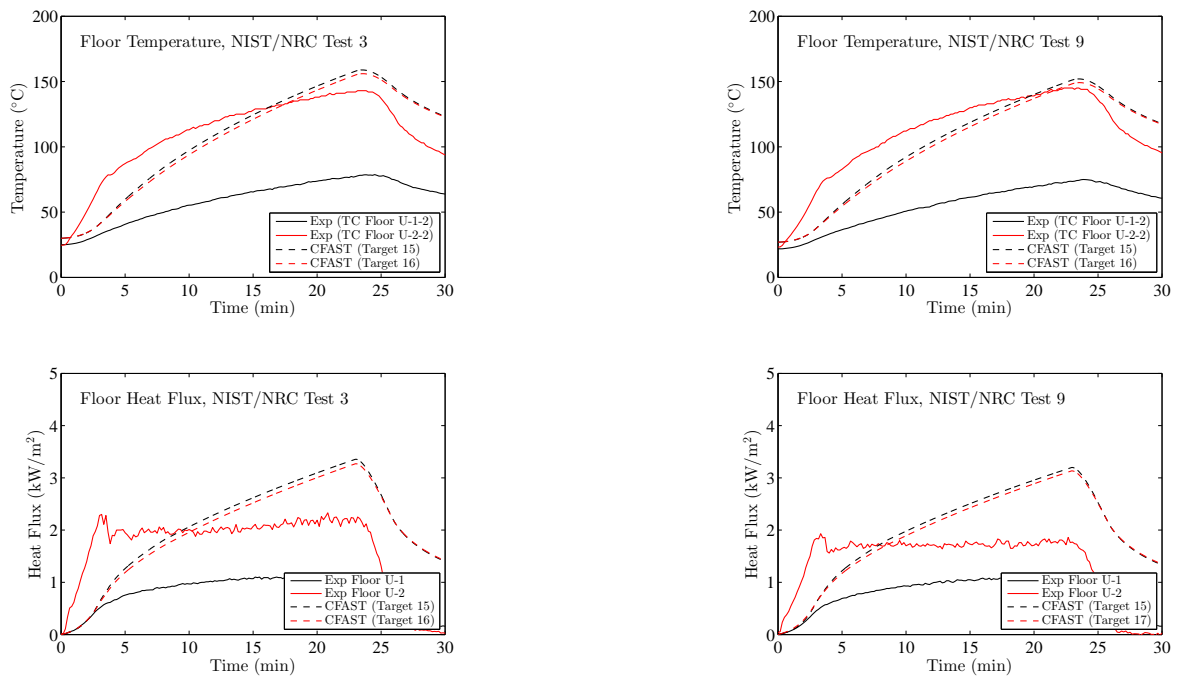


Figure B.91: NIST/NRC Series, Floor Temperature and Heat Flux, Replicate Tests 3 and 9.

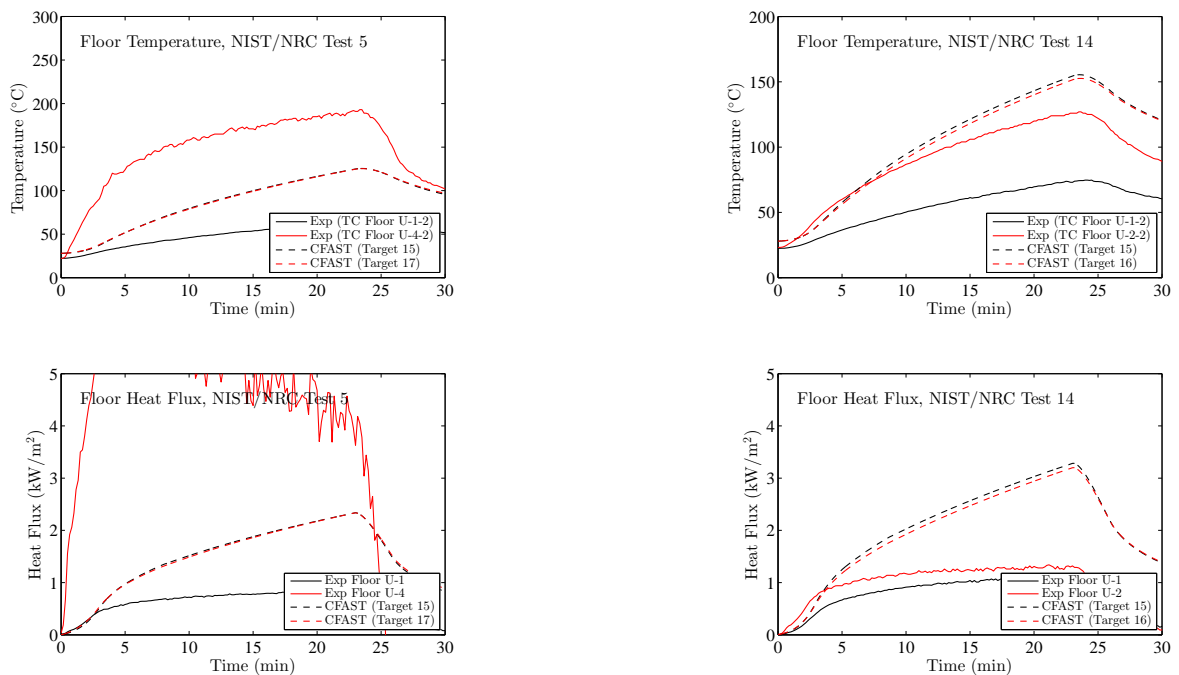


Figure B.92: NIST/NRC Series, Floor Temperature and Heat Flux, Replicate Tests 5 and 14.

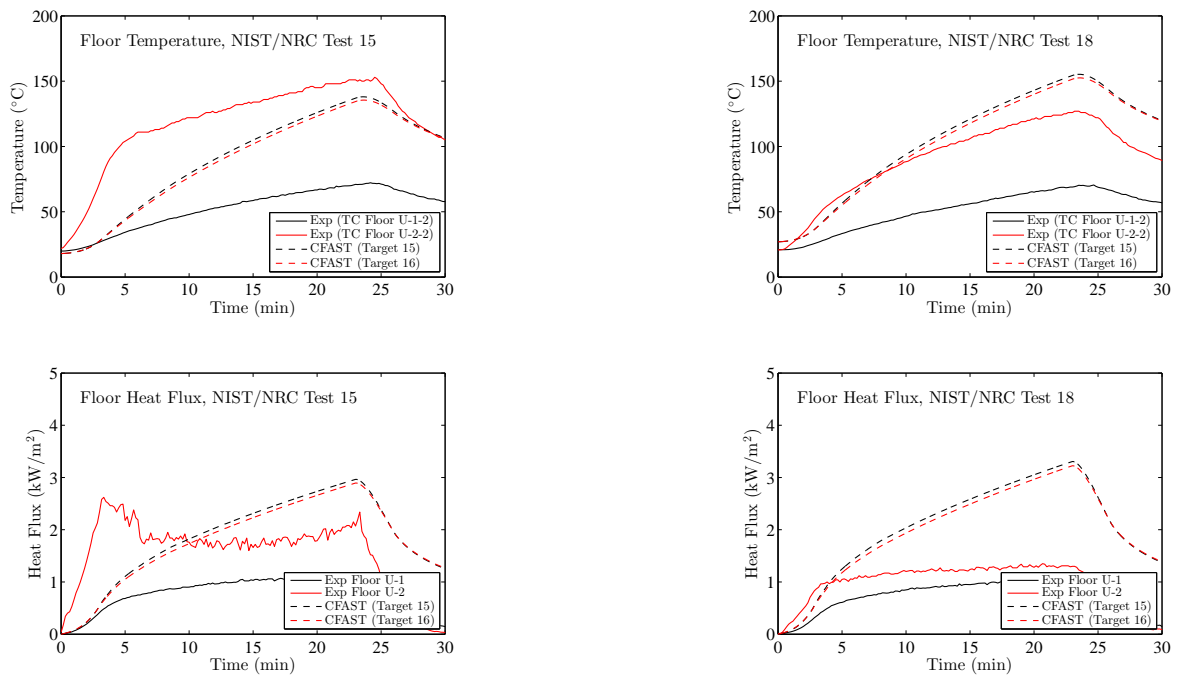
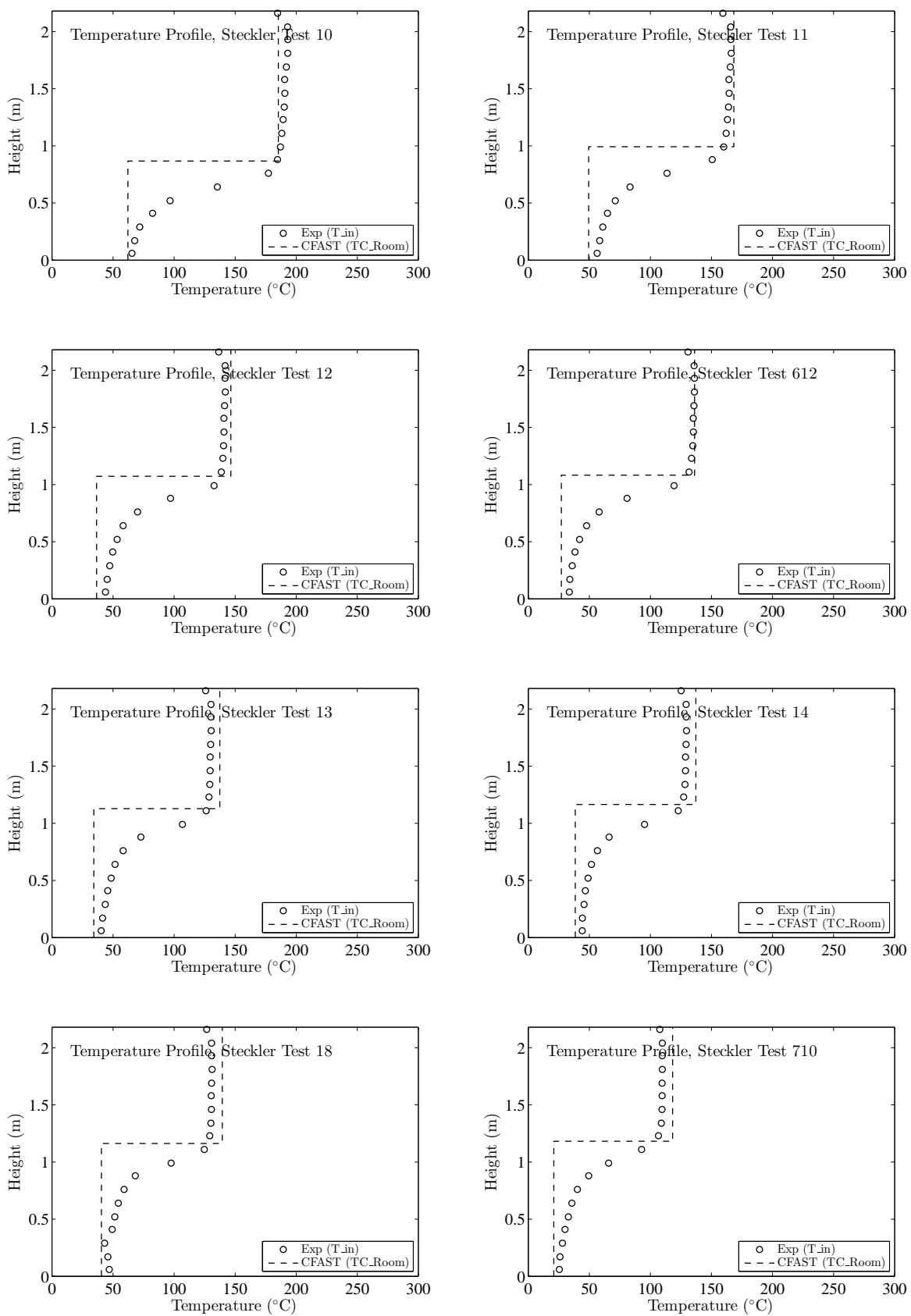
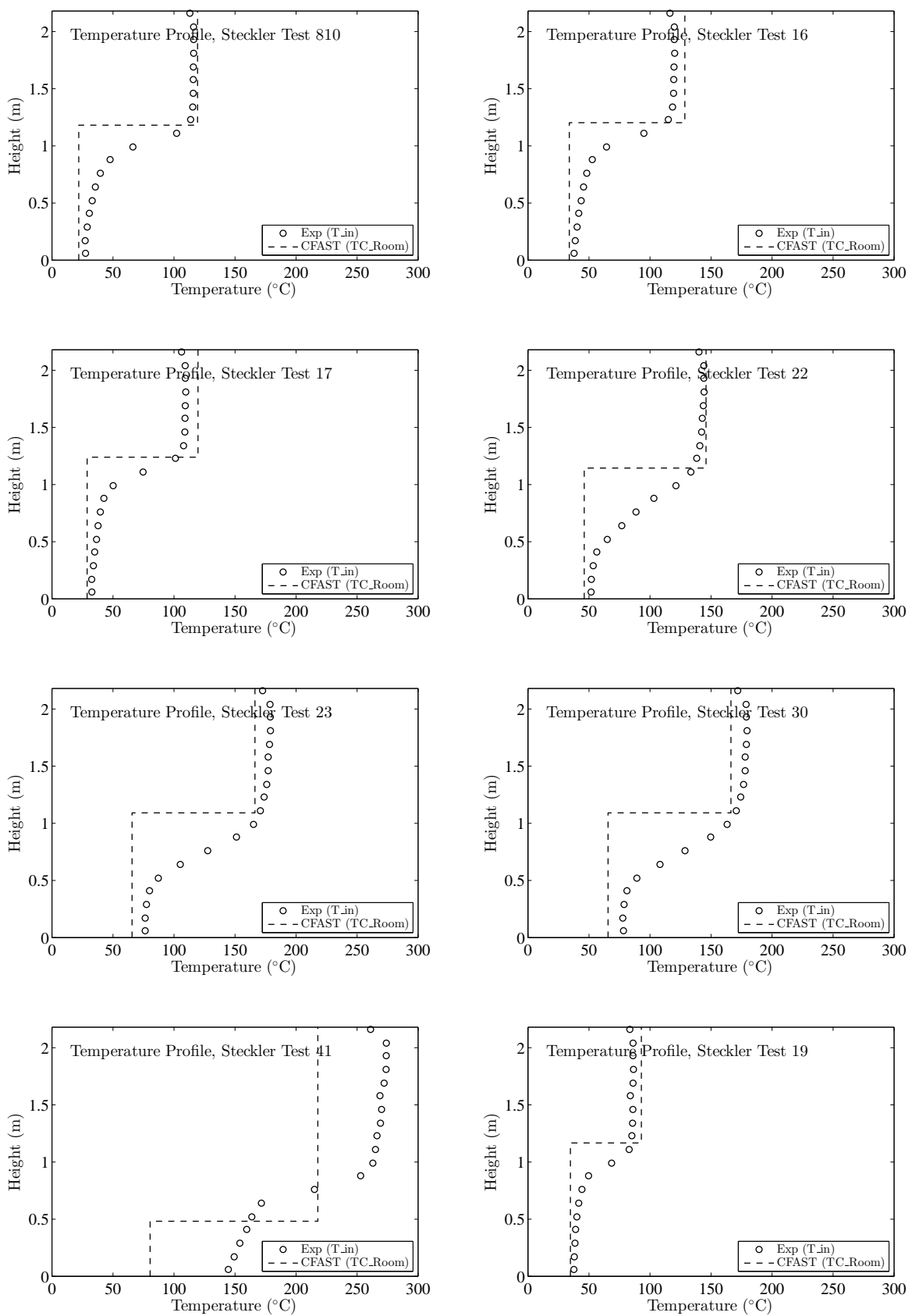


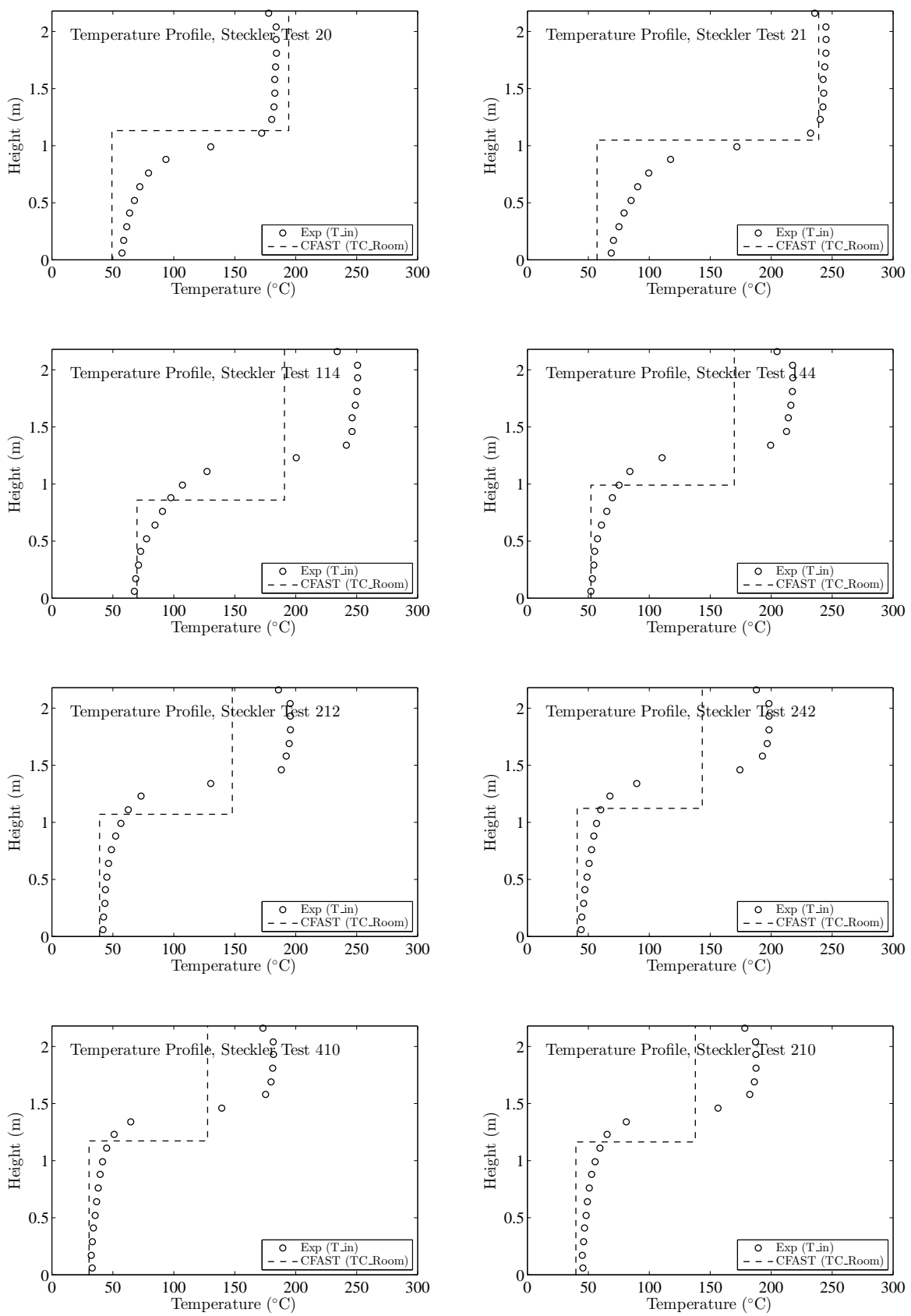
Figure B.93: NIST/NRC Series, Floor Temperature and Heat Flux, Replicate Tests 15 and 18.

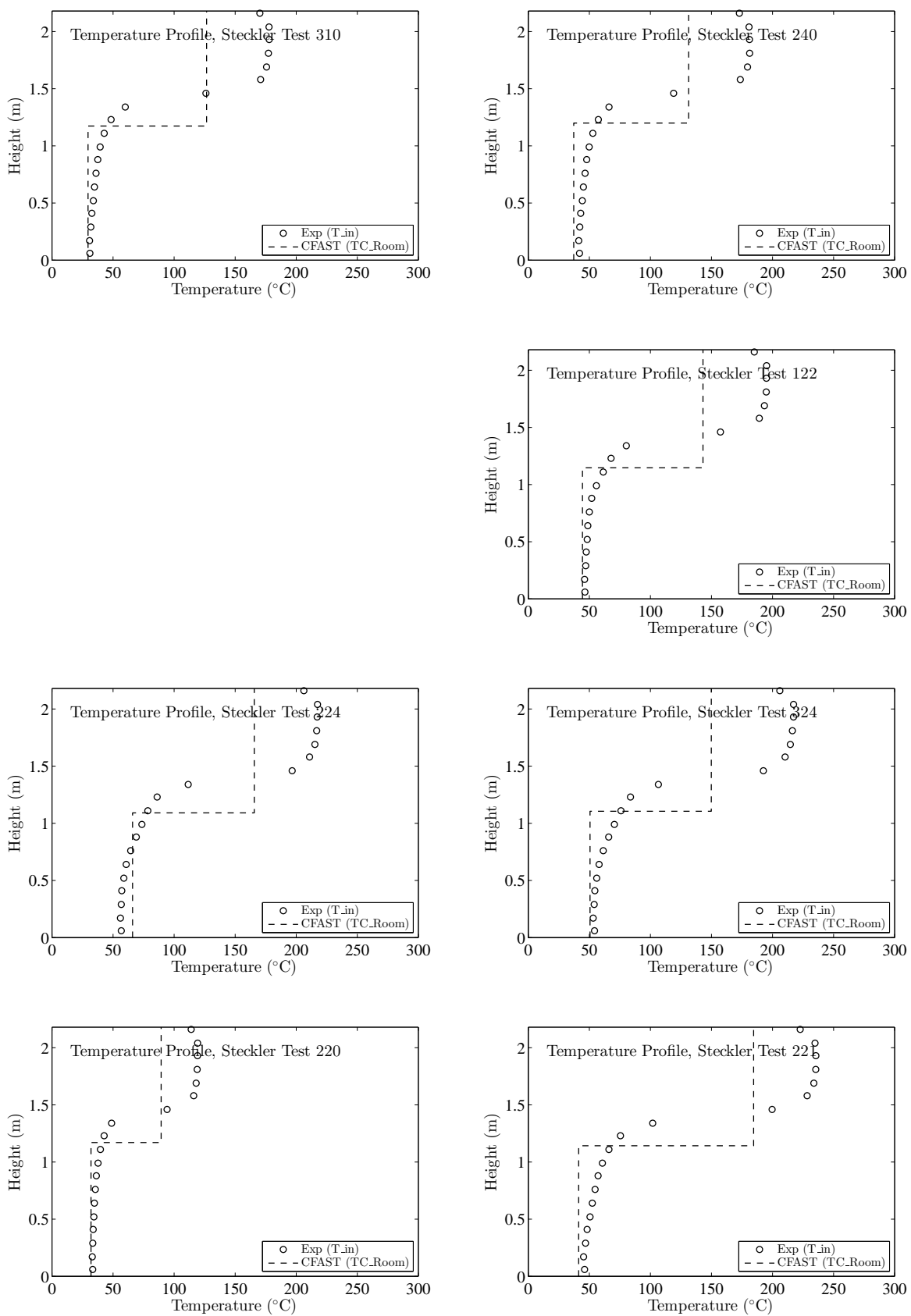
B.10 Steckler Compartment Experiments

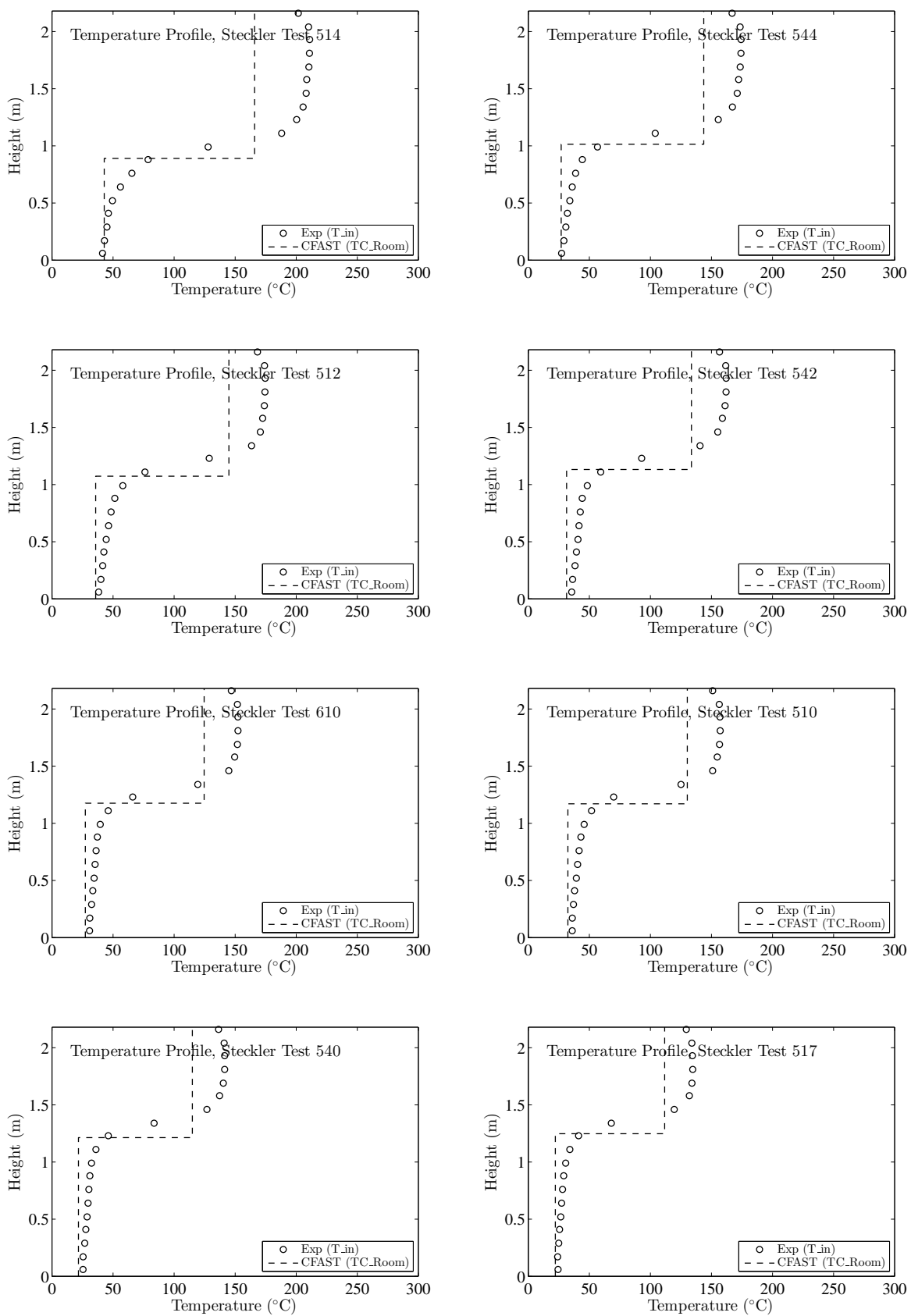
Steckler *et al.* [77] mapped the doorway/window flows in 55 compartment fire experiments. The test matrix is presented in Table 5.5. Shown on the following pages are the temperature profiles inside the compartment compared with model predictions. To quantify the difference between prediction and measurement, the maximum temperatures were compared.

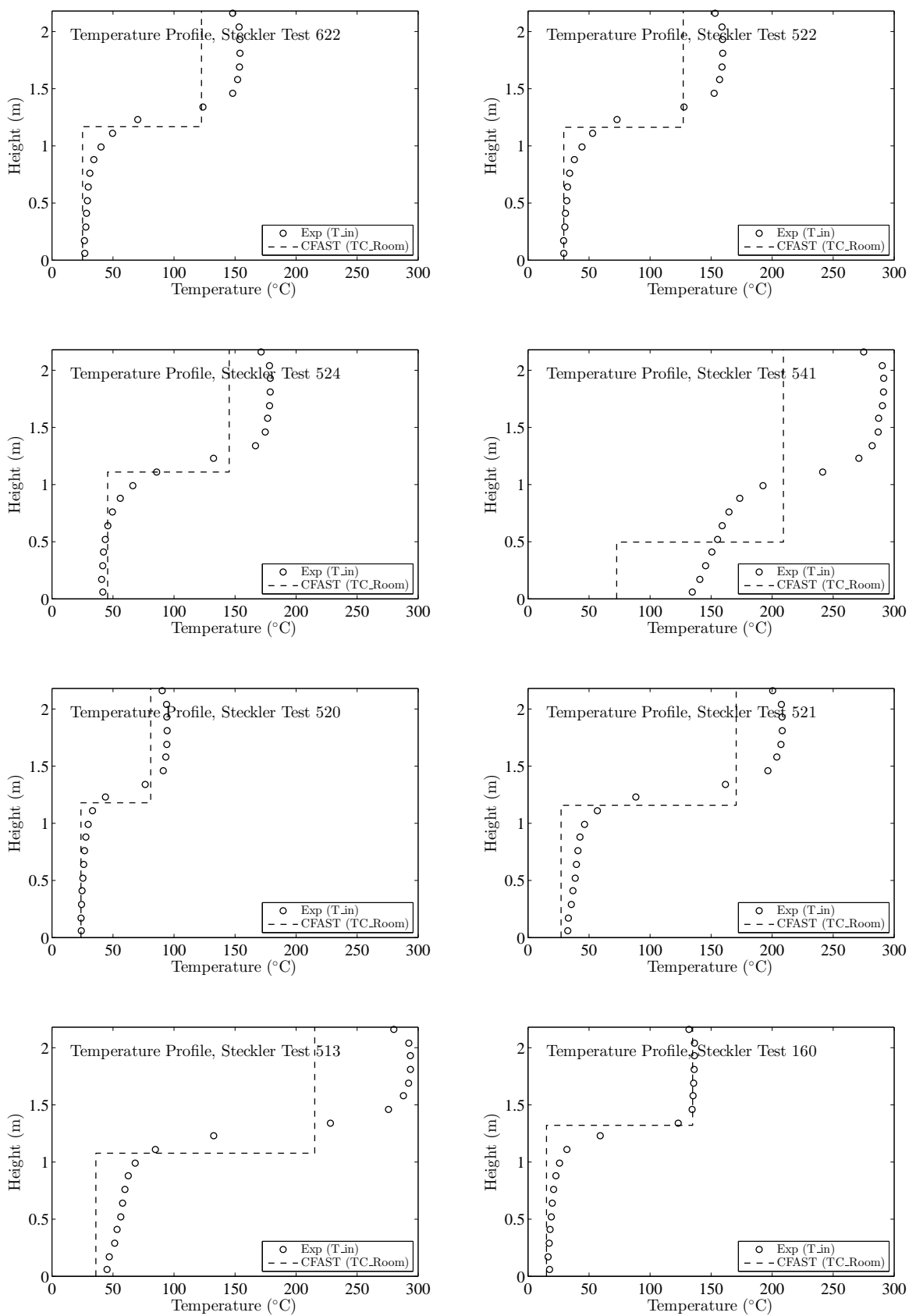


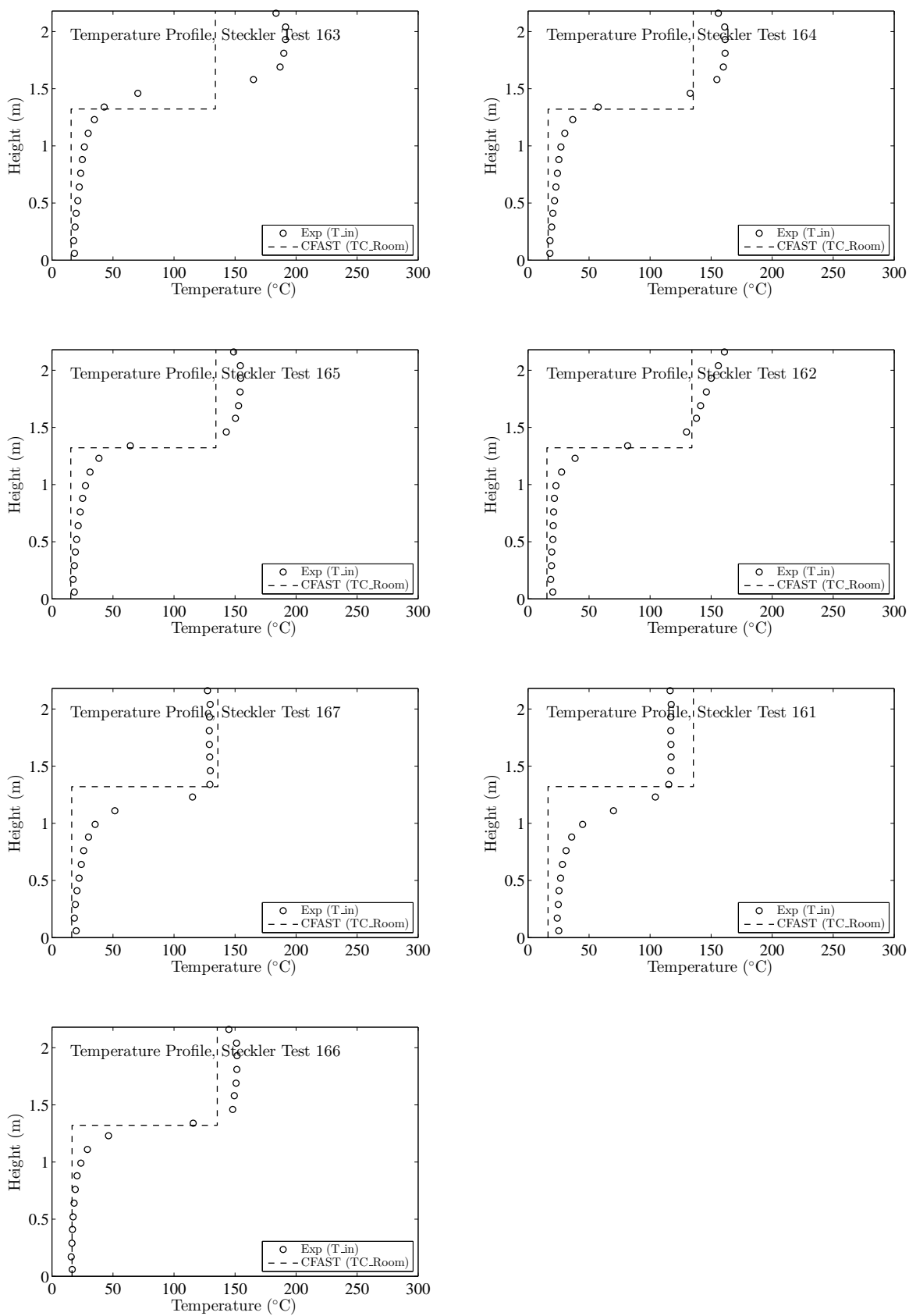






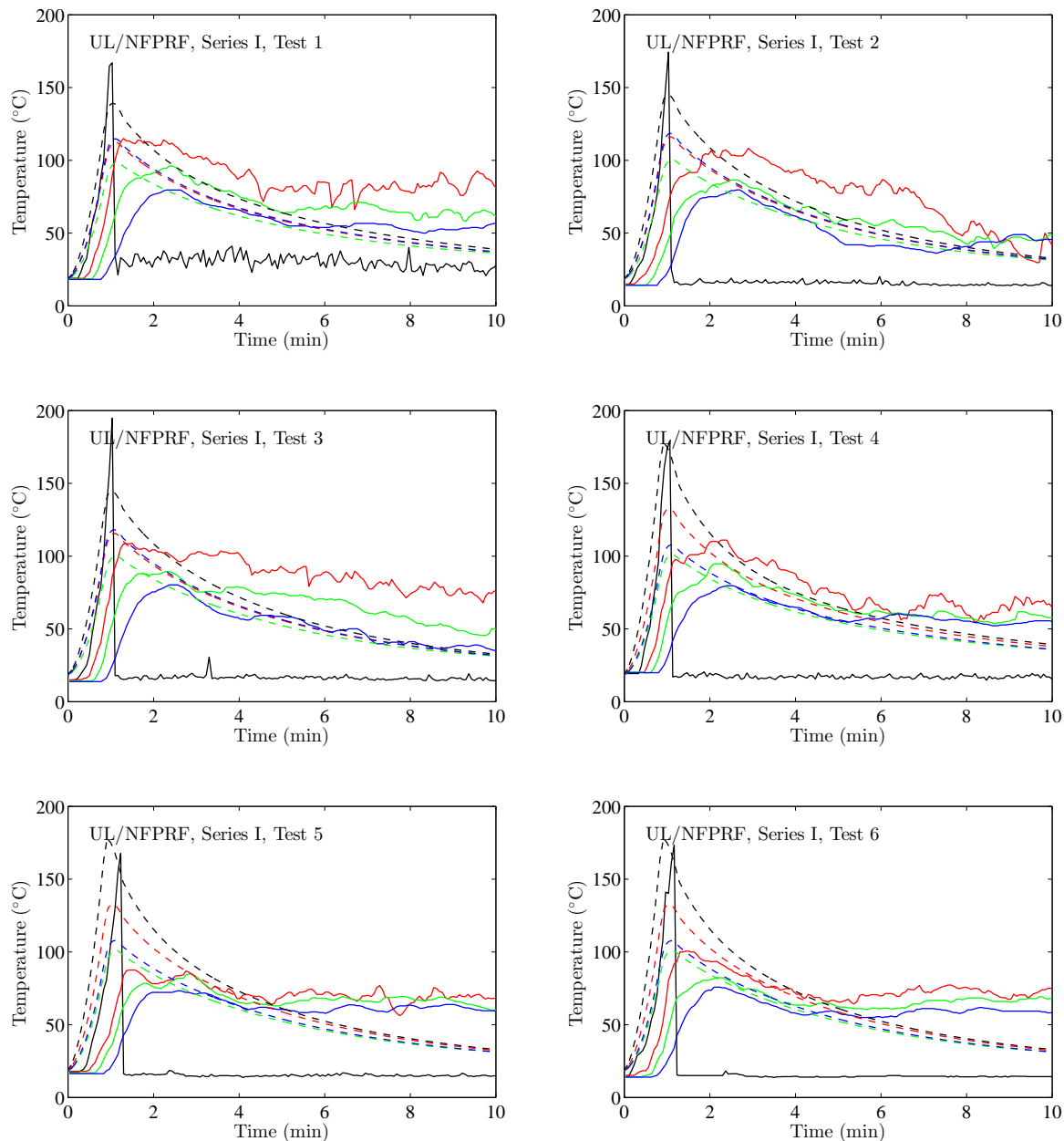


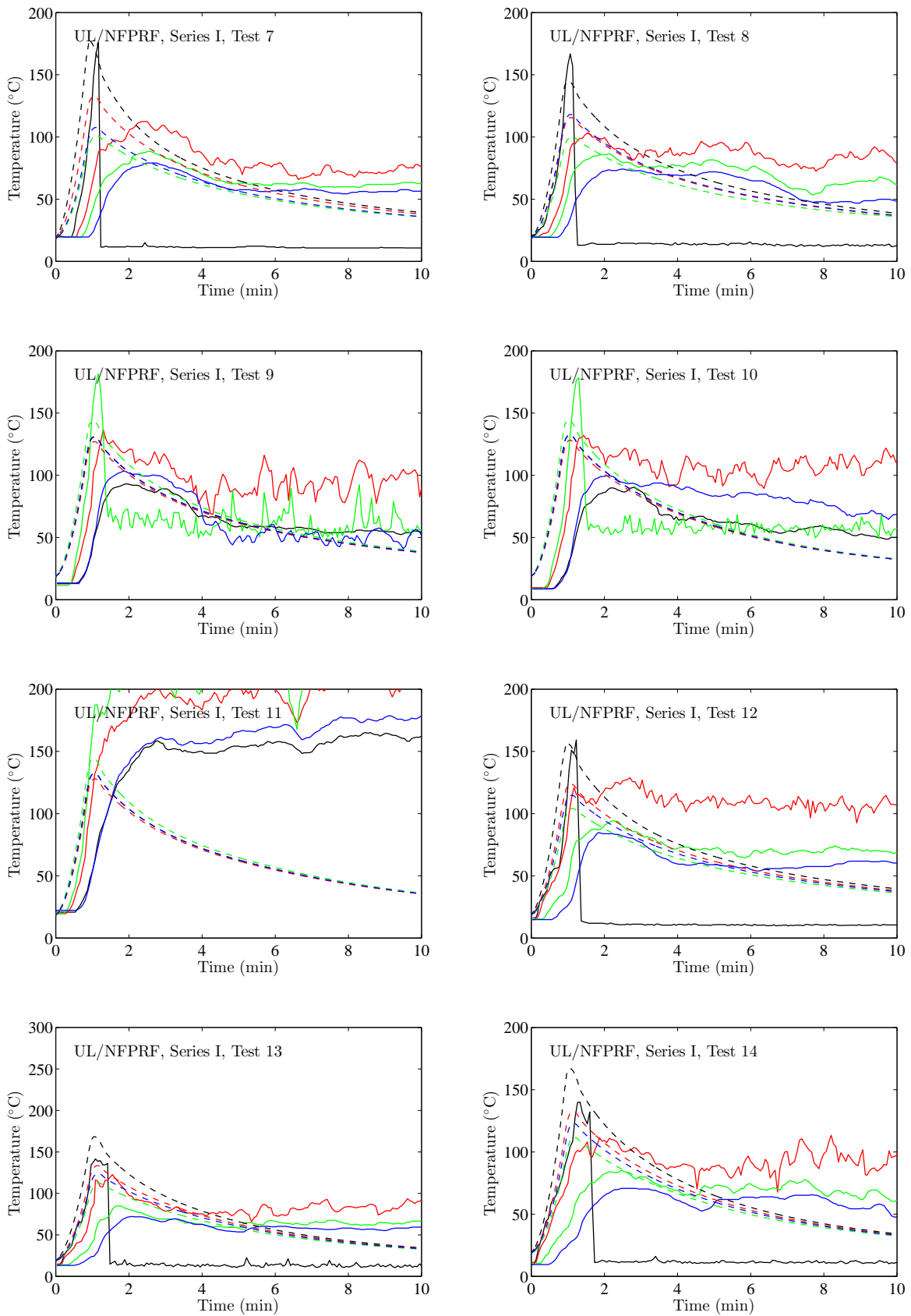


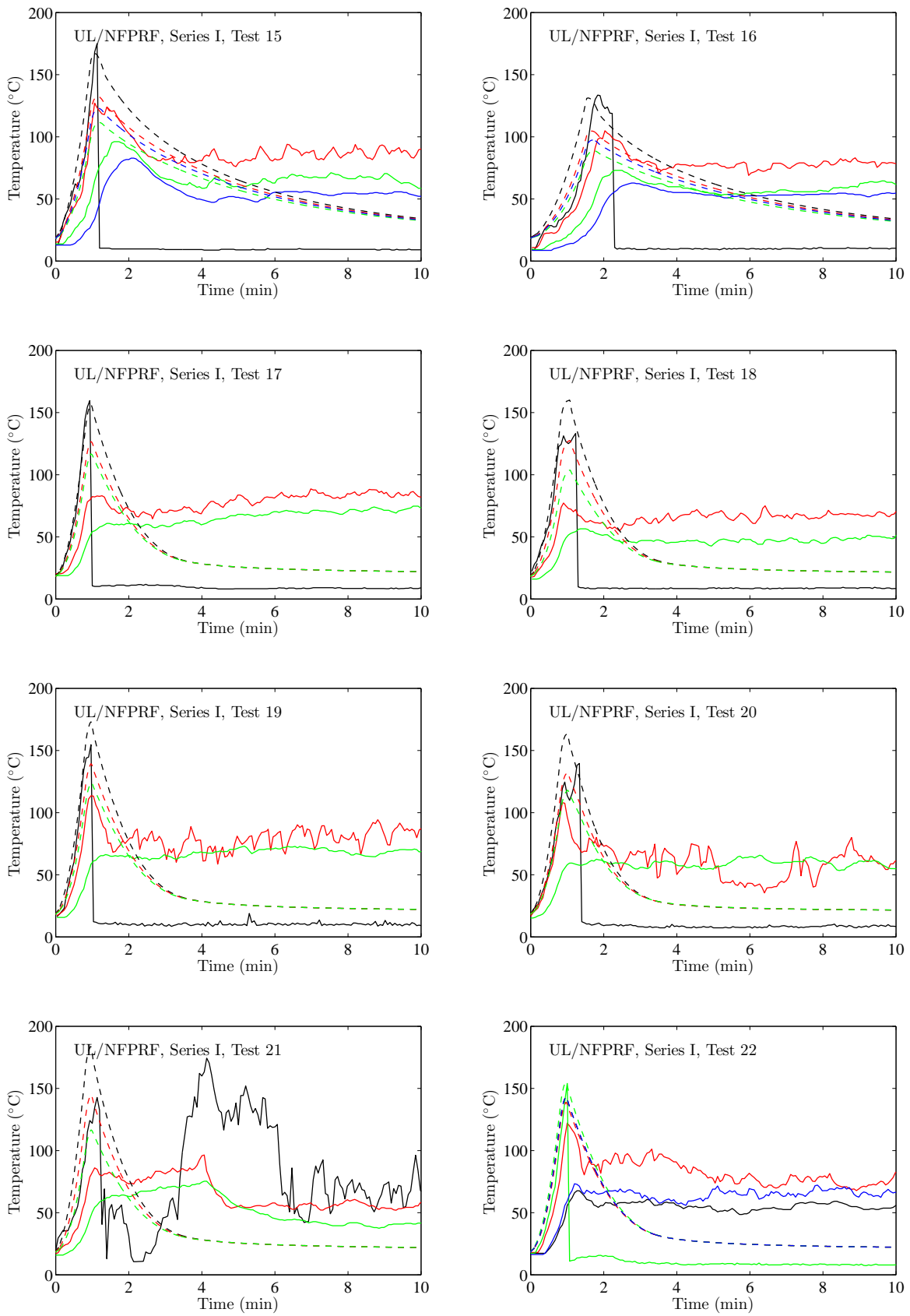


B.11 UL/NFPRF Series I Experiments

The primary purpose of the UL/NFPRF experiments was to measure sprinkler activation times for a series of heptane spray burner fires. To determine activation times, thermocouples were affixed to each sprinkler, and a sudden drop in temperature indicated activation. These same thermocouple temperatures can be compared to ceiling jet temperature predictions. Referring to Fig. 5.21, the chosen measurement locations are 56, 68, 86, and 98, providing comparisons as close to, and as far away from, the fire as possible.

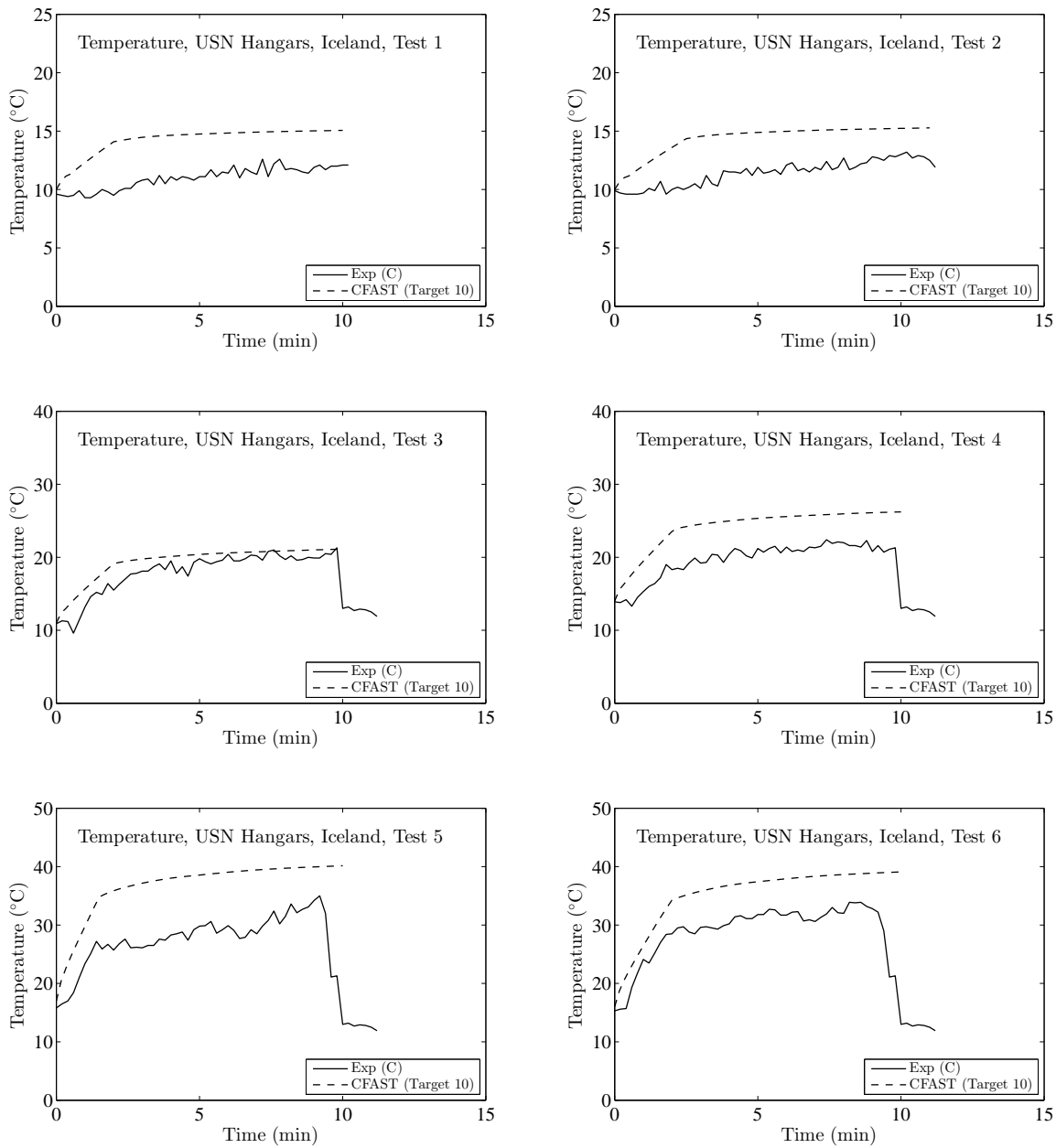


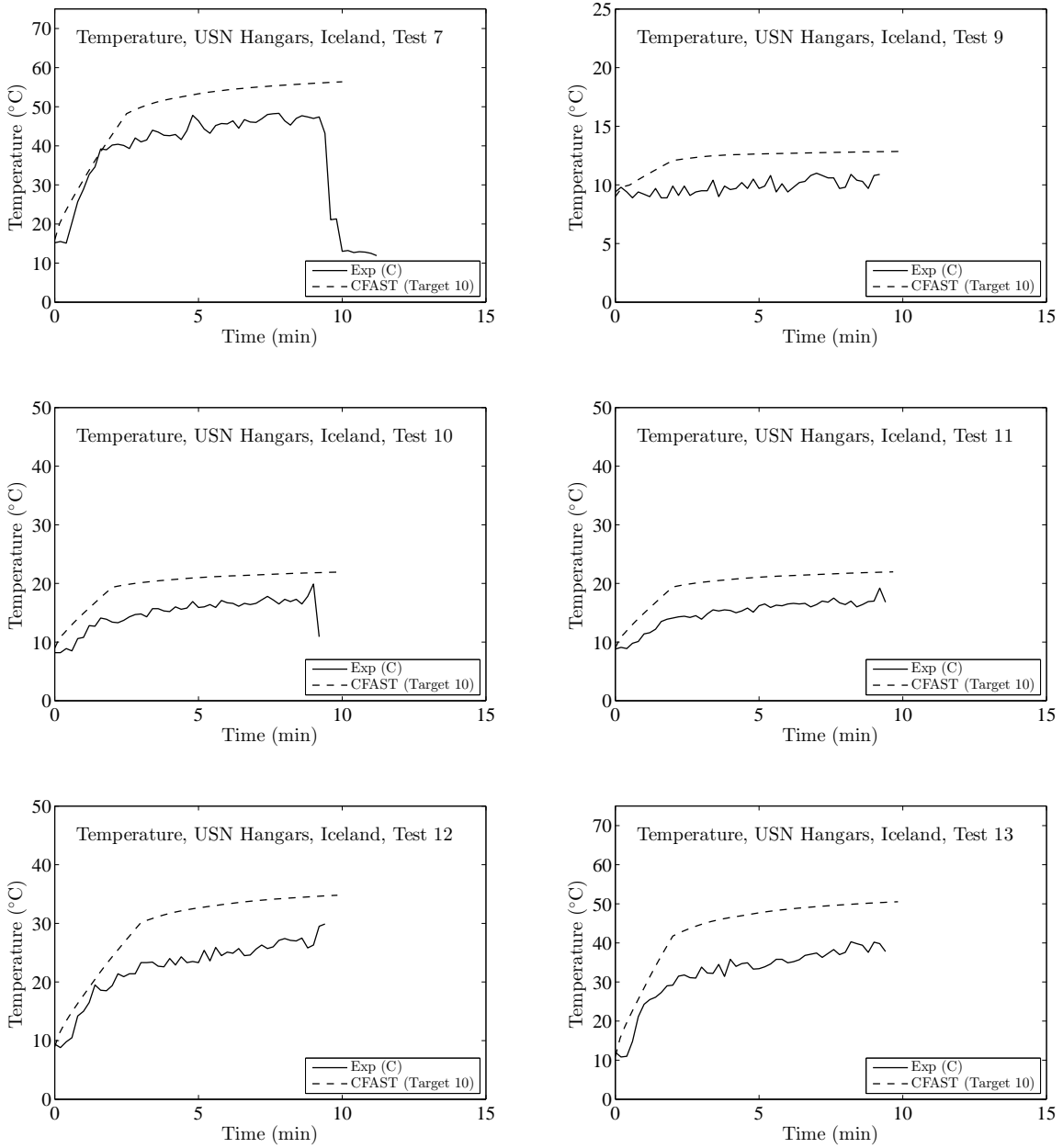


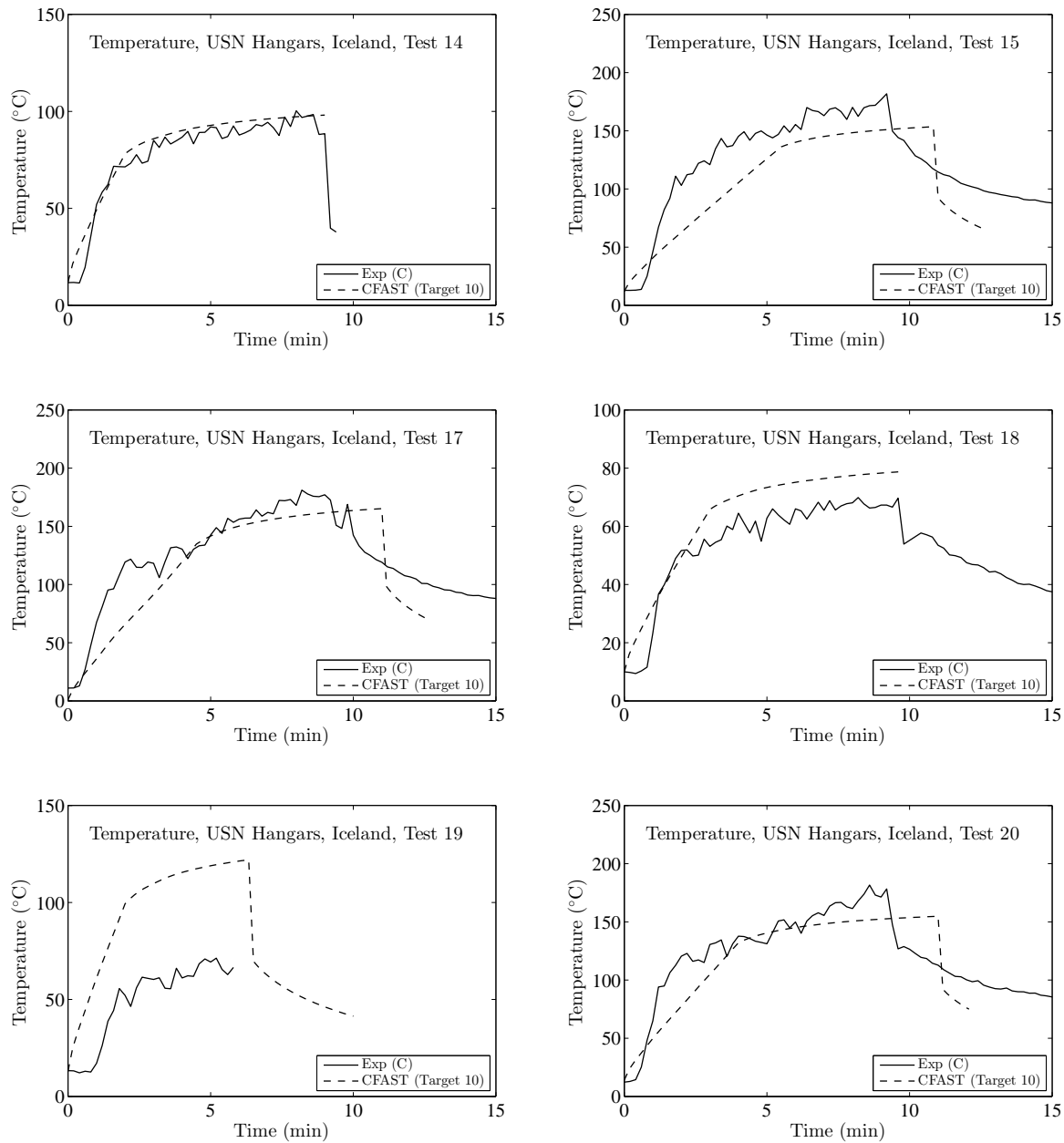


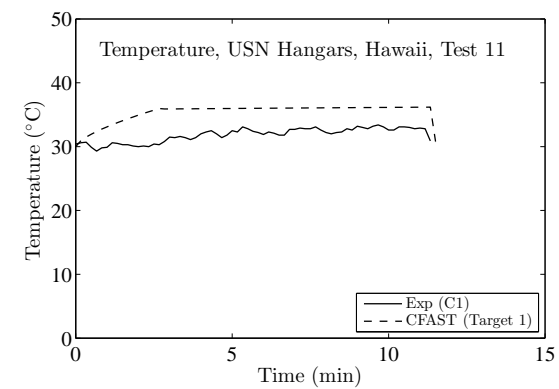
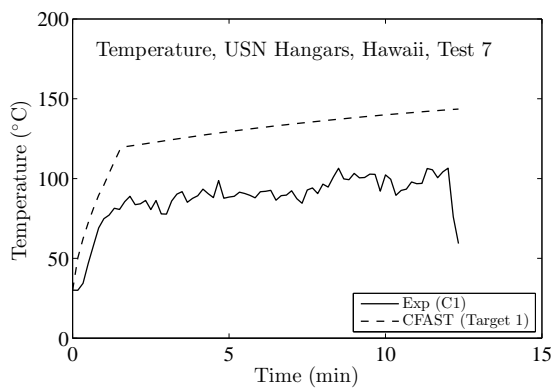
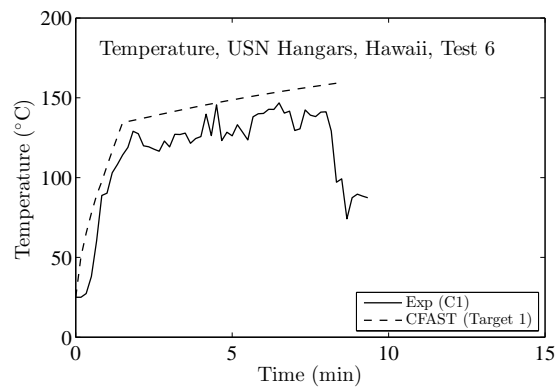
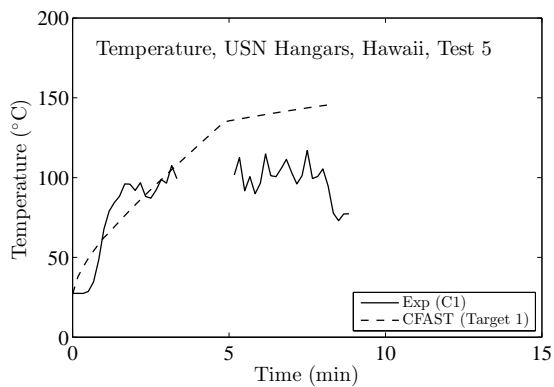
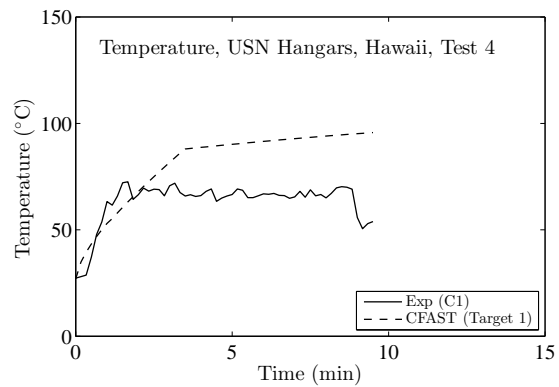
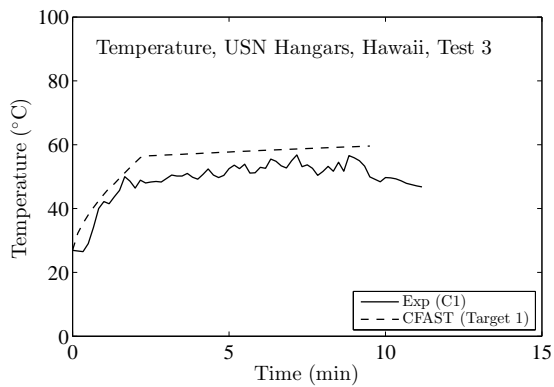
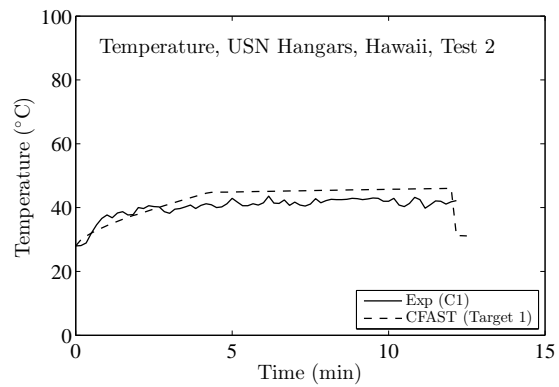
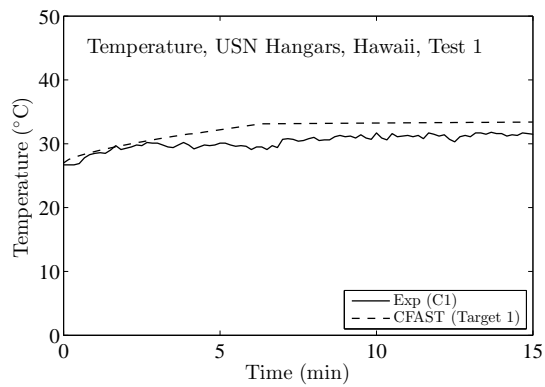
B.12 USN High Bay Hangar Experiments

A large number of plume temperature measurements are available from the US Navy experiments conducted at Keflavik, Iceland, and Barber's Point, Hawaii. The hangars were very large in size (22 m high in Iceland and 15 m high in Hawaii) and the heat release rates varied from 100 kW to 33 MW. All experiments made use of a fuel pan filled with either JP-5 or JP-8 jet fuel, positioned in the center of the hangar.



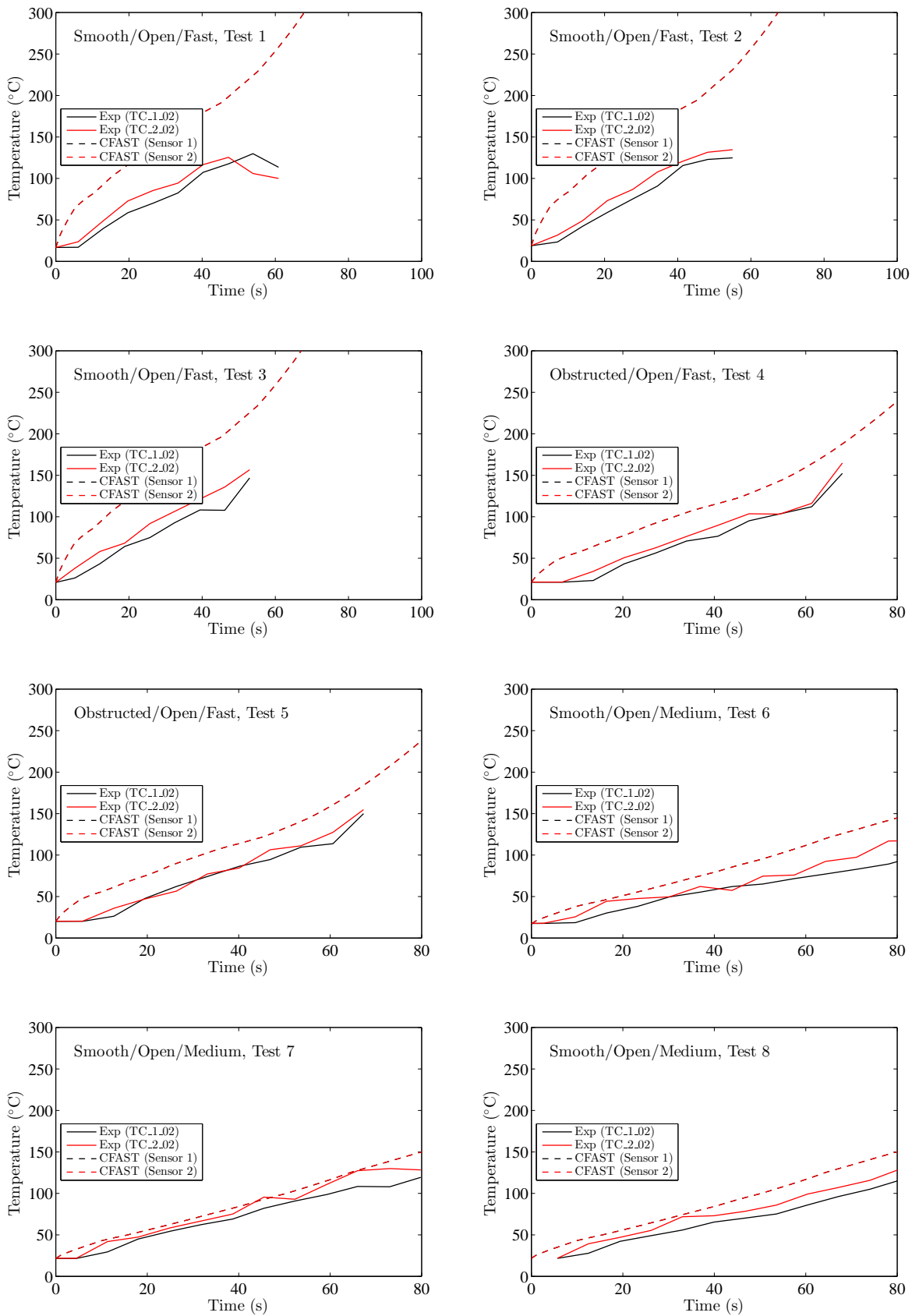


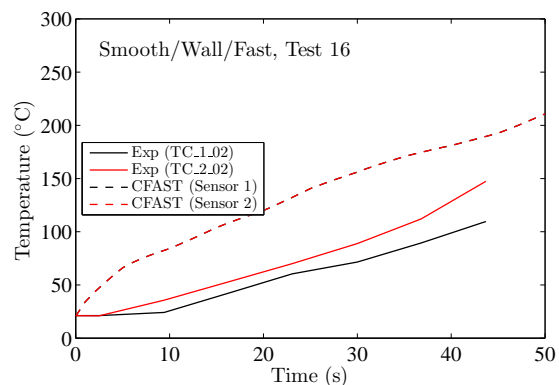
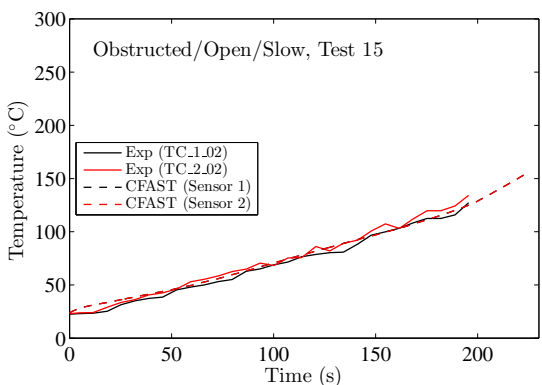
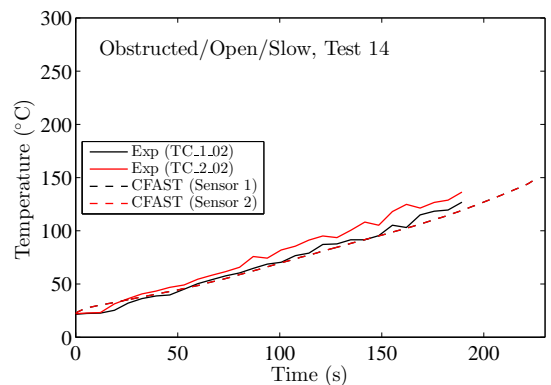
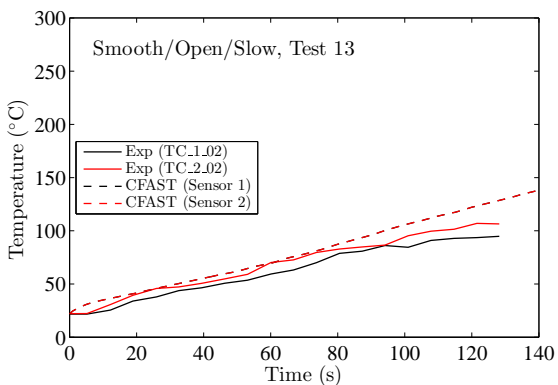
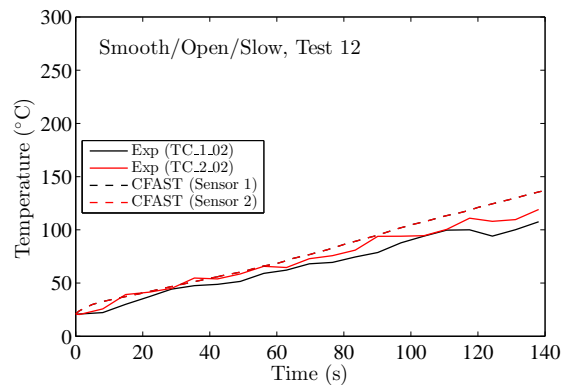
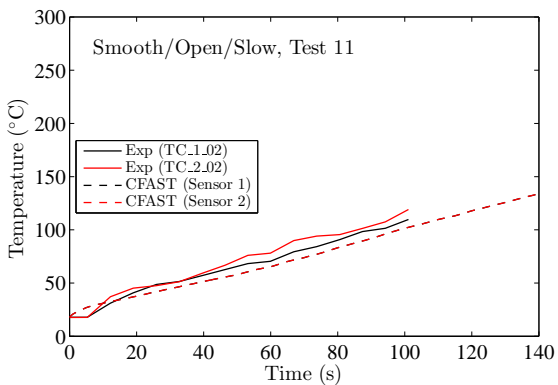
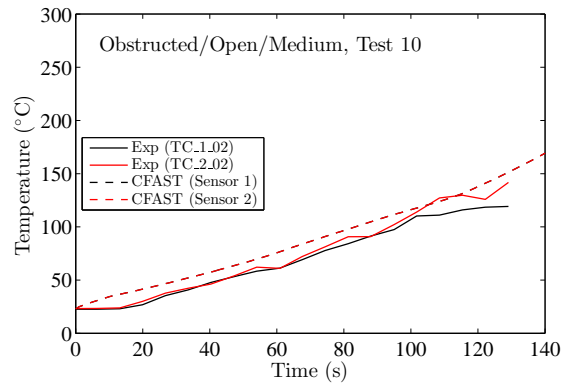
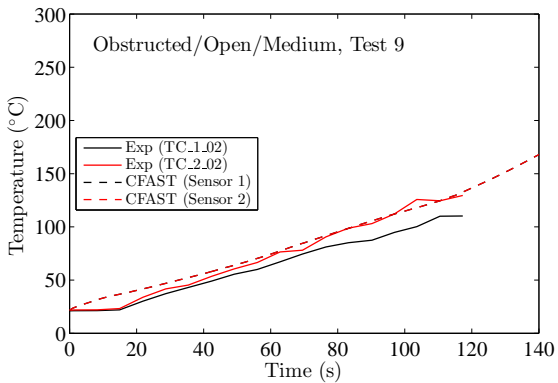


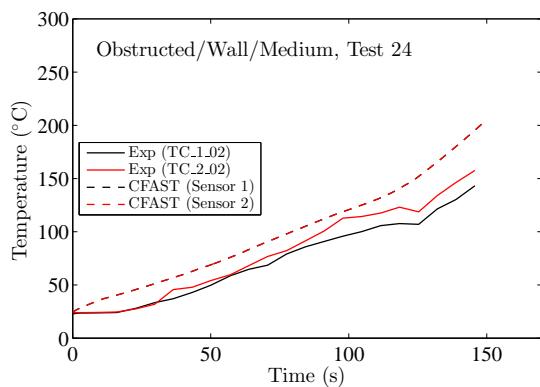
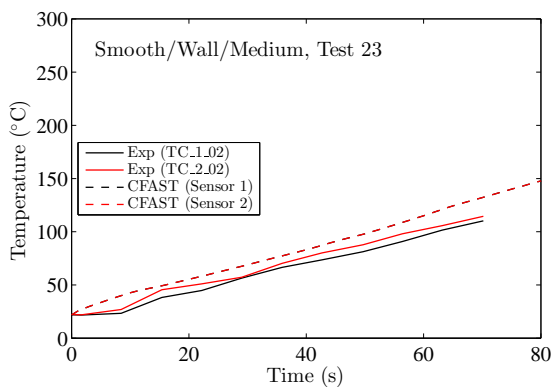
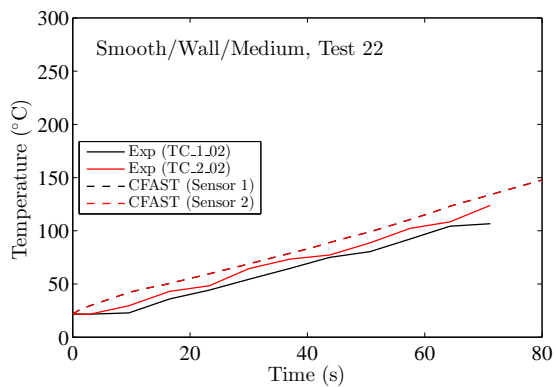
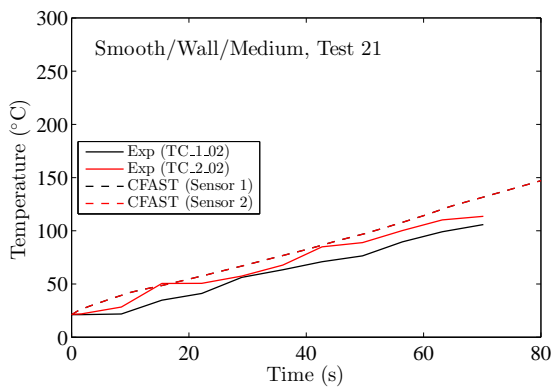
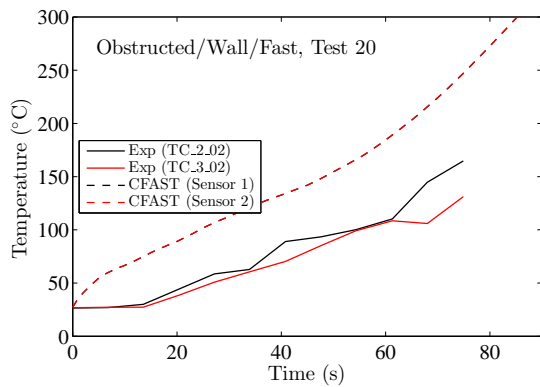
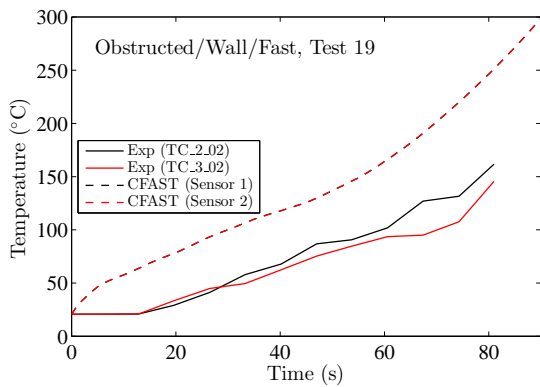
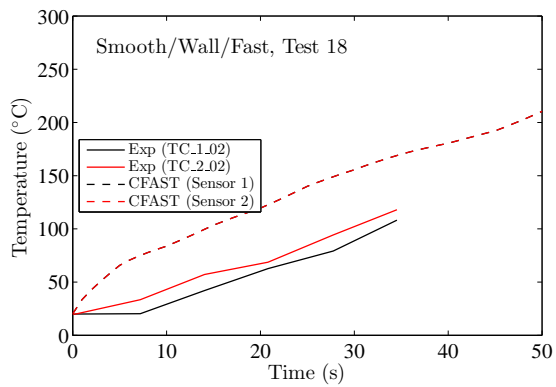
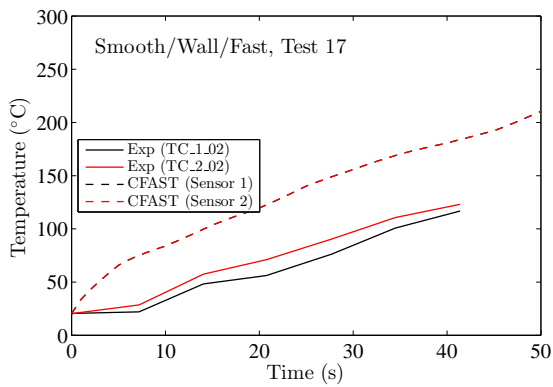


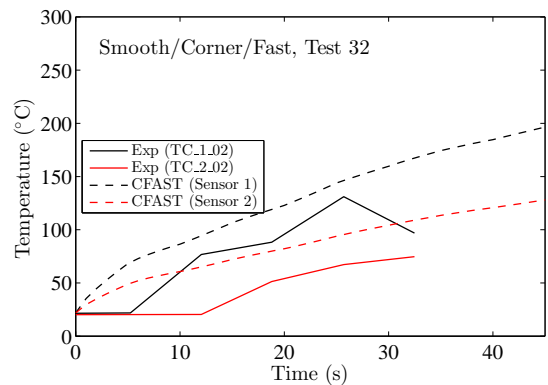
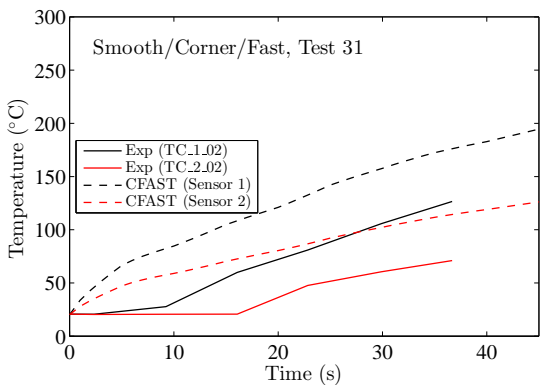
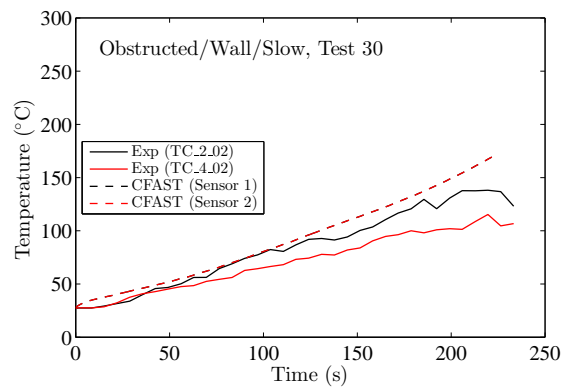
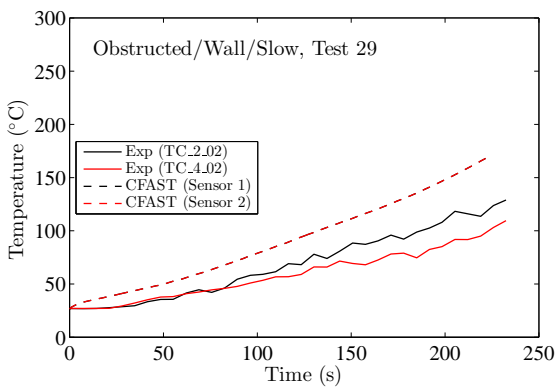
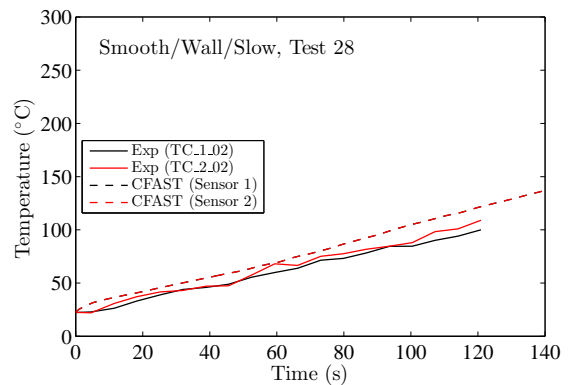
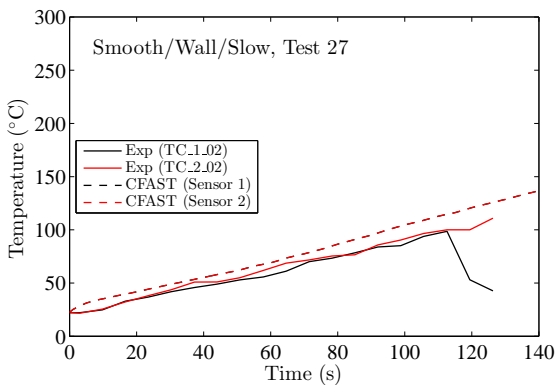
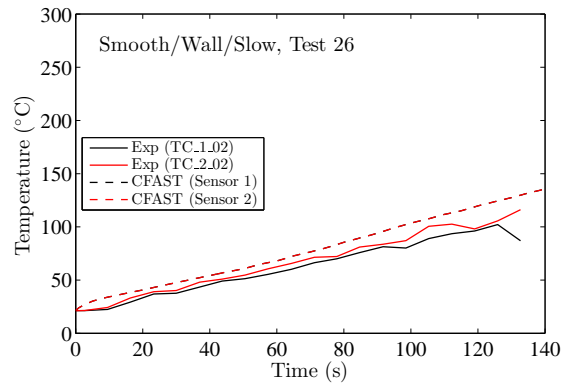
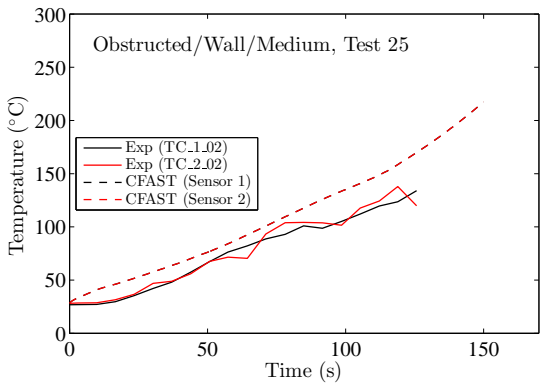
B.13 Vettori Flat Ceiling Experiments

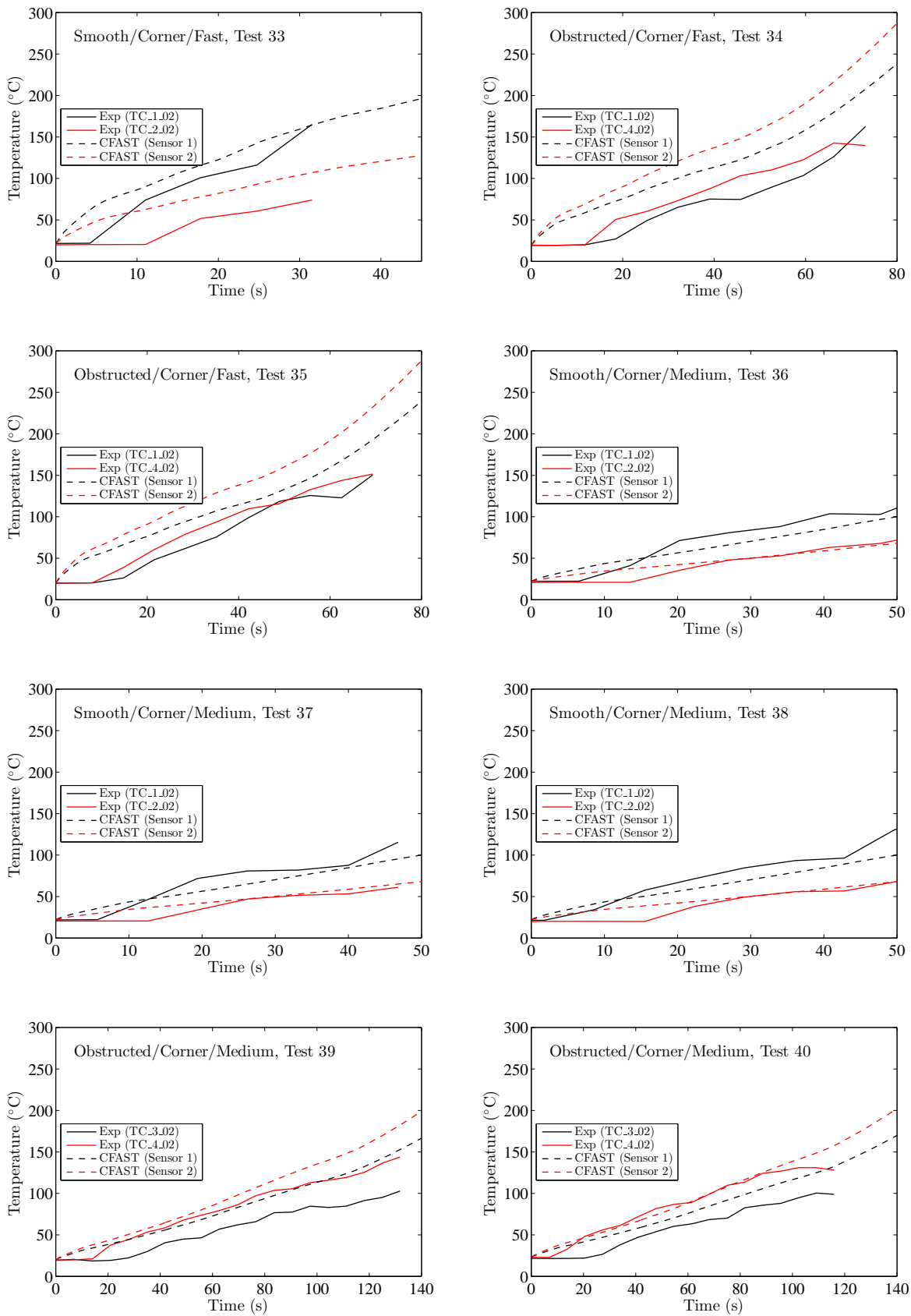
For these experiments, the measured and predicted thermocouple temperature at the location of the first two activating sprinklers are compared. The experiments consisted of either Smooth or Obstructed ceilings; Slow, Medium or Fast fires; and a burner in the Open, at the Wall, or in the Corner. The experiments included three replicates of each of the smooth ceiling configurations and two replicates of each of the obstructed ceiling configurations.

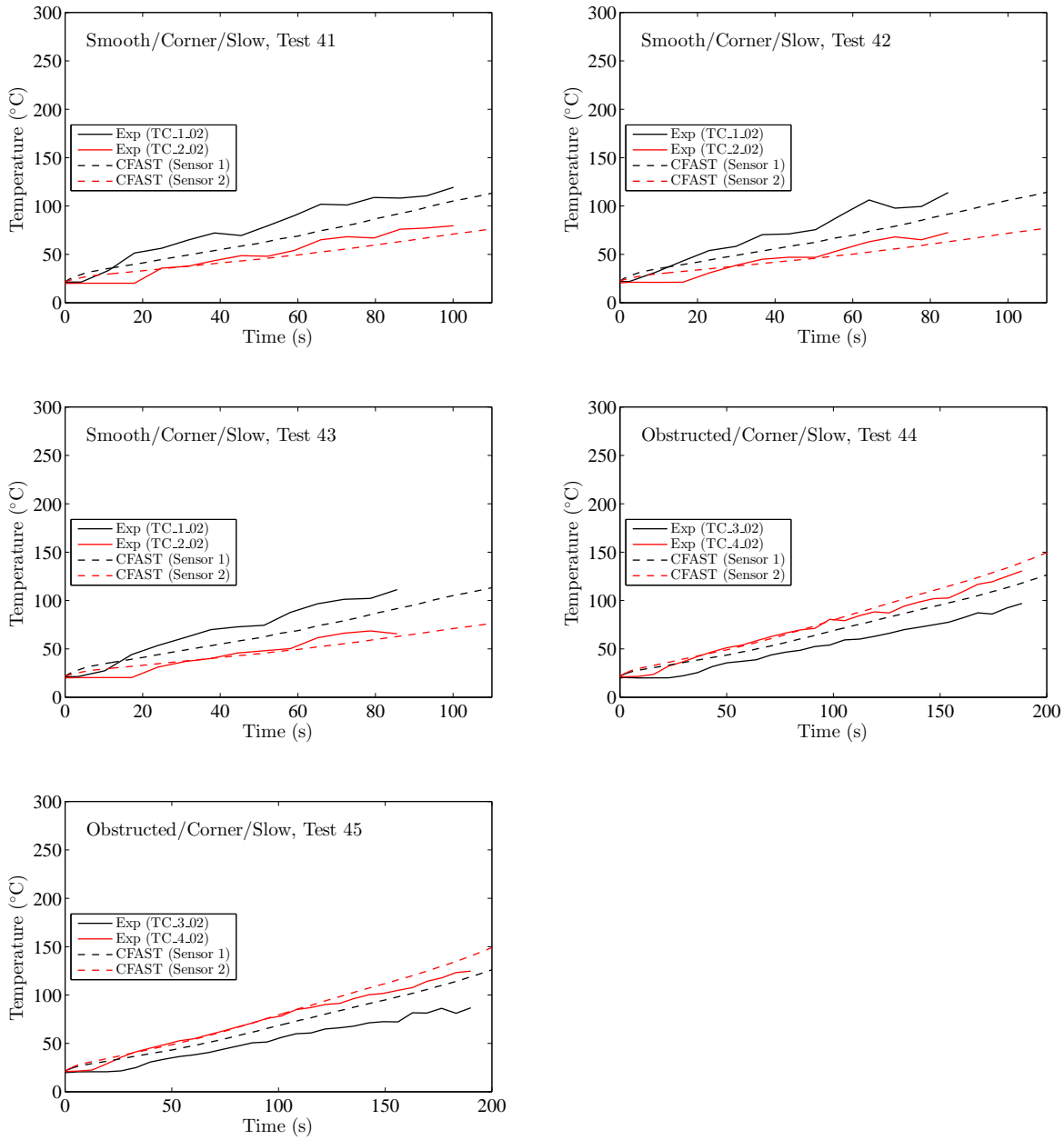












B.14 VTT Large Hall Tests

The experiments are described in reference [82]. The series consisted three unique fire scenarios with replications for a total of 8 experiments. The experiments were undertaken to study the movement of smoke in a large hall with a sloped ceiling. The tests were conducted inside the VTT Fire Test Hall, with dimensions of 19 m high by 27 m long by 14 m wide. Each test involved a single heptane pool fire, ranging from 2 MW to 4 MW.

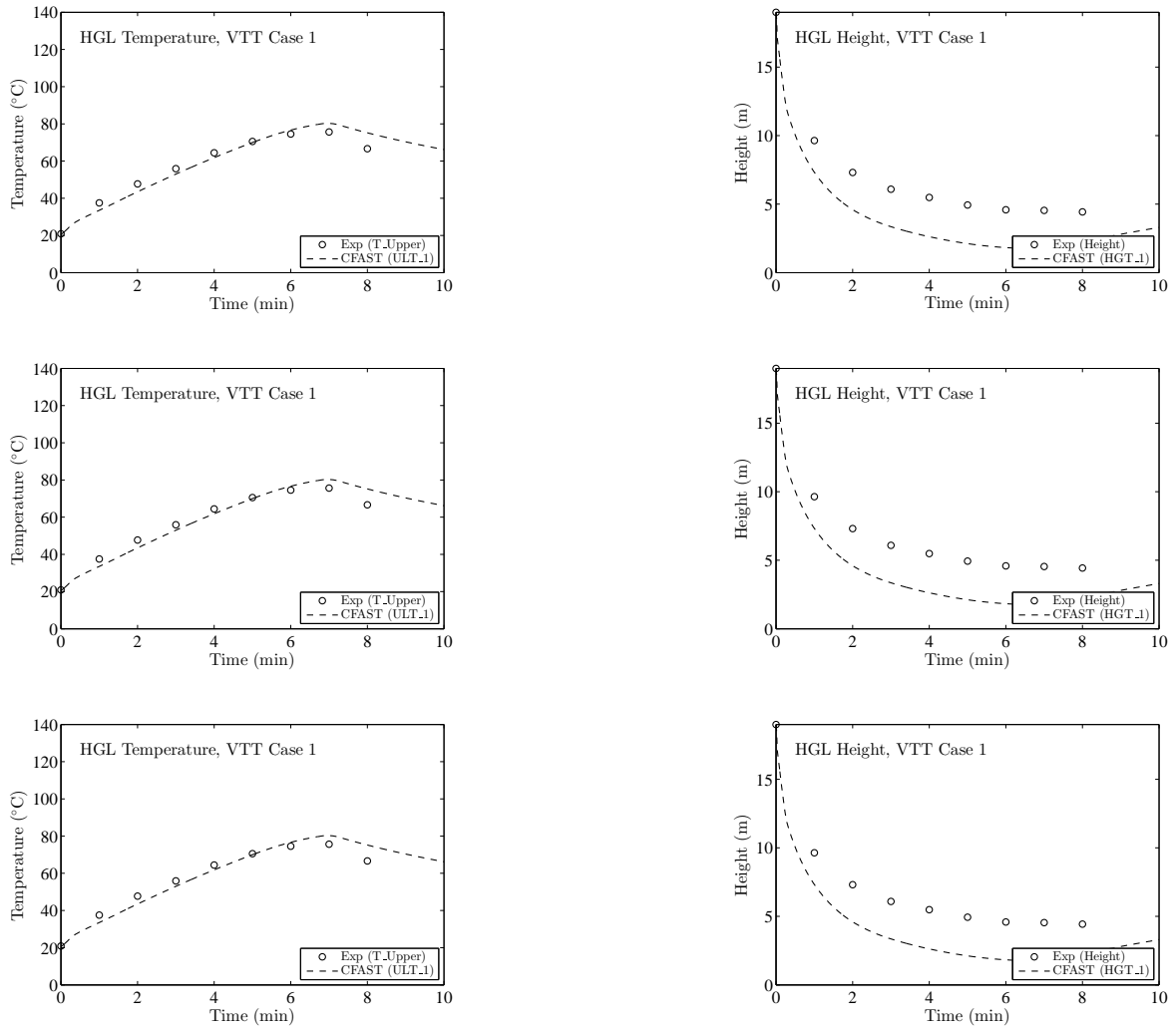


Figure B.94: Predicted HGL Temperature and Height for the VTT Large Hall Tests.

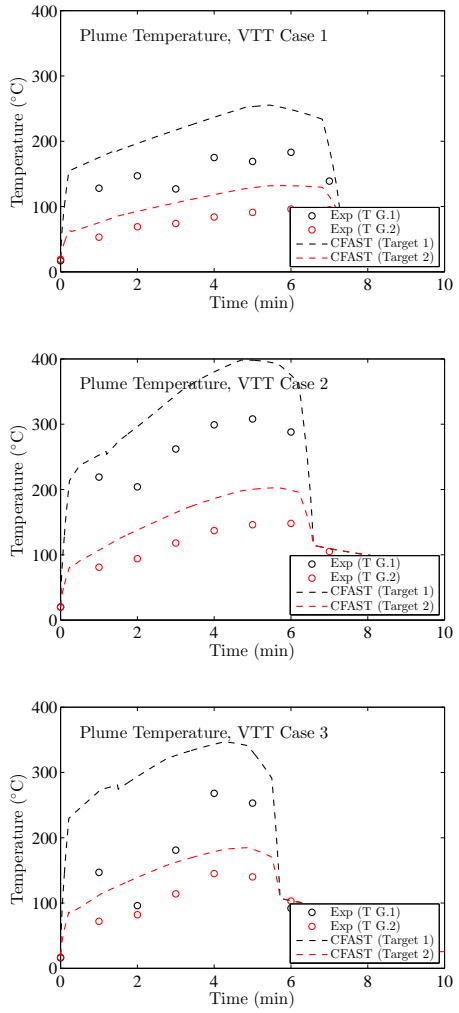
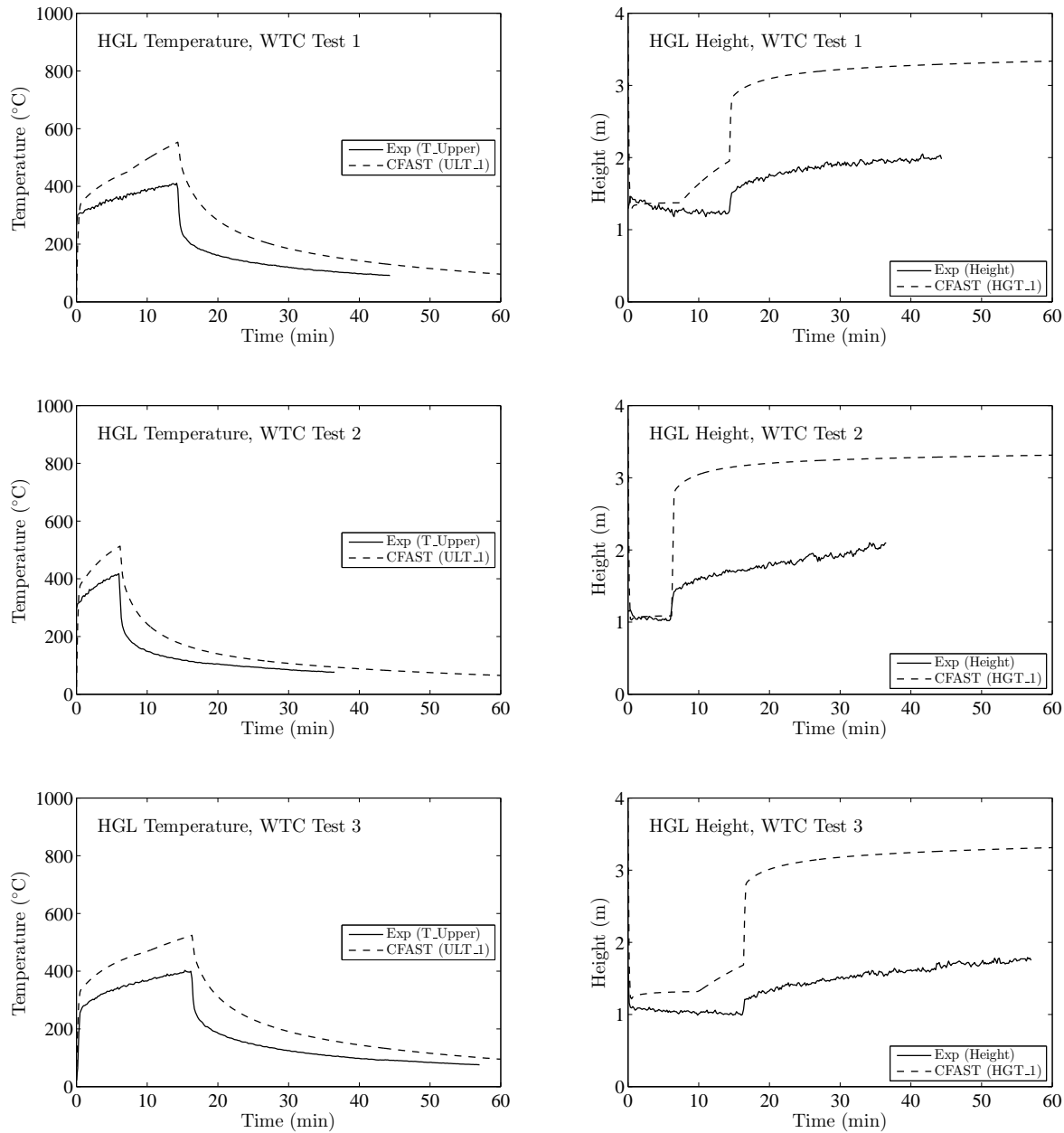
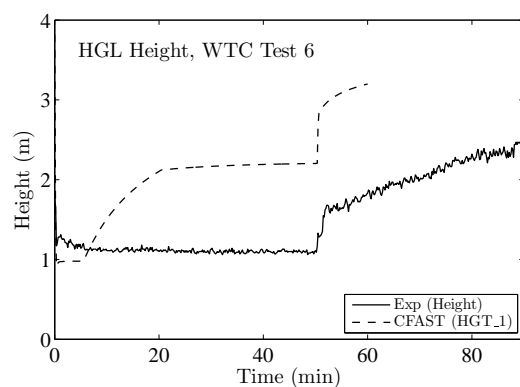
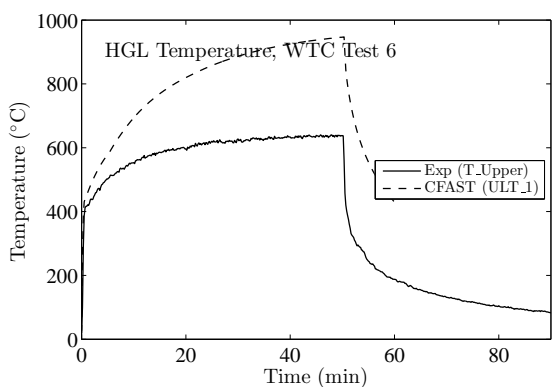
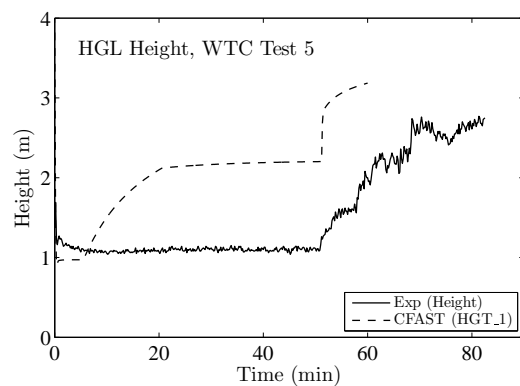
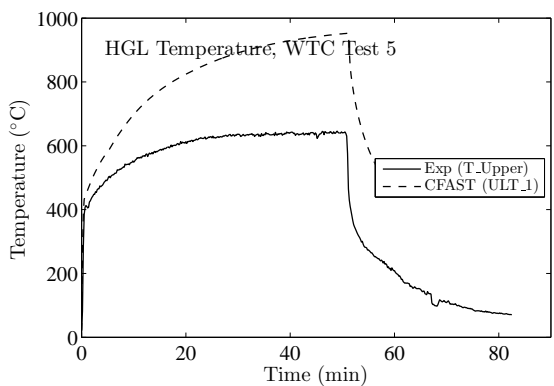
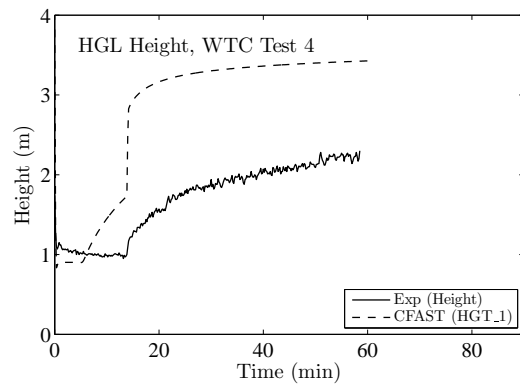
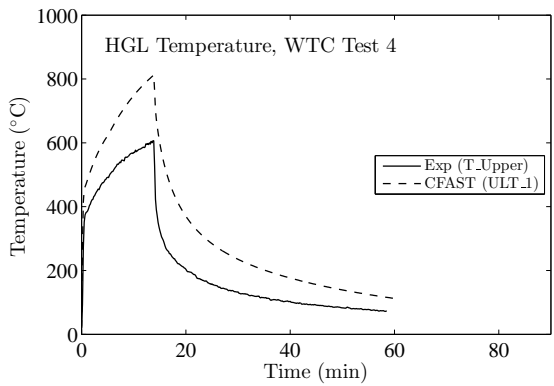


Figure B.95: Predicted Plume Centerline Temperature for the VTT Large Hall Tests.

B.15 WTC Test Series

The HGL temperature and height for the WTC experiments were calculated from two TC trees, one that was approximately 3 m to the west and one 2 m to the east of the fire pan (see Fig. 5.28). Each tree consisted of 15 thermocouples, the highest point being 5 cm below the ceiling.

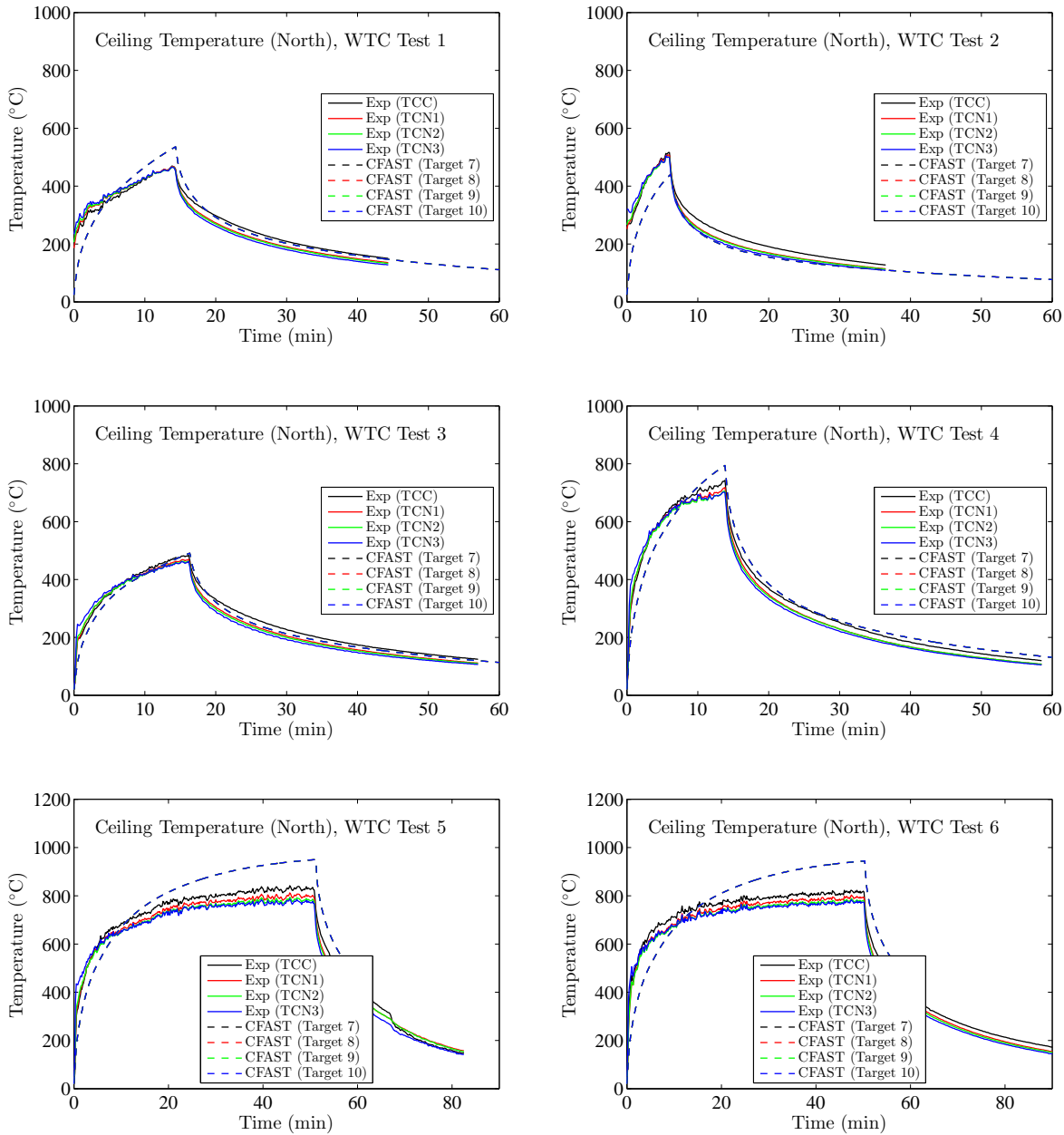


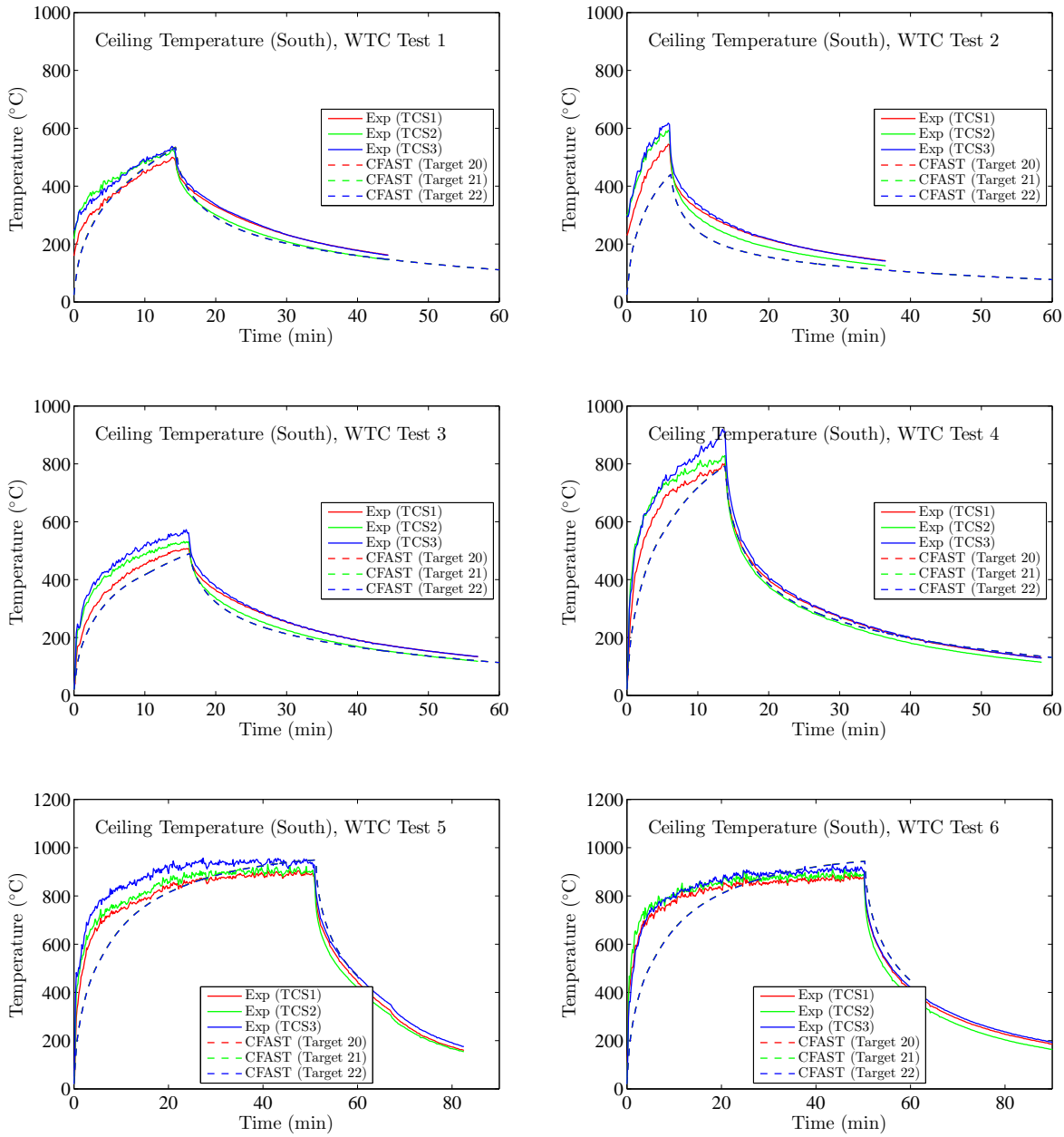


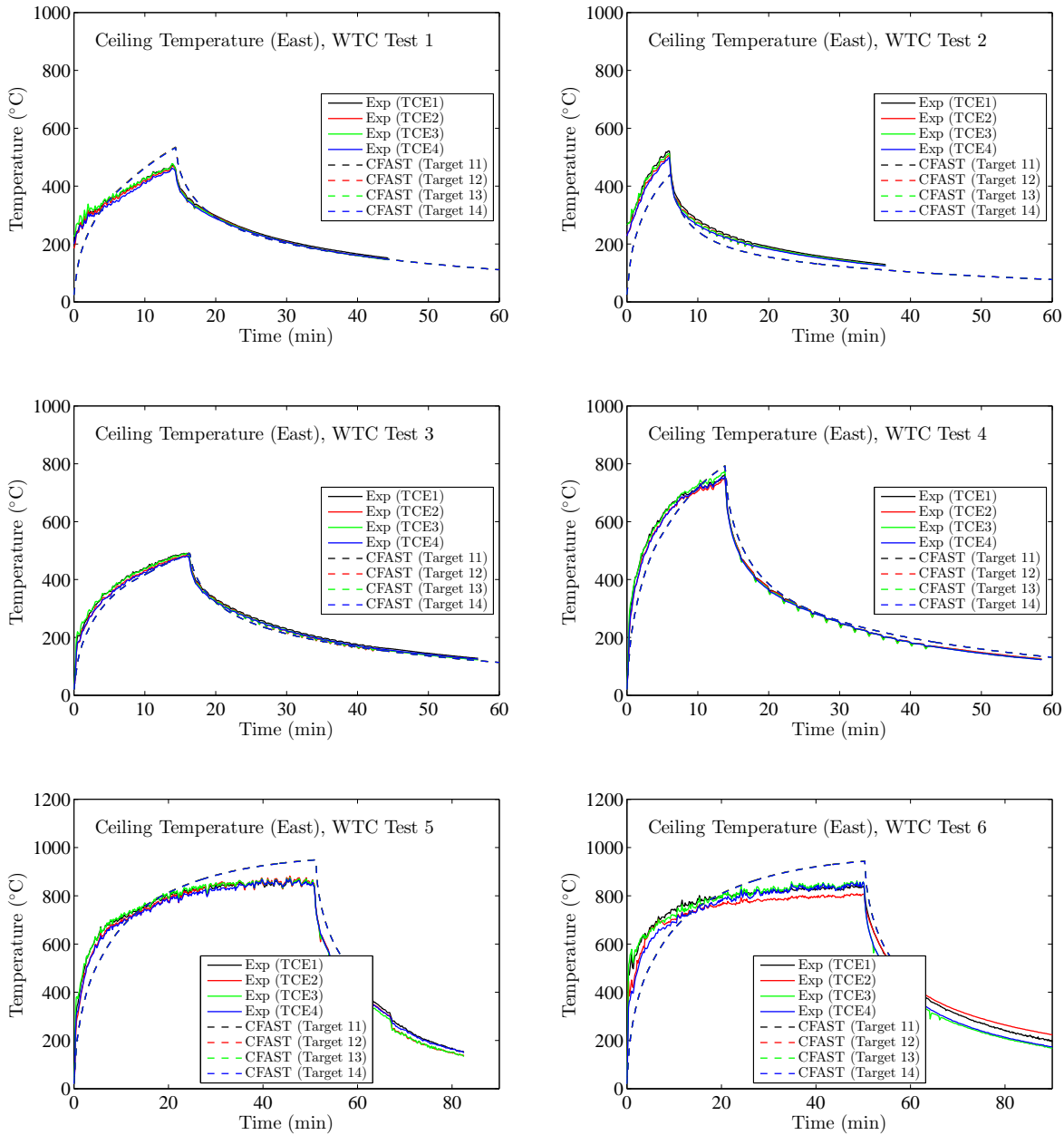
The following pages contain comparisons of predicted and measured ceiling temperatures, both at the surface and beneath a layer of marinite board. Table B.1 below lists the coordinates of the measurement locations relative to the center of the fire pan. Names with “IN” appended are measurements made under the marinite board.

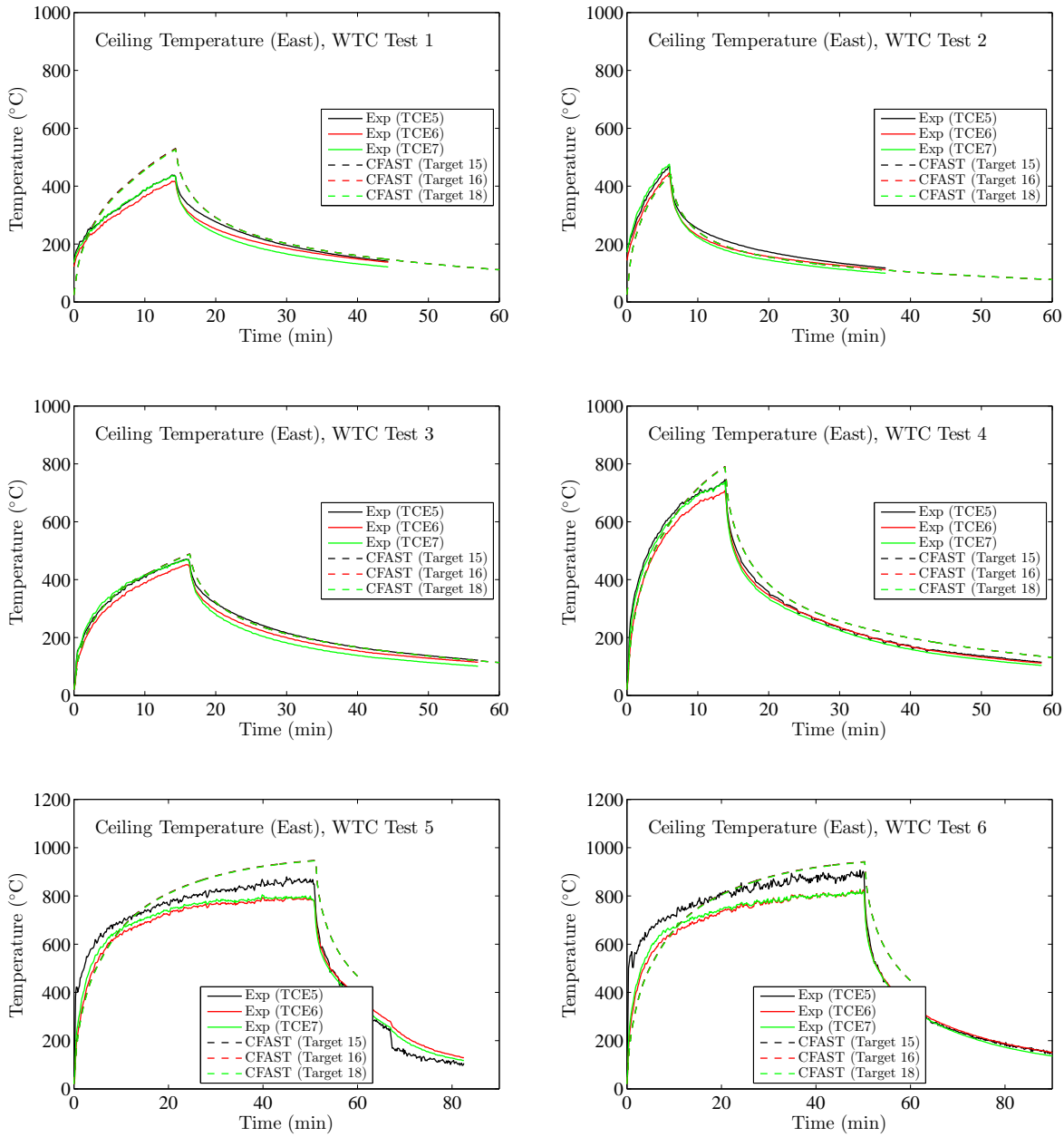
Table B.1: Locations of ceiling surface temperature measurements relative to the fire pan in the WTC series.

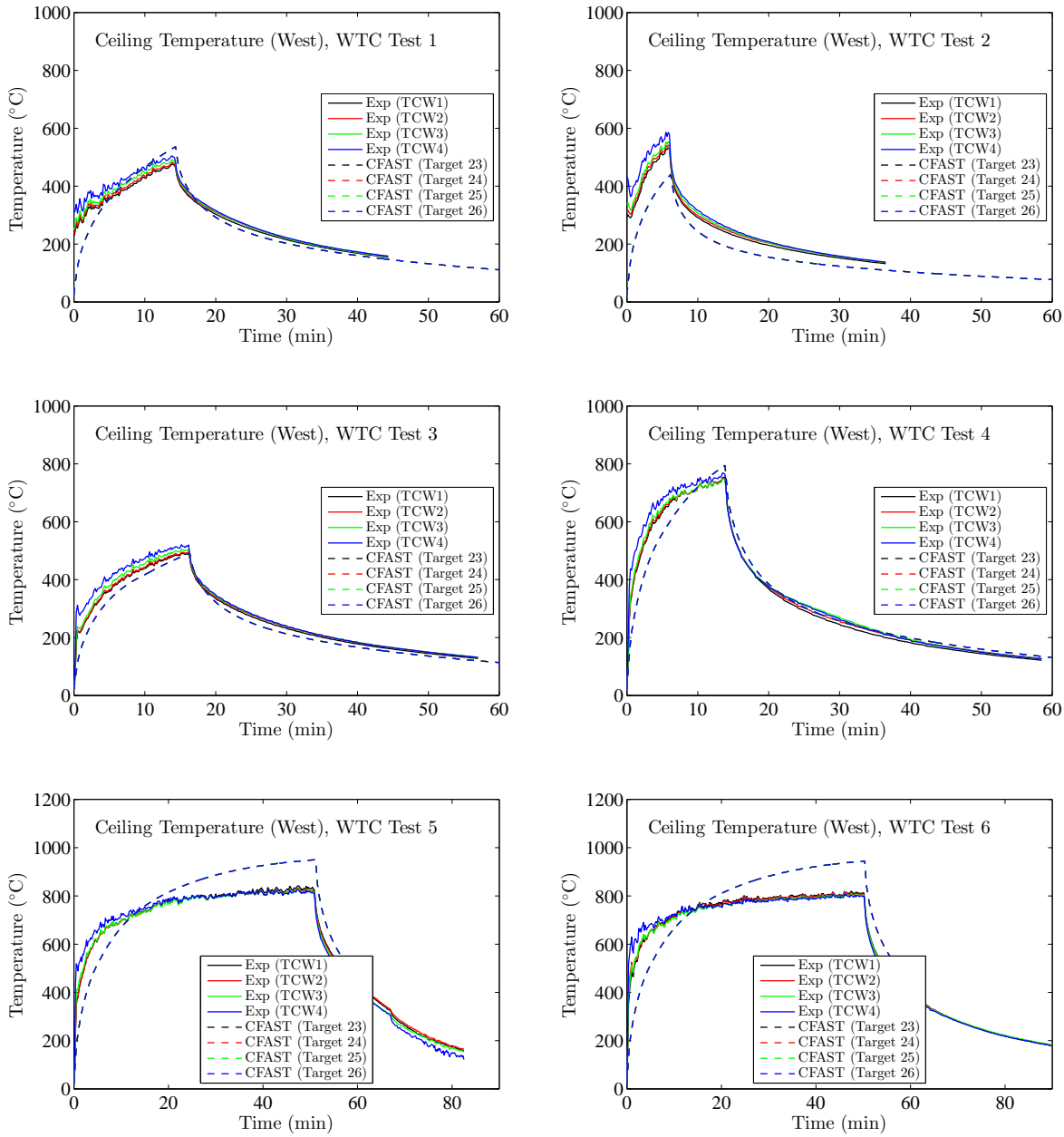
Name	x (m)	y (m)	z (m)
TCC	0.62	0.07	3.82
TCN3	0.62	0.67	3.82
TCS3	0.62	-0.53	3.82
TCE7	2.18	0.07	3.82
TCW7	-1.15	0.07	3.82
TCCIN	0.62	0.07	3.83
TCN3IN	0.62	0.67	3.83
TCS3IN	0.62	-0.53	3.83
TCE4IN	1.28	0.07	3.83
TCW4IN	0.05	0.07	3.83

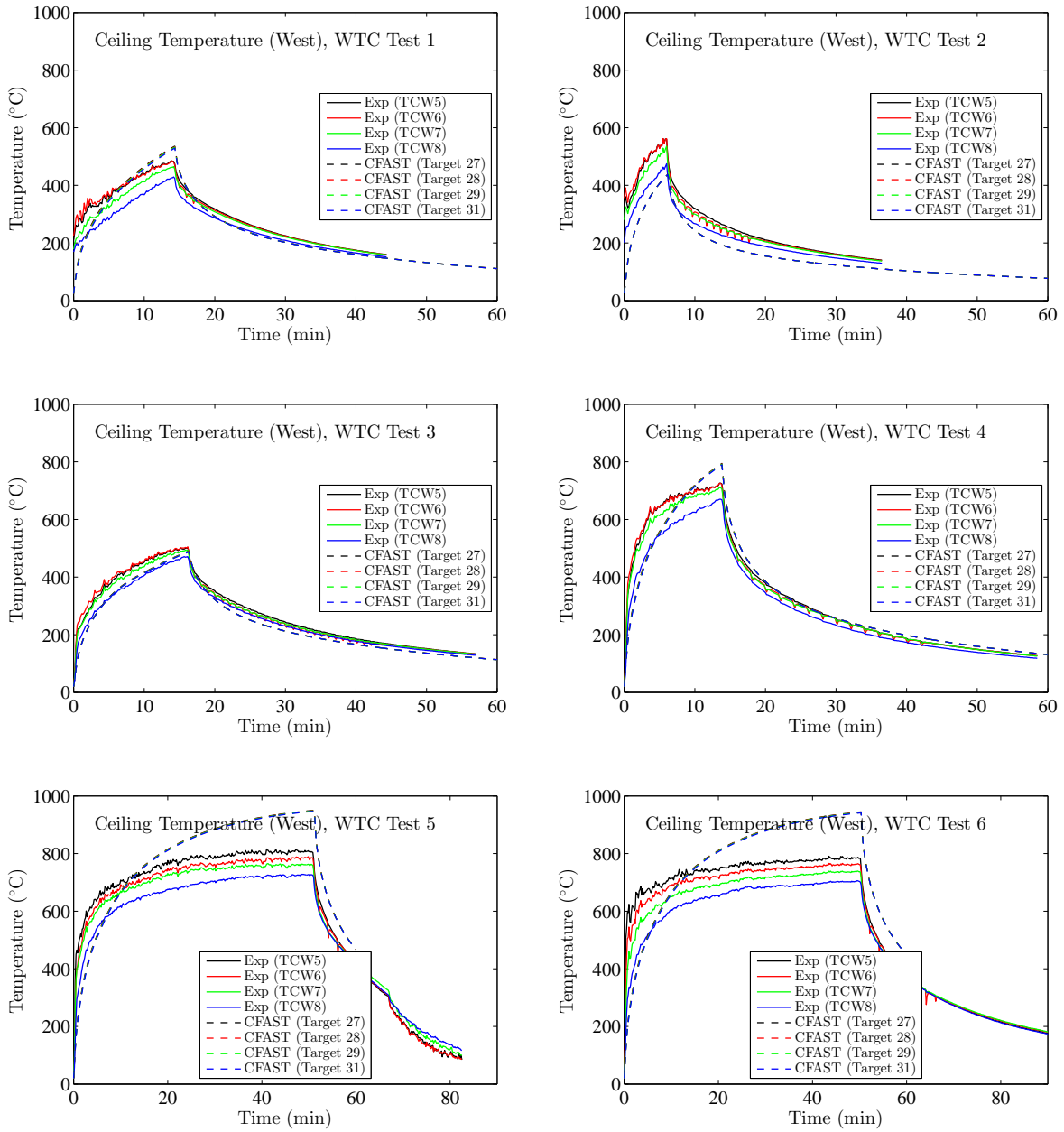


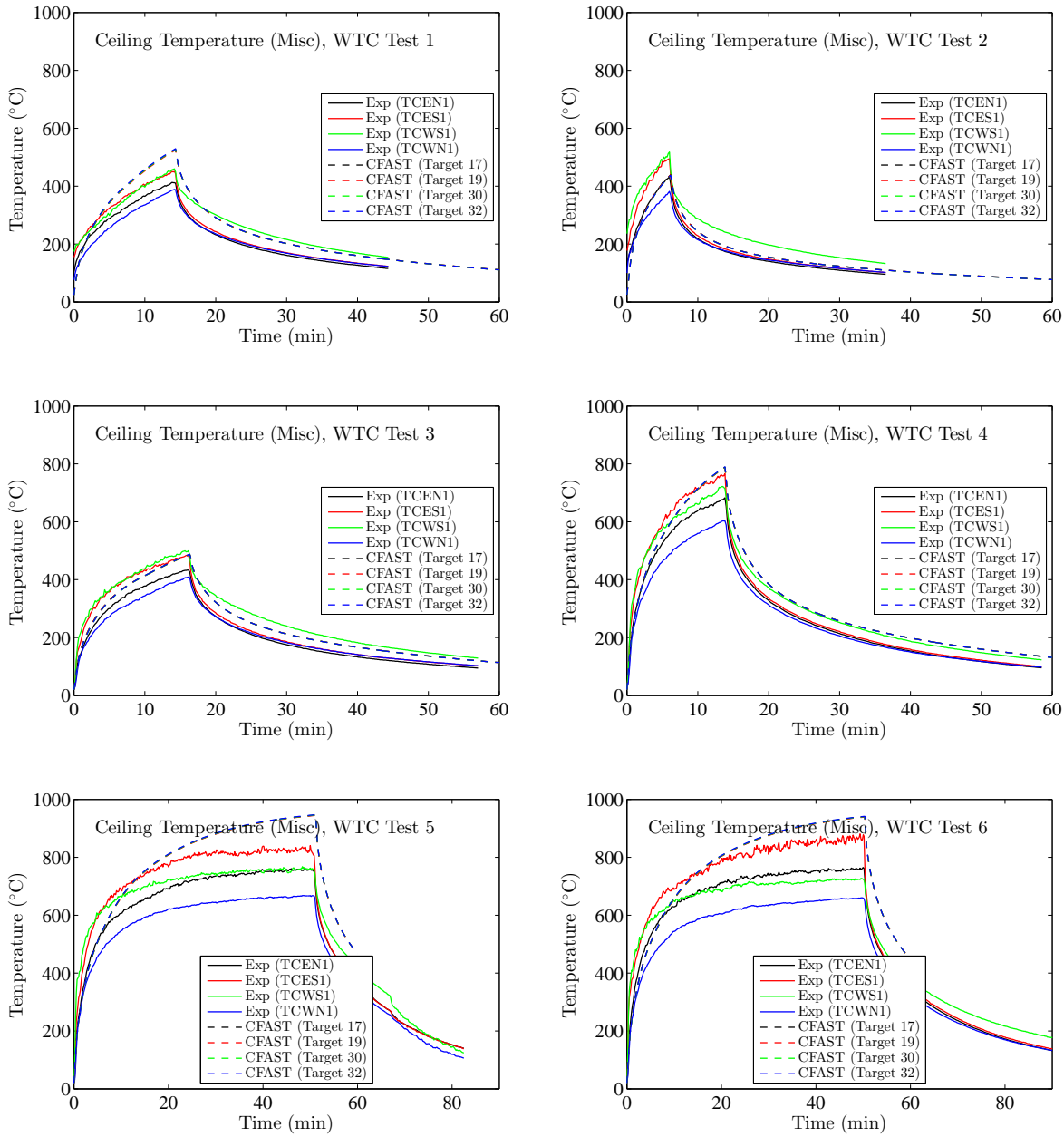


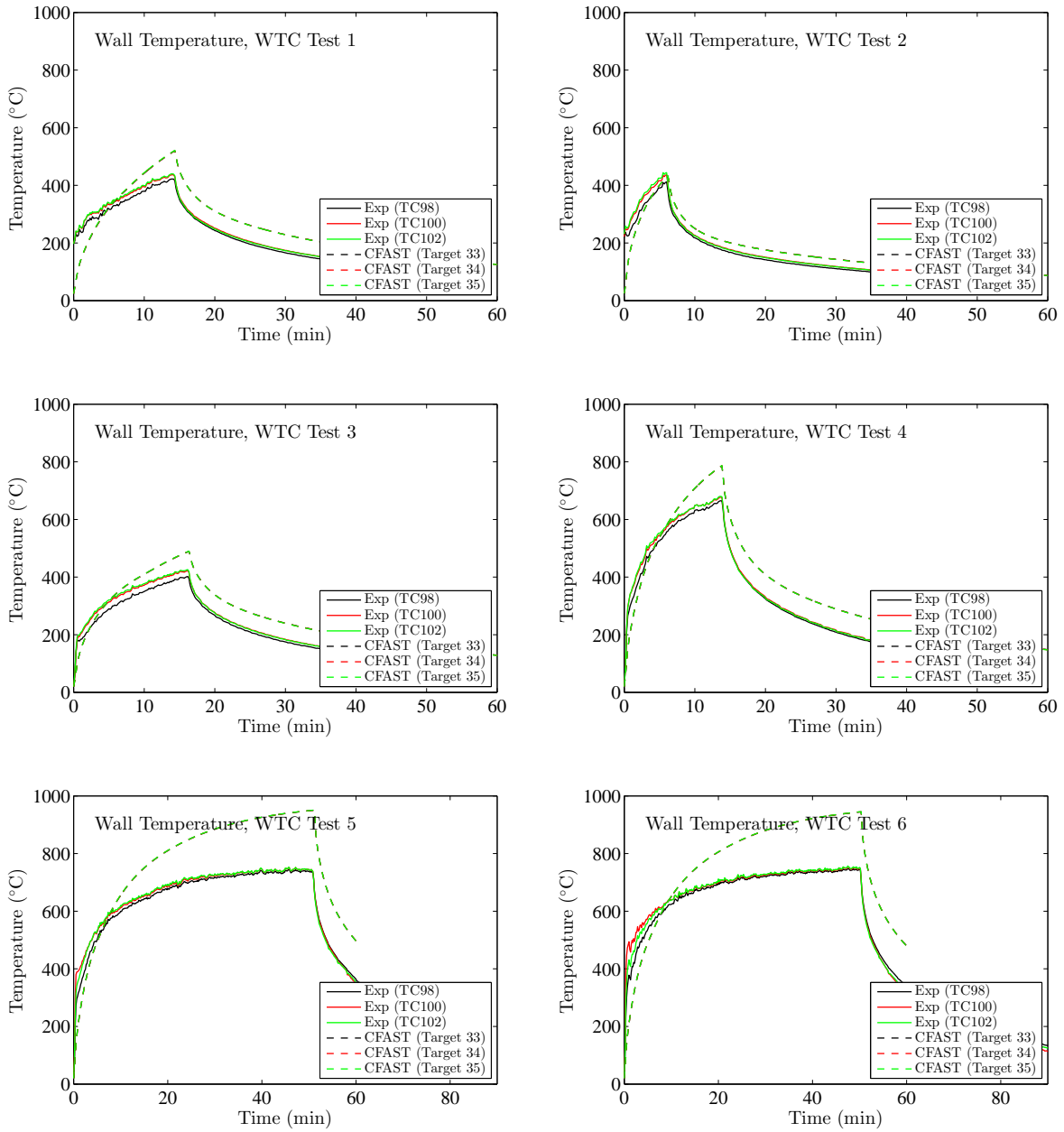


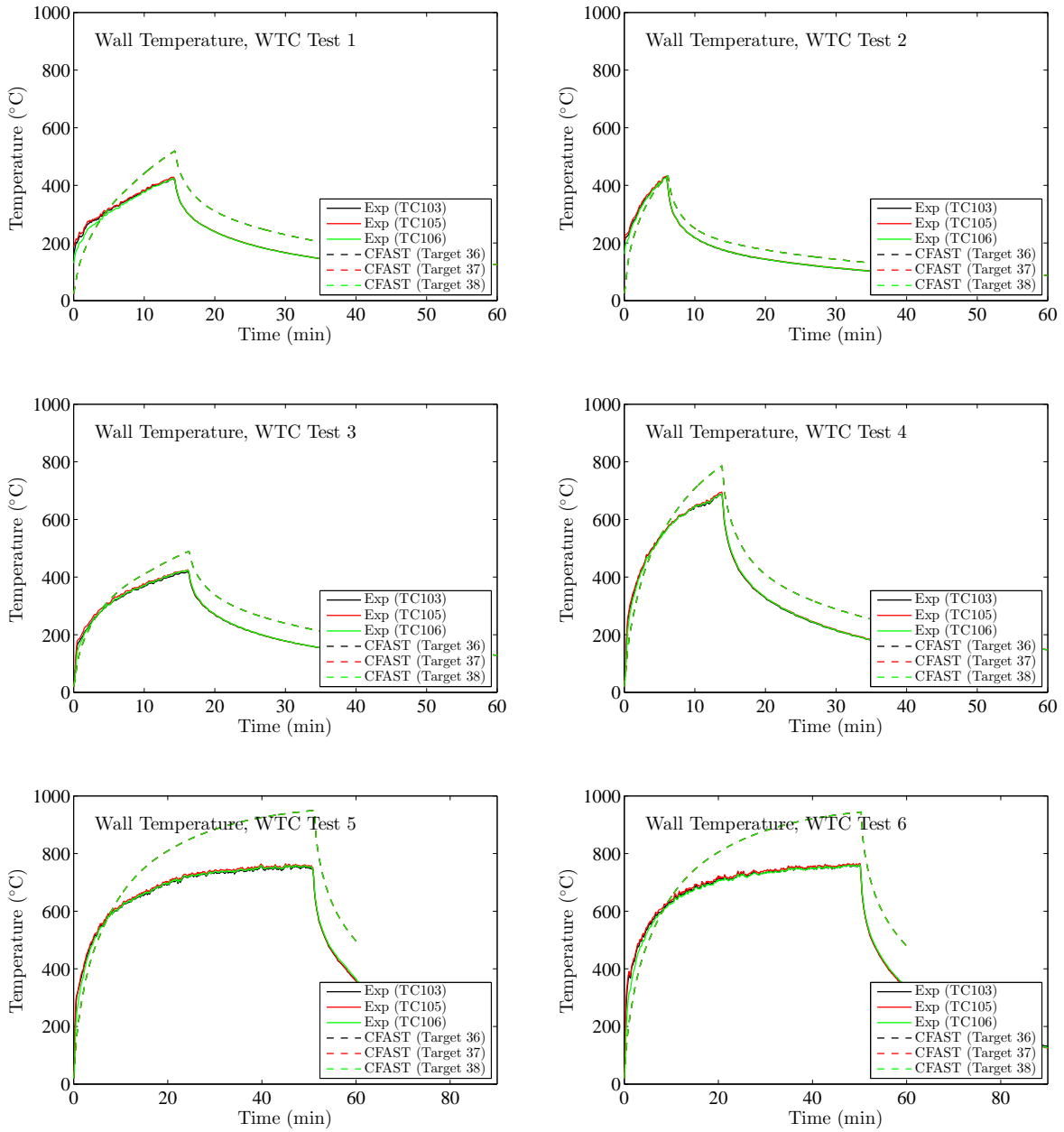


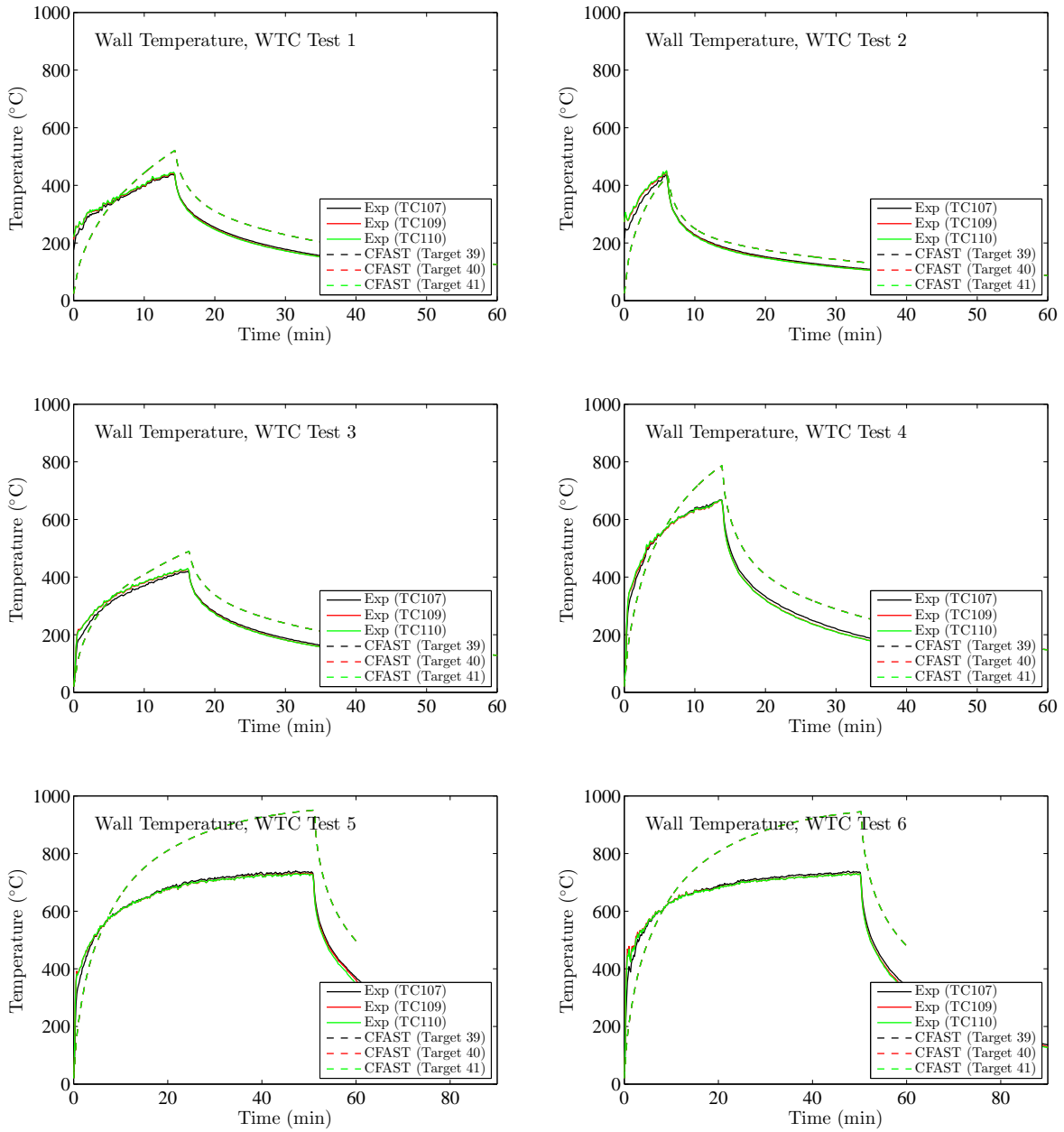




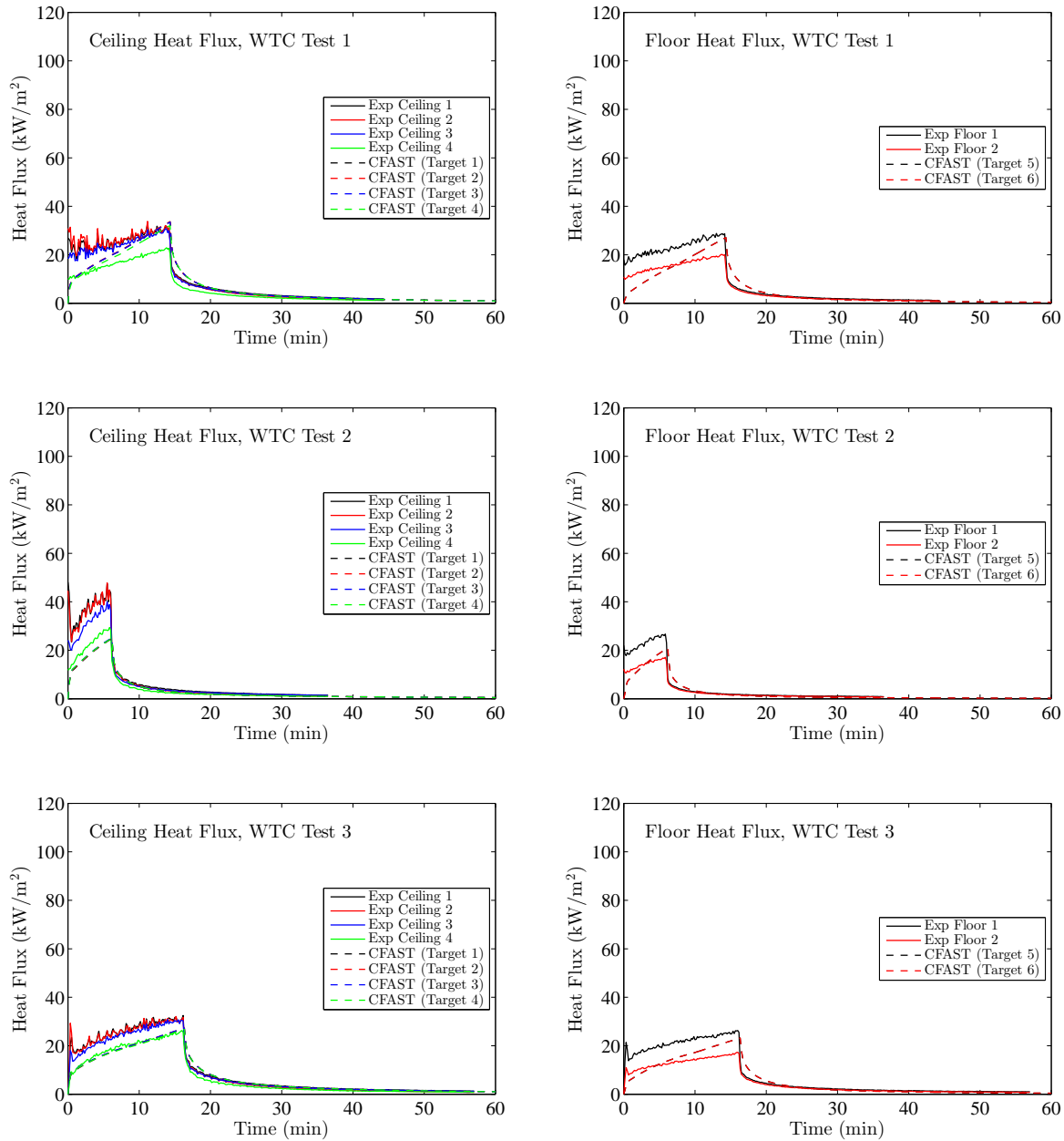


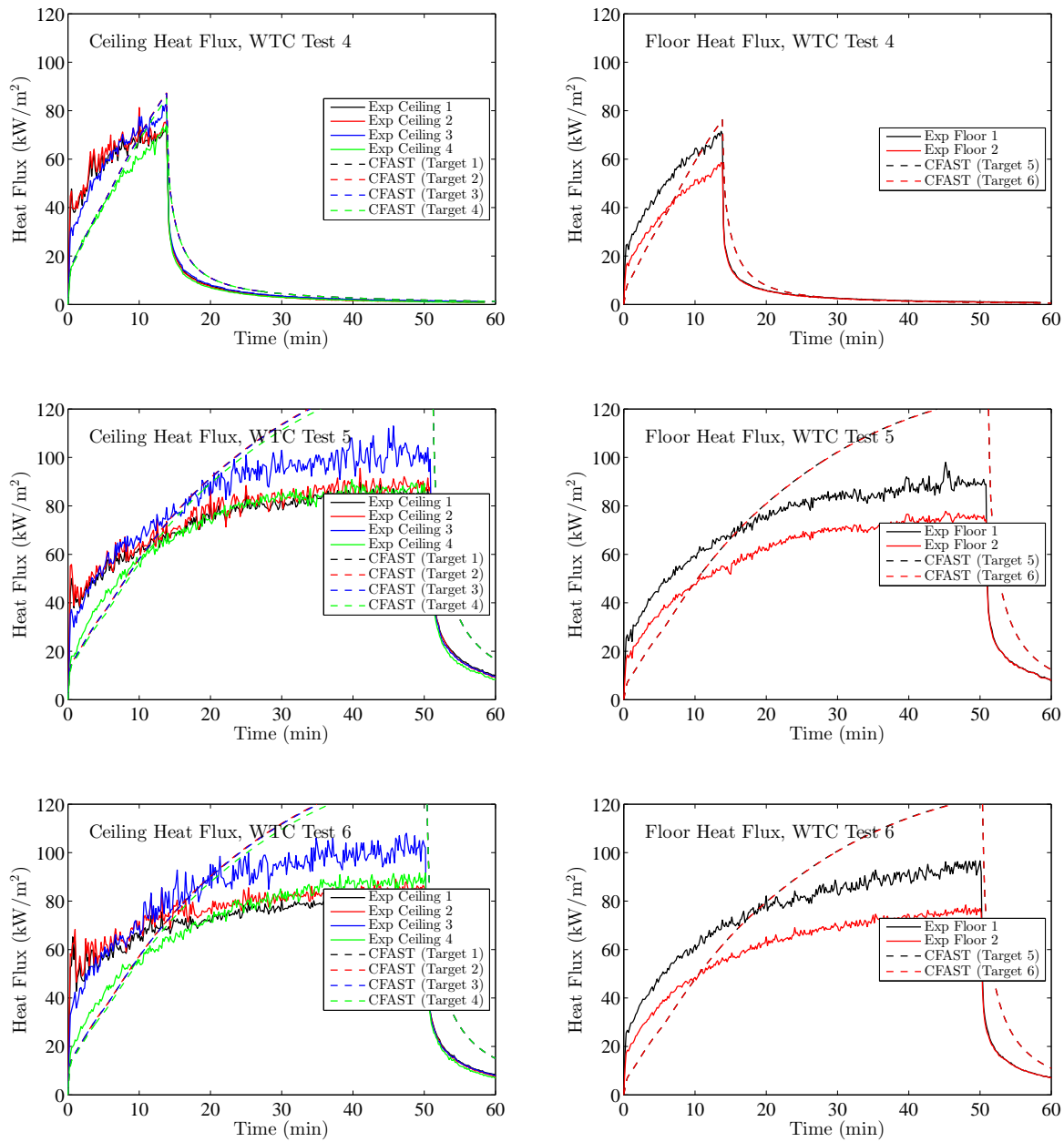






Heat flux to the ceiling and the floor were measured with a series of Schmidt-Boelter, water-cooled heat flux gauges.





The following pages present comparisons of oxygen and carbon dioxide concentration predictions and measurements for the WTC experiments. There was only one measurement of each made near the ceiling of the compartment roughly 2 m from the fire.

